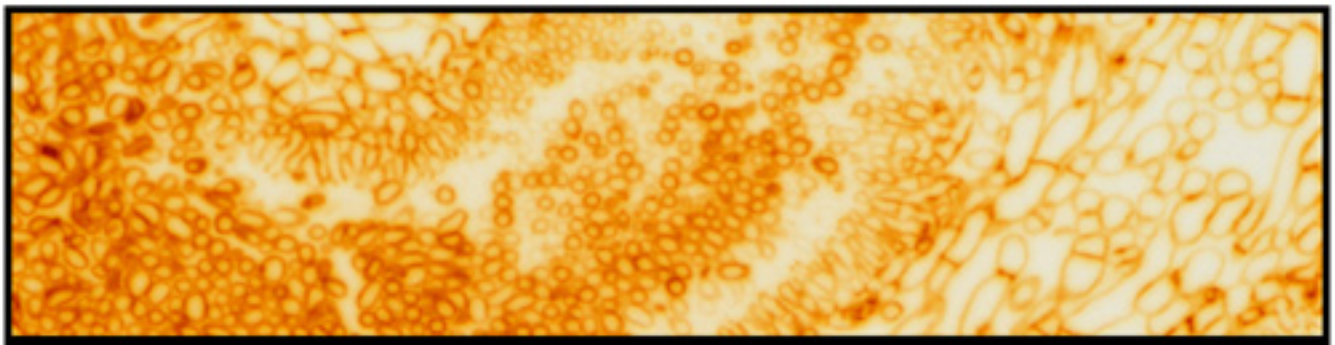

Sabine Ivison

The phytopathogenic interaction between *Claviceps purpurea* and rye: significance of enzymes involved in the response to active oxygen species

2002

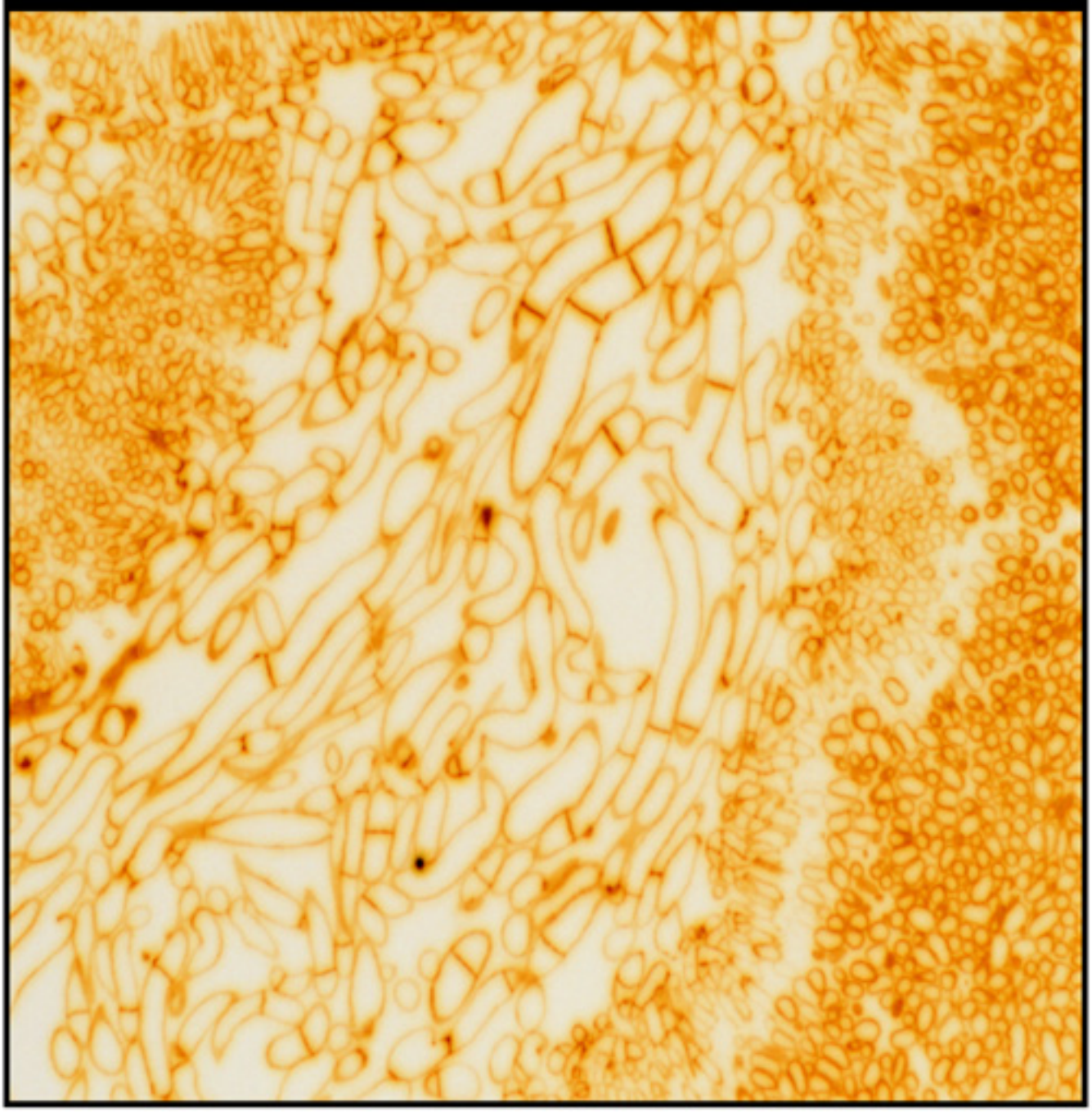

Mikrobiologie

The phytopathogenic interaction between *Claviceps purpurea* and rye: significance of enzymes involved in the response to active oxygen species

Inaugural-Dissertation
zur Erlangung des Doktorgrades
der Naturwissenschaften im Fachbereich Biologie
der Mathematisch-Naturwissenschaftlichen Fakultät
der Westfälischen Wilhelms-Universität Münster

vorgelegt von
Sabine Ivison
aus Victoria, BC, Kanada
-2002-

Dekan:	Pr. Dr. Paul
Erster Gutachter:	Pr. Dr. Tudzynski
Zweiter Gutachter:	Pr. Dr. Meinhardt
Tag der mündlichen Prüfung:	17.07.2002
Tag der Promotion:	17.07.2002

Index

Abbreviations

β	beta
Δ	difference
λ	lambda
®	registered trademark
Σ	sum
°C	degrees Celsius
µg	microgram
µl	microlitre
µM	micromolar (micromol/l)
µmol	micromol
µs	microsecond
(v/v)	volume/volume
(w/v)	weight/volume
A	absorption
A	adenine
A. nidulans	*Aspergillus nidulans*
A. niger	*Aspergillus niger*
A_{340}	absorption at 340 nm
aa	amino acids
ABA	abscisic acid
ABARE	abscisic acid response element
ABC	ATP-binding cassette
Ac	acetate
Acc.#	accession number
ACE	activation of copper enzyme
acyl-coA	acetyl-coenzyme A
Ag	silver
AIDS	acquired immune deficiency syndrome
AnCF	*A. nidulans* CCAAT factor
AOS	active oxygen species
app.	appendix
approx.	approximately
APS	ammonium persulfate
ATCC	American type culture collection
ATP	adenosine triphosphate
AT-rich	adenine and thymine rich
av	avirulence
BCA	bathocuproine disolfonic acid
BCIP	5-bromo-4-chloro-3-indolyl phosphate
bp	base pairs
BSA	bovine serum albumine
C	carbon
C	cytosine
C. purpurea	*Claviceps purpurea*
C. fulvum	*Cladiosporum fulvum*
C. fusiformis	*Claviceps fusiformis*
C. neoformans	*Cryptococcus neoformans*
Ca	calcium
ca.	circa
cAMP	cyclic adenosine monophosphate
CAT	catalase
Cd	cadmium
cDNA	complementary DNA
CDPK	calcium-dependent protein kinase
Ce	cerium
Cf (or CF)	in genes, refers to *claviceps fusiformis*
Cl	chlorine
cm	centimetre
CMS	cytoplasmic male sterile
CODE-HOP	consensus-degenerate hybrid oligonucleotide primers
cp	in genes, refers to *claviceps purpurea*
C-terminus	carboxy-terminus
CTT	cytosolic catalase
Cu	copper
Cu(I)	copper (oxidation state I)
CuRE	copper response element
CW	cell wall
CWDE	cell wall degrading enzymes
CYB	cytochrome b2
d	days
DAB	diaminobenzidine
dATP	2'-deoxyadenosine 5'-triphosphate

dCTP	2'-deoxycystidine 5'-triphosphate
ddATP	2',3'-dideoxyadenosine-5'-triphosphate
DDC	diethyldithiocarbamate
ddCTP	2',3'-dideoxycystidine 5'-triphosphate
ddGTP	2',3'-dideoxyguanosine 5'-triphosphate
ddH_2O	double destilled H_2O
ddTTP	2',3'-dideoxythymidine 5'-triphosphate
DEPC	diethyl pyrocarbonate
dGTP	2'-deoxyguanosine 5'-triphosphate
DMF	dimethyl
DMSO	dimethylsulfoxide
DNA	desoxyribonucleic acid
dNTP	desoxynucleotide triphosphate
dpi	days post inoculation
DS	differential screening
DTT	1,4-dithiothreitol
dTTP	2'-deoxythymidine 5'-triphosphate
e	base of natural logarithms
e^-	electron
E	enzyme
E. amylovora	*Erwinia amylovora*
E. coli	*Escherichia coli*
e.g.	exempli gratia (for example)
EC-SOD	extracellular SOD
Ed. (or Eds.)	editor (or editors)
EDTA	ethylenediamine tetra acetic acid
EMBL	European molecular biology laboratory
EMBO	European molecular biology organisation
ER	endoplasmatic reticulum
EST	expressed sequence tag
et al.	et alii
EtBr	ethidium bromide
etc.	et cetera (and so on)
eV	electronvolt
F. neoformans	*Filobasidiella neoformans*
FASEB	federation of American societies for experimental biology
Fe SOD	iron-containing SOD
Fe	iron
Fe(III)	iron (oxidation state III)
FEBS	federation of European biochemical societies
FEMS	federation of European microbiological societies
FeRE	iron response element
Fig. (or fig.)	figure
FMN	flavin mononucleotide
g	gram
G	guanine
G-6-P	glucose-6-phosphate
G6PDH	glucose-6-phosphate dehydrogenase
GFP	green fluorescent protein
GPx	glutathione peroxidase
GR	glutathione reductase
GSH	glutathione (reduced)
GSSG	glutathione (oxidised)
GST	glutathione-S-transferase
h	hour
H	hydrogen
HAP	heme activating protein
HI	homologous integration
HR	hypersensitive response
HRE	heat response element
HSF	heat shock factor
HSP	heat shock protein
i.e.	id est (that is to say)
IEF	isoelectric focusing
IMD	isopropyl malate dehydrogenase
IRE	iron response element
ITPG	isopropylthio-β-D-galactoside
JA	jasmonic acid
K	in DNA, guanine or thymine
K	potassium
kB	kilobase
kDa	kilodalton
kg	kilogram
K_m	Michealis-Menton constant
l	litre
LB	Luria Bertani medium
LBM	LB with magnesium sulfate
LBMM	LBM with maltose
Li	lithium
LSD	lysergic acid diethylamide

lx	lux
M	in DNA, adenine or cytosine
M. grisea	*Magnaporthe grisea*
MA	Mantle medium
mA	milliampere
MA-C	Mantle medium devoid of carbon source
MAP	mitogen-activated protein
MAPK	mitogen-activated protein kinase
mCu	milliCurie
MED	culture filtrate
Me^{ox}	metal (oxidised)
Me^{red}	metal (reduced)
mg	milligram
min	minute
ml	millilitre
mM	millimolar (millimol/l)
MM	minimal medium
Mn SOD	manganese-containing SOD
Mn	manganese
MRE	metal response element
mRNA	messenger RNA
MTF	metal-responsive transcription factor
MW	molecular weight
MYC	mycelia
N	nitrogen
N	normal
N. crassa	*Neurospora crassa*
n.a.	not available
n.c.	not countable
n.d.	not detectable
Na	sodium
NAD	nicotinamide-adenine dinucleotide
NADH	nicotinamide-adenine dinucleotide (reduced)
$NADP^+$	nicotinamide-adenine dinucleotide phosphate
NADPH	nicotinamide-adenine dinucleotide phosphate (reduced)
NBT	nitro blue tetrazolium
ng	nanogram
nm	nanometre
NO	nitric oxide
N-terminus	amino-terminus
O_2	oxygen
OD_{600}	optical density (at 600 nm)
ORF (or orf)	open reading frame
ox	oxidase
P	phosporus
P1	an alkaloid production strain from *C. purpurea*
PAA	polyacrylamide
PAGE	polyacrylamide gel electrophoresis
p.	page(s)
PCD	programmed cell death
PCR	polymerase chain reaction
PEG	polyethylene glycol
pers. comm.	personal communication
pfu	plaque forming unit
pH	potential of hydrogen
phleo	phleomycin
pI	isoelectric point
pK	negative logarithm of the ionisation constant (K) of an acid
pmol	pico mol
PR	pathogenesis related
ps	peptide synthase
PTS	peroxisomal targeting signals
Px	peroxidase
R	in DNA, guanine or adenine
R	residue
rDNA	recombinant DNA
re	random expectation
RF	replacement fragment
RNA	ribonucleic acid
RNase	ribonuclease
rpm	revolutions per minute
R-SH	reduced electron donor (protein)
RSSR	oxidised electron donor (protein)
RT	room temperature
RT-PCR	reverse transcriptase PCR
S	in DNA, guanine or cytosine
s	seconds
S	sulphur
S. cerevisiae	*Saccharomyces cerevisiae*
S. pombe	*Schizosaccharomyces pombe*

S. sclerotium	*Sclerotinia sclerotium*
SA	salicylic acid
SAR	systemic acquired resistance
SDH	sorbitol dehydrogenase
SDS	sodium dodecyl sulphate
SOD	superoxidedismutase
STRE	stress response element
T	thymine
T_A	annealing temperature
TEMED	N,N,N`,N`-tetramethylethylene-diamine
TF	transcription factor
™	trademark
Tris	tris(hydroxymethyl)-aminomethane
t_S	synthesis time
U	units
URS	upstream repressing sequences
UV	ultraviolet light
V	volt
vol (or Vol.)	volume
vs.	versus
W	in DNA, adenine or thymine
w/v	weight per volume
WT	wild type
x	factor
X/XO	xanthine/xanthine oxidase
X-Gal	5-bromo-4-chloro-3-indolyl-β-D-galactopyranoside
Y	in DNA, cytosine or thymine
Zn	zinc

1 Introduction

1.1 Oxygen toxins: the price of an aerobic lifestyle

In the mid to late pre-Cambrian era, about 3.8 to 0.5 billion years ago, the atmosphere of the earth became increasingly enriched with oxygen. During this time, protozoan life forms evolved from purely anaerobic organisms which produce their energy by fermentation and anoxygenic photosynthesis, to aerobic organisms, which harness energy by oxygenic photosynthesis or respiration. The use of dioxygen as a terminal electron acceptor instead of more reduced compounds such as nitrate or sulfate represented a more efficient means of energy production; this allowed the development of increasingly complex forms of life which eventually led to the evolution of eucaryotes and the rapid development of diverse metazoans in what is known as the Cambrian explosion. However, the organisms which profited from the high energy yield of aerobic metabolism were also confronted with new and lethal toxins which arose from the partial reduction of dioxygen.

Fig. 1.1: Oxygen in the atmosphere visible as the aurora borealis. Green aurorae are caused by the excitation of atmospheric oxygen after collision with particles of solar wind (mostly electrons and protons); transition from a high energy state into a lower energy state results in the emission of green light. Picture taken from http://www.cityofmelfort.ca/lights.gif

1.1.1 The toxicity of oxygen

The toxicity of dioxygen lies in its ability to exist in several redox states, some of which are exceedingly reactive. The reduction of dioxygen to water involves the acceptance of four electrons, which can take place in univalent steps, as shown in fig. 1.2. The intermediates are the superoxide radical (O_2^-), hydrogen peroxide (H_2O_2) and the hydroxyl radical ($OH^{\cdot}$). These compounds are collectively known as active oxygen species or AOS. A look at the standard reduction potentials of these compounds show that, while the superoxide radical can function as both oxidant and reductant, hydrogen peroxide and especially

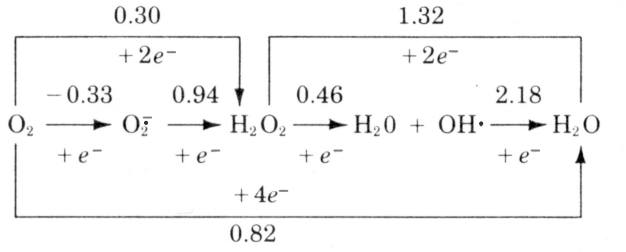

Fig. 1.2: The reduction of dioxygen to water. Each reaction is shown with standard reduction potential in eV. Drawing taken from Gralla and Kosman (1992).

the hydroxyl radical are powerful oxidants. Although superoxide can cause oxidative damage by inactivation of enzymes containing 4Fe-4S clusters such as aconitase (Gardner and Fridovich, 1991), and hydrogen peroxide is known to attack thiol groups of proteins (Thompson et al., 1987), most oxidative damage caused by superoxide and hydrogen peroxide is attributed to their ability to generate the hydroxyl radical. The direct reduction of hydrogen peroxide with superoxide to form the hydroxyl radical, known as the Haber-Weiss reaction (1), is a thermodynamically favourable but kinetically slow reaction (Koppenal et al., 1978). This reaction is strongly catalysed by transition metal ions such as Cu^{3+} and Fe^{2+}, which are reduced by superoxide (2) and oxidised by hydrogen peroxide (3) (Haber and Weiss, 1934).

(1) $O_2^{-\cdot} + H_2O_2 \rightarrow O_2 + OH^{\cdot} + H_2O$

(2) $O_2^{-\cdot} + Me^{ox} \rightarrow O_2 + Me^{red}$

(3) $H_2O_2 + Me^{red} \rightarrow OH^{\cdot} + H_2O + Me^{ox}$ **Equation 1.1**

The iron-catalysed breakdown of hydrogen peroxide, first suggested by Fenton in 1894, is referred to as the Fenton reaction; metal-generated hydroxyl-radical production is generally known as Fenton chemistry.

The exceedingly high reduction potential of the hydroxyl radical enables it to strip almost any compound which it may encounter of an electron or hydrogen atom; as a result, this potent toxin can cause direct injury only to molecules close to its site of generation (Czapski, 1984). However, the toxicity of the hydroxyl radical can be potentiated by the initiation of a free radical cascade. Typical candidates for chain reactions resulting in the spread of oxidative damage far from the site of initiation are unsaturated membrane lipids; oxidised fatty acids react with molecular oxygen to form lipid peroxyl radicals which are themselves capable of oxidising neighbouring lipids (Buettner, 1993). Damage of integral and peripheral membrane proteins as well as increased permeation of the lipid bilayer is the inevitable result of lipid peroxidation; disruption of ion homeostasis is the most immediate cause of necrotic cell death after severe oxidative insult. Oxidative damage of proteins and DNA can result in longer-term injury; although most oxidised proteins are subject to rapid recycling (Grune et al., 1997), some accumulate in the cell and have been implicated in neurodegenerative diseases. Oxidised bases such as 8-hydroxydeoxyguanosine (used as a marker for oxidative damage) result in conformational changes in the DNA, leading to replication errors with long term significance as well as perturbing cell homeostasis by causing errors in transcription and regulation (Kehrer, 2000).

Apart from the "classical" AOS: superoxide, hydrogen peroxide and the hydroxyl radical, there are many other important types of oxidative toxins such as nitric oxide ($NO^{\cdot}$) which is formed enzymatically in a reaction using molecular oxygen, as well as peroxynitrate ($OONO^-$) and hypochlorous acid (HOCl), which are formed in second degree reactions in which the "primary" AOS react with other

substances (Miller and Britigan, 1997). However, this thesis focuses primarily on the classical AOS types and their scavengers.

1.1.2 Sources of active oxygen

The reduction potentials of the reactions which form AOS shown in fig. 1.2 demonstrate that the formation of superoxide is endergonic, while all other AOS species can be formed spontaneously at physiological pH. The most abundant source of superoxide production in a healthy aerobic cell is the mitochondrial respiratory chain (in plants also the photosynthetic electron transfer) where it is estimated that about 1-2% of all transported electrons contribute to superoxide formation (Boveris and Chance, 1973). Most of this occurs in complex I with the NADH:Q reductase (Joseph-Horne et al., 2001), in which electrons are transferred from NADH to ubiquinone via flavin mononucleotide (FMN) and several Fe-S clusters. Almost all other sources of cellular superoxide are generated by similar enzymes; xanthine oxidase and aldehyde oxidase, two potent generators of superoxide (Fridovich, 1986), are also flavin-containing dehydrogenases which use dioxygen as a substrate; as does the cytochrome P_{450} oxidases and NADPH oxidase. These reactions all involve transfer from a exclusively two-electron carrier (NADH) to active centres which can only accept single electrons (Fe-S clusters) as well as high concentrations of dioxygen.

Superoxide can also be formed non-enzymatically with the help of compounds capable of redox cycling (such as quinones), which is the alternative acceptance and donation of single electrons (Winterbourne et al., 1991). Similar to the enzymatic formation of superoxide, the mechanism of these xenobiotics probably employs molecular oxygen as well as NAD(P)H as a reductant (Kim et al., 1996). An alternative source of superoxide is found in singlet-oxygen-generating photosensitisers; these compounds (such as cercosporin) absorb light energy which can be transferred to dioxygen, generating the first excited state of the oxygen molecule known as singlet oxygen which can accept an electron to form superoxide without needing additional energy (Daub and Ehrenshaft, 2000, Baker and Orlandi, 1995). Stress caused by UV light, injuries, hyperoxia, temperature fluctuations and a variety of other factors are known to elevate superoxide concentrations in aerobic cells (Scandalios, 1993); presumably, these factors could compromise enzyme function, creating "holes" in the carefully knit chains of electron transport .

At physiological pH, superoxide protonates to form its conjugate acid, the hydroperoxyl radical ($HO_2^{\cdot}$), which has a pK_s of 4.8; this dismutates non-enzymatically to form H_2O_2. The same reaction is enzymatically catalysed by superoxide dismutases at about 10^8-10^9 times the speed (Steinman, 1982). Thus, superoxide is quickly converted to hydrogen peroxide. Peroxidases can also produce H_2O_2 in a complex reaction stimulated by monophenols; this complex reaction, which (as usual) involves the production of superoxide by reduction of molecular oxygen with the concomitant oxidation of NADH,

is thought to be the source of hydrogen peroxide in the synthesis of lignin (Halliwell, 1978). Other sources of hydrogen peroxide include a variety of oxidases, only some of which are microbody-associated reactions such as those involved in the β-oxidation of fatty acids in the peroxisome. Typical substrates of other hydrogen peroxide-producing oxidase reactions, catalysed in a variety of different mechanisms, are oxalic acid, amines and glucose.

As most of the "unplanned" formation of hydrogen peroxide stems from spontaneous dismutation of superoxide, and the detoxification reaction of superoxide itself (catalysed by superoxide dismutase) produces hydrogen peroxide, the two substrates of hydroxyl radical formation (see equation 1.1) will often be found together. As stated above, biologically significant amounts of hydoxyl radical are probably only generated in the presence of transition metal catalysts. Although cellular concentrations of such metals are kept to a minimum (Rae et al. (1999) report that, in yeast, free copper ions are limited to less than one per cell), there is a certain amount of autocatalysis as the superoxide radical attacks 4Fe-4S clusters of enzymes, resulting in the release of free iron (Liochev and Fridovich, 1999). Some of the more exotic AOS such as peroxynitrite have also been implicated in the formation of the hydroxyl radical. Its exceedingly short half life renders *in vivo* localisation of the hydroxyl radical all but impossible; therefore information as to its source is mostly theoretical, and ascertainable only by the damage it has caused.

1.1.3 Survival as an aerobe

Aerobic organisms have evolved a complex set of anti-oxidant mechanisms, many of which have been conserved in the evolution from bacteria to mankind. Defense strategies include those which aim at preventing the formation of AOS and those which scavenge AOS.

The most important defense strategy is prevention. Electron transport processes in the respiration chain, photosynthesis and in a variety of redox reactions are carefully constructed in order to keep electron leakage to a minimum. The concentration of Fenton-susceptible metal ions in the cell is meticulously guarded; high and low affinity transporters are regulated to deal with environmental fluctuations in concentration; once in the cell, they are kept tightly bound to metallothioneins from which they are chaperoned to the proteins which require them.

In places with a high expectation of AOS formation, specialised enzymes await them; superoxide dismutase catalyses the dismutation of superoxide to hydrogen peroxide, catalases degrade hydrogen peroxide to water and oxygen and peroxidases use a variety of cofactors to reduce hydrogen peroxide to water. Mitochondria, the site of respiratory electron transport processes which represent the major source of superoxide, are equipped especially with their individual superoxide dismutases and peroxidases (as are chloroplasts in plants); peroxisomes (and in plants, glyoxysomes) have their own catalases to deal with the hydrogen peroxide generated within their boundaries. Extracellular and

periplasmatic spaces, which are exposed to more oxygen than the cytoplasma, are also equipped with superoxide dismutases, and to a certain extent, catalases.

As AOS can crop up throughout the cell, either as by-products of enzymatic reactions or general stress, or as the result of toxic substances, the cytosol is laced with enzymatic and non-enzymatic AOS scavengers. Cytosolic superoxide dismutases and catalases are part of the enzymatic defense array, as are peroxidases. There are many different types of peroxidases, each which use their individual co-factor as an electron donor. Some peroxidases have less importance as components of the AOS scavenging system, for instance fungal lignin peroxidase employs the oxidative power of H_2O_2 to pry electrons from the lignin polymer in the biodegradation of lignin (Reddy and D'Souza, 1994). Others, such as cytochrome c, ascorbate and glutathione peroxidase are important AOS scavenging enzymes. The heme-type cytochrome c and ascorbate peroxidases are found in mitochrondia and chloroplasts, respectively; while several different selenocysteine-type glutathione peroxidases (GPx1-4) patrol cytosol and membranes, detoxifying hydrogen peroxide and fatty acid hydroperoxides with the help of electrons drawn from glutathione (Arthur, 2000).

The tripeptide glutathione (γ-glutamylcysteinylglycine or GSH) is the central component of one of the major antioxidant enzyme systems in eucaryotic cells (Grant et al., 1996). The sulfhydryl group of its cystein moiety acts as electron donator in a number of enzymatic and non-enzymatic reactions, after which two molecules of oxidised product combine to form the disulfide GSSG. The ratio of GSH to GSSG indicates the redox status of the cell; under normal conditions, over 98% of glutathione is present in its reduced form. Oxidative stress causes accumulation of GSSG in a number of reactions involving enzymes such as glutathione peroxidase, glutathione-S-transferase (which catalyses the thiol-disulfide exchange of oxidatively damaged proteins) and dehydroascorbate reductase (which regenerates the reduced form of ascorbate) as well as non-enzymatic radical quenching reactions. GSSG is regenerated by the glutathione reductase, which utilises reduction equivalents from NADPH (Wang and Ballatori, 1998, Noctor and Foyer, 1998). Furthermore, the ratio of GSH:GSSG is directly implicated in the regulation of gene transcription; this is thought to be (in part) mediated by transcription factors whose activity is controlled by the glutathiolation of cystein residues (Klatt et al., 1999). Another important member of the redox-homeostasis system are the thioredoxins; these are small, cystein-containing proteins which partake in similar redox cycles as those described for glutathione (Inoue et al., 1999).

Besides the complex array of enzymatic defense systems, numerous small molecules are important for non-enzymatic AOS-scavenging. Hydrophobic AOS scavengers such as α-tocopherol (vitamin E), melatonin and flavonoids are essential for their ability to scavenge lipid hydroperoxides; water soluble radical traps include uric acid, mannitol and free amino acids as well as ascorbate and glutathione.

1.1.4 A closer look at two AOS scavenging proteins: Cu,Zn SOD and catalase

Most AOS are initially formed by the reduction of oxygen to superoxide. Enzymatic detoxification of superoxide is carried out by superoxide dismutases, which dismutates superoxide to hydrogen peroxide. As the combination of superoxide and hydrogen peroxide can produce the potent hydroxyl radical, superoxide dismutases must work in concert with hydrogen peroxide degraders such as catalases. Only together can these enzymes build an efficient AOS scavenging system.

1.1.4.1 Cu,Zn SOD

Using a metal ion (Me) cofactor which is bound in their active centre, all superoxide dismutases catalyze the following reaction (Steinman, 1982, Bannister et al., 1987):

$$\begin{aligned} \text{E-Me}^{ox} + O_2^{-\cdot} &\rightarrow \text{E-Me}^{red} + O_2 \\ \text{E-Me}^{red} + O_2^{-\cdot} + 2H^+ &\rightarrow \text{E-Me}^{ox} + H_2O_2 \\ \hline \Sigma \quad 2H^+ + O_2^{-\cdot} + O_2^{-\cdot} &\rightarrow + H_2O_2 + O_2 \end{aligned}$$

Equation 1.2

Depending on the type of catalytic metal, superoxide dismutases can be divided into three major groups: the Fe SOD, the Mn SOD and the Cu,Zn SODs. Structural similarities indicate that Fe SOD (the sole SOD of obligate anaerobes) and Mn SOD have a common evolutionary ancestor (Asada et al., 1980), while the Cu,Zn SOD is thought to have evolved separately, probably from a copper-storage protein (Getzoff et al., 1989, Chary et al., 1990). The latter idea is supported by the fact that binding of copper alone prevents oxidative stress by decreasing the concentration of potential Fenton catalysts (Gralla and Kosman, 1992) as well as by the copper-dependent regulation of the yeast enzyme (Greco et al., 1990). Although prokaryotes and plants have been documented which posses all three enzyme types, fungi and animals usually have SODs which are either of the Cu,Zn SOD-type or the Mn SOD-type (Scandalios, 1993). As the charged substrate of these scavengers can not easily pass cell membranes, superoxide must be detoxified in the compartment in which it is generated (Fridovich, 1995). Typically, Mn SOD is mitochondrial, Fe SOD is plastidic and Cu,Zn SOD can be subdivide into intracellular and extracellular forms.

Intracellular Cu,Zn SODs are highly homologous enzymes, showing over 50% primary structure conservation between fungi and higher eucaryotes. Although they are mostly cytosolic, they have been found in the nucleus and peroxisomes of mammalian cells (Crapo et al., 1992), as well as in the periplasmatic space of prokaryotes (reviewed in Fridovich, 1995). They are small proteins, with a typical monomer size of about 150 amino acids which are arranged in an 8-stranded antiparallel β-barrel and contain one atom of Cu and Zn. The functional enzyme is a homodimer which exhibits no kinetic links between the two active centres (Gralla and Kosman, 1992). Highly conserved regions include residues involved in the interface between the two monomers, residues which ligand the two

metals and residues which build a tertiary loop structure called the electrostatic channel (Bordo et al., 1994). A tight packing of the dimer interface, an interchain disulfide bond as well as an extensive network of hydrogen bonding contribute to the high stability of this enzyme (Barra et al., 1979). The catalytic function of Cu,Zn SOD, recognised for its ability to inhibit the superoxide-mediated reduction of cytochrome c, was first elucidated by McCord and Fridovich in 1969. The catalytic copper ion is liganded to one water molecule and four histidine residues, one of which is a bridging ligand to the adjacent Zn which buffers the active centre (Steinman, 1982) but does not take an active part in catalysis, as suggested in the following structure-based proposal for the enzymatic mechanism:

Catalysis, as shown above, is a two step reaction: in the first, the active centre, located in the bottom of an "electrostatic channel" uses positive charged residues to suck in the negatively charged superoxide (Getzoff et al., 1983). There, it associates with an arginine residue, resulting in the displacement of water and the transfer of an electron from superoxide to Cu(II). No longer negatively charged, the oxygen diffuses from the electrostatic channel and a water molecule takes its place. Protonation of the bridging ligand histidine results in the breakage of the bond to Cu(I). In the second step, another superoxide is electrostatically drawn into the channel, displaces the water ligand, and forms hydrogen bonds with the arginine, an adjacent molecule of water and the histidine proton. Transfer of the Cu(I) electron to the superoxide is accompanied by the acceptance of protons from the histidine and the water molecule, forming hydrogen peroxide. The Cu(II) moves back into its original liganding position with the histidine, the neutral H_2O_2 diffuses from the channel, and protons are relayed to the active site to refurbish the water molecule which is again liganded to the copper (Hart et al., 1999).

The extracellular form of Cu,Zn SOD (EC-SOD), which until now has only been found in eucaryotes (such as nematodes: Liddell and Knox, 1998, crayfish: Johansson et al., 1999, and mammals: Marklund, 1982) differs slightly from the cytosolic form. The monomer size, encompassing more than 200 aa, is larger than the cytosolic enzyme and includes about 100 amino acids at the N-terminus which contains a signal sequence for secretion. As about half of the EC-SOD primary sequence is highly homologous to that of the intracellular Cu,Zn SOD and contains almost all of the amino acids which are invariant in the latter, the catalytic mechanism of both enzymes is probably similar. In contrast to the homodimeric cytosolic enzyme, the active form of the extracellular enzyme is a homotetramer. (Marklund, 1982). EC-SOD is a glycoprotein which contains a positively charged carboxy-terminus (Hjalmarsson et al., 1987), thought to be involved in ionic binding to the cell surface (Johansson et al., 1999).

1.1.4.2 Catalase

Catalases are enzymes which are able to catalyse the following reaction:

$2\ H_2O_2 \rightarrow 2\ H_2O + O_2$

All known catalases fall into one of three distinct subgroups: true catalases, catalase-peroxidases and manganese catalases (von Ossowski et al., 1993, Mayfield and Duvall, 1996)

The manganese catalases, also known as pseudocatalases as they contain a Mn atom instead of a heme moiety in their active centre (see below), have until now only been found in prokaryotes (Kono and Fridovich, 1983, Kagawa et al., 1999), and are thought to have evolved separately from the other two types of catalases (Zámocký and Koller, 1999). The bifunctional catalase-peroxidases, which are able to use a broad variety of cofactors, as well as H_2O_2 as electron donors in the reduction of H_2O_2, have been isolated from prokaryotes (reviewed in Zámocký and Koller, 1999) and fungi (Levy et al., 1992, Fraaije et al., 1996). These heme-containing enzymes show greater homology to peroxidases than to true catalases (Zámocký and Koller, 1999) and although their H_2O_2 turnover is slower than catalases their higher substrate affinity (Kobayashi et al., 1997, Obinger et al., 1997) renders them better scavengers at lower H_2O_2 concentrations.

The group of true catalases are homotetramers with a ferric heme prosthetic group bound within each subunit. They are found in almost all prokaryotic and all eucaryotic aerobes and have also recently been isolated from archaebacteria (Shima et al., 1999, Shima et al., 2001). The subunit size, which typically ranges from about 400 to 800 aa, contains a highly conserved core of 390 aa (Klotz et al., 1997). Catalases are extremely fast enzymes, catalysing the disproportionation of about 40 million H_2O_2 molecules per second, a rate close to that of diffusion. The subunit can be divided into four domains: 1) the N-terminal domain, which is important for quaternary structure, 2) the β-barrel domain which contains the heme moiety, 3) the wrapping domain, which is also involved in intersubunit binding and contains the proximal heme-ligand tyrosine, and 4) the α-helical rich domain. In some catalases, the latter domain is able to bind NADP (Kirkman and Gaetani, 1984), thought to be involved in the reversion of oxidised intermediates and the stabilisation of quaternary structure (Zámocký and Koller, 1999). A subgroup of large catalases contain an extra C-terminal domain of about 150 aa, referred to as the "flavodoxin-like domain"; this domain, whose function is unknown, contains a Rossmann fold typical for nucleotide binding (Melik-Adamyan et al., 1986).

The degradation of H_2O_2 by catalases is thought to occur in two steps (Halliwell and Gutteridge, 1999):

$$H_2O_2 + \text{Fe(III)-E} \rightarrow H_2O + \text{O=Fe(IV)-E}$$
$$H_2O_2 + \text{O=Fe(IV)-E} \rightarrow O_2 + H_2O + \text{Fe(III)-E} \qquad \textbf{Equation 1.3}$$

The heme of each subunit is exposed through a funnel-shaped channel which contains hydrophilic residues around the entrance and hydrophobic residues as the channel narrows; the small channel diameter restricts the access of large substrates (Belal et al., 1989). The heme is liganded to four nitrogen atoms of the protoporphyrin and, on the proximal side (facing the enzyme core) to the phenolic side chain of a tyrosine residue. H_2O_2 diffuses to the active site along the tunnel to the distal side of the heme (facing the surface), where sterical hindrance forces it to interact with a histidine residue. Although the exact mechanism is unclear, the reaction involves proton transfer from one peroxide oxygen to the other via the histidine, facilitate the co-ordination of the other peroxide oxygen with the heme Fe(III) and the release of a water molecule. This forms Fe(IV) and a radical heme intermediate, which is able to stabilise itself by giving up an electron, probably with help of the tyrosine ligand. A second molecule of H_2O_2 is oxidised to O_2 by transferring a hydrid ion to the intermediate, releasing water and the original enzyme (Fita and Rossmann, 1985). When the concentration of H_2O_2 is low, the Fe(IV)-containing intermediate can use low molecular weight alcohols such as phenol and methanol as reductant in a peroxidase-like reaction (Percy, 1984), giving rise to water and acids.

Typically, aerobic organisms have multiple catalases. In eucaryotes, one catalase form is confined to the peroxisome, where it represents about 40% of all matrix protein and is important for the detoxification of H_2O_2 which are produced by a variety of flavin oxidases during the metabolism of fatty acids, amino acids and other substances. Peroxisomal catalases are mainly constitutive, while other catalase forms are often strictly regulated by tissue type and/or developmental stage (McClung, 1997, Kawasaki et al., 1997). Cells do not typically contain special mitochondrial catalases, as peroxidases are more important for detoxification of AOS leaked from the respiratory chain. Other catalases are localised in the cytosol or are extracellular. Evidence for secreted catalases have been found in prokaryotes (Raynaud et al., 1998) and fungi (Fowler et al., 1993, Garre et al., 1998a). Usually, extracellular catalases are larger than the peroxisomal forms as they have the extra "flavodoxin-like" domain at their C-terminus.

Together, these enzymatic and non-enzymatic system of AOS-scavengers have enabled the survival of aerobic organisms despite the constant threat of oxygen poisoning. Just how important these mechanisms are for survival has been uncovered in the past two decades as AOS have been implicated in a number of human diseases, including prion-related sickness, AIDS, cancer and a number of neurodegenerative disorders. Furthermore, accumulative oxidative damage is now considered to be one of the main causes of aging (Raha and Robinson, 2000). These discoveries have led to intense research into the formation and scavenging of active oxygen species, as well as their contribution to pathogenesis in both plants and animals.

1.2 Harnessing the evil: AOS in plant pathogenesis

The oxidative burst describes the response of a cell or organism to pathogen attack by immediate production of large quantities of active oxygen (Mehdy, 1994). The oxidative or respiratory burst was first discovered in neutrophils of the mammalian immune system, which generate large quantities of hydrogen peroxide via a membrane-bound NADPH oxidase when attacked by microbes (Segal and Abo, 1993). The importance of the oxidative killing of microbial invaders for the human immune system is illustrated by severity of the chronic granulomatous disease, which is caused by dysfunction of the NADPH-oxidase; without treatment, sufferers are fatally plagued by bacterial and fungal infections (Johnston, 2001). A similar phenomenon was found in plants when Doke showed in 1983 that potato tubers inoculated with incompatible strains of *Phytophthora infestans* produced large amounts of superoxide. This initiated a flurry of similar research which documented the occurrence of an oxidative burst as an immediate response to pathogen attack in several different plants; today it is accepted as a widespread and crucial component of the general defense arsenal in plants.

1.2.1 Early response to attack determines compatibility of interaction

Plants are able to recognise small molecules (usually proteins, peptides or oligosaccharides), termed elicitors, which are released as a result of attempted invasion by pathogenic bacteria or fungi. Either synthesised by the attacker or derived from the plant cell wall, elicitors initiate signal cascades in the host plants which result in the induction of a number of defense mechanisms. These include alkalisation of the protoplast, rise in cellular Ca^{2+} levels, production of AOS, death of tissue surrounding the infection site (hypersensitive response), fortification of cell walls and expression of pathogenesis-related (PR) genes such as those which synthesise toxic phytoalexins. Should these defences deter the attacker, the interaction is referred to as incompatible, while pathogens which can evade or survive these defenses cause compatible interactions. Incompatibility can arise on a species level, in which plant defense strategies ward off intruders not specialised for invasion of their type of host plant (non-host incompatibility), or on a sub-species level in which a pathogenic species is unable to infect because it expresses avirulence genes. The coupling of avirulence (av) gene products with specific plant resistance (R) gene products in the process defined as the "gene-for-gene interaction" results in incompatibility; fungal or bacterial pathovars are defined by possession of avirulence genes as host cultivars are defined by possession of resistance genes.

1.2.2 Early response AOS production: the oxidative burst

The oxidative burst is now considered to be one of the earliest response of plants to attack by pathogenic microbes including fungi, bacteria and viruses. Experiments with bacterial elicitors and plant cell suspensions indicate that the AOS produced in response to pathogen attack can be divided into two phases, the first, appearing after a few minutes, is seen in response to attack by both compatible and incompatible pathogens, while the second and often more copious generation of AOS, occurring after one or more hours, is only observed in incompatible interactions (Baker and Orlandi, 1995). Concentrations of H_2O_2 measured only 10 min after elicitation of soybean cells with oligogalacturonide reached 1.2 mM (Apostol et al., 1989), similar to the rate of AOS production shown for attacked neutrophils (Morel et al., 1991). Generally, in experiments involving whole plants or plant segments, the first appearance of AOS after elicitation takes longer (2-4 h) (May et al., 1996), although the amount of AOS production and its appearance seems to depend to some extent on the elicitor (Levine et al., 1994, Wojtaszek, 1997). Pre-treatment of cell suspensions and whole plants with salicylic acid, a mediator of systemic acquired resistance (SAR), can potentiate the oxidative burst in some systems (Kauss and Jeblick, 1995, Fauth et al., 1996).

Although most investigations implicate H_2O_2 as the main component of the oxidative burst, this may be a result of the greater stability of this compound in comparison to the superoxide and hydroxyl radicals. It is likely that the composition of AOS in the oxidative burst varies in individual systems, depending on the mechanism of production and pH. In many systems, immunological and inhibitory studies show that the most likely source of the plant oxidative burst (as in the neutrophil respiratory burst in mammals) is a membrane-bound NADPH oxidase, which generates extracellular superoxide (Levine et al., 1994, Dwyer et al., 1996, Lamb and Dixon, 1997). This model suggests that elicitation increases cytoplasmatic Ca^{2+} levels, resulting in protein kinase C-mediated activation of the NADPH-oxidase and production of superoxide. Hydrogen peroxide may be generated from superoxide via spontaneous dismutation (favoured at low pH) or the activity of an apoplastic SOD. Another candidate for generation of apoplastic AOS is a cell surface flavoprotein; this protein, which is also associated with the plasma membrane and involved in iron uptake, utilises electrons from NAD(P)H for the concomitant reduction of oxygen and Fe^{3+} to superoxide and Fe^{2+} (Vianello et al., 1990). A further proposed source of AOS is a pH-dependent cell-wall peroxidase (Bollwell et al., 1995) which can produce H_2O_2 in a reaction similar to that of lignification-linked peroxidase activity (see 1.1.2). Evidence for this model is supplied by the fact that it is possible to trigger the oxidative burst in suspensions of French bean by alkalisation of the media (Bolwell, 1996). The cell wall peroxidase requires extracellular reductant, which is thought to be supplied in the form of cystein, glutathione or NAD(P)H (Bolwell et al., 1995). Recently, an elicitor-induced extracellular peroxidase was isolated

which is able to produce H_2O_2 using cystein as a reductant when expressed in a heterologous system (Blee et al., 2001), which provides further support for this model. Furthermore, inoculation of barley with strains of powdery mildew induces the transcription of a secreted peroxidase (Gregersen et al., 1997). The extracellular oxalate oxidase (germin), which produces H_2O_2 and CO_2 from oxalate, has also been implicated in the oxidative burst of cereals as it is strongly activated in wheat and barley in response to attack by pathovars of *Erysiphe graminis* (Dumas et al., 1995, Zhang et al., 1995). However, unlike the phase II AOS production observed in elicited cell suspensions of soybean and tobacco, production of H_2O_2 resulting from activation of germin was observed in both resistant and susceptible cultivars (Hurkman and Tanaka, 1996). Together, these results suggest that mechanisms involved in both the initiation and the production of oxidative burst AOS in plant pathogenesis vary with the host-pathogen system.

1.2.3 Functions of the oxidative burst

The production of AOS in the oxidative burst is thought to influence many aspects of plant defense. The simplest aspect, which plays a central role in the oxidative burst of phagocytes, is the direct anti-microbial activity of AOS. In plants, the energy contained in AOS such as H_2O_2 is also used by the attacked tissue to create physical barriers, slowing pathogen invasion by oxidative cross-linking of cell wall proteins. In both plant and animal systems, AOS is proposed to function in signaling pathways involved in the activation of antioxidant and cell death genes, as well as in the systemic acquired resistance in plants.

1.2.3.1 Direct antimicrobial activity

One of the major functions of the oxidative burst is proposed to be the direct killing or weakening of the invading microbe by oxidative damage. The cytotoxic effects of various AOS have been discussed in detail (see 1.1.1). Although oxidative killing of bacteria has been well documented in the respiratory burst of phagocytes, it should be taken into account that the phagocytosis of particles prior to AOS production allows the accumulation of lethal AOS concentrations within the phagosome; this may not be the case in plant/pathogen interactions, in which the AOS is released into the apoplast (Baker and Orlandi, 1995). While physiological H_2O_2 concentrations are able to kill pathogenic *Pseudomonas* species at low inoculum densities (Baker et al., 1997), and the inhibitory effect of superoxide and micromolar concentrations of H_2O_2 on the germination of fungal spores has been reported (Peng and Kuc, 1992, Ouf et al., 1993), the concentrations of hydrogen peroxide achieved by the oxidative burst (0.01-1 mM) are not able to inhibit growth of *Cladosporium* germ tubes (Lu and Higgins, 1999). Although experiments showing the ability of physiological concentrations of superoxide and hydrogen peroxide to directly kill or weaken fungi and bacteria *in vitro* are few, much

indirect evidence has been put forth to support this hypothesis. For instance, addition of antioxidants to tobacco cell suspensions is reported to increase survival rates of *Pseudomonas* (Keppler and Baker, 1989) and transgenic potato expressing H_2O_2-producing glucose oxidase is more resistant to pathogenic strains of *Erwinia* and *Phytophthora* (Wu et al., 1995), while lower levels of antioxidant enzymes correlates with higher cultivar resistance in bean (Buonaurio et al., 1987). However, the problem of observations *in vivo* is that oxidant function other than antimicrobial activity (see below) may be responsible for the documented effects.

1.2.3.2 Oxidative cell wall alterations

In 1992, Bradley et al. showed that fungal elicitors initiate the oxidative cross linking of hydroxyproline-rich structural proteins of the bean and soybean cell wall within 2-30 min of elicitation. This reaction, which was only observed in incompatible interactions, could be blocked by antioxidants such as catalase and mimicked by exogenous H_2O_2. Similar findings were reported by many other investigators, including Brisson et al. (1994) for bean leaves inoculated with incompatible strains of *Pseudomonas*, Wojtaszek et al. (1995) for French bean and Otte and Barz (1996) for chickpea. These findings have led to the postulation that one of the major functions of the oxidative burst is to provide H_2O_2 for the oxidative cross-linking of pre-existing cell wall proteins; this results in the immediate slowing of pathogen ingress, giving the plant time to muster longer-termed (transcription-based) defenses such as phytoalexin production. Oxidative cross-linking could be mediated by apoplastic peroxidases, one of the possible sources of oxidative burst H_2O_2, in a process similar to that found in normal cell wall polymerisation processes in plants (Iiyama et al., 1994). Cross-linking of cell wall proteins similar to that induced by the pathogen could be obtained *in vitro* using horseradish peroxidase (Otte and Barz, 2000).

In barley attacked by the powdery mildew fungus, an important component of resistance is the formation of cell wall appositions (papillae) directly under attacking hyphae (Carver et al., 1996, Hückelhoven and Kogel, 1998). Although no temporal link could be found between papillae formation and the oxidative burst in infected barley leaves (Hückelhoven and Kogel, 1998), the authors detected AOS by staining with nitro blue tetrazolium (NBT), which is able to detect superoxide, but not hydrogen peroxide. More recent experiments in the same pathosystem showed an accumulation of H_2O_2 which coincided with the formation of papillae, although no corresponding peroxidase activity could be measured (Vanacker et al., 2000). This agrees with the results of Hückelhoven and Kogel (1998), in suggesting that the generation of H_2O_2 is not dependent on superoxide, as is that of peroxidases. Similar phenomena to that observed in the barley/powdery mildew system have been documented for interactions involving potato and *Phytophthora infestans*, where front-line defense of leaf epidermal cells included erection of an cell wall apposition containing phenolic substances and callose in both compatible and incompatible strains (fig. 1.3). Subsequent defense reactions depended on the ability of

the fungus to penetrate the barrier (Freytag et al., 1994). The pathogen *Puccinia coronata* (rust fungus) induced cell wall alterations in barley leaves which probably involve the oxidative cross linking of feruloyl residues (Ikegawa et al., 1996) and the fungal elicitor cryptogein induces a drastic reduction of the digestibility of tobacco cell walls which can be partially blocked by inhibitors of the oxidative burst (Kieffer et al., 2000). Pathogen-induced cell wall alterations can involve lignification, as seen in the interaction between *Puccinia graminis* and wheat. Lignification is also an oxidative process involving H_2O_2 and apoplastic peroxidases. Not only does the erection of lignified barriers physically slow pathogen ingress but it also decreases the diffusion of water, nutrients and signal molecules between host and pathogen (Elstner et al., 1996).

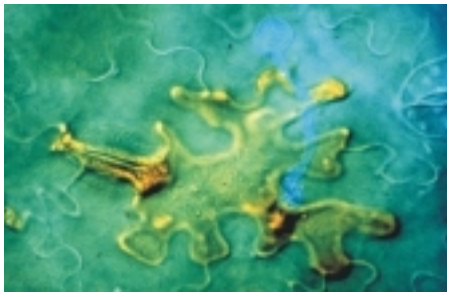

Fig. 1.3: Papilla formation in a potato leaf epidermal cell under attack by a *Phytophthora infestans* germling (blue fluorescent staining). The defense response of the plant cell includes morphological changes: dark brown papilla at the penetration site, brownish coloration and thickened cell wall. Photo taken from http://www.mpiz-koeln.mpg.de/~schmelze/potHRpub2a.gif.

1.2.3.3 AOS in gene activation during plant defense

In animals, H_2O_2 functions as a pleiotropic activator of genes involved in the immune and inflammatory response; in some cases, induction is mediated by redox-sensitive transcription factors such as AP-1. AP-1 homologues (yAP-1s) have been found in yeast (Schnell et al., 1992, Toone and Jones, 1999). Similar mechanisms may be involved in the plant defense response as an important proposed function of AOS in the oxidative burst is the induction of defense-related genes, in particular genes involving the biosynthesis of phytoalexins and the triggering of hypersensitive cell death (see below). In soybean, exogenous H_2O_2 resulted in the increased transcription of genes involved in the synthesis of phytoalexins, while elicitor induced transcription could be inhibited by addition of catalase (Apostol et al., 1989). Similarly, addition of SOD inhibitors decreased elicited phytoalexin production in potato (Doke et al., 1983). Although similar observations have been reported in different systems, transcriptional induction of phytoalexin biosynthesis genes are not always effected by oxidants or scavengers (Devlin and Gustine, 1992, Sasabe et al., 2000), suggesting AOS-independent mechanisms of defense gene transcriptional induction. The oxidant-mediated induction of genes involved in oxidant scavenging, especially members of the glutathione cycle such as glutathione-S-transferase (GST) and glutathione peroxidase (GPx), seems to be a more universal mechanism (Mehdy, 1994, Baker and Orlandi, 1995, Lamb and Dixon, 1997). That H_2O_2 functions as a diffusible signal molecule has been implied by several experiments (Levine et al., 1994, Chamnongpol et al., 1998). Although the short half-life and difficulty in crossing membranes renders superoxide a less likely candidate for a diffusible signal molecule, Delledone et al. (2001), report that the GST activator of soybean is superoxide. *In vivo* experiments in which the effects of exogenous oxidants on gene transcription are examined do not take into account that products of AOS damage, such as lipid peroxides, are equal candidates as mediators

of gene expression; for instance, production of soybean phytoalexins can be induced by fatty acid hydroperoxide (Degousée et al., 1994). Furthermore, jasmonic acid, which induces the expression of defense related genes (Reymond and Farmer, 1998), can be synthesised from lipid peroxide precursors. It may be that the ratio of cellular GST to GSSG is more important for gene activation than any single AOS (Mehdy, 1994). However, the relative stability and membrane permeability of H_2O_2, as well as its copious generation in the apoplast during the oxidative burst suggests that possible signaling functions, whether direct or indirect, are not only of interest for the host cells but may also alter gene expression in the pathogen.

1.2.3.4 Hypersensitive response

Both non-host and pathovar incompatibility are associated with the hypersensitive response (HR), which denotes a series of physiological mechanisms resulting in the death of an area of barricaded tissue immediately surrounding the site of infection and the death of biotrophic pathogens trapped within. The involvement of oxidative burst AOS in triggering and/or causing the death of cells in the HR is the subject of much discussion. The actual cause of death in cells undergoing the HR is controversial and may vary in different pathogen-host systems; while in some interactions typical signs of genetically induced cell deconstruction (apoptosis) such as blebbing of plasma membranes, DNA processing, and the presence of apoptotic corpses (shrunken cytosol remnants containing intact organelles) have been observed (Dangl et al., 1996), other interactions show cells undergoing the rapid disintegration, swelling and DNA degradation devoid of discreet processing intermediates which are typical signs of necrotic death (Gilchrist, 1998). AOS have been implicated in both necrotic and apoptotic cell death; although the extent and mechanism of the latter is still ambiguous (Clutton, 1997, Simon et al., 2000). Some evidence indicates that AOS is the direct mediator of the HR in soybean cell suspension cultures: elicited HR can be blocked by AOS-scavengers while treatment of cells with oxidants can induce it without elicitation (Lamb and Dixon, 1997). The creation of *Pseudomonas* mutants which fail to induce the HR despite eliciting the normal biphasic oxidative burst in tobacco cells (Glazener et al., 1996) contradicts these findings. Furthermore, the phase I burst of AOS resulting from compatible interactions, which in certain cases can produce levels of AOS comparable to those produced during phase II, is not able to invoke the HR; as is the strong oxidative burst caused by addition of heat-killed bacteria (Baker and Orlandi, 1995). Similar evidence against AOS as direct mediators of the HR is shown by superoxide staining of different resistant cultivars of barley infected with powdery mildew; although both cultivars in which the penetration of fungal hyphae was prevented by cell wall appositions did not undergo oxidative burst; one of these two strains underwent the hypersensitive response, showing that the HR can be detached from AOS (Hückelhoven and Kogel, 1998). Recent experiments implicate the involvement of nitric oxide (NO) in the signal cascades leading to plant cell death. In soybean, the interaction of H_2O_2 and nitric oxide is required for the induction of cell

death (Delledonne et al., 2001). Beligni and Lamattina (1999) suggest a dual role for NO, acting as an oxidative cell death potentiator in higher concentrations and a mediator of signals in lower concentrations, much as is postulated for hydrogen peroxide (Levine et al., 1994).

1.2.3.5 Other functions of the oxidative burst

The alkalisation of the plant cell protoplast is one of the most rapid responses to pathogen attack (Nürnberger et al., 1994, Wojtaszek, 1997.) It could decrease activity of cell wall degrading enzymes secreted by the pathogen, some of which are known to have acidic pH optima (ten Have et al., 2002). Although elicitation alters membrane permeability, causing influx of H^+ and Ca^{2+} (as well as efflux of Cl^- and K^+), the protonation of superoxide in the dismutation reaction which produces H_2O_2 is also thought to contribute to the rise in apoplastic pH (Otte et al., 2001).

Active oxygen species have been implicated in salicylic acid (SA)-mediated systemic acquired resistance (SAR), which describes non-specific resistance shown by plants after pathogen-induced HR. Exogenous application of salicylic acid is able to induce both SAR and the transcription of defence genes (Raskin, 1992), while plants which express an SA-degrading enzyme and are unable to accumulate SA do not show SAR after pathogen attack (Gaffney et al., 1993). The discovery that salicylic acid is able to bind to and inhibit catalase activity first led to the proposal that SAR was the result of higher levels of H_2O_2, which could diffuse as a second messenger within the plant and activate transcription of defense genes. (Chen et al., 1993). However, examination of H_2O_2 levels in plants undergoing SAR, as well as the discovery that H_2O_2 treatment alone was not able to induce SAR has weakened this hypothesis (Hunt et al., 1996). Further experimental evidence indicates that salicylic acid acts downstream of H_2O_2; for instance, treatment of plants with cytotoxic levels of hydrogen peroxide leads to accumulation of SA (Hunt et al., 1996); in tobacco this is thought to be due to the H_2O_2-mediated induction of an enzyme which releases salicylic acid from benzoic acid (Leon et al., 1995). Furthermore, SA accumulates in cells undergoing hypersensitive cell death, where it is thought to potentiate cell death (Shirasu et al., 1997). The exact mechanism of SA in SAR is still unclear (Cameron, 2000). In *Arabidopsis,* systemic micro-lesions are formed almost simultaneously with the oxidative burst in the course of incompatible interactions; both involve the participation of AOS and are prerequisites for SAR (Alvarez, 2000).

The functions which oxygen toxins are thought to fulfil in the interactions between plants and their pathogens, described in detail in the last sections, are summarised in schematic form (fig. 1.4).

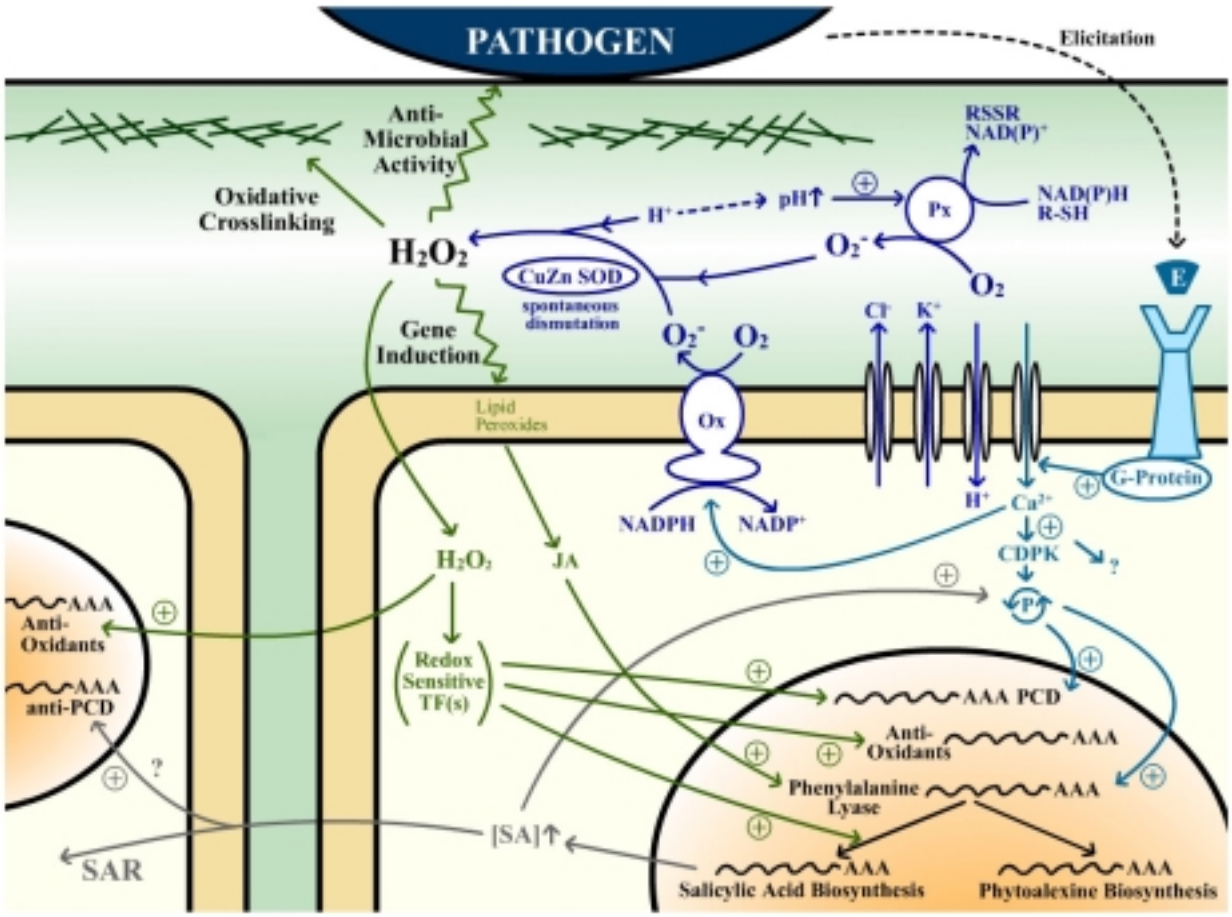

Fig. 1.4: Summary of AOS-involvement in plant-pathogen interactions. This information has been compiled from the results described for several different systems, described in detail in section 1.2. It is not meant to depict the reactions of any single system, but serves rather as an overview of some possible sources of and functions of active oxygen during pathogenesis. For the sake of simplicity, this picture, which leans heavily on those provided in Mehdy, 1994, and Lamb and Dixon, 1997, includes only hydrogen peroxide and superoxide and groups some pathway components by colour. The plant apoplast is shaded green, the membrane and protoplast of the host cell are orange. CDPK: Calcium-dependent protein kinase, E: elicitor, JA: jasmonic acid, Ox: oxidase, P: protein kinase (arrows indicate reversible phosphorylation), PCD: programmed cell death, Px: peroxidase, R-SH/ RSSR- thiopeptide reductant, SA: salicylic acid, SAR: systemic aquired resistance, TF: transcription factor. Curved lines tailed with AAA represent eucaryotic mRNA.

1.3 *Claviceps purpurea*

The fungal genus *Claviceps* comprises biotrophic parasites of more than 600 different members of the grass family, including such economically important species as rye, barley, wheat, oat and millet (Bove, 1970). Of the 30-36 species comprising the *Claviceps* genus (Taber, 1985), the species *Claviceps purpurea* is the most widely known in Europe, infecting at least 400 types of grasses with the disease known as ergot, derived from the French word for spur ("argot"). The name refers to the dark structures protruding from the ripe grass ear in the final disease stages (fig. 1.5). These structures, called sclerotia, contain a wide variety of

Fig. 1.5: Ergot-infected rye. Picture taken from: http://www-vetpharm.unizh.ch/jpg/pflanzen/0021_01b.jpg

physiologically active alkaloids which give ergot its significance; farmers fear the disease as even minimal contamination (0.3%) of seed with sclerotia can render the grain too poisonous for use (Agrios, 1988), and a considerable commercial interest is sparked by their effects on the mammalian vascular and nervous systems (Tudzynski et al., 2001).

1.3.1 Pathogenesis on rye

The life cycle of *Claviceps purpurea* (a brief depiction is provided in fig. 1.6) begins in the spring,

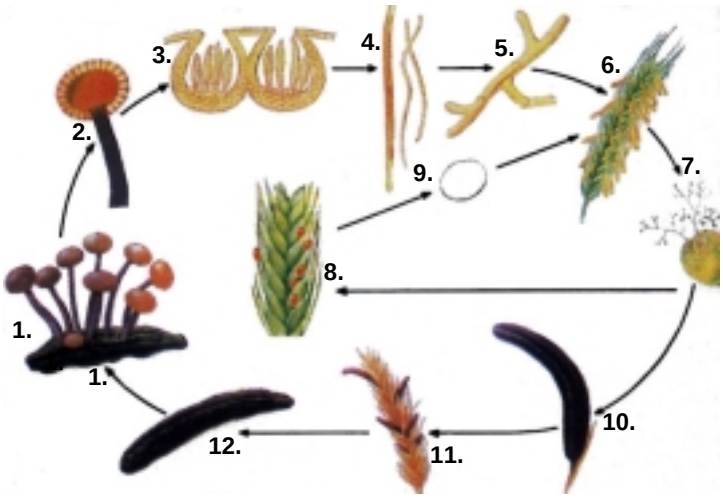

Fig. 1.6: Life cycle of *Claviceps purpurea.* In spring, the homothallic sclerotia germinate (1) and build the telomorph, which constists of stalked stroma (2) containing perithecia embedded in their periphery (3); there, caryogamy and meisosis give rise to needle like ascopores (4) which are carried by the wind to the pistils of their fluorescent host grasses, where they germinate (5,6). The fungus penetrates the pistil and grows down to the base of the ovary, where it extends hyphae into the vascular bundles, taking up the nutrients brought there for the ovule. Fungal growth does not extend beyond the ovary base and a stable host-parasite interface is established there. After about six days, the ovary is colonised and mycelia which break through the surface (7) produce conidia which are given up into a thick sugary fluid secreted simultaneously by the fungus. This fluid, known as honeydew (8), is the first macroscopic sign of infection on the rye ear. Insects attracted by the honeydew spread conidia to other plants (9), creating secondary infections. After conidiation (about 11 days post infection), the hyphae differentiate into lipid-rich sclerotial mycelia which ripen over a period of several weeks to the darkly pigmented sclerotia (20). The sclerotia, which protrude from the floral remnants in place of the seeds (11) and contain a variety of poisonous alklaoids, fall to the ground where they remain dormant throughout the winter (12). See text for details. Drawing taken from Agrios (1988).

when sclerotia germinate to form a number of stroma, consisting of stalks topped by spherical capitula which represent the teleomorphic stage of this homothallic fungus. In the periphery of the capitula, male antheridia and female archegonia are formed; fertilised archegonia develop into flask-shaped perithecia, which remain embedded in the capitula. The ascogenous hyphae give rise to needle-like ascospores; after forcible ejection from the perithecia they are borne by the wind to the exposed florets of host grasses (Taber, 1985, Tudzynski et al., 1995, and Tenberge, 1999).

Only ascospores which land and germinate on the pistils of their hosts are able to cause disease, as they are unable to penetrate any other part of the plant (Swan and Mantle, 1991), and formation of external mycelium is limited. As the ascospores must access the pistil, the time window in which infection is possible is constrained to the flowering period of the host plant, while at all other times the gynoecia is tightly enclosed by protective glumes. Penetration, which follows without the differentiation of specialised infection structures (Tudzynski et al., 1995, Tenberge, 1999), can probably occur at any place on the surface of the pistil or ovary. If penetration has occurred along the style, the fungus follows the pollen path around the ovule, whereas mycelia which has entered via the ovary wall grows

laterally through the carpal mesophyll; both routes directly target the ovary base which contains the vascular tissue (fig. 1.7) (Tudzynski et al., 1995, Tenberge, 1999). The vascular tissue is reached about 3 days post inoculation (dpi) (Luttrell, 1979); until this time, although some intracellular growth has been reported (Tenberge and Tudzynski, 1994), fungal growth is largely intercellular, fuelled by cell wall components and not affecting the host protoplasts in the ovary wall. After 4 dpi, this gentle mode of growth disappears as the hyphae proliferate rapidly throughout the ovary wall, replacing the plant tissue. During this time, the ovule within its protective integula remains untouched as fungal hyphae grow outwards, collecting under the ovary surface until it bursts (Luttrell, 1979).

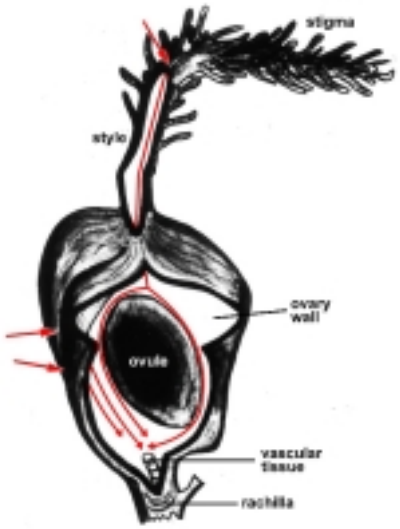

Fig. 1.7: Targeted growth of *Claviceps purpurea* in the rye ovary. Explanation in text. Drawing taken from Tenberge, 1999.

Fungal growth does not extend beyond the vascular tissue at the ovary base; instead, an interface between host and pathogen is formed there which is completed by about 6 dpi. In this interface, hyphae amass to a fungal foot which surrounds the vascular bundle in the rachilla, and contains a core of cells which extends intracellularly into phloem and xylem cells of the vascular bundle. In this way, the nutrient supply of the developing ovule, which has been separated from the vascular traces by the fungal foot, is usurped by the fungus (Luttrell, 1979, Tudzynski et al., 1995). The completion of the host-pathogen interface, which remains stable throughout the entire interaction, coincides with the appearance of honeydew on the ovary surface (Tudzynski et al., 1995). Plant sucrose taken up by the fungal foot are converted to a variety of sugars (mostly glucose, fructose and fructose oligosaccharides) and sugar alcohols (Mower and Hancock, 1975a) and exuded from the mycelia covering the ovary surface as honeydew. The external mycelia forms a superficial layer of phialidic conidiophors, which offer a succession of oblong conidia (Luttrell, 1979) into the surrounding honeydew. This viscous, sugar-rich substance serves the growing fungus as a food source, helps the establishment of a differential osmotic potential to increase the supply of further plant assimilates (Mower and Hancock, 1975b) and is crucial for the propagation of secondary infections. Although the sticky substance can spread the spores to neighbouring ears during head to head contact and can drip down to infect underlying florets, the most important propagators of secondary infection are insects, attracted by the sweetness of the honeydew (Tudzynski et al., 1995, Tenberge, 1999). Disease spreading via secondary infection is of utmost importance to *Claviceps* as it compensates for the time limitations imposed on primary infections.

After the establishment of a stable biotrophic relationship between host and fungus at about 6 dpi, the latter consumes the entire ovary including the ovule, replacing the plant tissue with loosely packed,

plectenchymatous sphacelial hyphae which are generated intercalarly from the fungal foot (Tulasne, 1853, Tudzynski et al., 1995); the sphacelial phase lasts until conidial sporulation is complete, after about 11 dpi (Tudzynski et al., 1995). At this time, the hyphae begin to differentiate into sclerotial tissue; this involves morphological as well as physiological changes: the hyphae develop a purple pigmentation and become interspersed with short, thick, bulbous and highly septate regions (Shaw and Mantle, 1980); physiological changes include decreases in RNA, malate, polyols and phosphate (Corbett et al., 1974), a massive accumulation of triglycerides, the biosynthesis of alkaloids and the respiration of lipids instead of sugars (Taber, 1985). Mycelia formed by the differentiation of sphacelial to sclerotial hyphae as well as that which is newly generated by the fungal foot gradually develop into a region of densely packed, longitudinally organised hyphae which forms the young sclerotium (Shaw and Mantle, 1980), conspicuous as early as 13 dpi (Luttrell, 1979). Ripening takes place over a period of about 4 to 5 weeks as the sclerotium elongates by proliferation of cells at the fungal foot (Shaw and Mantle, 1980), and the rind hardens and darkens to a purplish-black. The mature sclerotium, which protrudes conspicuously from the ripe ear, measures a few millimetres across and as much as 5 cm in length (Tenberge, 1999) and contains 30-50% triglycerides as well as up to 0.5% of its dry weight in alkaloids (Taber, 1985).

1.3.2 Ergot alkaloids of sclerotia

Consumption of ergot sclerotia causes ergotism, a malady with symptoms including gangrenous extremities, convulsions, madness and death. Ergotism had its heyday in the middle ages, when the disease (usually caused by eating contaminated rye bread) affected many thousands of people, resulting in the creation of an order to care for the afflicted, the patron saint of which is St. Anthony. The burning sensation experienced by the sufferers of ergotism led to the alternative name St. Anthony's fire. The symptoms of ergotism arise from the structural similarity between ergot alkaloids and neurotransmitters such as dopamine, noradrenaline and serotonine. As interactions with the receptors of these transmitters can be both agonistic and antagonistic, ergot alkaloids cause a wide variety of physiological effects involving the peripheral and central nervous system including contraction of smooth muscle cells, such as those in blood vessels and the uterus, as well as hallucinations (Řeháček, 1984, Tudzynski et al., 2001). The most notorious ergot alkaloid is indubitably lysergic acid, as addition of a diethylamide gives LSD (Hoffman, 1972). The broad-based toxicity of these compounds makes them interesting objects for the pharmaceutical industry, which exploits them for treatment of migraine and post-partum bleeding, as well as a number of neurodegenerative disorders (Tudzynski et al., 2001).

All ergot alkaloids are indol derivatives based on the tetracycline ergoline ring system (fig. 1.8, I). Typically, the N-6 is methylated and the C-8 is substituted with a methyl-, hydroxymethyl- or car-

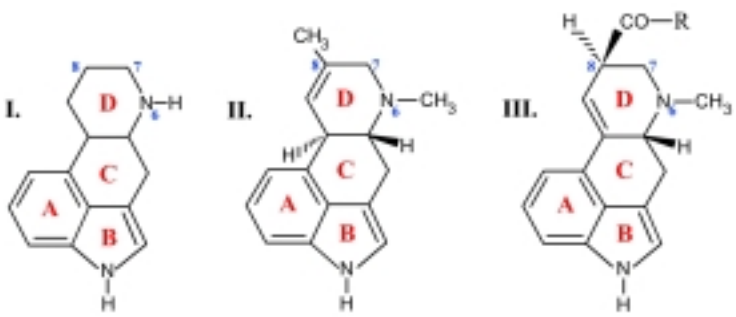

Fig 1.8: Structures of ergot alkaloids: I. ergoline: the tetrapyrol indol-derivate on which all ergot alkaloids are based II. agroclavine: the simplest example of a clavine; C-8 carries a methyl-group III: lysergic acid derivatives (in lysergic acid, R=OH); typically, this acid is bound to the amide of a short peptide or amine alcohol.

bonyl- group. The ergot alkaloids can be divided into two major groups. The first group are the clavines (as an example, agroclavine is shown in fig. 1.8, II), which carry simple substituents such as methyl- and hydroxymethyl-groups on C-8 (some carry additional hydroxyl groups on C-7 and C-8); these are intermediates for the second and more complex group of alkaloids, the lysergic acid derivatives (see fig. 1.8, III; in lysergic acid, R=OH). In the latter, the carbonyl-moiety at position 8 is attached to an amide; typically, the amide is part of a tripeptide (which is cyclic in the ergopeptines and non-cyclic in the ergopeptams) or an amino alcohol (such as ergometrine) (Keller, 1999).

Although ergoline-based alkaloids were first discovered in *Claviceps*, similar compounds have been isolated from grass endophytes of the Clavicipitaceae family (Schardl, unpublished) as well as from non-related fungi such as *Aspergillus* and *Penicillium* and from members of the Convolvulaceae family of plants (Vining, 1973). In the natural life cycle of *Claviceps*, alkaloids are found exclusively in the sclerotia (Ramstad and Gjerstad, 1955), where the content varies from 0.01 to 0.2% w/v (Tudzynski et al., 1995, Young and Chen, 1982). Large variations in alkaloid content can be observed even in sclerotia on the same ear; in one study, Young and Chen (1982) report a fifty-fold variation. Generally, alkaloid content of sclerotia is highly unpredictable, varying with infecting strain, weather, soil and host plant (Taber, 1985). No correlation could be found between the amount of sclerotial alkaloids and virulence of *Claviceps* strains (Békésy, 1956).

In order to escape the environmental uncertainties and limited harvests involved in the *in planta* cultivation of sclerotia for industrial production, most modern production methods involve axenic cultivation in fermentors. Due to its short stint as a saprophyte in its life cycle (see fig. 1.6), *Claviceps* is a hemibiotroph (Tenberge, 1999) and is easily grown in axenic culture. However, most wild-type isolates do not produce alkaloids in axenic culture (Mantle and Tonolo, 1968, Taber, 1985) and poorly sporulating mutant strains are used for mass production (Soĉiĉ and Gaberc-Porekar, 1992), which can yield as much as 20% alkaloid per dry weight (Řeháček, 1984). Induction of alkaloid production in culture is usually done by taking mycelia formed during rapid growth in a rich medium and subjecting it to conditions which facilitate slower growth, usually by phosphate exhaustion (Vining, 1973). This corresponds to the *in planta* conditions at the time of differentiation from sphacelial to sclerotial tissue: high sucrose and low nitrogen and phosphate reflect the use of phloem sap as a food source in

comparison to the metabolite-rich ovary tissues (Tudzynski et al., 2001). In axenic culture, as *in planta*, a morphological differentiation of hyphae from the filamentous sphacelial type to the pigmented, lipid-rich, thick and bulbous sclerotial type can be observed. While alkaloids are produced only in sclerotial hyphae, even non-producing wild-type isolates demonstrate this morphological switch under conditions of stress (Kirchhoff, 1929). Although intense investigation into the molecular genetics behind the synthesis of ergot alkaloids has unearthed a cluster of genes involved in biosynthesis (Tudzynski et al., 1999), the forces which govern their regulation are not completely understood.

1.3.3 The molecular biology of parasitic growth

The molecular mechanisms involved in the pathogenesis of *C. purpurea* have been intensely investigated in its interaction with rye (*Secale cereale*). This research is built on two basic approaches which differ in their selection of potential pathogenicity factors for analysis. Firstly, potential pathogenicity factors (such as signaling components, hydrophobins and cell wall degrading enzymes) are selected on the basis of existing knowledge about the infection process in this and other phytopathogenic systems. Secondly, random sequencing of a parasitic EST library provides information about the transcriptome of the infecting fungus, from which new potential pathogenicity factors may be drawn. Genes of interest are isolated and disrupted to determine their importance for the interaction. Expression studies in axenic culture and *in planta*, as well as accompanying cytological analysis, help to decipher the function of the selected genes.

1.3.3.1 A short summary of past results and present research

The absence of specialised infection structures (used to build up turgor pressure for penetration) as well as the largely intracellular pathway of *Claviceps* as it grows towards the vascular tissue indicates that secretion of cell wall degrading enzymes (CWDE) is likely to be crucial for parasitic development. After cytological analysis has indicated the depletion of the corresponding substrate in the ovary during pathogenesis, several genes encoding CWDEs have been isolated and disrupted. Important candidates as pathogenicity factors are cellulases, xylanases and pectinases, which degrade β-1,4-polyglucanopyranoses, β-1,4-polyxyloses and α-1,4-polygalacturonates, respectively. Although disruption of a putative cellulose-degrading cellobiohydrolase did not affect pathogenic development (Müller, 1997), the double-disruption of two xylanases caused a slight delay in pathogenesis (J. Scheffer, P. Heidrich, S. Giesbert, B. Oeser and P. Tudzynski, unpublished). In both cases, it is thought that similar enzymes are able to compensate for the missing activities. Recently, the simultaneous inactivation of two endopolygalacturonases was shown to have an important impact on virulence, as these mutants are almost completely unable to infect rye (Oeser et al., 2002); this is an unexpected result as pectins play less of a structural role in the cell walls of monocots as compared to di-

cots. A further interesting object of study is the β1,3-glucanase which is presumed to be involved in the degradation of vascular callose, allowing a more efficient exploitation of host phloem sap (Brockmann et al., 1992, Tudzynski et al., 1995). Although ample immunological evidence has been provided for this theory (Tenberge, 1999), more evidence awaits the isolation and disruption of this gene.

Since disruption of the hydrophobin (small secreted fungal proteins capable of forming an amphipathic polymer on the surfaces of aerial structures) MPG1 in *Magnaporthe grisea* resulted in a decreased ability to form appressoria (Talbot et al., 1996), hydrophobins have been considered putative pathogenicity determinants. Hydrophobic interactions between the cuticle of the host plant and fungal penetration structures are thought to influence signal interchange between host and pathogen (Talbot et al., 1996). In *C. purpurea*, a novel protein encoding five adjacent hydrophobin units, dubbed the pentahydrophobin CPPH1, was isolated, disrupted and shown to have no effect on pathogenicity (G. Mey, pers. comm.). Analysis of a similar oligomodulic (tri-)hydrophobin in *C. fusiformis* showed that the mature protein was not processed into single units (De Vries et al., 1999), indicating that this hydrophobin may be involved in different aspects of fungal growth than the monohydrophobin MGP1.

Another area of research which is rapidly expanding concerns components of the signal chain pathway. Disruption of genes encoding high-hierarchy signaling molecules, such as the MAP-kinases, allows the inactivation of a broad spectrum of genes at once, increasing the probability of finding a virulence-altering phenotype. In *M. grisea*, two MAP-kinases, MPK1 and MPS1 have been shown to be essential for pathogenicity in rice (Xu and Hamer, 1996, Xu et al., 1998); two homologous genes have been isolated and disrupted in *C. purpurea*. Both types of mutants are unable to infect rye, and, interestingly, are able to complement the corresponding mutants in *M. grisea* despite considerable differences in the infection strategies of the two pathogens (Mey et al., 2002a and b). The challenge which now arises from the creation of such broadly-disturbed mutants is the identification of underlying signal components as well as their target genes. Investigation of signal transduction components also focuses on those which involve directed growth, an area of research particularly suited to *Claviceps* as its pathogenesis involves the unique single-minded targeting of a small area of tissue, the ovary vascular bundles.

An EST-library was established from parasitically growing *C. purpurea*; sequencing of these clones unveiled a number of interesting genes. Hybridisation with the transcriptome of different infection phases allowed the temporal classification of some these genes (Oeser et al., 2001). A number of genes expressed in the first stages of infection, such those which encode the putative transcription factors CPTF1 and CPTF2, as well as a number of genes which show no homology to other sequenced genes, are interesting focal points for further research.

1.3.3.2 Implications for the involvement of AOS in pathogenesis

The involvement of AOS in the host-parasite interactions is, as described in section 1.2, a general phenomenon which has been observed in many systems. The main focus of AOS research in plant pathology centres around the hypersensitive response, which is an important factor in the determination of interaction compatibility. Although ovary necrosis has been documented after staggered inoculation of wheat with two different strains of *C. purpurea* (Swan and Mantle, 1991), the ability of incompatible *Claviceps* strains to invoke the HR has not been reported. In contrast, *C. purpurea* has a tremendous range of potential hosts, encompassing more than 600 grass species. It has been suggested that the ovary, which is the only plant organ this fungus is naturally able to colonise, is not likely to evolve a HR as genetic elements involved in the triggering and implication of cell death can not be passed on to the next generation (Tenberge, 1999). However, AOS are involved in many aspects of host defense, such as antimicrobial activity and the construction of cell wall barriers, which can be detached from the HR. Pathogen-induced cross-linking of phenolic compounds has been observed in the rachilla of rye ovaries (A. Hambrock, K. Tenberge and P. Tudzynski, unpublished observations) which are the site of the host-pathogen interface; the erection of physical barriers, which in barley and many other plants are correlated with oxidative processes, may participate in the restriction of fungal growth beyond this point. Ovaries are sites of intense ontological development which involve the production of AOS, for instance in the lignification process. Cytological analysis of rye ovaries shows intensive staining for hydrogen peroxide and superoxide (K. Tenberge and M. von den Driesch, unpublished data). As *Claviceps* must confront these toxins in the course of ovary colonisation, the possession of AOS scavenging enzymes could be an important requirement for virulence. Although the ability of H_2O_2 to diffuse through membranes could render intercellular AOS-scavengers crucial for survival, front-line fungal defense against oxygen toxins will probably involve secreted detoxification systems. Protein analysis of axenic and parasitic cultures of *Claviceps* shows that this fungus does secrete AOS scavenging enzymes such as catalases and SODs.

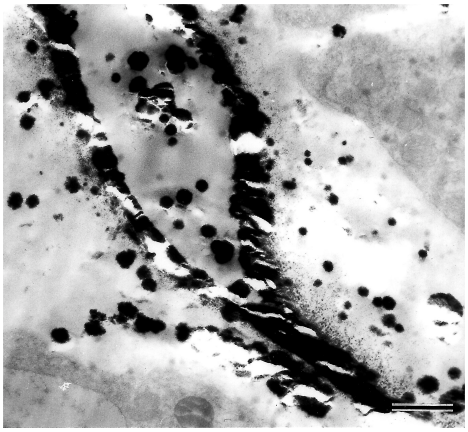

Fig. 1.9: *In situ* localisation of H_2O_2 in non-infected rye ovaries using $CeCl_3$. Massive precipitation of cerperhydroxide indicates the presence of H_2O_2 in the cell walls between differenciating xylem cells of the ovary rachilla. This picture is kindly provided by K.B. Tenberge

Activity staining for catalases following gel electrophoresis of crude protein extracts shows that *C. purpurea* expresses at least four catalase isoforms, dubbed CATA-CATD. CATA, produced in parasitic and axenic culture, is always associated with the mycelia and is therefore thought to be of peroxisomal origin. CATB is also produced in both culture types and can be isolated both from myce-

lia and the culture filtrate, indicating that this catalase is associated with the cell wall. CATC and CATD, found in axenic culture filtrate and in honeydew, respectively, are secreted (Garre et al., 1998a). Genomic library screening with a gene encoding a secreted catalase from *A. niger* (CatR) led to the isolation of *cpcat1*, which encodes a large (ca. 700 aa) catalase containing a signal peptide for secretion. Targeted inactivation of this gene led to the loss of both CATC and CATD activities, indicating that both isoforms were encoded by the same gene (Garre et al., 1998b). Although virulence of mutants lacking functional *cpcat1* was unchanged on rye in comparison to the wild type, the cell wall associated CATB activity may be able to compensate for lack of CATC/D (Garre et al., 1998b).

As many sources of oxygen toxins have their root in the production of superoxide, and enzymatic AOS scavenging systems such as peroxidases and catalases break down hydrogen peroxide, the SOD is an important component of the anti-oxidant arsenal. In an alkaloid-producing strain of the closely related sorghum parasite *Claviceps fusiformis*, N-terminal sequencing of proteins associated with the cell wall revealed a peptide fragment with strong homologies to Cu,Zn SODs (Moore, 1997). This discovery, representing the first indication for an extracellular SOD in a phytopathogenic fungus, indicated that *Claviceps* species are equipped with an entire extracellular arsenal of AOS scavenging enzymes, and strengthened the conviction that detoxification of oxidative toxins may be an important requirement of survival in the host ovary.

1.3.3.3 Focal points of research

A major focal point of research will be the investigation into "classical" AOS scavengers such as catalases and superoxide dismutases. Thus, the putative cell-wall associated Cu,Zn SOD homologue in *C. purpurea* will be characterised and an attempt will be made to locate and characterise new catalase genes. Furthermore, differential expression techniques will be employed in the search for new genes involved in the response to oxidative stress. Characterisation of genes includes sequencing of the genomic region, promotor analysis, *in vitro* and *in vivo* expression analysis, and where possible, visualisation of enzyme activities. The significance of the investigated genes for pathogenicity will be determined by assaying the virulence of targeted deletion mutants. This research should extend the knowledge of genes involved in the AOS response of *Claviceps purpurea* and further investigate their significance for survival during parasitic growth.

2 Experimental Procedures

Notes to experimental procedures:

1. The centrifuges used in the described experiments were as follows:

Eppendorf centrifuge 5417R	0.1-2 ml (Eppendorf tubes, etc.)
Sigma 202	2-12 ml (falcon tubes)
Sorval RC-5B Dupont	SS34 rotor 12-30 ml
Sorval RC-5B Dupont	GSA rotor 30-150 ml
Savant Speedvac	vacuum-accelerated drying of protein and DNA in Eppendorf tubes

2. The composition of media, and a list of chemicals, can be found in appendices D and C, respectively.

3. Buffer composition is given in the procedures.

2.1 Strains

2.1.1 *E. coli*

E. coli Top10F`	F[lac^{q}Tn10(tet^{R})], mcrA, Δ(mrr-hsdRMS-mcrBC), Φ80lacZ ΔM15, ΔlacX74, deoR, recA1, ara Δ139, Δ(ara-leu)7697, galU, galK, rpsL, endA1, nupG (Invitrogen).
E. coli XL1-Blue MRF´	Δ(mcrA)183 Δ (mcrCB-hsdSMR-mrr)173 endA1 supE44 thi-1.recA1 gyrA96 relA1 lac [F‘ proAB lacI^{q}ZΔM15 Tn10 (Tet^{r})].
E. coli LE392	F(-) hsdR514(r(-)k, m(-)k) supE44 supF58 lacY1 galK2 galT22 metB1 trpR55 lambda(-).

2.1.2 Claviceps

Claviceps purpurea T5	Field isolate from rye (Düvell et al., 1988).
Claviceps purpurea 20-1	Benomyl-treated T5 derivative. The DNA content is reduced by ca. ½ (Müller, 1997).
Claviceps purpurea P1	Alkaloid-producing strain 1029N5 (Keller, 1983).
Claviceps fusiformis	American Type Culture Collection (ATCC) strain 26245, originally of interest for its high production of clavine alkaloids and thought to be a strain of *C. purpurea*, was later identified as *C. fusiformis* (Pažoutová and Tudzynski, 1999).

Neurospora crassa	Allel V2M304, *nmr*1-deletion mutant; this strain was created in the lab of G. A. Marzluf, Ohio, USA.
Δcpsod1	*C. purpurea* 20-1-derived strain lacking *cpsod1* through homologous integration of the disruption vector pDV-1.
cΔsod1	Complemented strain of Δcpsod1 created by ectopic integration of vector $pComp1_a$.
cΔsod2	Complemented strain of Δcpsod1 created by ectopic integration of vector $pComp1_c$.
Δcpcat2	*C. purpurea* 20-1-derived strain lacking *cpcat2* through homologous integration of the replacement vector pRV-1.

2.1.3 Rye

All pathogenicity assays involved the use of *Secale cereale* cultivars Halo (Winterroggen) or CMS (Lo37-PxLo55-N; cytoplasmic male sterile) from F. von Lochow-Petkus GmbH.

2.2 Culture conditions

2.2.1 *E. coli*

E. coli were cultivated at 37°C and 180 rpm in LB-medium (Miller, 1972), and varied according to the required application:

1: for plasmid isolation by adding 80 mg/l ampicillin or 50 mg/l kanamycin (for isolation of pBK-CMV derivatives only).

2: *E. coli* LE392 (for the infection by EMBL-3 lambda phages) and *E. coli* XL1-Blue (for the infection with Stratagene lambda-ZAP-vectors) was cultivated by adding 0,2 % $MgSO_4$ (LBM or NZY) and 0,2 % maltose (LBMM).

E. coli were cultivated on solid media (LBM) overnight at 37°C. Recombinant clones were cultivated on media to which either ampicillin or kanamycin had been added, in the concentrations described above. X-Gal and ITPG (see 2.4.9.2) for blue-white screening of clones carrying first-time recombinant plasmids.

2.2.2 *Claviceps*

2.2.2.1 Cultivation of sporulating mycelia from *C. purpurea* (20-1)

To induce sporulation, mycelia of *C. purpurea* was cultivated on solid Mantle medium (MA) (Mantle and Nisbet, 1976) for ca. 12 d at 28°C.

2.2.2.2 Cultivation for protein, RNA and DNA analysis of *C. purpurea* (20-1)

Spores were taken up in sterile ddH_2O by rubbing the colony surface with a sterile pipette tip; mycelial remnants were filtered through sterile glass wool, and the spore concentration of the filtrate was determined by counting under a light microscope. 10^6 spores were routinely cultivated in 100 ml liquid medium in 300 ml Erlenmeyer flasks for 4 d at 28°C and 180 rpm. If not otherwise described, Mantle (MA) medium was used as a base. Inductive supplements for northern and protein analysis were added as described in section 2.6. Cultivation under conditions which can induce the production of alkaloid is described in the next section. Cultivation of mycelia for transformation and selection of transformants is described in section 2.8.

2.2.2.3 Cultivation for induction of alkaloid production in axenic culture

The non-sporulating *Claviceps purpurea* strain P1 was cultivated as follows: 1 ml of mycelia, ground in ddH_2O, was used to inoculate 50 ml InocN-medium in a 300 ml Erlenmeyer flask for initiation of the first preculture. This was then cultivated for 5 d at 24°C and 200 rpm, after which a second preculture was inoculated, using 1 ml of the first culture and otherwise the same conditions as described above. After 5 d the mycelia was collected by centrifugation for 20 min at 4°C and 6000 rpm. After washing the pellet once by resuspension in 50 ml ddH_2O and centrifugation as described above, the pellet was taken up in ddH_2O to a concentration of 0.1 g/ml. This was used as inoculum in the final culture: 5 ml were added to 50 ml of T25N-medium (with varying phosphate concentration) in a 300 ml Erlenmeyer flask and cultivated in the same manner as the pre-cultures for 5-7 d. Cultures in which the production of alkaloids were induced contained media with 0.5 g KH_2PO_4/l and were harvested after 5 d, while non-induced cultures contained 2.0 g KH_2PO_4/l, and were harvested after 7 d.

C. purpurea strain 20-1 was cultivated under conditions which induce alkaloid production in the strain P-1 with both 0.5 and 2.0 g KH_2PO_4/l, with the following modifications: only one pre-culture, inoculated with 200 µl of a concentrated spore solution, was implemented. The final culture was harvested after 5 and 8 d.

2.2.2.4 Cultivation of *C. fusiformis*

For the cultivation of *C. fusiformis* the following conditions were used: a ca. 1 cm^2 mycelial mat, which had been grown on solid MA, was finely ground in 500 µl medium and used to inoculate

100 ml aliquots of minimal medium (MM) in 300 ml Erlenmeyer flasks. The cultures were shaken for 6 d at 28°C and 200 rpm.

Unless described otherwise, *Claviceps* mycelia grown in liquid culture was harvested using a Büchner-funnel covered in a paper filter (Schleicher and Schuell 595) and sucked dry of medium using a vacuum. The mycelial mat was peeled off, frozen in liquid nitrogen and dried under a vacuum.

2.2.3 Rye

Seeds were germinated on moist paper for 5-6 weeks at 4°C. 4-5 young seedlings (about 2-3 cm in length) were then planted in a pot containing clay-rich soil and compost in a ratio of 3:2.

The seedlings were first cultivated at 9-10°C with a day phase (6 000-10 000 lx) of 9 h for vernalisation. Shoot extension was initiated by raising temperatures during the day (8 000 lx for 15 h) to 16-18°C and during the night to 13-15°C and increasing the length of the day phase; the plants were fertilised once a week. Under these conditions the rye began to bloom after 8-9 weeks.

2.3 Vectors, libraries and primers

2.3.1 Vectors

pBluescriptIISK⁻ (pBS) Stratagene phagemid vector used for the cloning of DNA fragments in *E. coli* (Short et al., 1988).

ZAP-Express® phagemid-containing vector used for the synthesis of the cDNA library (Stratagene).

pBK-CMV vector derived from excision of the ZAP-Express® phagemid (Stratagene)

pCR®2.1-TOPO® vector used for the cloning of PCR fragments in *E. coli* (Invitrogen).

pAN7-1 fungal transformation vector containing the hygromycin b phosphotransferase gene from *E. coli*, flanked by the glyceraldehyde-phosphate A (*gpdA*) promotor and the tryptophan C (*trpC*) terminator (hygromycin gene cassette), both from *Aspergillus nidulans* cloned into pUC-18 (Punt et al., 1987).

pOliHP fungal transformation vector containing the hygromycin resistance gene cassette from pAN7-1 cloned via *Sal*I/*Hin*dlll into pBS (Weltring, unpublished).

pAN8-1 fungal transformation vector containing the gene for a phleomycin-bleomycin binding protein (phleomycin resistance) from *Streptoal-*

loteichus hindustanus flanked by the *gpdA* promotor and the *trpC* terminator from *Aspergillus nidulans* (Punt et al., 1988).

pDVF1-4 *cpsod1* disruption vector consisting of a 756 bp PCR fragment amplified from λ S28/1 (T5 genomic library), cloned via pCR2.1-derived *Eco*RI sites into the corresponding site of pAN8-1.

pComp1$_a$ Δcpsod1 complementation vector containing a 5.0 kb *Sal*I/*Hin*dIII fragment of λS26/6 (T5 genomic library), with edges blunted by Klenow treatment, cloned into the *Eco*RV site of pOliHP. Orientation of the *cpsod1* gene and the hygromycin resistance gene is identical.

pComp1$_c$ Δcpsod1 complementation vector containing a 5.0 kb *Sal*I/*Hin*dIII fragment of λS26/6 (T5 genomic library), with edges blunted by Klenow treatment, cloned into the *Eco*RV site of pOliHP. The *cpsod1* and the hygromycin resistance genes are inversely oriented.

pRV-1 pAN8-1-based *cpcat2* replacement vector; the phleomycin cassette is flanked on both sides by identically oriented fragments of *cpcat2*, which were amplified from genomic DNA of *C. purpurea* strain 20-1: a 953 bp *Bgl*II and a 1052 bp *Xba*I, cloned into the corresponding sites of pAN8-1.

2.3.2 Libraries

T5 genomic library The library was constructed from genomic fragments of *C. purpurea* strain T5 which were not subjected to prior size fractionation, using EMBL-3 lambda phages (Smit and Tudzynski, 1992).

Cu-excess cDNA library: The library, containing cDNA-inserts of *C. purpurea* strain 20-1 derived from cultures challenged with 50 µM $CuSO_4$, was constructed in lambda-based ZAP-Express® phages from Stratagene which contain the pBK-CMV phagemid carrying kanamycin-resistance. See 2.5.1 for details.

alkaloid-producing cDNA library The library, containing cDNA-inserts of *C. purpurea* strain P-1 derived from alkaloid-producing cultures, was constructed in lambda-based Uni-ZAP® XR vector phages from Stratagene, which contain the pBS phagemid carrying ampicillin-resistance (T. Correia, unpublished).

2.3.3 Primers

All primers were synthesised by MGW-Biotech. Sequencing primers were labelled with 7-deaza-dGTP for use in automatic sequencing (see 2.4.10).

2.3.3.1 PCR and RT-PCR Primers

Included here are the sequences of the degenerate primers used in the isolation of *cpsod1* (with corresponding translation) and of primers used during RT-PCR, during sequencing and for construction and screening of fungal transformants. The annealing temperature (T_A) and synthesis time (t_s) for each primer pair are also shown. When primers were used in more than one combination, the primer pairs are indicated.

Primer sequence	T_A, t_s	Primer pair
Primers used for the isolation of *cpsod1* (degenerate)		
SOD1.1: 5' -GCC GGC CCY CAY TWY AAY CC –3' A G P H F/Y N P	53°C, 0.5 min	
SOD2.1: 3' -CTC AAG ACT GGN AAY GCN GG- 5' L K T G N A G		
Primers used for RT-PCR		
RT-SOD-F: 5'- GTT GGC GGC ACC GTC GTC TTT G -3' **RT-SOD-R:** 5'- CAT TGC CCT GGC CAT CCG TCT C -3'	62°C, 0.75 min	
RT-cat2-F: 5' –TCA ATC GCG AGA AAA TCC CAG AGA-3' **RT-cat2-R:** 5' –GAC CCA GTC CCA ATT TCC ATC CTG-3'	59°C, 0.75 min	
RTHF: 5' –TCC TTC ATC ATC TCC ATC ATG G –3' **RTHR:** 5' –GAA ATG CAC AGA ACA CCC TGT C –3'	60°C, 0.75 min	
RT-DH-F: 5' –AAC CTA CCC AAG GAG ATG AAG G-3' **RT-DH-R:** 5' –TTA CAC CAA CTG TCT CGT GAC C-3'	60°C, 0.75 min	
WSF: 5' –CAG GGC TCA GCG GAA ACG TC–3' **WSR:** 5' –GGG TCT AGA TGC GGG CCT GC–3'	62°C, 0.75 min	
Primers used in the construction of deletion vectors		
DVF1: 5' -GGT AAG ATG TCC TCG GCC –3' **DVR1:** 5' -TGT GCA GTC GAT CAA CGC –3'	55°C, 0.5 min	
RVF1: 5' –AGA TCT GGT CAA GCA CAG GAC C –3' **RVR1:** 5' –AGA TCT CCC AAT TTC CAT CCT GC –3'	59°C, 1 min	
RVF3: 5' – TCT AGA GTC CAT GCT CAA CGT–3' **RVR2:** 5' –TCT AGA TGC ACG ACA AAA TTA CG–3'	57°C, 1 min	

Primer sequence	T_A, t_s	Primer pair
Primers used in the screening of transformants		
HIF1: 5' -CGA GAC TTC ACT TCC ACT TCG –3'	58°C, 0.5 min	HIF1+HIR1
HIR1: 5' -GCT CGA CGT ATT TCA GTG TCG –3'	58°C, 0.5 min	HIF1+HIR2
HIR2: 5' -TCA GAG ACT CTT CGT TGT CGC -3'		
HIF4: 5' –GTA CCT GAC AGG TCA AGA TAT ACC G-3'	57°C, 0.5 min	HIF4+HIR1
HIF5: 5' –CTA TGA GTC GTT TAC CCA GAA TGC -3'	58°C, 0.5 min	HIF5+HIR4
HIR4: 5' –CTC ATT CGT GGA TTT GCT ATG C -3'	58°C, 0.5 min	HIF6+HIR4
HIF6: 5' –GGT CTG TTT GAA TAT CCC CAT G -3'		
Primers used for miscellaneous purposes		
NC1: 5'-GGT GAC TCT AAC GTC AAG GGC –3	60°C, 0.5 min	
NC2: 5'-GTC TTG AGG GAC TCC TCG TTG –3'		
B-DHF: 5' –CCG CCG CCA AGG TGT TCA AGT-3'	60°C, 0.5 min	
B-DHR: 5' –GCC TCT ATG TAG TCC CCT CGT TCC -3'		
S6F2: 5' –ACG CAA GGC GCA ATT GAC GAC C-3'	62°C, 1 min	
S6R: 5' –CCG AGA TGG TGG TTA CTG GAT GGA-3'		

2.3.3.2 Sequencing primers

Primer sequence	T_A, t_s	Primer pair
REVERSE: 5' –CAG GGT TTT CCC AGT CAC GAC GT-3'	65°C, 0.5 min	
UNIVERSE: 5' –ACA CAG GAA ACA GCT ATG ACC AT-3'	58°C, 0.5 min	
pAN-T: 5' –CCC AGA ATG CAC AGG TAC AC-	360°C, 0.5 min	
S8M: 5' –TGG GCA GTC TTC GTC ATC CGT CTC-3'	65°C, 0.5 min	
S8R: 5' –TCA GGA GGC GCA GAA GCA GAT A-3'	58°C, 0.5 min	
SMCOR: 5' –CCA GGG CTA CGA TGC CAC GG-3'	65°C, 0.5 min	
SEQ-SOD1: 5' –TCA CGA CAA TCA CCA CGA AAC ACC-3'	59.5°C, 0.5 min	
SEQ-SOD2: 5' –GAT TCG GAC TCC TGC TCA AAG ACG-3'	59.5°C, 0.5 min	

2.4 General procedures in molecular genetics

2.4.1 Isolation of DNA and RNA

2.4.1.1 Isolation of lambda-DNA

For isolation of DNA from EMBL-3 lambdas containing the genomic library, phage lysate was prepared as follows: *E. coli* LE392 was cultivated as described in 2.2.1 to an OD_{600} of 1.5-2.0, centrifuged for 10 min at 3000 rpm and dissolved in 50 ml 10 mM $MgSO_4$. 150-300 µl of a phage lysate were combined with 20-100 µl of the *E. coli* suspension and were allowed to adsorb for 20 min at 37°C. After adsorption, the mixture was added to 50 ml LBM-medium and incubated over night at 37°C and 180 rpm. To kill surviving bacteria, the mixture was shaken with 500 µl chloroform for an additional 15 min.

Small scale isolation of lambda-DNA was done according to Sambrook et al. (1989), with a few modifications. The cell debris of 1 ml culture was pelleted briefly by centrifugation and transferred to a fresh Eppendorf container. To remove the bacterial DNA, 7.5 µl DNaseI (1 mg/ml) were added and incubated for 30 min at 37°C. After the DNAseI was inactivated by addition of 7.5 µl diethylpyrocarbonate (DEPC), followed by 2 min of vortexing, 250 µl TES buffer (1 M Tris/HCl, 100 mM EDTA, 1% SDS, pH 8.0) were added and the mixture was heated to 80°C for 20 min. Proteins were precipitated with 125 µl 5 M KAc by incubation on ice for 30 min and then separated by centrifugation (15 min, 10 000 rpm). The phage-DNA was precipitated from the supernatant with 0.45 vol isopropanol, centrifuged, washed with 70% ethanol, dried and dissolved in ddH_2O.

2.4.1.2 Isolation of genomic DNA from *Claviceps*

After lyophilisation, mycelia was ground to a fine powder under liquid nitrogen, and genomic DNA was isolated according to Cenis (1992), and modified as described by Müller (1997).

2.4.1.3 Isolation of total RNA from *Claviceps*

Total RNA was obtained from 50 mg aliquots of ground lyophilised mycelia through use of the RNAgents® Total RNA Isolation System from Promega, according to instructions of the supplier for 2 ml tube size. All experiments with RNA comprised the use of DEPC-treated water (stirred with 0.1% (v/v) DEPC over night and then autoclaved).

2.4.1.4 Isolation of mRNA from *Claviceps*

mRNA was isolated directly from 20 mg aliquots of ground lyophilised mycelia using Dynabeads® (Dynal), according to instructions provided by the manufacturers. The mycelia was lysed in lysis/binding buffer C (100 mM Tris, 500 mM LiCl, 10 mM EDTA, 1% SDS and 5 mM DDT), and the bound beads were washed twice in washing buffer D (10 mM Tris, 1 M LiCl, 2 mM EDTA and 10% SDS), once in washing buffer E (same as D without SDS), and finally, once in Li-free OW2 washing buffer from the Oligotex™mRNA Mini Kit (Quiagen) to remove last traces of Li which could potentially impede cDNA synthesis. After elution in buffer F (10 mM Tris) at 65°C, the mRNA was precipitated over night at –70°C after the addition of 1/8 vol 2 M NaAc, pH 4.0 and 2.5 vol of ice-cold ethanol.

2.4.1.5 Isolation of plasmid DNA

All plasmid isolation protocols are based on the method of alkaline lysis described by Birnboim and Doly (1979).

For restriction analyses of recombinant plasmids, buffers provided by Genomed (for large scale plasmid isolation) were used on 1 ml over-night cultures. After centrifugation at 5000 rpm, the cell pellet was suspended in 100 µl E1, cells were lysed and DNA was denatured in 100 µl E2 for 5 min, and plasmid DNA was renatured in 100 µl E3. Cell remnants were spun down at 15 000 rpm for

10 min, and the plasmid DNA was precipitated from the supernatant with 0.7 vol isopropanol.

Plasmid DNA for sequencing was obtained from 5 ml cultures grown over night using the Jet Star Plasmid Miniprep Spin Kit from Genomed, as described by the manufacturers.

Large scale plasmid isolation was done using the Jet Star Midi Prep kit from Genomed by subjecting 50 ml over night cultures to alkaline lysis with buffers E1, E2 and E3, followed by a purification with an affinity chromatography column, as described by the manufacturers.

2.4.1.6 Determination of RNA and DNA concentrations

Small concentrations of DNA (>50 ng/µl) were determined as described in 2.4.3; larger concentrations of DNA and RNA were determined photometrically using the GeneQuant II RNA/DNA Calculator according to the instructions provided by the manufacturers (Pharmacia).

2.4.2 Restriction, precipitation and washing of DNA

DNA was digested with Fermentas restriction enzymes in One-Phor-All buffer (10 mM Tris/HAc pH 7.5, 10 mM $Mg(Ac)_2x\ 4H_2O$ and 50 mM KAc). For optimal enzyme activity, the buffer concentration was adjusted between 0.5x, 1x and 2x according to the recommendations of Pharmacia. Approximately 10 U enzyme were used to digest 1 µg plasmid for at least 2 h at 37°C. When digesting genomic DNA and lambda DNA, 1% BSA was added and the mixtures were incubated over night. When digesting lambda-DNA, 0.25 µg/µl spermadine (Sigma) and 1 µg DNAse-free RNAse (Genomed) was also included.

If not otherwise described, DNA was precipitated from aqueous solution by the addition of 1/10 vol 3 M NaAc and 2 vol ice-cold ethanol. After 10-20 min at –20°C, the DNA was pelleted by centrifugation (15 min, 14 000 rpm, 4°C) and washed by addition of 700 µl 70% ethanol and centrifugation (5 min, 14 000 rpm, 4°C) before drying.

2.4.3 Gel electrophoresis of DNA and RNA

DNA was separated in 1 to 2 % agarose gels using a saltfree-buffer (10 mM EDTA, 40 mM Tris/HCl, pH 8,2 with acetic acid). Size standards were provided by *Hin*dIII or *Hin*dIII/*Eco*RI restricted lambda-DNA, or the 1 kb ladder (Pharmacia). The DNA was made visible under UV-light after dyeing with ethidium bromide (50 µg/ saltfree buffer). DNA amount could be estimated by comparison with defined amounts of *Hin*dIII-digested lambda DNA.

RNA was separated in 1.4% agarose gels containing 1.5% formaldehyde, according to Sambrook et al. (1989). An RNA-size-marker (Gibco BRL) served as a size standard and was detected after blotting onto membranes (see 2.4.6.1) by exposure to a UV-handlamp (254 nm). After lying the gel on a silica gel plate with UV-fluorescence-indicator for 254 nm (Kieselgel 60 F_{254}, Merck), the RNA could be

made visible by exposure to a UV-handlamp (254 nm).

2.4.4 Isolation of DNA from agarose gels

DNA fragments for cloning or radio-labelling were isolated using the Jet Quick Gel Extraction Spin Kit from Genomed according to the instructions of the manufacturers.

2.4.5 Hybridisation of DNA and RNA with α-^{32}P-dCTP-labelled probes

These techniques were typically used to locate specific DNA fragments on Southern blots, phage plaque- or bacterial colony- filters and RNA fragments on northern blots.

2.4.5.1 Radio-labelling of DNA fragments

For use as probes in hybridisation experiments, DNA fragments were radio-labelled using a random-priming approach as follows: In a total volume of 20 µl: 10-50 ng denatured DNA fragment (created by heating for 5 min at 100°C and cooling on ice), 3 U Klenow fragment (Fermentas), 1 µl of nucleotide mixture containing 0.5 mM each of dGTP, dATP and dTTP (Fermentas), 2 µl (2.5 µg/µl) random hexamers (Boehringer) and 1µl α-^{32}P-dCTP (ca. 10 mCu) (DuPont) were combined in 1x Klenow buffer (Fermentas) and incubated for 1-2 h at 37°C.

Free nucleotides were separated via gel filtration on a Sephadex G-50 column, as described in Ausubel et al. (1987). The eluted fragments were denatured prior to addition to the hybridisation solution by heating to 100°C for 3-5 min and cooling on ice.

2.4.5.2 Synthesis of radio-labelled cDNA from mRNA template

1 µg mRNA/10 µl ddH_2O was combined with 1 µg Oligo dT $_{12\text{-}18}$ (Gibco), heated for 2 min at 70°C and cooled on ice for 5 min. To this, 2 µl of a dNTP mixture containing 10 mM each of dATP, dTTP, dGTP (Fermentas) were added, as well as 2 µl 0.1 M DDT (Gibco), 1 µl 25 600 U/ml RNAse inhibitor (RNA Guard, Pharmacia), 5 µl first strand buffer (Gibco) and 2 µl α-^{32}P-dCTP (Amersham). After primer-annealing for 2 min at 37°C, 1 µl 10 U/µl Superscript™ reverse transcriptase (Gibco) was added and the mixture incubated for 1 h at 37°C. Then, 1 µg of non-radioactive dCTP and 1 µl of reverse transcriptase was added and the solution was again incubated for 1 h. The reaction was stopped by addition of 1 µl 0.5 M EDTA and 1 µl 10% SDS. The mixture was then incubated with 3 µl 3 M NaOH for 30 min at 65°C to hydrolyse the mRNA. After neutralisation by the addition of 10 µl 1 M Tris/HCl pH 7.5 and 3 µl 2 M HCl, the free nucleotides were separated as described in 2.4.5.1.

2.4.5.3 DNA-DNA hybridisation

DNA-DNA hybridisation was carried out using the method of Denhardt (Sambrook et al., 1989). Filters were incubated in the prehybridisation solution for 1-2 h at hybridisation temperature (usually 65°C: stringent conditions for homologous hybridisation). After adding the denatured, radio-labelled DNA-probe, the hybridisation was continued over night. The filters were washed with 2x SSPE, 0.1% SDS for 5-10 min at room temperature (20x SSPE stock: 3.6 M NaCl, 0.2 M NaH_2PO_4, 20 mM EDTA, pH 7.7). A more stringent washing buffer (1x SSPE, 0.1% SDS) was used if the background radioactivity was estimated to be strong with a Geiger-counter. The filters were wrapped in plastic foil and exposed to X-ray film (Retina) for between 1 h and 10 d (depending on the signal strength) at -20°C.

2.4.5.4 RNA-DNA hybridisation

RNA-DNA hybridisation (hybridisation of northern blots) was carried out as described in 2.4.5.3, with the exception of the (pre)hybridisation buffer, which comprised: 1.1 M NaCl, 0.3 M Na_2HPO_4, 0.01 M Na_2EDTA, 1.85% N-lauroylsarcosine (Sigma) and 18.5% dextran sulfate (Eppendorf). Hybridisation took place over night at 60°C. Filters were washed in 2x SSPE, 0.1% SDS for 5 min at hybridisation temperature.

2.4.6 Analysis of DNA and RNA on membranes

2.4.6.1 Downward blotting of DNA and RNA

DNA (1 µg plasmid or 10 µg genomic-DNA) and RNA (15-20 µg total RNA) were transferred from agarose gels to membranes (Nylonfilter HybondN$^+$, Amersham) with a „downward-blot“, as described by Ausubel et al. (1987), to create Southern blots. 0.4 N NaOH was used as a transfer buffer for DNA. The transfer of high molecular weight genomic DNA was eased by a 15 min treatment with 0,25 M HCl (depurination) prior to blotting. Blotting of RNA (for northern blots) was done with RNA-blot buffer (20 mM NaOH, 0.75 M NaCl, 75 mM sodium citrate, pH 7.0). After a maximum 2 h blotting time, RNA was covalently bound to the membrane by baking for 30 min at 80°C.

2.4.6.2 Dot Blots

Dot Blots were done according to the technique described by Ausubel et al. (1987), for the manual preparation of dot blots.

2.4.6.3 Preparation and screening of bacterial colony filters

Colony filters were made to screen a large number of bacterial clones for specific inserts by hybridisation. Round nitrocellulose filters (Schleicher and Schuell "Optitran", ∅ 8.2 cm) were placed on the agar plates (∅ 9 cm) containing a bacterial clone array. After a few seconds, the nitrocellulose fil-

ters were placed with the bacteria imprint facing upwards for 3 min on 750 µl 0.5 M NaOH (denaturing step), for 5 min on 750 µl 1 M Tris/HCl pH 7.5 (neutralisation step), and once for 5 min on 750 µl 0.5 M Tris/HCl and 1.5 M NaCl pH 7.5. Between each step the filters were briefly dried on Whatman-paper. Plasmid DNA was affixed to the filters by baking for 2 h at 80°C. Hybridisation of the colony filters with specific radio-labelled probes enabled the localisation of those colonies which contained a hybridising insert.

2.4.6.4 First- and second-round preparation of phage plaque filters for genomic and cDNA library screening

For the isolation of genomic and cDNA gene sequences, ca. 60 000 phages from the corresponding libraries were screened. *E. coli* strain LE392 (for infection with EMBL-3 phages containing genomic sequences) and *E. coli* strain XL-Blue (for infection of the lambda-ZAP phages containing cDNA phagemids) were prepared as described in 2.2.1. Cultures were pelleted by centrifugation and taken up in 10 mM $MgSO_4$ to an OD_{600} of 0.5-1.0.

In each case, approx. 10 000 phages were mixed with 600 µl bacteria, allowed to adsorb at 37°C for 15 or 30 min (cDNA and genomic phages, respectively), added to 10 ml liquid LBM top-agar (which had been previously cooled to 48°C) and poured onto a large LBM or NZY agar plate (∅ 14 cm). After incubation over night at 37°C, plaques appeared in the bacterial lawn. DNA from the phage plaques were im printed onto nitrocellulose membranes (Schleicher and Schuell "c", ∅ 13.2 cm), according to Sambrook et al. (1989), in a procedure similar to that described in 2.4.6.3. DNA was affixed to the filters by baking for 2 h at 80°C.

After hybridisation with a radio-labelled probe, signals hybridising to the probe were purified in a second screening round. By comparison of signals on the X-ray film to the plates used in the plaque-imprinting the signals could be localised; the area giving rise to the signal was stamped out with the wide end of a pasteur-pipette and transferred to a 300 µl aliquot of phage buffer (100 mM NaCl, 10 mM Tris, 10 mM $MgSO_4$ pH 7.5) to produce phage stock solution. After addition of 5 µl chloroform and shaking for 30 min at 37°C to kill bacterial cells and allow the diffusion of phages into the buffer, the mixture was diluted 1:10 and 1:100 in phage buffer and used to infect *E. coli* XL-Blue (cDNA libraries) or *E. coli* LE392 (genomic DNA library). For this, 5 µl diluted phage stock were adsorbed to 200 µl bacteria as described above and then added to 4 ml liquid LBM top-agar (cooled to 48°C) and poured onto small LBM agar plates (∅ 9 cm) and incubated over night at 37°C. Plates with generously spaced plaques were used to imprint a new set of filters and hybridised to allow the identification of single phages which contain hybridising fragments. These were stamped out with the narrow end of a pasteur pipette and used to create a stock solution as described above.

2.4.7 Excision of phagemid vectors from lambda-ZAP vectors

The *in vivo* excision of the pBK-CMV phagemid vector from ZAP-Express® phages (Cu-induced cDNA library) and the *in vivo* excision of the pBluescript (pBS) phagemid vector from the Uni-ZAP® XR vector (alkaloid production-induced cDNA library) were done according to the protocols provided with the cDNA library synthesis kits (Stratagene), with a few small modifications.

E. coli strain XL-Blue was prepared as described in 2.2.1. To infect *E. coli* with both non-lysogenic helper phage (ExAssist™) and lambda-ZAP phage carrying phagemid vector and cDNA insert, 60 µl lambda-ZAP phage stock were combined with 1 µl non-lysogenic helper phage, were vortexed and the phage mixture was added to 200 µl XL-Blue. Following adsorption for 15 min at 37°C, the mixture was added to 3 ml LB and shaken at 37°C and 180 rpm for 3 h to cultivate bacteria. During this time, the bacteria and their phages replicate, and the non-lysogenic helper phage is released into the medium. The mixture was then incubated at 70°C for 15 min to lysate the lambda phages, and spun down to remove the bacteria cells from the mixture. The supernatant, which comprised helper phages carrying either their own genome or excised phagemid vector (which contained replication signals for the helper phage), was used to infect *E. coli* XL-Blue.

Infection of XL-Blue with helper phages and selection for cells containing pBS were done as follows: 1 µl 1:100 diluted supernatant was combined with 150 µl XLBlue, allowed to adsorb for 15 min at 37°C and then plated on LB with ampicillin.

Infection of XL-Blue with helper phages and selection for cells containing pBK-CMV containing helper phages were done after an extra amplification step: 10-100 µl supernatant were adsorbed as described above to 150 µl XL-Blue and shaken for 45 min at 37°C and 180 rpm. 200 µl of this mixture were then plated on LB with kanamycin.

After excision, the phagemid vector is referred to as a plasmid.

2.4.8 PCR and RT-PCR

The polymerase chain reaction (PCR) was performed a in 50 µl volume which included 1 U Sigma RED-Taq™ DNA polymerase, 1x corresponding buffer (Sigma), 1 µM (homologue conditions) or 1-2 µM (heterologue conditions) of each primer, 2 mM nucleotides and ca. 0.1-100 ng template. For PCRs with plasmids or transformation vectors the template was added by "inoculation" with a sterile toothpick.

Conditions were as follows:

$$\mathbf{94°C\ 3\ min \rightarrow (94°C\ 0.5\ min \rightarrow X°C\ X\ min \rightarrow 72°C\ 1\ min/kb)_{36X}}.$$

Primer sequences, annealing temperature and synthesis time of the various reactions is provided in 2.3.3.1. When PCR fragments were to be cloned, a post-treatment at 72°C for 6 min was added for the

addition of adenine, which was needed for the cloning into the PCR vector (see 2.4.9.1).

RT-PCR was done in a two step procedure. First, 1 µg of total RNA was combined with 200 ng reverse primer in 14 µl ddH_2O, heated to 70°C for 3 min, cooled on ice and collected by brief centrifugation. After addition of 2 µl 10 mM dNTP, 2 µl first strand buffer (Gibco) and 1 µl (25 600 U/ml) RNAse inhibitor (RNA guard, Pharmacia), the mixture was incubated for 2 min at 42°C for annealing of the primers. Then, 1 µl 10 U/µl Superscript™ reverse transcriptase (Gibco) was added and the reaction was incubated for 1 h at 42°C. The reaction was stopped by incubation at 95°C for 5 min. In the second step, 3-5 µl of this reaction were used as template in a homologous PCR as described above.

2.4.9 Cloning of DNA fragments

2.4.9.1 Ligation of DNA fragments into cloning vectors

Isolated restriction fragments were ligated into the linearised cloning vector pBluescriptIISK$^-$ (pBS), fungal transformation vectors, or derivatives of these vectors. 1-2 µg of vector DNA were prepared by restriction, precipitation and washing. After purification by gel electrophoresis and isolation from agarose gel, they were taken up in 100 µl ddH_2O.

Vectors linearised with one restriction enzyme only were treated with 0.1 U/µg DNA calf intestinal alkaline phosphatase (Pharmacia) in 1x OPA for 30 min at 37°C directly following restriction to prevent recirculisation by removal of the 5'-phosphate residue. After the phosphatase was inactivated at 85°C for 15 min and the DNA renatured for 20 min at room temperature, the vector was precipitated and purified as described above.

Insert fragments were purified by gel electrophoresis and re-isolation from the gel segment. For ligation into blunt-ended vectors, overhanging 5' ends were filled in a Klenow reaction according to Ausubel et al. (1987).

Approximately 10-20 ng vector were ligated with threefold the molar amount of fragment in a 20 µl reaction mixture with 2 or 0.5 U ligase (Fermentas or Gibco, respectively) in the corresponding buffer. Ligation took place either over night at 13°C, or for 1-2 h at room temperature. In blunt end ligation reactions, 4 µl PEG 4000 (Fermentas) was added to the ligation mixture and ligation took place over night.

For the cloning of PCR fragments, the TOPO™ TA Cloning® Kit (Invitrogen) was used according to the manufacturer's instructions.

2.4.9.2 Transformation of ligated vectors into *E. coli* and selection of recombinant clones

Transformation of competent Top10F$^-$ *E. coli* cells was done according to Sambrook et al. (1989). Transformants were selected by cultivation on LB-agar containing 80 mg/l ampicillin. Where possible,

recombinant clones were selected by blue-white screening on agar additionally containing 40 mg/l X-Gal (5-bromo-4-chloro-3-indolyl-β-D-galactopyranoside) and 50 mg/l ITPG (isopropylthio-β-D-galactoside). The clones were analysed either by isolation, digestion with restriction enzymes and gel electrophoresis, or by colony filter hybridisation.

2.4.10 DNA sequencing

Thermo-cycle sequencing was done with either the DYEnamic Direct Cycle Sequencing Kit with 7d-Z-dGTP (Amersham) and infrared fluorescence dye (IRD) labelled primers (MWG Biotech) according to instructions provided by the manufacturers, with slight modifications: linear PCR for the DNA sequencing reaction was performed as follows: 500 ng plasmid were combined with 1-2 pmol sequencing primer in a volume of 12 µl. After vortexing and collection by centrifugation, 3 µl were added to four separate aliquots of 0.5 µl thermo-sequencing mix (Amersham or Biozym), which included polymerase, polymerase buffer, dNTPs and one of either ddGTP, ddATP, ddTTP or ddCTP. After renewed vortexing and collection by centrifugation, the thermocycling reaction was carried out as follows:

$$\mathbf{94°C\ 3\ min \rightarrow (94°C\ 0.5\ min \rightarrow X°C\ 0.5\ min \rightarrow 72°C\ 0.5\ min)_{30X}}$$

3 µl of dye-containing stop solution as supplied by the manufacturer were added to each reaction. After denaturing, 0.7-1.1 µl of the reaction were used for sequencing.

Sequencing was carried out with the aid of LI-COR sequencing automats "DNA-sequencer models 4000 and 4200" (from MWG Biotech), according to instructions provided by the manufacturers. The sequencing gel was made by combining 24 ml Sequagel XR® with 6 ml Sequagel® complete buffer reagent (Biozym-Diagnostics) and polymerising by the addition of 240 µl 10% (w/v) APS (ammonium persulfate).

Primers and annealing temperatures are provided in 2.3.3.1.

2.5 Creation and differential screening of a copper-induced cDNA-library

2.5.1 Creation of a copper-induced cDNA-library

2.5.1.1 Cultivation of mycelia

Mycelia of the haploid pathogenic *C. purpurea* strain 20-1 was grown in shaken cultures (at 200 rpm and 28°C) for 4 d in 100 ml of MA medium (containing 10% sucrose) to which 50 µM (10 µl of a 125 mg/ml $CuSO_4$ x 5 H_2O sterile-filtered solution) were added directly prior to inoculation with

10^6 conidia. From this mycelia, a total of 9.5 µg mRNA were isolated directly from six aliquots of 20 mg lyophilised mycelia as described in 2.4.1.4.

2.5.1.2 Synthesis of the cDNA library

The creation of the cDNA library from 5 µg mRNA was done with the ZAP Express® cDNA-synthesis kit and ZAP Express® cDNA Gigapack III Gold cloning kit (Stratagene), according to the protocol supplied by the manufacturers. The protocol was modified only in substituting non-radioactive dNTPs for α-^{32}P-dNTPs and eliminating controls based on radioactivity.

With the use of this kit, the first strand was synthesised from the mRNA template with an oligo-dT primer and reverse transcriptase; the second strand was created through the simultaneous digestion of the mRNA-half of the resulting chimera with RNAse and the filling in of missing sequences with dNTPs using a DNA-polymerase. In this way, the RNA-remnants served as initial primers for the DNA synthesis. After a nuclease treatment to blunt the ends of the cDNA, adapters containing *Eco*RI sites were ligated onto both sides. Digestion of the resulting constructs with *Eco*RI and *Xho*I (whose restriction site is contained in the original oligo-dT primer) released a double-stranded cDNA population which could then be ligated into the arms of the λ-ZAP phagemid vector from Stratagene; construction of the first strand reaction using methylated dNTPs shields mRNA-internal restriction sites from digestion. In order to ensure that the library contained a large proportion of full-length cDNAs, the population was fractioned according to size via filtration through a gel c

olumn prior to ligation. After ligation of cDNAs and phagemid arms, the constructs were packaged into λ-phages to yield the primary bank

The library synthesis was attempted for the first time without the use of radioactivity (in contrast to the kit protocol) so that verification of successful first and second strand synthesis reactions was not possible. Furthermore, an accurate estimation of the fragment sizes after gel fractionating was also not possible. The first experimental control which could be carried out involved the determination of DNA concentration of the different fractions; this was done by dropping 0,5 µl from the total of 5 µl purified DNA on an ethidium bromide-containing agar plate and comparing the fluorescence under UV-light with that emitted from a row of standards (fig. 2.1). In contrast to fractions 1-4, which do not contain detectable amounts of cDNA, fractions 5-12 show fluorescence comparable to that of the standards, confirming the success of the cDNA synthesis.

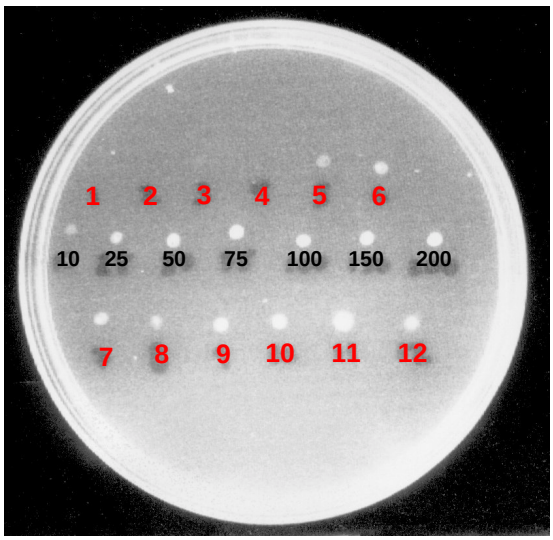

Fig. 2.1: Determination of the cDNA concentration in the size fractions after gel filtration. 0.5 of each 5 µl fraction were dropped on an agar plate containing EtBr and was illuminated with UV-light. The fractions (1-12) are indicated in red. 0.5 µl aliquots of DNA corresponding to 10, 25, 50, 75, 100, 150 and 200 ng of pUC19 DNA were used as standards.

As the principle of gel filtration dictates that the fractions eluted first contain the longest cDNAs, the 100 ng needed for the ligation reaction were drawn from fractions 5 and 6. The concentrations of fractions 5 and 6 were estimated at 20 and 40 ng/µl respectively, so that the remaining 4,0 µl of fraction 5 were combined with 0.6 µl of fraction 6 to make a total of 104 ng cDNA for the ligation reaction with the arms of the λ-ZAP Express vector.

Packaging of 3 µl of the 5 µl ligation reaction into λ-phages yielded the primary library in a total volume of 500 µl. Both the titre of the primary library, as well as the proportion of phages which contained an insert, was determined by infecting *E. coli* (strain XL1-Blue) aliquots of the primary library and plating out the infected bacteria in agar containing X-Gal and ITPG. As the insertion of cDNA into the λ-ZAP vector disrupts the (ITPG-induced) β-galactosidase gene, the ability of this enzyme to break down the X-Gal substrate into a blue product is lost by recombinant phages, rendering their plaques colourless, while phages lacking inserts create blue plaques.

A secondary library was created by the amplification of 10^6 primary plaques according to the instructions provided with the cDNA library synthesis kit (Stratagene).

2.5.2 Differential cDNA screening

Differential screening of a cDNA library involves plating out library clones so that single plaques can be isolated, transferring the plaque DNA from each plate onto double sets of membranes and hybridising each membrane with differential populations of radioactively labelled mRNA. Differentially expressed clones can be found by comparing the signal patterns of both membranes.

For all differential cDNA screenings, 7x 1000 cDNA phages from the Cu-induced cDNA library were plated out, and phage DNA from each plate was transferred onto two separate nitrocellulose membranes in two successive imprinting steps. As the second DNA transfer from the same plate of phage plaques invariably produces weaker hybridisation signals than the first, these membranes were incubated with the induced mRNA population, so that signals appearing stronger after hybridisation result from a higher proportion of mRNA in the probe rather than from a higher amount of DNA template on the membrane.

Cultivation of all mycelia used for isolation of mRNA template was done as follows: 10^6 spores of the haploid pathogenic *C. purpurea* strain 20-1 were used to inoculate 100 ml of MA medium (containing 10% sucrose) and grown in shaken cultures at 200 rpm and 28°C for 4 d. The differences between induced and non-induced conditions are described below.

2.5.2.1 Non-stringent differential cDNA screening

Induction of mycelia with excess copper was done by adding 10 µl of a 125 mg/ml $CuSO_4$x 5 H_2O sterile-filtered solution (Millex GV 0.22 µM filter units) directly prior to inoculation, while non-induced mycelia was cultivated identically without the addition of $CuSO_4$. 1 µg of each mRNA population was used as template in radio-labelled cDNA synthesis (see 2.4.5.2).

The hybridisation of membranes containing phage DNA with induced and non-induced radio-labelled cDNA was done in two identical plastic containers by gently shaking in a water bath at 65°C overnight. Filters were washed in 2x SSPE with 0.1% SDS for 10 min and exposed to film for 1-5 d (see 2.4.5.3 for the composition of SSPE). After comparison of films obtained with hybridisation of induced and non-induced cDNA, 13 signals appearing stronger in the former were isolated according to 2.4.6.4 (procedure for second screening round). After excision and isolation of the phagemid vector containing the cDNA insert, each was twice subjected to digestion with *Eco*RI and *Xho*I to release the vector, and analysed via Southern blotting with induced and non-induced radio-labelled cDNA to determine differential expression.

2.5.2.2 Stringent differential screening

Conditions of copper starvation Non-induced mycelia was obtained by addition of 1 mM ascorbic acid (100 µl of a 176 mg/ml solution in ddH_2O) and 33 µM bathocuproine disulfonic acid (BCS, Sigma) (20 µl of a 93 mg/ml solution in DMSO) to 100 ml of media directly prior to inoculation. These conditions are based on a protocol described in Osiewacz and Nuber (1996). 4 h prior to harvest, 15 µl ddH_2O were added to the cultures.

Conditions of copper excess Induced mycelia was obtained by the addition of 75 µM $CuSO_4$ (15 µl of a 125 mg/ml solution in ddH_2O) as well as 100 ml ddH_2O and 20 µl DMSO directly prior to inoculation. 4 h prior to harvest, 75 µM $CuSO_4$ were again added to the cultures.

Mycelia obtained from these cultures was used to produce induced and non-induced radio-labelled cDNA. After hybridisation, the differential signals were isolated and excised as described in 2.4.6.4 (procedure for second screening round). A mixture of excised colonised was used for the inoculation of cultures for plasmid isolation. Plasmids isolated from 101 excised signals were subjected to gel

electrophoresis to estimate if the phage stock was homogenous or heterogeneous. For samples containing plasmids of different sizes, six single clones were picked from the corresponding excision plates and re-analysed. The signal was subdivided into a, b or c, each containing a single plasmid of a different size.

A total of 139 plasmids originating from the 101 differential signals were subjected to a second round via dot blot analysis. Two identical dot blots were created by dropping 1 µg plasmid DNA on a membrane as described in 2.4.6.4, hybridised with either induced or non-induced radio-labelled cDNA, washed for 10 min at 65°C in 2x SSPE with 0.1% SDS and exposed to X-ray film (Retina) for 4 h-1 d. As a control of quantity, the membranes were dehybridised and re-hybridised as described above with radio-labelled pBK-CMV.

2.6 Induction of mycelia for northern and protein analysis

All induction experiments, unless mentioned otherwise, were conducted in the base medium MA (10% sucrose), and cultivated as described in 2.2.2.2. In all cases, the spores were derived from *C. purpurea* strain 20-1.

2.6.1 Induction with copper and iron

Induction with the transition metals copper and iron was done by adding the metals to the media as described below:

50 – 100 µM copper: 10-20 µl of a 125 mg/ml $CuSO_4$ x $5H_2O$ solution were sterilised by filtration (Millex GV 0.22 µM filter units) and added directly prior to inoculation.

118 µM iron: 100 µl Fe stock solution (33 mg $FeSO_4$ x $7H_2O$/ml 0.1 N HCl)/100 ml MA medium were added with all other media ingredients prior to autoclaving. This is the routine concentration of Fe used in the cultivation of *Claviceps*.

500 µM iron: 421 µl Fe stock solution (see above) were added/100 ml MA medium to the media prior to autoclaving.

Cultivation of non-induced mycelia involved use of media to which either no copper or no iron had been added.

2.6.2 Induction with AOS

2.6.2.1 Induction with hydrogen peroxide

Induction with H_2O_2 was done by adding 102 µl ddH_2O or 102 µl 10^2, 10 or 1x diluted 30% (v/v) H_2O_2 stock solution (Perhydrol, Merck) to 100 ml cultures (cultivated for 4 d as described above), creating 0, 0.1, 1 or 5 mM H_2O_2, respectively.

2.6.2.2 Induction with sources of superoxide

Extracellular superoxide was generated enzymatically by addition of xanthine oxidase and xanthine to a mycelia-containing incubation buffer (50 mM KPP buffer, pH 8.0) as described by Fridovich (1970). 500 ml buffer were prepared, 31 mg xanthine (Sigma) (formerly dissolved in 1 ml ddH_2O by addition of a few drops of 20% (w/v) NaOH) were added to achieve a final concentration of 400 µM. 30 ml aliquots of sterile filtered xanthine-containing buffer were added to 100 ml sterile Erlenmeyer flasks. Mycelia was cultivated as described above, filtered through sterile Mira-cloth (Calbiochem), rinsed in 50 mM KPP buffer, pH 8.0, and drained. Mycelial aliquots of 30 mg were added to the incubation buffer. 100 U of xanthine oxidase (XO) (Sigma) were dissolved in 1 ml ddH_2O to make XO stock. 0, 6, 60 and 120 µl XO stock were brought to a total volume of 300 µl ddH_2O and added to the incubation media. As described by Augustin et al., 1996, 12 000 U/ml catalase were added to the buffer to degrade H_2O_2 produced by spontaneous dismutation of superoxide. 22.5 mg of 16 000 U/mg bovine liver catalase (Sigma) were added to each 30 ml of buffer. Incubation followed at 150 rpm at 28°C; mycelia was harvested and freeze-dried after 1, 5 and 24 h.

Intracellular superoxide was generated within the cells by the addition of the redox cycler paraquat (methyl viologen, Sigma), as described in De Groote et al., 1997. Two separate experiments, paraquat I and paraquat II were undertaken.

Paraquat I: Cultures were prepared as described above. After 4 d growth, paraquat was added. Aliquots of 2.6, 12.9, 25.7 and 128.5 mg were dissolved in 500 µl ddH2O and added to the 100 ml cultures, while 500 µl ddH2O were added to the controls. After incubation for 30 min, 1 h, 5 h and 24 h, the mycelia was harvested.

Paraquat II: This induction experiment examined the effect of low sucrose as well as the combination of excess copper with paraquat. MA base medium containing 1% and 10% sucrose was prepared. Otherwise, culture conditions were as described above. 10 µl of 125 mg/ml $CuSO_4$ (50 µM) were added directly prior to inoculation for the induction of cultures with copper. After 4 d, 5 h prior to harvest, 257 mg paraquat were dissolved in 800 µl of ddH_2O and added to 100 ml of culture to create 10 mM, while 800 µl ddH_2O were added to the control cultures.

2.6.3 Induction with polyols

Mycelia was cultivated as described above and shifted to an MA medium devoid of all carbon sources (yeast extract, asparagin and cystein) (MA-C) to which either 2% sucrose (control), sorbitol, mannitol or xylitol had been added. The harvested mycelia was filtered over sterile Mira-cloth and rinsed in MA-C; aliquots of 4 mg were each added to 100 ml medium. After incubation at 180 rpm and 28°C for 5 and 24 h, the cultures were harvested.

2.7 Protein-biochemical methods

2.7.1 Extraction of proteins from *C. purpurea*

For the extraction of proteins from axenic mycelia, *C .purpurea* was cultivated as described in 2.2.2.2, unless otherwise specified. For the extraction of proteins from parasitic culture, the fungus was cultivated as described in 2.8.3; at 5 and 10 dpi, infected ovaries were harvested. After lyophilisation, 50 mg aliquots of infected rye ovaries were used for the extraction of proteins.

For isolation of mycelial proteins the mycelia was finely ground under liquid nitrogen, while for the isolation of cell-wall bound proteins the mycelia was left intact. Proteins were extracted with 1-1.5 ml of 50 mM KPP buffer (pH 7.8); the mixture, in 2 ml Eppendorf tubes, was placed horizontally on ice for 30 min on a gentle shaker. Mycelial remnants were separated by centrifugation for 30 min at 4°C and 14 000 rpm. The supernatant was dialysed over night in ddH_2O at 4°C. The dialysate was spun down as described above and the supernatant was aliquoted into five equal volumes and frozen in liquid nitrogen. Before gel electrophoresis, the protein extracts were freeze-dried.

Proteins of the culture filtrate were precipitated with ammonium sulfate in a two step procedure. 20.9 g $(NH_4)_2SO_4$ were gradually added to 100 ml of culture filtrate, under stirring on ice, to achieve 35% saturation. The solution was then transferred to GSA-tubes and centrifuged at 10 000 rpm for 30 min at 4°C. After 411 g/l $(NH_4)_2SO_4$ were added to the supernatant, as described above, to achieve 90% saturation, the precipitated proteins were spun down as already described. The two pellets were combined in 5 ml ddH_2O and dialysed against ddH_2O over night. After centrifugation of the dialysate in SS34 tubes, the supernatant was divided into ten aliquots of equal volume, frozen with liquid nitrogen and lyophilised.

2.7.2 Determination of protein concentration in extracts

The concentration of total protein in the extracts was determined using the method from Lowry et al. (1951), with slight modifications. 10 µl of the protein extract was combined with 190 µl ddH_2O and incubated with 1 ml of Lowry-solution (made directly prior to use by combining 25 ml of solution A (750 mM Na_2CO_3 in 0.1 M NaOH) with 500 µl of solution B (20 mM $CuSO_4$ and 35 mM KNa-tartrate in 0.1 M NaOH) for 10 min at RT). Then, 100 µl of Folin-Ciocalteau-Phenol Reagent (Merck) were added, the solution was mixed and left to incubate for 30 min at RT. Extinction of the resulting solution was measured at 660 nm and compared with a BSA (Fermentas)-based calibration curve to obtain the protein concentration. Results obtained in three separate measurements were averaged.

2.7.3 Isoelectric focussing (IEF) gel electrophoresis

Lyophilised proteins were taken up in a buffer consisting of 3.3 % (v/v) ampholytes 5-8 or 3-10 (Serva) and 20 % (v/v) glycerol in ddH_2O.

The gel was made by combining 9.91 ml ddH_2O, 3.4 ml 50% glycerol, 2.84 ml (40 %) PAA (National Diagnostics) and 850 µl ampholytes (same as used for the protein buffer), degassing for 10 min by stirring in a vacuum and adding 34 µl TEMED and 34 µl 10% (w/v) APS to initiate polymerisation.

Proteins were separated using the Vertical Slab Gel Unit Model SE 280 "Tall Mighty Small" (Hoefer Scientific Instruments), and 25 mM HAc and 20 mM NaOH as anode and cathode solutions, respectively.

After a pre-run of 30 min at 100 V, wells were loaded with 15% glycerol in ddH_20 and protein extracts were added with a Hamilton needle under the protective glycerol layer to prevent denaturing. Electrophoresis was performed at 4°C as follows: 1 h at 250V, 3 h at 500 V and 30 min at 750 V.

The IEF-mix 3.6-9.3 (Sigma) (10-20 µl of a 3.6 mg/ml solution) was used as an IEF marker. After electrophoresis the marker was severed from the rest of the gel and stained with silver precipitate as described below.

2.7.4 Silver staining of protein gels

This method, suitable for use in both IEF and SDS gels, was kindly provided by J. Cordewener (pers. comm.). The proteins were incubated first in fixing solution (50% ethanol and 10% acetic acid) for 30 min and then incubated in 1:10 diluted fixing solution for 15 min. After rinsing 3x 5 min in ddH_2O, the gel was incubated for 1 min in priming solution 0.2 g/l $Na_2S_2O_3$ x $5H_2O$. This was followed by 3x rinsing in ddH_2O for 30 s. The gel was then incubated for 20 min in silver soln (2 g $AgNO_3$ and 750 µl formaldehyde/l). After removing the silver soln with abundant ddH_2O, the proteins

were made visible by precipitating bound Ag^{2+} in developing solution (60 g Na_2CO_3, 0.5 ml formaldehyde and 20 ml 0.2 g/l $Na_2S_2O_3$ x $5H_2O$/l). Orange to brown bands appeared after 2-10 min and the reaction was quickly stopped by dousing the gel in 5% HAc.

2.7.5 Zymogram techniques

2.7.5.1 Staining for SOD activity

Staining for SOD activity was based on the procedure described by Beauchamp and Fridovich (1971), with slight modifications. 0.2 g of agarose were dissolved in 17 ml 50 mM KPP buffer (pH 7.5) and cooled to about 60°C. To this, 15 mg nitro blue tetrazolium (NBT; dissolved in 1 ml 50 mM KPP), 2 ml 1 mg/ml riboflavine (Serva) and 100 µl TEMED were added. After brief stirring the mixture was poured between two glass slabs (preheated to 60°C) and left to harden in the dark (ca. 5 min). Following gel electrophoresis, the gel was briefly rinsed in 50 mM KPP buffer (pH 7.5). After the IEF gel was spread on a glass plate, the overlay was placed directly on top and left to diffuse into the gel for 20 min in the dark. The enzyme reaction was initiated by removal of the overlay and exposure to light (40 watt bulb at a distance of ca. 20 cm) for 5-10 min. After light was absorbed by riboflavine, which transfers electrons to atmospheric oxygen, NBT was reduced by the superoxide, creating dark, indigo-coloured formazan. In gel areas which contained SOD, this reduction was prevented, creating lighter spots in the indigo-coloured background.

2.7.5.1.1 Inhibition of Cu,Zn SOD activity with DDC

The copper chelator diethyldithiocarbamate (DDC), which specifically inhibits Cu,Zn SOD (Cocco et al., 1981) was used to differentiate between the activities of Cu,Zn SOD and Mn SOD during SOD staining of IEF gels. After IEF electrophoresis, the gel was washed briefly in 50 mM KPP, pH 7.8 and divided into two identical halves.

An agarose overlay for detection of SOD activity was prepared; a second overlay, identical but for the addition of DDC (Fluka) to a final concentration of 1 mM, was also prepared. The detection of SOD activity followed the procedure as described above.

In an alternative experiment using the method of Iqbal and Whitney (1991), the gel was shaken gently for 1 h at 28°C in 50 mM KPP, pH 7.8 containing 50 mM DDC, while an identical gel was subjected to the same treatment without DDC. After rinsing the gels in 50 mM KPP, the gel was stained for SOD activity.

2.7.5.2 Staining for catalase activity

The staining of catalase activity was based on a method described by Clare et al. (1984). A peroxidase solution was made by dissolving 2.5 mg (w/v) horseradish peroxidase (Grade II, Roche) in 50 ml

50 mM KPP (pH 7.5). After IEF gel electrophoresis, the gel was rinsed briefly in KPP buffer (pH 7.5) and then gently shaken in peroxidase solution for 45 min at RT. After addition of 30 µl H_2O_2 to the solution, the gel was shaken further for 10 min. After removing the peroxidase solution and rinsing the gel briefly with ddH_2O, DAB solution (25 mg diaminobenzidine tetrahydrochloride x $2H_2O$/50 ml 50 mM KPP, pH 7.5) was poured over the gel. Within 2-5 min, the peroxidase used H_2O_2 to oxidise DAB, creating a brown stain. In gel areas containing catalase, the staining was prevented, creating colourless areas in the brown background.

2.7.6 Western Blotting

2.7.6.1 SDS-PAGE

SDS-PAGE was done according to the method of disc electrophoresis described by Lämmli (1970). A 12% (PAA) separation gel was created by combining 2.76 ml ddH_2O, 1.5 ml separation gel buffer (1.5 M Tris/HCl, pH 8.8), 1.83 ml 40 % PAA, 60 µl 10 % SDS, 3 µl TEMED and 30 µl 10 % (w/v) APS. The mixture was then poured between gel slabs of a MINI PROTEAN II™ gel apparatus (BIORAD), leaving about 3 cm space at the top of the plates, and overlaid with isopropanol. After at least 1 h of polymerisation followed by removal of the isopropanol, the stacking gel was added to the top of the separation gel. The stacking gel was created by combining 1.84 ml ddH_2O, 0.85 ml stacking gel buffer (0.5 M Tris/HCl, pH 6.8), 0.66 ml 40 % PAA, 35 µl 10 % SDS, 3.5 µl TEMED and 50 µl 10 % (w/v) APS; after insertion of a well comb, the gel was left to polymerise for at least 1 h. The gel-containing glass slabs were inserted into the apparatus as described by the manufacturers and filled with electrophoresis buffer (0.1 % SDS, 25 mM Tris, 192 mM glycine).

Lyophilised proteins were diluted 1:1 in 2x SDS-protein buffer (0,1 M Tris-HCl, 4% SDS, 20% glycerol, 0,002% bromphenol blue, pH 6,8), denatured by heat-treatment (100°C, 5 min) and added to the wells. Electrophoresis was performed at 25 mA for 2-3 h.

2.7.6.2 Blotting of gel proteins and Ponceau S staining

Proteins were transferred onto a nitrocellulose membrane (Schleicher and Schuell BA85) using the tank-blot method described in Ausübel et al. (1987) in a blotting buffer comprised of 25 mM Tris, 192 mM glycine and 20% glycerol (pH 8.3 without adjustment). The blotting took place over night at a constant current of 1.25 mA/cm^2 of membrane. Successful protein transfer was checked using the reversible Ponceau S (Sigma) staining technique: the blot was shaken for 5 min in staining solution (0.5 g Ponceau S dissolved in 1 ml 100% HAc ad. 100 ml ddH_2O) and de-stained in ddH_2O for 2 min, which resulted in the emergence of red-coloured protein bands. The blot was then de-stained in abundant ddH_2O.

2.7.6.3 Immuno-staining of blot proteins

The immuno-staining of CpSOD1 was done with primary antibodies directed against the *C. fusiformis* Cu,Zn SOD, produced from rabbit as described in De Vries et al. (1999), which were kindly provided by Onno De Vries. They were supplied as 1 ml aliquots of freeze-dried polyserum, which was taken up in 1 ml ddH_20, aliquoted and stored at -70°C.

The immuno-staining was done according to the method of A. Frey (pers. comm.) as follows: after rinsing the de-stained membrane briefly in TBS Buffer (0.137 M NaCl, 10 mM Tris/HCl, pH 7.8), it was shaken in blocking buffer (TBS-blotto), made by dissolving 5% (w/v) Glücksklee milk powder in TBS, for 30 min at 37°C. Extraneous blocking buffer was then removed from the membrane by 3x 10 min washing in TBST (10% Tween-20 in TBS). The membrane was then shaken for ca. 5 h in primary antibody solution, created by diluting the anti-CfSOD polyserum 1:500 in TBS-blotto. This was followed by three successive washing steps as described above. The secondary antibody (Anti-rabbit IgG, AP conjugate, Sigma) diluted 1:1 000 in TBS-blotto, was then added to the membrane and shaken for 1-2 h. After threefold washing, as described above, the membrane was equalibriated by 1 min incubation in AP-buffer (100 mM NaCl, 0.1 mol Tris/HCl pH 9.5, 5 mM $MgCl_2$). After pouring off the AP-buffer, the visualisation solution was then added to the membrane. The visualisation solution was created by adding 33 µl NBT-solution (100 mg in 1.9 ml 70% (v/v) DMF) and 17 µl BCIP-solution (100 mg BCIP in 1.9 ml DMF) to 5 ml AP-buffer. Where the secondary antibody had bound, alkaline phosphatase cleaved the phosphate group from BCIP and the resulting indol product was rapidly oxidised by NBT; reduced NBT (formazan) precipitate build an indigo-coloured stain, visible after about 5-10 min.

2.7.7 Determination of mycelial contamination of cell wall extracts with G6PDH

Determination of mycelial contamination was done by measuring the activity of glucose-6-phosphate dehydrogenase (G6PDH) in equal amounts of proteins from both fractions, using a method based on that described by Löhr and Waller (1965), and modified by G. Mey (pers. comm.). Enzyme activity is defined as the rate of NADPH increase, measured by monitoring the absorption at 340 nm. The increase of absorption at 340 nm was compared directly in both types of protein fraction as described below:

$$(\Delta A_{340}/min)_{cell\ wall} / (\Delta A_{340}/min)_{mycelia} \times 100\%$$

Enzyme buffer was prepared by combining 25 ml 0.1 M Tris, pH 7.4 and 1 ml 0.22 M $MgCl_2$ directly prior to use. 100 µg protein in 100 µl ddH_2O were added to 867 µl 1 enzyme buffer. To ¾ of the samples of each protein extract, 17 µl of a 16 mM $NADP^+$ stock (6.3 mg $NADP^+$/500 µl buffer) (Sigma) were added. To the fourth sample, 17 µl of buffer were added instead of NADP+. After de-

leting background absorbance at 340 mn, the reaction was started by the addition of 33 µl of a 4 mM glucose-6-phosphate (G6P) stock (1:5 diluted 5.6 mg G-6-P (Calbiochem)/ml buffer). The absorption at 340 nm was measured every 2 s for 100 s starting after 10 s. In two separate experiments, the rate of $NADP^+$-reduction was measured three times and a control to which no $NADP^+$ had been added was measured once. For each set of measurements, the A_{340} was plotted against time and the slopes of the three lines were averaged.

2.8 Generation and analysis of mutant strains

2.8.1 Transformation of *C. purpurea* strain 20-1 and derivatives

For the transformation of *C. purpurea* strain 20-1 and derivatives, which is based on a method described by van Engelenburg et al. (1989), mycelia was cultivated in one of two ways.

1: ca. 100 ml MA medium (with 1% glucose) were inoculated with 100 µl of a concentrated spore solution and cultivated on a rotary shaker at 180 rpm for 72 h at 28°C. The mycelium was harvested by washed once with sterile ddH_2O and suspended in protoplasting solution (1 g/ml).

2: 200 µl of a concentrated spore solution were plated out on cellophane-covered MA (10% sucrose) and incubated for 2-3 d at 28°C. The thin, hyaline-coloured fungal mat was peeled off the cellophane and transferred to a sterile petri dish containing 15 ml protoplasting solution.

The protoplasting solution contained 0.25 mg/ml Novozyme 234 (Novo, Bagsvaerd, Denmark) in SMaC buffer (0.2 M potassium maleate, 0.85 M sorbitol, 50 mM $CaCl_2$, pH 5.8) or 10 mg/ml Mutanase (Interspex Products, Inc, USA) and 2.5 mg/ml Driselase (Sigma, USA) in SMaC, pH 5.2. Following incubation on a rotary shaker at 80 rpm and 28°C for 1.5 h, the protoplasts were filtered through a sterile nytex membrane, pelleted by centrifugation, washed twice with STC buffer (0.85 M sorbitol, 10 mM Tris, 50 mM $CaCl_2$) and brought to a final concentration of 10^8 protoplasts/ml STC. Aliquots of 10^7 protoplasts were transformed with 10 µg vector as follows: 100 µl of protoplasts were combined with the DNA in 1x STC and 50 µl of a PEG solution (25% PEG 6000, 10 mM Tris-HCl, 50 mM $CaCl_2$, pH 7.5); after incubation for 5 min at RT, the 250 µl of solution were combined with 2 ml of PEG solution and incubated for a further 20 min at RT. The transformation process was stopped by dilution with 4 ml STC, added to 100 ml BII/8 agar (BII agar as described by Esser and Tudzynski, 1978, modified for transformation), which had been cooled to 48°C, and distributed among five petri dishes.

Selection of bleomycin-resistant transformants: after 4 h regeneration at 28°C, protoplasts were

overlaid with 10 ml BII/8 containing 100 µg/ml phleomycin (Cayla) (final concentration: 33 µg/ml). After 3-5 d growth at 28°C, bleomycin-resistant colonies were transferred to BII/8 plates containing 100 µg/ml bleomycin.

Selection of hygromycin-resistant transformants: after 24 h regeneration at 28°C, protoplasts were overlaid with 10ml BII/8 containing 4.5 mg/ml hygromycin B (Calbiochem-Novabiochem); after 3-5 d growth at 28°C, hygromycin-resistant colonies were transferred to BII/8 plates containing 1.5 mg/ml hygromycin.

2.8.2 Cultivation and analysis of *C. purpurea* transformants

Nine transformants and the recipient strain were inoculated with sterile toothpicks on one plate containing either 100 µg/ml phleomycin or 1.5 mg/ml hygromycin. After 6-8 d incubation at 28°C, mycelia was stamped from each transformant colony with the wide end of a sterile pasteur pipette and lyophilised. Genomic DNA, isolated according to 1.4.1.2, was taken up in 30 µl ddH_2O and incubated for 10 min at 60°C. After vortexing and collection by centrifugation, 2 µl DNA were used per PCR reaction with analytic primers. PCR (50 µl volume) was carried out in 96 well tube plates (Eppendorf); 10 µl of each reaction were analysed via gel electrophoresis.

2.8.3 Pathogenicity assays

Spores of the strains to be tested were obtained and their concentration determined as described in 2.2.2. As the virulence of strains is gauged by observing infections caused by inoculation of rye flowers with equal amounts of conidia, the germination rate of mutated strains was compared to that of the wild type by plating out a defined number of spores (200-500) on MA and counting colonies after 3-4 d.

For use as inoculum in the pathogenicity assays, spores were centrifuged at 14 000 rpm for 15 min and taken up in 60 % sucrose to a final concentration of 10^8. In this solution, they can be stored for 1-2 months at 4°C without affecting the germination rate (Platford and Bernier, 1975).

Pathogenicity assays were based on a method described by Voß (1996). All flowers of one ear were inoculated during the 1-2 d blooming period, preferably shortly before the emergence of the ripe pollen sacks from a majority of blossoms. Directly before inoculation, the spores were diluted 10^2-fold with ddH_2O to a concentration of 10^6. 5 µl of this suspension were pipetted once into each rye flower; one each ear, 40-80 flowers were individually inoculated. To prevent cross infection by insect vectors or ear to ear contact, paper bags were fastened over each infected ear, and disease was monitored through cellophane "windows" (prepared by tearing off one side of the bag and gluing a cellophane sheet in its place).

2.8.4 Testing paraquat sensitivity of wild type and mutant strains

The paraquat sensitivity of germinating conidiospores was examined according to Chary et al. (1994). 250 spores were plated on Mantle agar with and without 100 µM paraquat (methyl viologen, Sigma) and incubated at 28°C for 3-5 d. Growth tests were done by inoculating MA plates with and without 5 mM paraquat with mycelia from the various strains which were stamped out of plate-grown colonies using the large end of a pasteur pipette. After cultivation for 8 d at 28°C, the colony diameters were determined.

2.9 Computer-based analysis of DNA and protein sequences

Manipulation of sequence data: Raw sequence data was assembled into continuous sequences using SeqMan™ and edited in both SeqMan™ and EditSeq™. Conceptual translation and mapping were done in EditSeq™ and MapDraw™, respectively. Protein alignments and phylogenetic analyses were done with MegAlign™, while primers were determined with the help of PrimerSelect™. All of the above programs are part of the Lasergene package, Version 4.03, 1989-1999, DNA-STAR, Inc.

Creation of publishing formats: Publishing formats were created with the "publish" program from Heidelberg Unix Sequence Analysis Resources (HUSAR), German Cancer Research Centre Heidelberg.

Data base homology comparisons: These were done on the internet with the help of Blast provided by the National Centre for Biolotechnology Information (NCBI) at: **http://www.ncbi.nlm.nih.gov/BLAST** using the standard protein-protein Blast (BlastP) or translated Blast (BlastX).

Promotor analysis: This was done using "MatInspector professional (enhanced version)" offered by Genomatix at **http://transfac.gbf.de/programs/matinspector/matinspector.html** This program is based on a method developed by Quant et al. (1995).

Domain recognition: Protein sequences were scanned for conserved domains using PROSITE, a data base of protein families and domains (Bucher and Bairoch, 1994, Falquet et al., 2002) at: **http://www.expasy.org/prosite/** provided by the ExPASy Mo-

lecular Biology Server.

Localisation of targeting signals: Protein sequences were scanned for targeting signals using PSORTII prediction at PSORT (a prediction of protein sorting signals and localisation sites in amino acid sequences) at :**http://psort.nibb.ac.jp/** (Nakai and Kanehisa, 1992).

Source of published sequences: Published protein and DNA sequences for comparison were taken from the GenBank Database at NCBI using Entrez at: **http://www.ncbi.nlm.nih.gov/entrez/query.fcgi**

3 Results

3.1 Cloning and analysis of a cell-wall associated Cu,Zn SOD in *Claviceps purpurea*

During amino-terminal protein sequencing of abundant cell wall-associated proteins in the non-pathogenic alkaloid production strain *Claviceps fusiformis* 26245, a protein with strong homologies to Cu,Zn superoxide dismutases (CfSOD1) was identified. In order to investigate the importance of this protein for pathogenicity, polyclonal antibodies directed against this protein were isolated (Moore et al., 2002) and were used to probe for a homologous protein in the pathogenic strain *Claviceps purpurea.* After conditions were found in which this protein is highly expressed, cDNA template was generated for isolation of the corresponding gene using a heterologous PCR approach.

3.1.1 Identification of a CfSOD1-homologue in *Claviceps purpurea*

The CfSOD1 protein was first localised in 60% ethanol extract from cultures of *C. fusiformis* after 6 d growth in minimal medium (MM) (Moore , 1997). In order to investigate the expression of the homologous protein in the *C. purpurea* strain T5, the fungus was cultivated for 4 and 6 d in minimal and complete media. *C. fusiformis* was cultivated under conditions which express CfSOD1 as a positive control. Extracts obtained by washing intact mycelia with 60 % ethanol were separated using SDS-PAGE and subjected to western analysis followed by immuno-staining with the anti-CfSOD1 antibody. Analysis of proteins corresponding to 10 mg of freeze dried mycelia showed a strong signal at the 18 kDa position in the positive control lane, as well as a much weaker signal at the same position in the *C. purpurea* protein extracts after 4 d in a complete medium. No signal was seen in the other extracts from *C. purpurea* (data not shown).

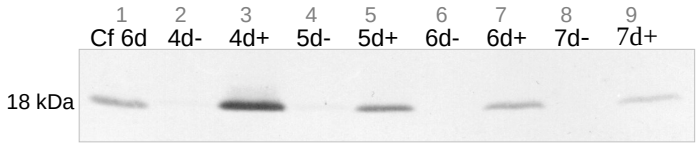

Fig. 3.1: Immuno-staining of *C. purpurea* proteins extracted from cultures grown with and without copper supplement. Each lane contains proteins extracted from the cell wall with 60 % ethanol corresponding to 10 mg freeze-dried mycelia. Separation of proteins using SDS-PAGE was followed by western blotting and immuno-staining with the anti-CfSOD1 polyserum. Lanes 1-9 (left to right): 1. *C. fusiformis* 6 d MM without copper (positive control). Lanes 2-9: *C. purpurea* MA without (-) and with (+) supplementation of 50 µM $CuSO_4$, harvested after 4-7 d, respectively. The antibodies were kindly provided by Onno MH DeVries.

As in *S. cerevisiae* the CuZn SOD activity was doubled by supplementing the media with copper (Greco et al., 1990), *C. purpurea* was cultivated in MA-medium with and without a 50 µM copper supplement and har-

vested after 4-7 d. The proteins were extracted and analysed as described above. The results are shown in fig. 3.1. The *C. fusiformis*-derived positive control in lane 1 shows a band at the 18 kDa position. In the *C. purpurea* extracts, a signal at the same position, which is strongly copper-dependent, reacts with the antibody. The signal is strongest after 4 d and weakens with each continuing day of culture. Apart from some (probably unspecific) staining in the region which corresponds to the top of the separation gel, the 18 kDa band represents the only signal in the *C. purpurea* extracts (data not shown).

3.1.2 Analysis and localisation of SOD activity in axenic culture

In order to confirm the identity of the copper-induced protein which was recognised by the anti-CfSOD1 antibody as a functional superoxide dismutase, the cultures were examined for SOD activity. Protein extracts derived from the culture filtrate, the cell wall and the mycelia were separated by isoelectric focussing and the gel was stained for SOD activity. Proteins of the cell wall fraction were isolated by gentle washing of the lyophilised mycelia in buffer, while mycelial fractions were extracted in the same buffer from mycelia ground under nitrogen and homogenised by repeated vortexing and pipetting. To ensure that the activity present in cell wall fractions was not caused by leaking of cytoplasmatic content through the lyophilised (and possibly damaged) cell membranes, both fractions were examined for activity of a cytoplasmatic marker enzyme. As the SOD staining does not distinguish between Cu,Zn SOD, Mn SOD or other sources of superoxide decay, the effect of a Cu,Zn SOD inhibitor on the staining pattern was examined.

3.1.2.1 SOD activity in culture filtrate, cell wall and mycelia of *C. purpurea*

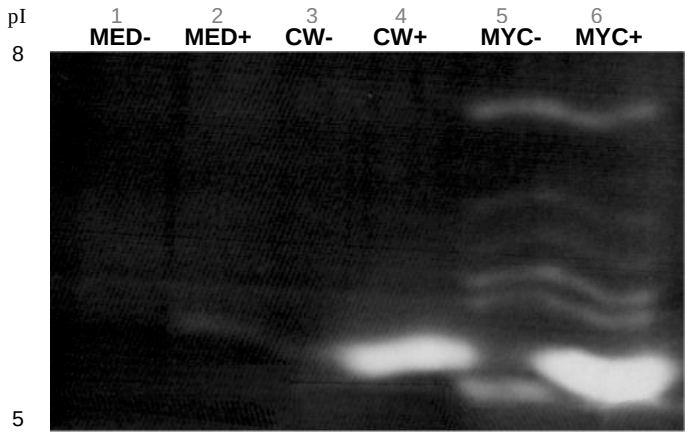

Fig. 3.2: Localisation of SOD activity in axenic culture of *C. purpurea*. Protein fractions, extracted from cultures with and without supplementation with 50 µM $CuSO_4$, were separated by isoelectric focussing within a native PAGE gel pI 5-8 and then stained for SOD activity. Each lane contains protein corresponding to 10 ml of culture filtrate or 10 mg of freeze-dried mycelia. Lanes 1-6: Proteins from the culture filtrate (MED), cell wall (CW) and mycelia (MYC) cultivated without (-) and with (+) copper. Numbers on the far left indicate pI.

After separation on a IEF gel, proteins isolated from cultures grown for 4 d in a complete medium with and without 50 µM copper supplement were stained for SOD activity. Fig. 3.2 shows such a gel; among the mycelial proteins (compare lanes 5 and 6) many weak but non-copper dependent bands of activity are visible as well as one strong band which is strongly copper-dependent. Comparison with the pI of isoelectric marker proteins places the pI of this activity at 5.2 (data not shown). The activity seen in these lanes corresponds

to 10 mg of mycelia, as does the activity seen in lanes 3 and 4, which show the SOD activity present in the cell wall extracts. Here, only one band of activity is visible; in pI and copper dependency it corresponds to the main band of the mycelial extract. In comparison, the amount of activity in the cell wall fraction is slightly less than in the mycelial fraction, which indicates similar activity within the cytoplasm. In lanes 1 and 2, in which proteins isolated from 10 ml of culture filtrate have been loaded, a slight activity band of a similar pI is visible among the proteins isolated from copper-induced culture.

These results all point to the presence of a strongly copper-dependent superoxide dismutase which is associated with the cell wall. Although there are other activities present in these cultures, the putative Cu,Zn SOD (named SODA) seems to be the main superoxide dismutase which is expressed under these conditions. To strengthen the evidence that this activity corresponds to the protein recognised by the anti-CfSOD1 antibody, the same protein fractions were subjected to western analysis, as depicted in fig. 3.3.

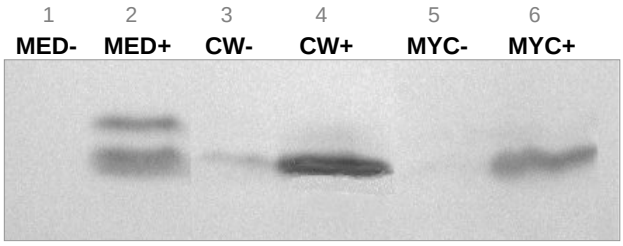

Fig. 3.3: Localisation of the protein recognised by the anti-CfSOD1 antibodies. Protein fractions, extracted from cultures with and without supplementation with 50 µM $CuSO_4$, were separated by SDS-PAGE and subjected to western analysis followed by immuno-staining with the anti-CfSOD1 antibodies. Each lane contains protein corresponding to 10 ml of culture filtrate or 10 mg of freeze dried mycelia. Lanes 1-6: Proteins from the culture filtrate (MED), cell wall (CW) and mycelia (MYC) cultivated without (-) and with (+) copper. Comparison of the main immuno-reactive band to molecular weight markers places its apparent molecular weight at 16-18 kDa (data not shown).

Here as well, the putative Cu,Zn SOD is present in culture filtrate, cell wall and mycelial fractions. Interestingly, two isoforms are present in the culture filtrate. Either the different apparent molecular weight does not result in variation of the pI, or there is a second protein recognised by the anti-CFSOD1 antibody which is only present in the culture filtrate and which lacks SOD activity.

3.1.2.2 Analysis of cytoplasmatic contamination in the cell wall fraction by measurement of G6PDH activity

Glucose-6-phosphate dehydrogenase (G6PDH), the first enzyme of the pentose phosphate pathway, is found only in the cytoplasm. In order to assess the amount of cytoplasmatic contamination in the cell wall protein fractions, the activity of this enzyme, defined by the rate of NADPH production (measured by absorption at 340 nm), was compared in the same amount of protein from cell wall and mycelial fractions. The contribution of other, possibly cell wall-associated, enzymes to the rate of $NADP^+$ reduction was determined by the inclusion of controls to which no glucose-6-phosphate had been added. While the controls showed no detectable increase of NADPH concentrations, measurement of cell wall and mycelial fractions show that the contamination of cell wall proteins with cytoplasmatic proteins is about 13% (table 3.1).

$(\Delta A_{340}/min)_{cell\ wall}$	$(\Delta A_{340}/min)_{mycelia}$	% contamination
0.0117 (± 0.0029)	0.0867 (± 0.0064)	13
0.0060 (± 0.0017)	0.0480 (± 0.0075)	12.5

Table 3.1: Comparison of G6PDH activity in protein extracts derived from cell wall-associated and mycelial protein extracts. Each value is derived from 3 separate measurements of the same extract; the standard deviation is shown in brackets. The first and second experiment was done with 100 and 75 µg protein, respectively.

3.1.2.3 Direct comparison of SODA activity in cell wall and mycelial protein fractions.

As comparison of protein fractions to determine the amount of cytoplasmatic contamination in the cell wall fraction were based on equal amounts of protein rather than mycelia, the same amounts of protein (150 µg) were separated on an IEF gel and their SODA activity compared. Fig. 3.4 shows the amount of SOD activity in each lane. Despite the fact that only 13% leakage from the cytoplasm could contribute to the SODA activity in the cell wall fraction, there is at least the same amount of activity in both fractions, indicating that a substantial part of the SODA protein is secreted.

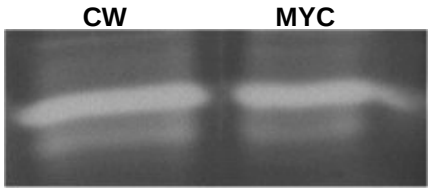

Fig. 3.4: Direct comparison of SODA activity in cell wall-associated and mycelial proteins. Each lane shows SOD activity staining after isoelectric focussing of 150 µg protein. Left: proteins of the cell wall fraction. Right: proteins of the mycelial fraction.

3.1.2.4 Determination of SOD-type using a Cu,Zn SOD inhibitor

As the applied protocol for activity staining does not distinguish between Cu,Zn-, Mn-, or Fe-SODs, the effect of diethyldithiocarbamate (DDC) on SODA activity was examined. DDC is a copper chelator and thus specifically inhibits the activity of Cu,Zn SODs (Holdom et al., 1996). In order to test the effect of DDC, mycelial protein fractions with and without copper were separated on an IEF gel and stained for SOD activity with and without inclusion of DDC in the staining overlay. The result is shown in fig. 3.5. The left side without DDC in the overlay shows strong SODA activity, while the right side in which DDC was added to the overlay shows a marked decrease in SODA activity.

In these experiments, only the activity of SODA was affected by the copper chelator. This indicates that the other activities originate from Mn SODs or other proteins with the ability to oxidise superoxide without the use of copper.

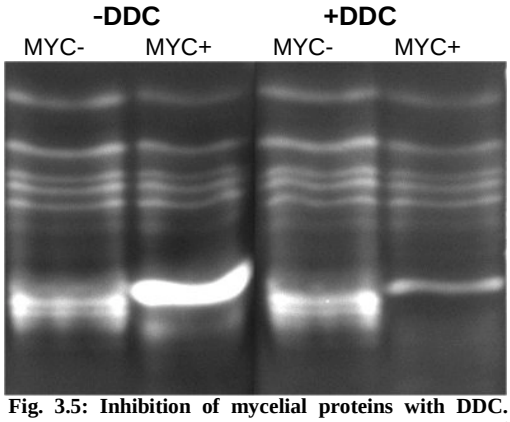

Fig. 3.5: Inhibition of mycelial proteins with DDC. Each lane contains proteins corresponding to 10 mg of mycelia (cultivated with and without supplement with 50 µM $CuSO_4$) separated by IEF gel electrophoresis and stained for SOD activity. Left two lanes: without inclusion of DDC in overlay for activity staining, without copper (MYC-) and with copper (MYC+). Right two lanes: same, with inclusion of 1 mM DDC in overlay.

3.1.3 Isolation and sequencing of a Cu,Zn SOD from *C. purpurea*

Cu,Zn SODs are highly conserved proteins with an overall primary sequence homology of about 50-56%; among yeast and fungi the homology rises to 68% (Gralla and Kosman, 1992). Proteins with this degree of homology can often be easily cloned using heterologous PCR with degenerate primers. As a template for gene isolation, mRNA has the advantage over genomic DNA in containing a larger ratio of the sought-after template to total nucleic acid as well as lacking introns which could jeopardise the binding of primers designed from protein sequences.

3.1.3.1 Heterologous PCR using cDNA template.

Using the CODE-HOP theory of primer design (Rose et al., 1998) in which the degree of degeneration is minimised using an invariant core region at the 5' end and a variable clamp region at the 3' end, primers SOD1.1, SOD2.1 and SOD2.2 were constructed against the most conserved regions of Cu,Zn SODs. Cultures of *C. purpurea* strain T5 were grown for 4 d in a complete medium and expression of the putative Cu,Zn SOD was confirmed via western analysis as described in 3.1.1 (data not shown). Template for the PCR reaction was generated from mRNA by cDNA synthesis using an oligo-dT primer. As primer degeneracy resulting in low concentrations of the "correct" primer is a major problem of heterologous PCR, primer concentrations of both 1 and 2 µM were tested. In order to be able to screen PCR products for homology to Cu,Zn superoxide dismutases, a 544 bp fragment spanning the most conserved regions of *ncsod1* (encoding a Cu,Zn SOD) was amplified from *Neurospora crassa* and, after ensuring via non-stringent Southern analysis that a homologue was present in genomic DNA from *C. purpurea* (data not shown), was used to probe the amplified fragments (fig. 3.6). The increase of primer concentration from 1 to 2 µM only results in an overall increase of all products without influencing the specificity of primer binding. The combination of primers SOD1.1 and SOD2.1 (lane 1) gives rise to a strong and specific PCR product of approximately the expected size (ca. 240 bp); lanes 3 and 4 show that each primer alone does not produce the same product. The combination of primers SOD1.1 and SOD2.2 does not produce any product. Hybridisation shows that the product amplified with SOD1.1 and SOD2.1 has homology with the gene

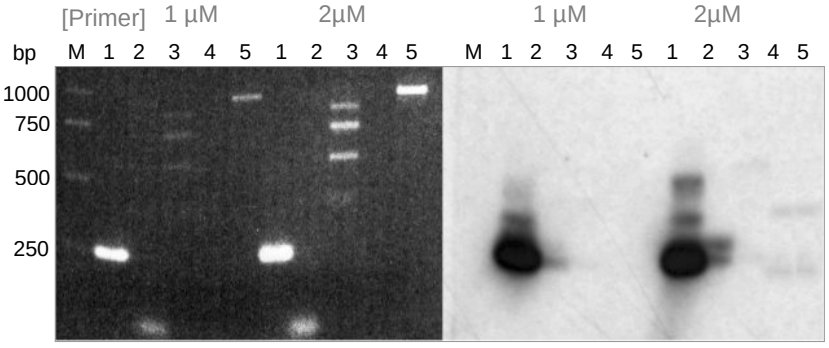

Fig. 3.6: Amplification of a Cu,Zn SOD gene fragment using heterologous primers. Left: Ethidiumbromide-stained PCR products after gel electrophoresis. Right: Southern analysis of the same gel; after blotting, the filter was hybridised at 56°C with the *ncsod1* probe. The PCR reactions 1-5 were repeated using a primer concentration of 1 and 2 µM. Lanes M: 1 kb DNA ladder, 1: SOD1.1 + SOD2.1, 2: SOD1.1 + SOD 2.2, 3-5: SOD1.1, SOD 2.1 and SOD2.2 only, respectively (negative control).

encoding the Cu,Zn SOD of *N. crassa*.

The hybridising PCR product was cloned into the PCR 2.1 vector and resulting clones were analysed by digestion with *Eco*RI and Southern analysis of the restriction products using the probe from *ncsod1* (data not shown). Clones which carried a hybridising fragment of the correct size were sequenced; BlastX analysis of the 245 bp fragment showed that the fragment was strongly homologous to other fungal Cu,Zn SODs (top homology was to SOD1 from *N. crassa*; score 353, probability $1.5e^{-42}$).

The gene corresponding to the sequenced cDNA fragment was named *cpsod1*. The cDNA fragment was then used to probe a genomic library of *C. purpurea* for isolation of *cpsod1*.

3.1.3.2 Isolation and sequencing of the *cpsod1* gene

After determination of the copy number via Southern analysis, the *cpsod1* gene was isolated from a genomic library, subcloned and sequenced. The derived protein sequence was compared with those of other Cu,Zn SOD genes and the promotor was searched for metal response elements.

3.1.3.2.1 Genomic Southern with the *cpsod1* probe

In order to determine the copy number of *cpsod1*, as well as to investigate the existence of further Cu,Zn SODs, a genomic Southern blot was hybridised with the *cpsod1* probe at 65°C and 60°C. Shown here (fig. 3.7) is the less stringent Southern analysis. As restriction with four different enzymes generates only one hybridising fragment, it was concluded that *cpsod1* is a single copy gene. Restriction with *Bam*HI and *Hin*dIII releases hybridising fragments of ca. 7.2 kb and 6.6 kb, respectively. The *Eco*RI fragment is too large to allow an accurate estimate of its size. Furthermore, the hybridisation at this temperature already results in a myriad of unspecific bands, indicating that no homologue of this gene is present in *C. purpurea*.

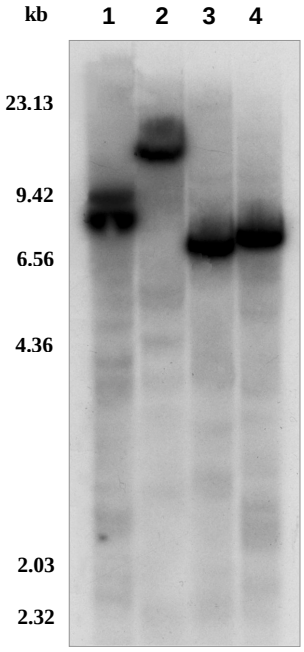

Fig. 3.7: Non-stringent Southern analysis with *cpsod1*. Genomic DNA from *C. purpurea* probed with *cpsod1* at 60°C. Lanes 1-4: DNA digested with *Bam*HI, *Eco*RI, *Hin*dIII and *Sal*I, respectively.

3.1.3.2.2 Isolation and sequencing of genomic *cpsod1*

A total of 50 000 λ-clones from the *C. purpurea* EMBL3 genomic library were screened for homology with the *cpsod1* probe. In the first round, plaques corresponding to eight signals were picked and plated in a further screening round; from those plaques, six were purified. The DNA of six λ-clones was isolated and digested with *Eco*RI and *Sal*I; four different λ-types were identified and subjected to further restriction and Southern analysis. As the hybridising fragment of all clones contained an *Xho*I site, both fragments released by *Sal*I/*Xho*I-restriction from the clones S2λ2/1and

S2λ8/1 were subcloned and sequenced. Fig 3.8 shows the subcloning strategy as well as a map of the sequenced region.

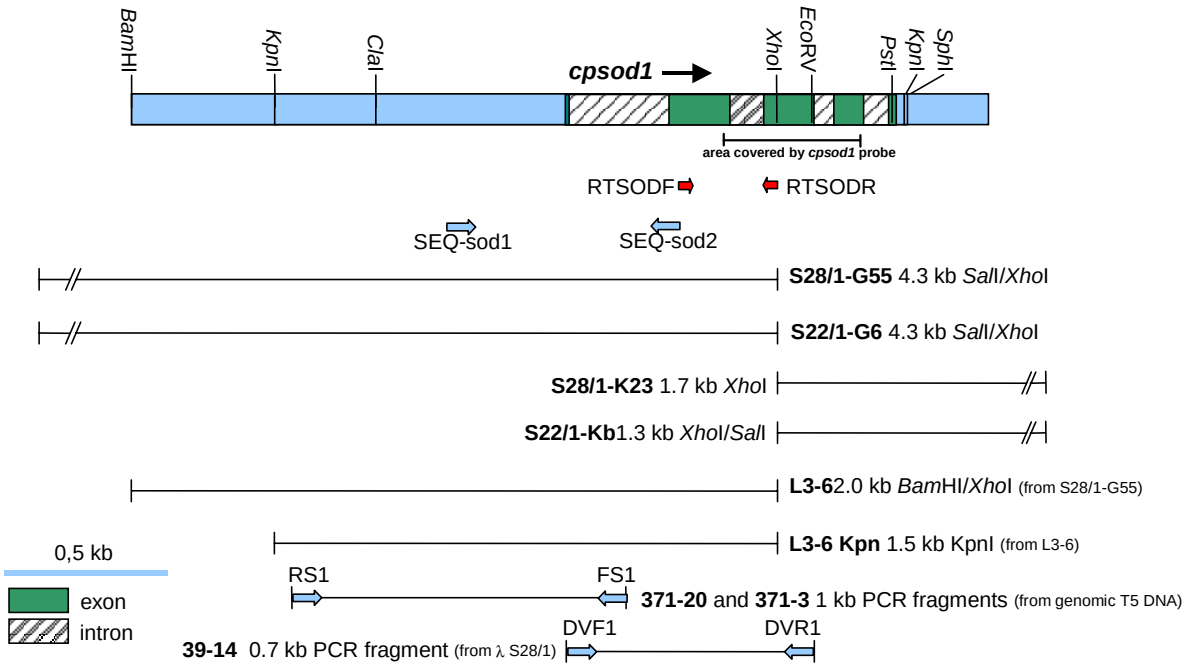

Fig. 3.8: Restriction map and subcloning strategy of the *cpsod1* genomic region. All subclones are derived from the λ-clones S2-2/1and S2-8/1. After restriction with *Xho*I both the large (G) and small (K) hybridising fragments were subcloned from each λ-clone, yielding the primary subclones S22/1-G6, S22/1-Kb, S28/1-G55 and S28/1-K23. All other clones were obtained either by subcloning these primary clones or by PCR of genomic (*C. pupurea* strain T5) or λ-DNA. All λ-fragments and their subclones were cloned into pBS; all PCR fragments were cloned into the PCR2.1 vector. In both cases, sequencing was done with universe and reverse primers. When raw sequence data was obtained from PCR fragments, at least two separate clones were sequenced each time. Primers are indicated by arrows; SEQ-sod1 and -sod2 are specific sequencing primers which were used to obtain data from the S28/1-G55 subclone. Red arrows denote RT-PCR primers. The intron and exon pattern was obtained by comparison with cDNA.

In order to determine the amount and position of introns within the *cpsod1* gene, the *C. purpurea* strain P1 cDNA library was screened for full-length clones. About 60 000 clones were screened with the *cpsod1* probe. Of the 19 positive signals in the first round, eight single signals were obtained in a second round. The pBS vectors carrying the cDNA inserts were excised; restriction with *Eco*RI and *Xho*I released the inserts from the vector in three of eight clones. Of those three clones, only one was full-length: S42d, with an insert length of 785 bp. Comparison of this clone to the genomic sequences revealed the exact position and number of introns, which are shown in the sequence below. The open reading frame is stretched along 1009 bp; this is interrupted by five introns which together account for 547 bp or 54% of the total nucleotides. The large numbers and size of the introns is typical for the *sod1* genes of other filamentous fungi (fig. 3.9).

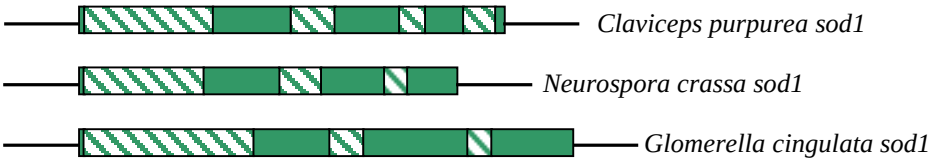

Fig. 3.9: *Sod1* exon pattern of filamentous fungi.

The sequenced region of 2.6 kb encompasses *cpsod1*, as well as 1.3 kb upstream and 0.3 kb downstream of the coding regions. The nucleotide sequence and its derived amino acid sequence is shown in appendix A.1. The putative Cu,Zn SOD comprises 154 aa with an estimated molecular weight of 15.8 kDa and a predicted pI of 6.2. PROSITE analysis of the putative protein shows both signatures for Cu,Zn superoxide dismutases (see A.1).

As the Cu,Zn SOD is a very small protein (ca.150 aa), which folds into a highly compact monomer, and two monomers associate to form a tightly-knit dimer in the active form, a large amount of residues are invariant. The seven residues which ligand the copper and zinc ions are conserved in *cpsod1*(see A.1), as are residues making up and stabilising the active centre and those building an electrostatic gradient designed to tunnel the negatively charged superoxide towards the catalytic copper ion. The conserved cysteins at positions 58 and 147 form a disulfide bridge across almost 2/3 of the primary sequence, contributing to the high stability of the monomer. Other invariant residues are those along which the monomer associates into its dimeric form; furthermore, a large number of glycins are conserved for their small size, crucial in such a tightly compact protein (Bordo et al., 1994). The conservation of residues invariant in other Cu,Zn SODs supports the identity of the *cpsod1*-derived protein as a functional enzyme.

The homology of the derived protein product of *cpsod1* and other fungal Cu,Zn SODs was compared by clustal analysis (a phylogenetic tree is shown in fig. 4.1). The overall homology is very high, ranging from 85 % with *N. crassa* SODC (gene product of *sod1*) to 64% with the *Filobasidiella neoformans* SODC protein. The *cpsod1* gene product groups with the other filamentous fungal Cu,Zn SODs, while the yeast proteins group together.

3.1.3.2.3 Promotor analysis

The 1 kb sequence directly preceding the *cpsod1* start codon, defined as the ATG directly upstream of the termination of homology with other fungal Cu,Zn SODs, was analysed for putative promotor elements and indicated in red type in A.1). An N-terminal signal sequence for secretion (as defined by von Heijne, 1986) could not be located. The choice of start codon could be supported by the nucleotides immediately preceding the start codon; the consensus CA(C/A)(A/C) for bases at position –4 to –1 is fulfilled with CACA (Ballance, 1991).

Since the protein thought to correspond to *cpsod1* is induced by copper, the promotor was examined for elements involved in copper regulation. In yeast, two major copper response elements (CuREs) have been identified: the ACE-binding domain, responsible for inducing the transcription of genes under conditions of excess copper, and the MacI-binding domain, which binds a positive regulatory protein only under conditions of copper deprivation (Winge et al., 1997). Transcriptional sensing of copper could also be under the control of a less specific metal response element (MRE), as is the case in the promotor of the rat Cu,Zn SOD (sod1) (Yoo et al., 1999). Interesting would also be the presence of iron-sensing elements; because of their role as Fenton catalysts, both copper and iron are potential oxidative threats. In yeast, the Aft1 protein is a MacI functional homologue for iron sensing; under conditions of excess iron, it mediates the repression of genes such as those involved in high-affinity iron uptake (Martins et al., 1998). Of these elements, a putative inverted ACE-binding region was found at –460 bp, and two putative MREs were found at –106 and –615 bp (indicated in blue type in app. A.I). Of the latter, one adheres perfectly to the consensus sequence TGC(A/G)CNC, TCGACTC at –615 bp, while the second (TGCTCTC at –106 bp) deviates slightly at the variant position. No putative elements involved specifically in iron-sensing could be found in the *cpsod1* promotor.

3.1.4 Expression analysis of *cpsod1*

3.1.4.1 Expression of *cpsod1* in axenic culture

The influence of different factors on the expression of *cpsod1* in axenic culture was investigated using northern analysis. Because of the presence of a putative ACE-binding region in the promotor as well as the copper-dependency of SODA activity, the influence of copper on the expression of cpsod1 was examined. Copper is also a Fenton catalyst and may indirectly induce transcription by raising the concentration of superoxide, hydrogen peroxide and other species of active oxygen (see 1.1.1). If this is the case, then iron, another powerful Fenton catalyst, should also increase transcription. Furthermore, the putative metal response elements in the promotor could mediate the regulation of metals by transcription. The effect of more direct sources of AOS on the transcription of *cpsod1* was also tested. Superoxide generators such as the redox cycler paraquat and the enzyme system xanthine/xanthine oxidase, as well as H_2O_2, were used in these experiments. The results are summarised in fig. 3.10.

In the copper- and iron-induction experiments, the metal was added as a sulfate salt to the medium directly before inoculation. As the media contained yeast extract and no chelator was added, the non-induced cultures will have contained trace amounts of metal. Addition of 75 µM $CuSO_4$ (A) to the cultures results in a strong induction of the *cpsod1* transcript. Addition of 118 µM or 500 µM iron sulfate (B) also seems to induce transcription of this gene in comparison to cultures to which no iron had

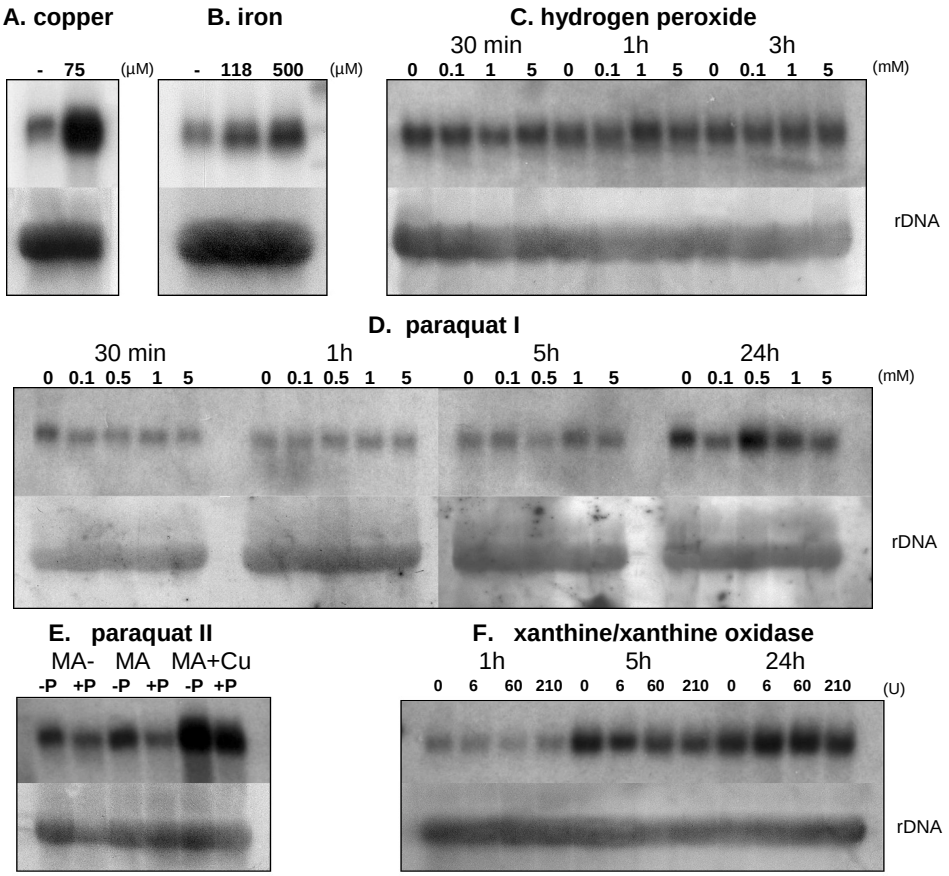

Fig. 3.10: Effect of metals and AOS on the expression of *cpsod1*. Total RNA was isolated from cultures grown for 4 d in MA (with the exception of the two leftmost lanes in (E), which were grown in MA^-) and probed with the 245 bp cDNA fragment of *cpsod1*. In each case, hybridisation with rDNA (*Giberella fujikuroi*) provides a loading control. When variant, the concentration of added substances and induction-times are given in the figures; units are indicated on the right. The effect of copper and iron is shown in (A) and (B); 75 µM $CuSO_4$, 118 µM or 500 µM $FeSO_4$ were added to cultures directly before inoculation. The effect of AOS on transcription is shown in (D)-(F); here, addition of AOS or AOS generating substances was done at the indicated time prior to harvest. (C) H_2O_2 (D) paraquat I (E) paraquat II (concentration of paraquat in +P cultures was always 10 mM, added 5 h prior to harvest; MA+Cu refers to supplementation of medium with 50 µM of $CuSO_4$). (F) Xanthine/Xanthine oxidase (the substrate concentration was constant at 400 µM and units of xanthine oxidase were varied as indicated in the picture.) Here, mycelia was transferred to a special buffer for the incubation period (details are given in 2.6). To avoid induction by general stress involved in treating the cultures, controls were treated with the same volume of water.

been added.

Interestingly, both AOS and AOS generating systems do not induce transcription of *cpsod1*; (C) shows that direct addition of H_2O_2 in concentrations between 0.1 and 5 mM does not result in an increase of signal strength compared to the control (to which H_2O was added) when monitored 30 min, 1 h or 3 h afterwards. The effect of superoxide generating systems such as paraquat or xanthine and xanthine oxidase were also examined and found to have no inductive effect. Unlike H_2O_2, which can easily pass through membranes, superoxide will stay on the side of the membrane on which it is generated, so that external and internal generation should result in the activation of different signal pathways. Alterations in the level of *cpsod1* transcription was measured 30 min, 1 h, 5 h and 24 h after the addition of 0.1, 0.5, 1 and 5 mM of paraquat, which causes generation of superoxide within the cytoplasm; in each case there was no significant difference to the control, to which H_2O had been added (D). In fact, a further experiment, in which the effects of simultaneous addition of high concen-

trations of paraquat (10 mM) and copper were tested (which theoretically should result in a vicious production of the hydroxyl radical) showed that while addition of copper with or without paraquat induced transcription, addition of paraquat caused a reduction of transcription (E, four rightmost lanes). The reduction of transcript amount, which is probably a result of general cell damage due to the high concentrations of toxin rather than the triggering of AOS dependent signal pathways, is also seen in the first two lanes of (E), in which cultures grown in reduced sugar were tested for reaction to paraquat.

Treatment of the cultures with xanthine and xanthine oxidase, which generates extracellular superoxide, had no effect on *cpsod1* transcription (F). Interestingly, the transcript amount seems to be increased 5 h and 24 h after addition of the inductors; as this is also true for the H_2O–treated controls, this effect can not be superoxide-mediated.

Together, these results indicate that although *cpsod1* can be induced by metals such as iron and copper (factors which contribute to the generation of AOS), it does not seem to be induced by either internally or externally generated superoxide or hydrogen peroxide. Furthermore, there is some indication of other (yet unknown) factors mediating changes in *cpsod1* transcription, as induction of control cultures can be seen after 5 h (F) as well as after 24 h in (D) and (F).

3.1.4.2 *In planta* expression analysis of *cpsod1* using RT-PCR

In order to investigate the *in planta* expression of *cpsod1*, total RNA from rye infected with *C. purpurea*, strain T5, was used as a template in RT-PCR experiments. The infection is temporally divided into four phases, the earliest of which is phase I, in which the mycelia targets ovary vascular tissue and establishes the host-pathogen interface; phase I mycelia is harvested about 5 dpi. Conidiating phase II mycelia is harvested during honeydew production after about 10 d, while phase III is harvested five days later, when the entire ovary has been colonised with sphacelial mycelia and the differentiation to sclerotial mycelia has begun. The final phase of infection, represented by phase IV, is harvested about 20 dpi. At this time the young sclerotia is fully formed although not yet ripe. To ensure that the amplified fragments originate from *Claviceps* and not rye mRNA, the products were hybridised with *cpsod1*. The results are shown in fig. 3.11.

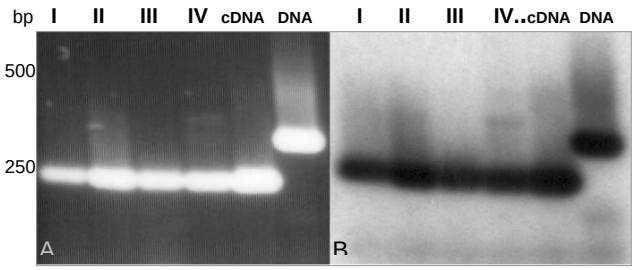

Fig. 3.11: Expression of *cpsod1 in planta*. A. RT-PCR products. Template for the PCR: Phase I-IV mRNA, S42d (cDNA), genomic 20-1 DNA. B. Southern analysis. The gel shown in A was blotted and probed with the 245 bp cDNA fragment of *cpsod1* at 65°C. The positions of the 250 bp and 500 bp fragments of the 1 kb ladder are indicated on the far left in bp.

Lanes I-IV of (A) represent the phases I to IV as described above. In each lane, a strongly amplified band is present which corresponds to the expected size of 228 bp and hybridises with *cpsod1* (B). The *in planta* expression of *cpsod1* thus seems to be con-

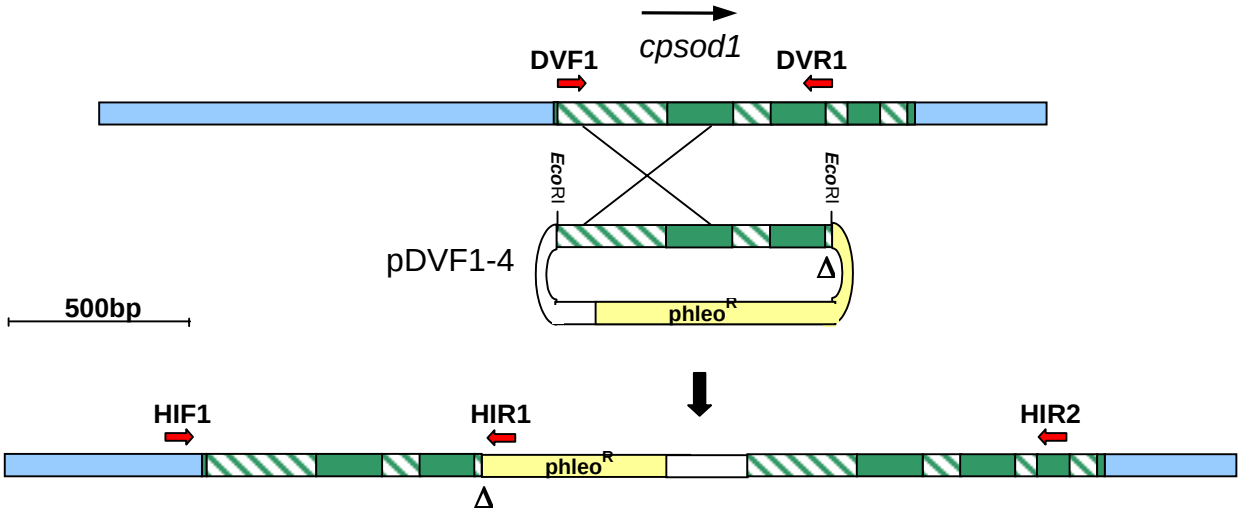

Fig. 3.12: Gene disruption strategy for *cpsod1*. ***Cp****sod1* is depicted in green, exons are solid and introns are striped, surrounding genomic regions are blue. Red arrows are PCR primers: DVF1 and DVF2 were used to amplify the disruption fragment, and HIF1, HIR1 and HIR2 were used in analysis of the transformants. pDVF1-4 is pAN8-1 derived circular transformant vector, containing the phleomycin cassette (yellow) and pUC18 (white) as well as the disruption fragment. All DNA is shown to scale with the exception of the pAN8-1 derived regions of the disruption vector. Black arrows indicate transcription direction. Details are described in the text.

stitutive throughout infection. The fact that the product amount in phase I is slightly less than that of the other phases is most likely due to the a high ratio of rye mRNA to *Claviceps* mRNA in the template rather than any phase-dependent fluctuation of expression. To ensure that the products in lane I-IV are of mRNA and not DNA origin, the products of parallel RT-PCR reactions in which cDNA and genomic DNA have served as respective templates are shown (lanes cDNA and DNA, respectively); the size of the genomic fragment corresponds to the expected 349 bp.

3.1.5 Creation of mutants lacking *cpsod1* for functional analysis

The identity of *cpsod1* as the cell-wall associated Cu,Zn SOD is supported by strong evidence: non-stringent Southern analysis suggests that only one Cu,Zn SOD is present in the *C. purpurea* genome; protein analysis shows only one major band of Cu,Zn SOD activity which corresponds in expression and localisation with the protein recognised by the antibody directed against the cell-wall associated Cu,Zn SOD of *C. fusiformis*. Furthermore, both gene and protein activity are strongly induced by copper. On the other hand, there exists a discrepancy between the pI of the predicted protein from *cpsod1* (6.2) and the actual pI of the major Cu,Zn SOD (5.2), and (most uncomfortably) *cpsod1* lacks a signal peptide for secretion. The clearest evidence could most easily be provided by gene deletion and protein analysis of the mutant. Moreover, should this gene encode the cell-wall associated SOD, the importance of this protein for pathogenicity could be assessed by comparing the virulence of the deletion mutant with the wild-type recipient strain.

3.1.5.1 Construction of the *cpsod1* disruption vector pDV1

Targeted gene disruption involves the homologous integration of a gene fragment which lacks essential information at both the 5' (usually the promotor) and the 3' ends. The fragment approaches the genome as a circular disruption vector, usually accompanied by a selection marker, and a single cross-over event leads to the generation of two partial gene copies separated by the rest of the plasmid (see figure 3.12). The method of gene disruption as opposed to gene replacement offers greater ease in generation and preparation of the vector, as only one (non-oriented) and not two (oriented) gene fragments are involved and the isolation of large amounts of linear vector fragment is no longer necessary. This is balanced by a theoretical lack of stability in the disruption mutant; the entire gene is still present. Unlike in gene replacement in which parts of the gene have been irrevocably removed, one homologous recombination between adjacent DNA regions is enough to restore gene function. However, as gene disruption is a fast and widely accepted method of targeted mutation, it was applied to *C. purpurea* for the mutation of *cpsod1*. This was the first time that a disruption approach had been tried in *Claviceps*.

A schematic representation of the disruption strategy is shown in fig. 3.12. The primers DVF1 and DVR1 were used to amplify a gene disruption fragment from λ S28/1 DNA with PCR. The amplified fragment of 756 bp lacks both the promotor and coding region corresponding to 39 aa of the C-terminus, containing many residues important for enzyme integrity and function including His_{121}, which is involved in the co-ordination of the copper ion and R_{144}, which is crucial in guiding the superoxide anion towards the active centre (see 1.1.4.1). After cloning into the PCR 2.1 vector, the disruption fragment was excised using vector-derived *Eco*RI sites. This was then cloned into the *Eco*RI site immediately preceding the phleomycin resistance cassette in the transformation vector pAN8-1, creating disruption vector pDV1-4, which was then used to transform the haploidised *C. purpurea* strain 20-1.

3.1.5.2 Transformation of *C. purpurea* and analysis of pDV1-4 transformants with PRC

Two aliquots of 10^7 *C. purpurea* strain 20-1 protoplasts were transformed with 10 and 15 µg of circular pDV1-4 DNA and selected for phleomycin-resistance. As a control, one further aliquot of 10^7 protoplasts was subjected to the transformation protocol without DNA and plated with and without a phleomycin-containing overlay. After 4 d incubation at 28°C, the control plates without phleomycin showed a dense growth of colonies and the plates overlaid with phleomycin were empty. The amount of colonies growing on the transformant plates were too high to count. Of these, 180 apparent transformants were picked onto plates containing a threefold higher concentration of phleomycin. Only 42 % of the transformants were able to grow under the more stringent selection conditions. Fifty transformants displaying true phleomycin resistance were selected for further analysis.

With the help of analytical PCR, the phleomycin-resistant transformants were screened for

homologous integration of the circular disruption vector. The product of homologous integration of pDV4-1 into the genomic sequence of *cpsod1*, as well as the binding regions of the primers used in the analytical PCR are shown in fig. 3.12 (see above). Primer HIF1, directed against a sequence within the promotor region of *cpsod1* upstream of the disruption fragment, was used in combination with HIR1, a primer which binds within the promotor of the phleomycin cassette. These two primers can amplify a 992 bp fragment only after homologous integration of pDV4-1. To determine if a functional gene copy was still present, primer HIF1 was combined with primer HIR2 which binds within the terminal 3' region missing in the disruption fragment. Should the entire gene be present, a fragment of 937 bp would be amplified.

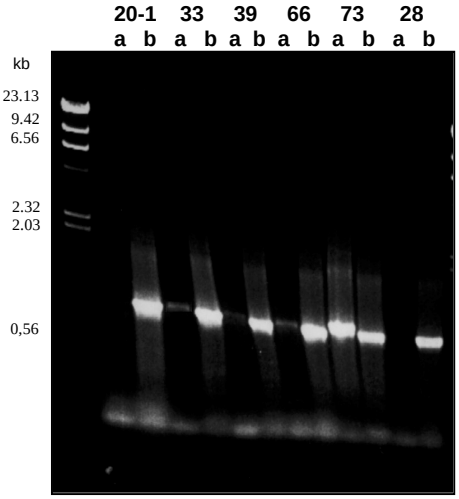

Fig. 3.13: Analytical PCR of pDV1-4 transformants. DNA strains are listed at top of picture; the sizes of the DNA marker (λ x *Hin*dIII) are shown on the left. The PCR was performed with two different primer combinations **a**: HIF1 and HIR1 (shows homologous integration) and **b**: HIF1 and HIR2 (shows wild type gene copy).

Of the 50 transformants subjected to analytical PCR, only the transformant T1-73 showed a strong product with the primers HIF1 and HIR1, indicating a homologous integration. Interestingly, in 17 cases a very weak product could be obtained with the same primers. In all cases, a strong band was obtained with primers HIF1 and HIR2, indicating the presence of the functional gene copy. The PCR with both primer combinations was repeated with four of the transformants showing the fragment for homologous integration as well as with one additional transformant which did not show a product with HIF1 and HIR1 (T1-28) and the recipient strain 20-1 as negative controls. The result of this PCR is shown in fig. 3.13. The negative controls 20-1 and T1-28 show a product of the correct size only with the wild-type gene copy primer combination. The transformants T1-33, T1-39 and T1-66 show only a weak product with the primer combination for detection of homologous integration, while T1-73 gives rise to a strong product of the expected size. All transformants seem to carry the wild-type gene copy. The PCR product from T1-73 arising from amplification with primers HIF1 and HIR1 was cloned into the PCR2.1 vector and sequenced to confirm the identity of the fragment.

The presence of the wild-type gene copy in a strain which shows homologous integration of the vector into this gene indicates either contamination with an ectopic transformant (very possible in this case due to the high density of transformants on the first plates) or that the transformed protoplast contained more than one nucleus (either from the beginning of protoplasting or due to the merging of different protoplasts during PEG treatment), rendering the transformant a heterocaryon. In both cases, isolation of colonies arising from a single mononuclear conidiospore is an efficient means of genetic

purification. After two successive rounds of single spore isolation, progeny of T1-73 showed no trace of wild-type gene contamination after analysis with PCR.

3.1.5.3 Analysis of T1-73

The *C. purpurea* transformant strain T1-73 was compared with the recipient strain 20-1 via Southern analysis to confirm the loss of the wild-type gene copy and check the number of integration events. The effect of *cpsod1* disruption on SODA was investigated using both SOD activity analysis in IEF gels and western analysis.

3.1.5.3.1 Southern analysis of T1-73

In order to confirm homologous integration and disruption of the *cpsod1* gene, the transformant T1-73 was subjected to Southern analysis. The restriction of genomic DNA with *Hin*dIII releases a 6.6 kb fragment containing *cpsod1*. As *Hin*dIII sites are not present within the 6.8 kb disruption vector integration should cause this fragment to shift to the 13.4 kb position. The results are shown in fig. 3.14. As expected, the 6.6 kb fragment which is present in the WT is replaced with a much larger fragment in two single spore isolates of T1-73 (a and g). As a size comparison, the λ-marker has been digested with *Bgl*II to release a 13.2 kb fragment; this appears at the same position as the hybridising fragment in the disruption mutant. As expected both isolates show no remnant of the wild-type gene copy; furthermore, no additional ectopic copy of the vector is present.

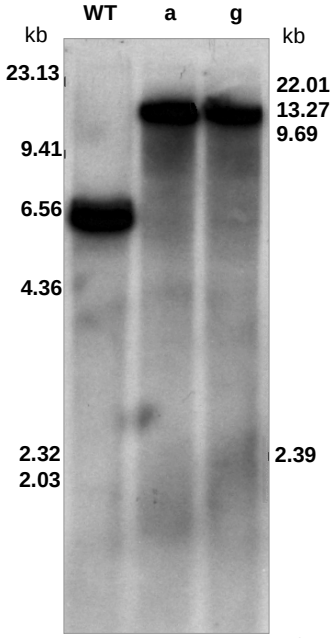

Fig. 3.14: Southern analysis of T1-73. Genomic DNA was digested with *Hin*dIII; the 245 bp fragment from *Cpsod1* served as a probe at 65°C. Lanes: WT(20-1), a(T1-73a), b(T1-73g). Size markers in kb: left shows *Hin*dIII-digested λ, while right shows *Bgl*II-digested λ..

3.1.5.3.2 Protein analysis of T1-73

The relationship between SODA and *cpsod1* was examined by investigating the mutant for changes in copper-dependent SOD activity patterns. Protein extractions of the cell wall were made from wild type and T1-73 cultures with and without copper supplement, separated by isoelectric focussing and stained for SOD activity. The same proteins were also subjected to western analysis and immuno-stained with the anti-CfSOD1 antibodies. The results are shown in fig. 3.15 A and B.

In protein extracts of the disruption mutant, the main and copper-dependent SOD activity seen in the wild-type strain 20-1 is no longer present. The immuno-staining shows that the protein recognised by the anti-CfSOD1 antibodies is also missing (A and B, compare lanes WT+Cu and T1-73g+Cu). Staining of the blot with Ponceau red prior to treatment with the antibodies shows that the lack of immuno-signal is not the result of less loaded protein (data not shown). These results confirm the identity of the *cpsod1* gene product as the cell-wall associated Cu,Zn SOD and the major source of SOD activ-

ity seen in axenic culture. The transformant T1-173 was dubbed Δcpsod1.

There are also many other faint bands of activity visible in all lanes. Although a minor band of activity, which is not induced by copper, appears in the mutant at pI 5.5, no major SOD activity is induced (under these conditions) to replace the missing SODA activity. The faint bands may be caused by unspecific metalloproteins; such proteins may well have slight superoxide dismutase activity as their bound metal ions could be in the position to accept an electron from superoxide. Another, somewhat stronger, band of activity appears just beneath that of SODA and is clearly repressed by copper. Inhibition with the copper chelator DDC has shown that none of these bands are the product of other Cu,Zn SODs or any copper-dependent enzyme (see 3.1.2.4).

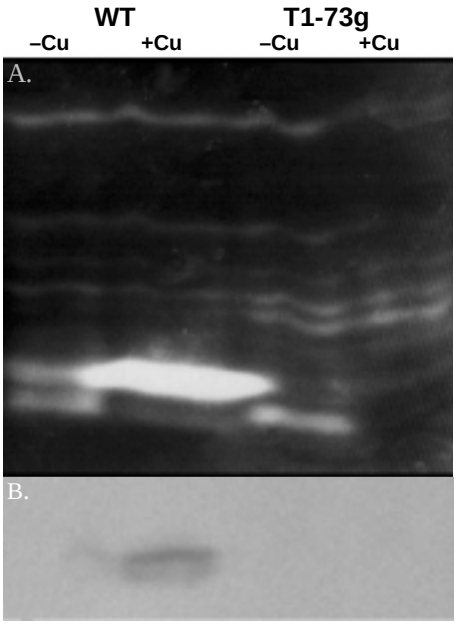

Fig. 3.15: Protein analysis of the *cpsod1* disruption mutant. Each lane in A and B contains cell wall associated proteins corresponding to 10 mg of mycelia (cultivated with and without 50 µM $CuSO_4$ supplement) in the order (left to right) WT with and without copper, T1-73g with and without copper A: IEF-gel electrophoresis (pI 3-10) followed by SOD activity staining. B. Immunostaining of western blot proteins with anti-CfSOD1. Ponceau S staining of the western blot prior to immunostaining indicated that all lanes contained comparable amount of protein (data not shown).

3.1.5.4 Complementation of Δcpsod1

In order to prove that phenotypes arising in the course of testing Δcpsod1 were really the result of the lack of the Cu,Zn SOD, two approaches were considered. Even in the case of targeted gene disruption/replacement, phenotypes arising from mutant strains can be caused by genomic rearrangements which can take place in the course of transformation. It is also possible that the mere presence of the transformation vector in the genome can effect the biochemistry of a mutant in such a way as to cause a phenotype. An indirect way of proving that a phenotype is caused by a certain specific mutation is to test multiple mutant strains as well as an ectopic transformant. Should all mutant strains behave in the same way, and the ectopic mutant behave as the wild type does, the evidence linking mutation and phenotype is solid. A more direct way of proving the same thing is complementation of the mutant with the functional gene. As complementation is usually fulfilled with an ectoptic integration of the healthy gene, and activity staining could be used to verify the functionality of the re-introduced gene, this course was chosen.

3.1.5.4.1 Construction of the complementation vectors pComp1$_a$ and pComp1$_c$.

For the construction of a complementation vector, a 5.0 kb *Sal*I/*Hin*dIII fragment of λS26/6 carrying the complete *cpsod1* gene was cloned into *Sal*I/*Hin*dIII-digested pBS. The fragment was released from the vector with *Sal*I and *Hin*dIII, the overhanging 5' ends were filled using the Klenow fragment and the blunt-ended fragment was then cloned into the *Eco*RV site of the fungal transformation vector

pOliHP. The construction of the complementation vector is schematically described in fig. 3.16. Because transcription of the selection cassette has been suspected of being continued past the terminator region (from the *trpC* gene of *Aspergillus nidulans*) in *G. fujikuroi* (B. Tudzynski, pers. comm.) and

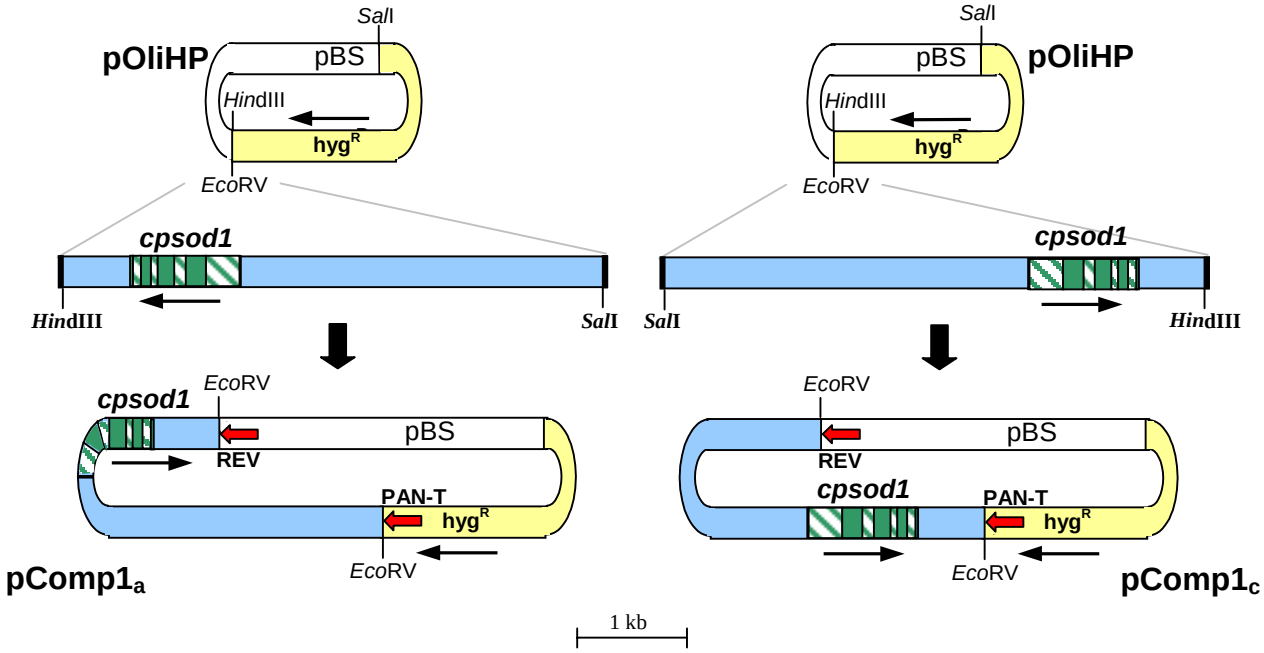

Fig. 3.16: Construction of the *cpsod1* complementation vectors pComp1$_a$ and pComp1$_c$. The fungal transformation vector pOliHP comprises a hygromycin cassette (Hyg^R), shown in yellow, cloned into *Sal*I/*Hin*dIII sites in pBS (white). The λ-subclone which carries *cpsod1* is depicted in blue; the coding region of *cpsod1* is in green, introns are striped, exons are solidly coloured. Restriction enzymes written in bold type indicate sites rendered non-functional by filling to blunt ends. After ligation of the subclone into the *Eco*RV site of pOliHP, two products are created: left, pComp1$_a$ and right, pComp1$_c$. Red arrows denote sequencing primers REV (REVERSE) and PAN-T while black arrows indicate the direction of transcription. All non-curved elements are to scale.

this may interfere with the transcription of adjacent genes, two forms of the complementation vector were differentiated. The difference between the two vectors lies in the orientation of the *cpsod1* subclone within the *Eco*RV site of pOliHP. The *cpsod1* gene is located towards one end of the subclone; in pComp1$_a$, *cpsod1* is adjacent to the pBS side of the pOliHP component, while in pComp1$_c$, *cpsod1* is directly adjacent to the terminator of the hygromycin cassette. Should the terminator of the hygromycin cassette not be fully functional in *C. purpurea*, transcription of the hygromycin gene could interfere with the transcription of *cpsod1*. In order to test this, both vectors were used to transform the Δcpsod1 strain.

3.1.5.4.2 Screening pComp1 transformants for integration of functional *cpsod1*

Two aliquots of 10^7 *C. purpurea* strain Δcpsod1 protoplasts were transformed with 10 µg of circular pComp1$_a$- and pComp1$_c$-DNA and selected for hygromycin resistance. As the amount of primary transformants obtained with both vectors was too high to count, no transformation rates were determined. Of the 75 transformants picked from each of the primary transformants, 32 pComp1$_a$ and 17 pComp1$_c$ transformants were screened for integration of an intact *cpsod1* gene copy with the primers

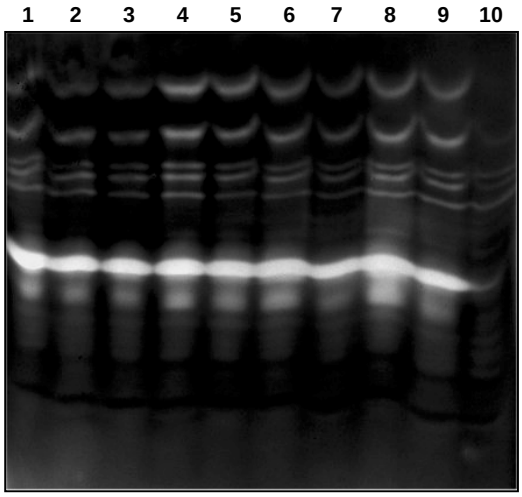

Fig. 3.17: SOD activity staining of complementation mutants. Cell wall associated protein fractions, extracted from cultures supplemented with 50 µM $CuSO_4$, were separated by isoelectric focussing within a native PAGE gel, pI 3-7 and then stained for SOD activity. Each lane contains protein corresponding to 10 mg of freeze dried mycelia. Lanes 1-10: WT 20-1, T_a13, T_a16, T_a20, T_a25, T_a45, T_a48, T_c18, T_c62 and Δcpsod1.

HIF1 and HIR2 used in PCR analysis of the Δcpsod1 transformants (see 3.12). Both wild-type strain 20-1 and Δcpsod1-DNA functioned as controls. While PCR with the Δcpsod1 strain showed no amplification, the 20-1 and 13 transformants showed a product which corresponded to the expected size of 937 bp. Of these, nine were from the transformation with the pComp1$_a$ vector (T_a transformants), and four were from the pComp1$_c$ vector (T_c transformants), revealing that about 25 % of each transformant type carried intact *cpsod1* gene copies (data not shown).

Well-sporulating strains resistant to both hygromycin and phleomycin were cultivated in medium supplemented with 50 µM copper sulfate to induce transcription of *cpsod1*; protein extracts were isolated from the cell wall and then analysed for SODA activity using IEF-focussing and SOD activity staining. The wild-type strain 20-1 and the recipient strain Δcpsod1 were included as positive and negative controls, respectively. While Δcpsod1 showed no SODA activity, all ten tested transformants showed a restored SODA activity comparable to that of the wild-type strain (fig. 3.17). Furthermore, the two T_c transformants exhibit a SODA activity comparable to that of the eight T_a transformants. As Southern analysis of T_c62 (see below) shows that only one copy of functional *cpsod1* is present, it can be concluded that the strong band of activity is not derived from many weakly expressed gene copies. Therefore, the *trpC* terminator of the hygromycin cassette is either fully functional in *C. purpurea* or the extended transcription does not severely interfere with the transcription of *cpsod1*, which ends about 600 bp upstream of the end of the trpC terminator.

3.1.5.4.3 Southern and western analysis of the selected complementation mutants cΔsod1 and cΔsod2

The strains T_a16 and T_c62, selected for further analysis, were respectively renamed cΔsod1 and cΔsod2. In order to be sure that the mutant strains were not contaminated by wild-type or other non-complemented strains, they were each subjected to two rounds of single spore isolation. The purity of the strains was then tested by Southern analysis (fig. 3.18). The wild-type strain shows the familiar 6.6 kb hybridising fragment after digestion with *Hin*dIII. This is lacking in the three other strains. Instead, the ca. 13 kb fragment containing the disruption vector appears in each of the three strains. While Δcpsod1 carries only the disrupted copy of the gene, the two complementation mutants show an

additional hybridising fragment which corresponds to the reintroduced *cpsod1* gene.

With the purity of the complementation mutants having been established, the protein size, antigenic properties as well as the copper sensing ability of the products of the newly introduced gene copies were tested in western analysis. Cell-wall associated proteins, isolated from cultures grown with and without copper supplement, were subjected to SDS-PAGE, western blotting and immuno-staining with the CfSOD1 antibodies (fig. 3.19).

The results show that the reintroduced proteins react with the anti-CfSOD1 antibody, and that the ability to be induced by copper has been preserved. A comparison of the wild type and cΔsod2 protein sizes shows that they are both about 17 kDa, while the size of the cΔsod1 protein is less clear; the staining pattern indicates two to three forms of the protein. Southern analysis shows only one copy of the reintroduced gene, so the presence of different forms must be a product of either differences in post-transcriptional modifications or protein stability. As SOD activity staining of the purified strain in cell wall fractions is comparable to the activities of the wild type and cΔsod2, the appearance of multiple isoforms in cΔsod1 does not seem to have effected the complementation.

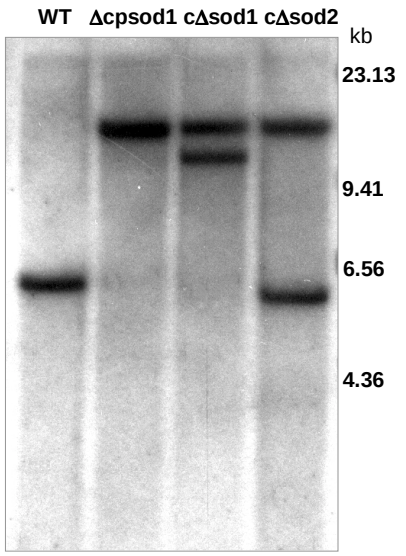

Fig. 3.18: Southern analysis of cΔsod1 and cΔsod2. Genomic DNA was digested with *Hin*dIII and hybridised with the 245 bp fragment from *cpsod1*. Lanes (left to right) WT (20-1), Δcpsod1, cΔsod1 and cΔsod2. Size of DNA marker is indicated in kb on the far right.

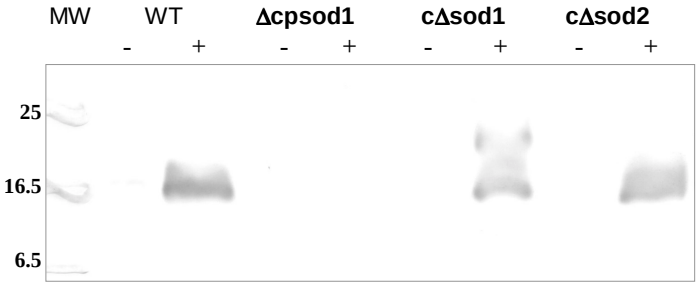

Fig. 3.19: Western analysis of cΔsod1 and cΔsod2. Cell wall associated proteins corresponding to 10 mg of freeze dried mycel cultivated with and without addition of 50 µM $CuSO_4$ were loaded on each lane of an SDS-PAA gel (14 % PAA in separation gel). After electrophoresis and western blotting the blot was immunostained with anti-CfSOD1. Lanes left to right: molecular weight marker in kDa (New England Biolabs), WT(20-1) – and + Cu, Δcpsod1 – and + Cu, cΔsod1 – and + Cu, cΔsod2 – and + Cu.

3.1.6 Analysis of Δcpsod1 phenotypes in axenic and parasitic culture

The importance of the major Cu,Zn SOD during growth under conditions of extreme oxidative stress (caused by the redox cycler paraquat), was tested in axenic culture. Further experiments examined the germination rates of conidiospores on paraquat-containing media. The effect of *cpsod1* deletion on parasitic growth was tested in comparative pathogenicity analysis on rye infected with the

wild-type strain 20-1 and Δcpsod1.

3.1.6.1 Axenic growth of Δcpsod1 with and without oxidative stress

Comparison of Δcpsod1 and wild-type cultures, grown 4-5 days in liquid culture for protein analysis, showed that although dry weight varied considerably with each experiment, the mutant grew between 40 and 80% slower then the wild type. Oxidative stress in the form of supplemented copper (50-75µM) did not significantly change these values. In individual experiments, both complementation mutants tended to grow faster than the Δcpsod1 and slower than the wild type (between 50 and 95% of wild type growth); again, the addition of copper had no significant effect on growth rates. It was concluded that deletion of *cpsod1* tended to slow down growth in liquid culture.

To assess the importance of *cpsod1* for axenic growth with and without oxidative stress provided in the form of an intercellular superoxide generator, the wild type, Δcpsod1 and the complementation mutants cΔsod1 and cΔsod2 were grown on agar plates with and without 5 mM paraquat and the colony diameters were compared. Fig. 3.20 shows the results of the growth tests. Comparison of wild-type and Δcpsod1 colony growth on medium without paraquat shows that the disruption of *cpsod1* already slows growth by about 30%. Addition of paraquat to the medium results in a ca. 40% reduction of wild-type growth; this reduction does not significantly increase in the Δcpsod1 mutant. The complementation mutants show at least a partial restoration of the growth rate without paraquat but in both cases growth on paraquat is even more hampered then in the mutant strain; cΔsod1 shows about 60% and cΔsod2 about 65% reduction in growth compared to rates on medium without paraquat.

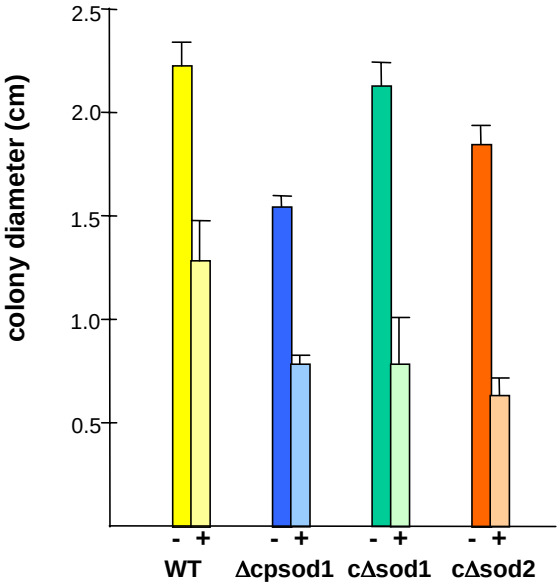

Fig. 3.20: Axenic growth with and without paraquat. Strains were inoculated on MA plates with and without addition of 5 mM paraquat. After 8 d growth at 28°C the colony diameter was measured. Each value is an average of 5 experiments; standard deviation is indicated by vertical lines. Strains are listed beneath the growth columns; dark colours indicate growth without paraquat (-), pale colours indicate growth with paraquat (+).

These results indicate that while the presence of *cpsod1* is important for normal growth, it plays no essential role in helping the fungus cope with the oxidative stress caused by paraquat.

Deletion of the major Cu,Zn SOD in *Neurospora crassa* was reported to result in paraquat sensitivity of germinating spores (Chary et al., 1994). The experiment was repeated with the *C. purpurea* mutant. Spores were plated on medium containing 100 µM paraquat and the germination rates of the

wild type, Δcpsod1 and the complementation mutant cΔsod2 were compared. Fig. 3.21 shows that the germination rates of wild-type spores are not significantly affected by paraquat and that deletion of *cpsod1* does not increase the sensitivity of germinating conidiospores to this toxin.

To investigate if the lack of paraquat sensitivity in the Δcpsod1 mutant resides in the induction of another cytoplasmatic superoxide activity, mycelial extracts of the wild type and Δcpsod1, grown in a complete medium with and without oxidative stress, were examined for alternative SOD activity. Induction of oxidative stress was achieved by the addition of paraquat, copper and both substances simultaneously (as described in fig. 3.10 E). Mycelial proteins were separated by IEF-gel electrophoresis and then stained for SOD activity. The copper–induced SODA activity, missing in Δcpsod1, is the only major SOD activity in all cultures (data not shown). Therefore, application of oxidative stress does not result in the induction of other, soluble SOD activities, either in the wild type or in the strain lacking *cpsod1*.

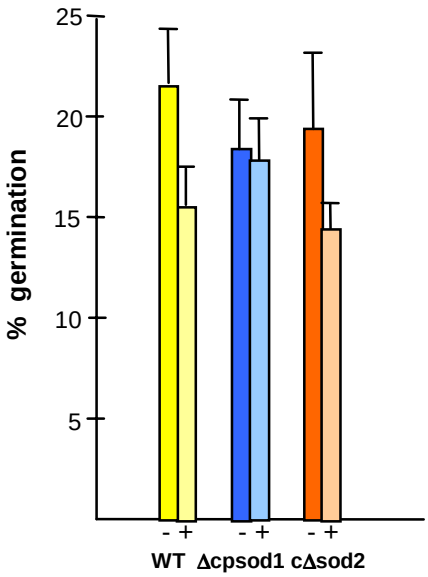

Fig.3.21: Germination rates with and without paraquat. 250 spores of each strain were allowed to germinate on MA plates with and without 100 µM paraquat. After 4-5 d growth at 28°C the number of colonies were determined. Each value is an average of 3 experiments; standard deviation is indicated by vertical lines. Strains are listed beneath the growth columns; dark colours indicate growth without paraquat (-), pale colours indicated growth with paraquat (+).

3.1.6.2 Testing the virulence of Δcpsod1 on rye

Flowering ears of the male-sterile rye cultivar CMS, containing between 60 and 80 florets, were infected with conidospores from the wild-type strain 20-1 and Δcpsod1. The time between inoculation and the appearance of honeydew, which marks the first visible sign of successful pathogenesis, was used as a criterion for virulence. In a further experiment, rye ears infected with both strains were examined for SOD activities.

3.1.6.2.1 Pathogenicity assays with Δcpsod1

Each floret of a flowering ear was individually inoculated with 5000-10000 conidiospores of Δcpsod1 or 20-1. Because of difficulties involving the sporulation of the two complemented strains, analysis was at first restricted to wild type and disruption mutant strains. A total of 29 ears were infected; of these, 16 were inoculated with Δcpsod1 while 13 were inoculated with 20-1. The amount of honeydew observed was recorded in one of five categories ranging from one colourless drop on one floret (+) to intensive amber droplets completely covering the entire ear (++++). An interpretation of the assays on the CMS strain is given in fig. 3.22.

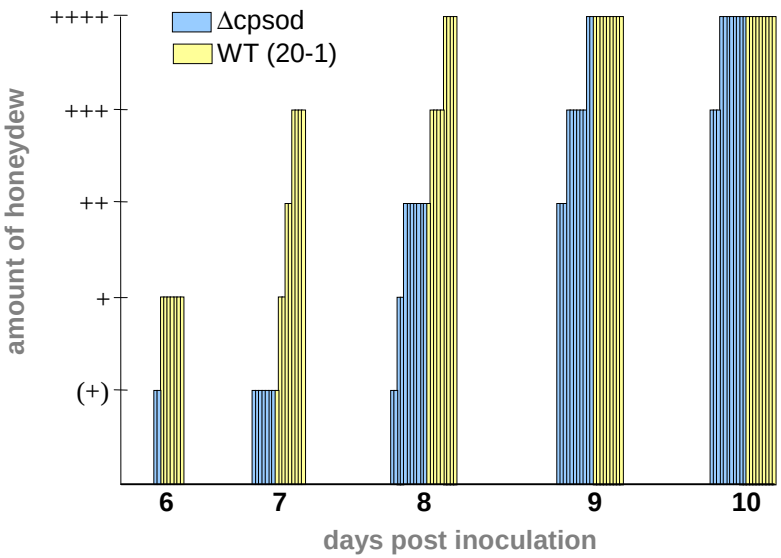

Fig. 3.22: Comparison of time and amount of honeydew production in Δcpsod1 and WT(20-1) strains. Each pathogenicity assay is represented by one rectangle; assays with Δcpsod1 are depicted in blue and the WT in yellow. The amount of honeydew was assessed 6-10 dpi; grading is as follows (+): one colourless droplet on one floret, +: amber droplets on 1-3 florets, ++: 3-6: florets show honeydew, +++: thick honeydew on many florets, ++++: excessive honeydew covers entire ear.

As almost all of the rye infected with Δcpsod1 shows maximum production of honeydew (++++) by 10 dpi, it can be concluded that the lack of SODA activity does not seriously impede infection. The time of the first appearance of honeydew is slightly delayed in infections with the mutant; although the majority (7/9) of the WT assays shows honeydew 6 dpi, the majority of the mutant assays shows first honeydew production at 7 dpi (7/11); furthermore, in all cases the amount of honeydew in the very early stages of visible infection is less and the honeydew shows less colour and turbidity in mutant than in wild type infections. The wild-type strain induces maximum honeydew amounts also one to two days earlier than the mutant strain. These observations confirm the results of preliminary pathotests, in which a one day delay of honeydew production in the Δcpsod1 as compared to strain 20-1 was recorded (Drauschke, 1999). However, all differences between the infection patterns in the two strains have vanished by about 10 dpi. As in the wild type, the protrusion of sclerotial tissue was observed in late phase III (between 17 and 20 dpi) after infection with Δcpsod1; this tissue ripened to sclerotia which were morphologically identical (on a macroscopic level) to those produced in the course of wild type infection.

3.1.6.2.2 *In planta* analysis of SOD activities in the Δcpsod1 and WT strains

In order to investigate the SOD activities present in the fungus during growth *in planta*, proteins were isolated from rye ears infected with the wild type and mutant strains. As the differences in the pathogenicity were was confined to phase I and II of infection. After 5 and 10 dpi, the infected rye ears were harvested and the proteins were extracted from ground florets. Non-infected blooming florets served as a control. Proteins were subjected to IEF-gel electrophoresis and stained for SOD activity. The results are shown in fig. 3.23. Lane 1 shows SOD activities present in non-infected rye. Comparison to lanes 2 and 3, which show phase I from wild type and mutant infections, shows that all of the activities which are visible in these extracts seem to originate from the rye. The ratio of rye to fungal proteins after only 5 dpi is so high that this is not surprising. More interesting are the lanes 4

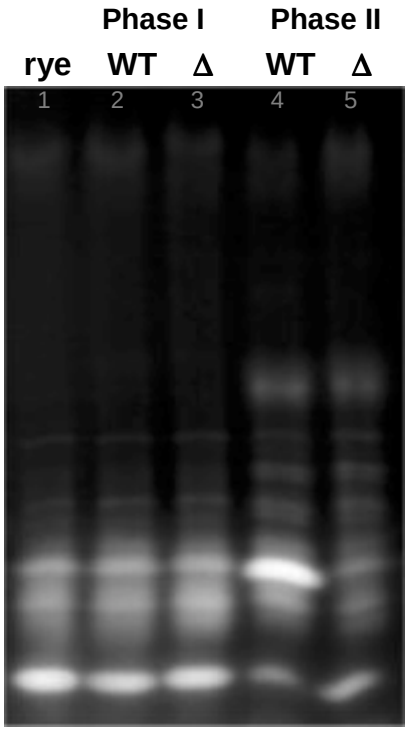

Fig. 3.23: *In planta* SOD activities of Δcpsod1 and WT (20-1). Each lane contains 100 µg proteins extracted from ground florets separated with IEF gel electrophoresis (pI 3-10) and stained for SOD activity. Lanes: 1-florets from uninfected rye, 2 and 3-from rye infected with the wildtype 20-1 (WT) and Δcpsod1 (Δ) after 5 dpi (phase I), respectively, 4 and 5- from rye infected with the wildtype and Δcpsod1 after 10 dpi (phase II), respectively. Isoelectric points were calculated by comparison to a silver stained marker mix (data not shown).

and 5 which show phase II activities from the wild type and the mutant; visible in these lanes are a few SOD activities which are probably of fungal origin (it is impossible to distinguish fungal proteins from fungus-induced rye proteins). The strongest activity visible in wild-type extracts is that of CpSOD1 at pI 5.2, which is missing in the mutant extract. Another band appears in both extracts at pI 6,7; this activity is not inhibited by DDC (data not shown) so it is either a Mn SOD or another, non-copper-dependent protein with SOD activity. Important is the fact that no other major SOD activity is induced *in planta* in the Δcpsod1 strain which could compensate for the lack of SODA. These results indicate that (soluble) SOD activity is not necessary for survival of *C. purpurea* during colonisation of rye; if AOS is a significant component of the interaction, it seems likely that H_2O_2 rather than $O_2^{-\cdot}$ is of importance. This shifts the focus of interest from superoxide dismutases to H_2O_2 scavengers such as catalase.

3.2 Characterisation and functional analysis of a putative catalase gene

During the sequencing of genomic regions containing genes involved in alkaloid biosynthesis of the non-pathogenic alkaloid production strain P1 of *Claviceps purpurea*, a gene fragment with homology to catalases was found (Tudzynski et al., 1999). As sequencing of the entire gene confirmed the homology to catalases, it was denominated *cpcat2* (this was the second putative catalase gene identified in *C. purpurea*, see 1.3.3.2). Southern analysis revealed the presence of a highly homologous gene in the pathogenic strain 20-1 and the gene was disrupted in this strain to assess both its importance for pathogenesis and its role in the biosynthesis of alkaloids.

3.2.1 Sequencing of *cpcat2*

A 6 kb *Xba*I fragment of the genomic lambda clone p25 from strain P1 was partially subcloned and sequenced to reveal the open reading frames of *cpcat2* as well as 854 bp upstream of the putative start codon and 60 bp downstream of the stop codon. A cDNA screening of ca. 60 000 clones from alkaloid producing mycelia of strain P1 revealed 54 positive clones; of these 4 were sequenced to identify introns. Fig. 3.24 depicts a restriction map of the genomic region of *cpcat2* as well as the putative

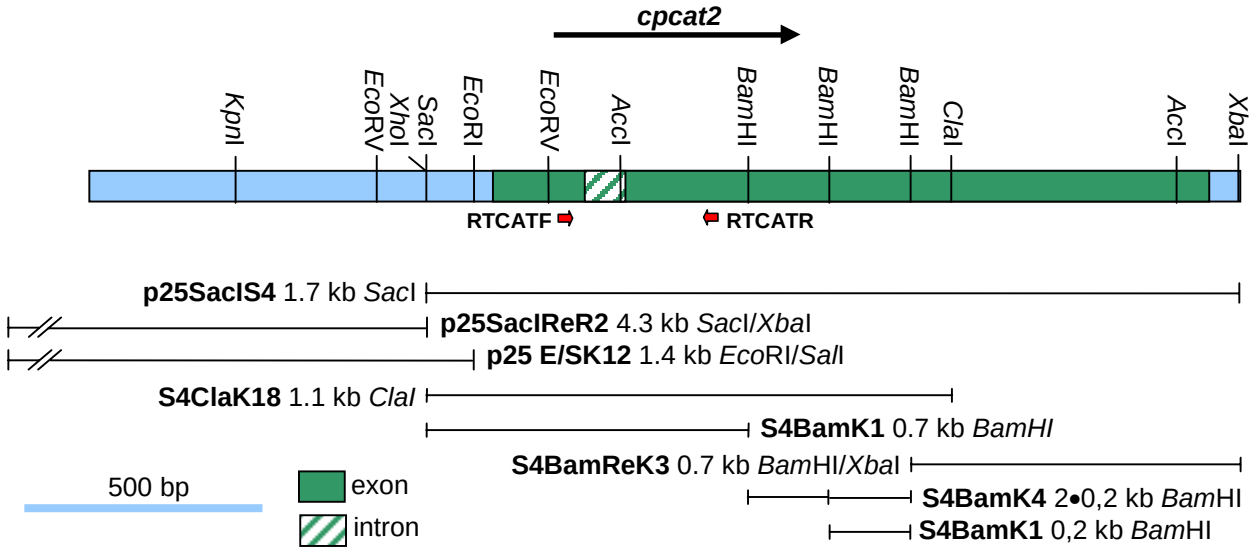

Fig. 3.24:Restriction map and subcloning strategy of the *cpcat2* genomic region. All subclones were derived from a 6 kb *Xba*I subclone from λ p25. Clones denominated p25 are direct subclones of the *Xba*I fragment, while clones denominated S4 are derived by subcloning the 1.7 kb *Sac*I fragment from p25*Sac*IS4. All fragments were cloned into the vector pBS; sequencing was done with universe and reverse primers. The intron (greem striped) and exon (solid green) pattern was obtained by comparison with cDNA clones and by information provided by intron consensus sequences and conserved regions of catalases from other organisms. Surrounding genomic regions are blue; the RT-PCR primers RTCATF and RTCATR are shown as red arrows., while a black arrow indicates direction of *cpcat2* transcription.

coding regions of the protein.

The sequence of the *cpcat2* genomic region as well as the derived amino acid sequence is shown in appendix A.2. The methionine immediately preceding the beginning of homology to similar catalases was chosen as the start codon. This choice is supported by the size of the putative protein, which is similar to that of related catalases, as well as by computer analysis using GENSCAN (Burge and Karlin, 1997), which shows that the coding potential of regions upstream of the chosen methionine is very low. The candidate region of the promotor and coding sequences of *cpcat2* is limited 726 bp upstream of the putative start codon by the stop codon of the preceding gene in the alkaloid gene cluster, *cpox2* (Tudzynski et al., 1999). The consensus sequence determined by Ballance (1991) for highly expressed fungal genes is not fulfilled by the regions preceding any of the possible start codons. The sequence contains one intron of 85 bp. A comparison of the intron/exon pattern of *cpcat2* with other similar catalases reveals that the only shared characteristic is a large exon (at least 1000 bp) at the C-terminus (data not shown).

3.2.2 Analysis of the *cpcat2*-derived protein and promotor region

The ORF of *cpcat2* encodes a putative protein containing 473 aa with an estimated pI of 5.4. Catalases are homotetramers with 4 prosthetic heme groups; each subunit is roughly globular with an extended N-terminal arm which links the subunits together. The globule contains the funnel-shaped substrate channel and the heme group at its end; the residues involved in forming these structures are a part of the catalase core, an area defined by Klotz et al. (1997), as comprising the residues 70-460 of CATA from yeast. The core is well conserved among typical catalases (as opposed to non-heme or Mn-containing catalases and catalase-peroxidases). The highest degrees of homology are found in the area around the essential distal histidine and the region of the proximal heme-binding tyrosine. This histidine is present in all heme catalases and is necessary for the correct binding and reduction of a peroxide molecule (Zámocký and Koller, 1999). The histidine and conserved surroundings are found in the *cpcat2*-derived protein (CpCAT2) and are shown as PROSITE catalase signature 2 in A.2 (blue type). The PROSITE catalase signature 1, containing the area around the essential proximal heme-Fe ligand tyrosine, is also conserved in CpCat2 (see A.2). The conservation of these residues supports the identity of CpCAT2 as a functional catalase.

As the product of *cpcat2* does not belong to the group of large subunit catalases and is thus a likely candidate for NADP-binding (see 1.1.4.2), the conservation of residues which interact with NADPH was examined. The review from Zámocký and Koller, 1999, gives detailed descriptions of NADPH–catalase binding where it has been investigated (for 3 catalases). In bovine liver catalase, residues important for NADPH binding are F_{197}, F_{445} and V (or L)$_{449}$ (hydrophobic interaction with adenine), as well as H_{304} (interacts with the pyrophosphate group). In CpCAT2 all of the former residues are

conserved (F_{177}, F_{414} and L_{418}) while the latter is not (L_{284}). Thus, sequence analysis does not allow a clear prediction of the ability of CpCAT2 to bind NADPH; only experimental evidence can clarify this.

BlastP analysis of CpCAT2 reveals strong homology with other fungal catalases; the top homologies are with peroxisomal enzymes: *Ajellomyces capsulatus* CATP (high score 281, probability $9e^{-75}$), *Aspergillus nidulans* CATC and *Glomerella cingulata* CAT1 (both 281, $1e^{-74}$). Peroxisomal enzymes are small subunit catalases; CpCAT2 with 484 amino acids is slightly smaller than the three similar proteins which have lengths of 503, 501 and 504 aa, respectively. The smaller length of CpCAT2 is reflected in a smaller enzyme core and does therefore not necessarily cast doubt on the choice of start codon. Proteins fated for peroxisomes carry peroxisomal targeting signals (PTS); most known peroxisomal enzymes, especially catalase, have both PTS1 and PTS2. PTS1 is easier to spot as it consists of 3-9 amino acids at or very close to the carboxy-terminus which contain a distinct tripeptide (SKL and functional variants, Subramani, 1998). PTS2 is more difficult to locate as the signal is transduced through tertiary rather than primary structure. In yeast, CATA deletion experiments show that it is localised in its amino terminal third (Kragler et al., 1993). Interestingly, the stop codon of CpCAT2 precedes a perfect PTS1 signal followed by a second stop codon (indicated in dark blue type, A.2).

The 723 bp region between the stop codon of *cpox2* and the putative start codon of CpCAT2 was analysed for promotor elements by MatInspector (Quandt et al., 1995). Interesting putative promotor elements are shown in red type in A.2.

Four distinct putative binding sites for the heme activator protein HAP-1 were found at positions -693, -641, -260 and –153. This protein is involved in the regulation of heme-containing proteins and antioxidant enzymes (Kwast et al., 1998). In yeast, HAP-1 interacts with promotors of genes involved in fatty acid metabolism, respiration and oxidative damage; although some, such as CTT, CTA (catalases T and A) and CYB2 (cytochrome b_2) contain heme as a prosthetic group, others such as SOD1 and SOD2 do not (Kwast et al., 1998). Heme is important for numerous cell processes which involve oxygen or oxygen sensing; in yeast it acts as a secondary signal for oxygen (Zitomer and Lowry, 1992), activating the transcription of aerobically induced genes in concert with the HAP-2345 complex (Forsburg and Guarente, 1989). A putative binding site for the latter complex was found at -174; this complex binds CCAAT-boxes about 50-200 bp upstream of the transcription initiation point in eucaryotic promotors (Bucher, 1990).

Another interesting result of the promotor analysis is the discovery of two putative ABA-inducible elements at positions –342 (ABF1-03) and –134 (ABF1-01). ABA (abscisic acid) is a plant hormone with pleiotropic effects on growth and development (Tudzynski and Sharon, 2002). Most ABA-responsive genes contain multiple ABARE (ABA-response elements) (Vasil et al., 1995).

A few putative promotor elements involved in stress-mediated responses were found. A putative ATF-1 binding element is present at –348. In fission yeast, the response of catalase to general stress (heat, UV and osmotic stress) is mediated by the ATF-1 transcription factor (Nakagawa et al., 2000); a homologue has been found in *C. purpurea* which is induced by H_2O_2 (Joshi et al., 2002b). Although the stress response element (STRE) of yeast is known to activate transcription of a number of stress-related genes such as CTT (cytosolic catalase) (Marchler et al., 1993), the single putative STRE at –111 of the *cpcat2* promotor may not be significant, as in stress-induced yeast promotors, STRE is found twice within 30-60 bp in the 600 bp region preceding the stop codon (Moskvina et al., 1998). Oxidative stress proteins such as catalase are often inducible by heat shock (Noventa-Jordão et al, 1999, Chary and Natvig, 1989, Kawasaki et al., 1997); a putative heat shock element (HRE) is present in the *cpcat2* promotor at –58.

Finally, as metal ions create oxidative stress, the promotor of *cpcat2* was checked for the presence of putative copper response elements (CuREs), ACE-binding regions and metal response elements (MRE). Copper induction has been reported for the yeast cytosolic catalase T (Lapinskas et al., 1993). No such elements could be found in the *cpcat2* promotor.

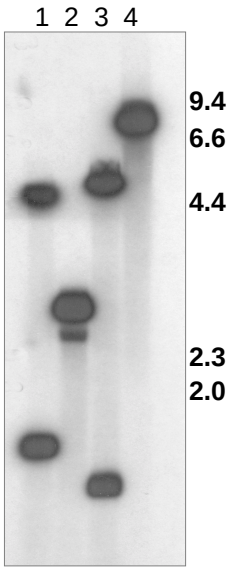

Fig. 3.25: Genomic DNA from strain 20-1 probed with *cpcat2*. Lanes 1-4: DNA digested with *Bam*HI, *Eco*RI, *Hin*dIII and SalI, respectively. Size marker fragments from *Hin*dIII-digested λ-DNA are indicated in kb on the far right. The 1.7 kb *Sac*I fragment from p25*Sac*IS4 (see 3.24) was used as a probe. Hybridisation was performed at 65°C.

3.2.3 Southern analysis of *cpcat2*

In order to confirm the presence of a *cpcat2* homologue in the pathogenic strain 20-1 and to investigate the copy number of this gene, Southern analysis was performed under stringent conditions at 65°C (fig. 3.25). According to the sequence of the *C. purpurea* alkaloid production strain P1, *Bam*HI should produce four hybridising fragments, two of which are too small to be detected in this gel (169 and 173 bp). *Eco*RI cuts once within the hybridising region; one of the fragments overlaps only 99 bp, with the probe which explains the weakly hybridising band. *Sal*I does not cut within the hybridising region; Southern analysis shows only one signal. The pattern of hybridising bands after digestion with *Hin*dIII does not conform to that expected from the sequence; obviously there are differences between the sequences of strain 20-1 and P1 which yields a *Hin*dIII site within the hybridising region. Nevertheless, the results indicate that there is a single-copy homologue of *cpcat2* in strain 20-1.

3.2.4 Expression analysis of *cpcat2*

3.2.4.1 Northern analysis in the pathogenic strain 20-1 and the alkaloid production strain P1

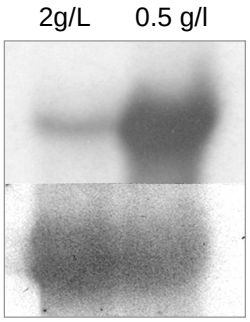

Fig. 3.26: Northern analysis of *cpcat2* in strain P1. Mycelia was cultivated in alkaloid production media with 2 and 0.5 g/l phosphate. The former represses the biosynthesis of alkaloids; when the phosphate is reduced to 0.5 g/l, de-repression occurs. Top: RNA probed with the 1.7 kb *Sac*I subclone of *cpcat2*. Bottom: The same blot was probed with rDNA from *G. fujikuroi* as a loading control. Comparison of the hybridising signals with an RNA marker indicated that the *cpcat2* messenger is ca. 1.5 kb in length (data not shown).

Northern analysis of *cpcat2* in axenic cultures in strain 20-1 did not yield a detectable transcript under any of the tested conditions. Induction with hydrogen peroxide or other AOS-producing systems such as paraquat and xanthine/xanthine oxidase also failed to produce a detectable transcript. As this strain, like most field isolates of *C. purpurea*, is unable to produce alkaloids in axenic culture (Tudzynski, pers. comm.), it is perhaps not surprising that a gene located in the alkaloid gene cluster is not expressed.

As the strain P1 does produce alkaloids under axenic conditions, it was examined for expression of *cpcat2*. In order to investigate the induction of *cpcat2*, the mycelia was cultivated with phosphate concentrations which repress the biosynthesis of alkaloids (2 g/l), and was compared to mycelia cultivated in 0.5 g/l under which the biosynthesis is de-repressed (Arcamone et al., 1970) (mycelia was kindly provided by Y. Lübbe). The results are depicted in fig. 3.26; the 1.5 kb *cpcat2* transcript is present even in conditions under which the alkaloid biosynthesis is repressed (2 g/l). De-repression leads to a strong induction of *cpcat2*; a phenomenon which was observed for other genes in the cluster (Y.Lübbe, pers. comm.). Similar cultivation of strain 20-1 was also tested for its ability to induce *cpcat2*-transcription but, again, no transcript could be detected in northern analysis.

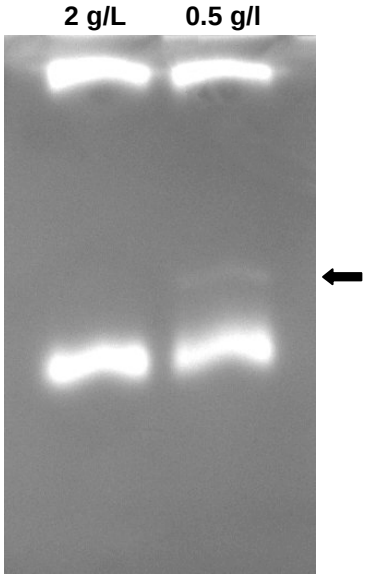

Fig. 3.27: Catalase activities of P1 strains differentially expressing genes of the alkaloid biosynthesis cluster. Protein fractions, extracted from cultures repressed and de-repressed for akaloid biosynthesis (2 and 0,5 g phosphate/l, respectively), were separated by isoelectric focussing within a native PAGE gel pI 5-8 and then stained for catalase activity. Each lane contains 300 µg protein. The arrow on the right indicates a weak catalase activity in the alkaloid-induced culture.

3.2.4.2 Catalase activity in strain P1

As the expression of *cpcat2* was detected in alkaloid

producing cultures of the strain P1, the same cultures were subjected to protein analysis in the hope of visualising a catalase activity which corresponded to the presence of the *cpcat2* transcript. Mycelial extracts of cultures repressed and de-repressed in the biosynthesis of alkaloids were separated using isoelectric focussing and then stained for catalase activity. Fig. 3.27 (see above) shows such a gel. Two major bands of activity are not induced by de-repression of the alkaloid biosynthesis cluster, whereas a faint band of catalase activity is present only in the alkaloid induced cultures (arrow). Whether or not this activity originates from *cpcat2* can only be decided by targeted disruption in the strain P1.

3.2.4.3 *In planta* expression of *cpcat2*

The method of RT-PCR was used in order to investigate the expression of *cpcat2* during parasitic culture. Total RNA from rye infected with *Claviceps purpurea*, strain T5, was used as a template. The RNA template originates from phases I-IV of infection as described in 3.1.4.2; hybridisation with *cpcat2* detects those products which result from specific amplification of *cpcat2*. For amplification, the primers RTCATF and RTCATR were used which span the 85 bp intron (see fig. 3.24); with mRNA template the expected product would be 249 bp; DNA would give rise to a 334 bp fragment. The results are shown in fig. 3.28 A and B. Although many different fragments were amplified in the RT-PCR reaction (A, lanes I-IV), only two of them produce a strong signal after hybridisation with the *cpat2* probe (B, lanes III and IV). The smaller of these signals (ca. 250 bp) was amplified from mRNA, while the larger hybridising fragment results from the amplification of DNA. The almost complete lack of an-mRNA-derived amplification product in phases I and II indicates that *cpcat2* is mainly expressed during late infection, during phase III and phase IV which entails the formation and ripening of sclerotia and the biosynthesis of alkaloids.

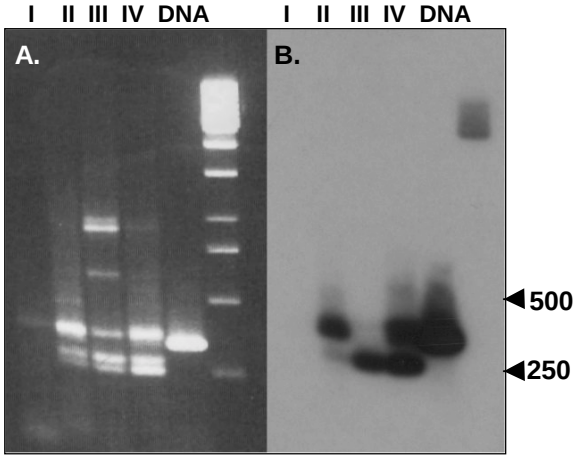

Fig. 3.28: *In planta* expression of *cpcat2*. A. RT-PCR products. Template for the PCR: Phase I-IV mRNA, genomic 20-1 DNA. **B. Southern analysis.** The gel shown in A was blotted and probed with the 1.7 kb *Sac*I fragment of *cpcat2*. Relevant size marker fragments are indicated on the far right in bp.

3.2.5 Targeted inactivation of *cpcat2*

The results of the expression studies indicated that *cpcat2* is co-regulated with genes of the alkaloid biosynthesis cluster. Sequence analysis of the derived protein indicates that the product of this gene is a functional catalase; a faint band of catalase activity was found whose presence correlated with to the

expression of *cpcat2*. In the pathogenic strain 20-1, this gene is only expressed during later stages of infection, rendering a role in the initial development of the fungus during pathogenesis unlikely. In order to ascertain the importance of CpCAT2 for sclerotial development during pathogenesis and the synthesis of sclerotial alkaloids, the gene was inactivated in strain 20-1. To avoid re-establishment of the wild type gene through internal recombination (a phenomenon attributed to the constant re-occurrence of wild type *cpsod1* in Δcpsod1 strains taken from glycerine stocks; data not shown), a targeted gene replacement was used to delete *cpcat2*. This method, which involves a double cross-over event with a linear replacement fragment resulting in irreversible deletion of parts of the targeted sequence, yields more stable mutants than those created by gene disruption.

3.2.5.1 Construction of replacement vector pRV-1.

The strategy of pRV-1 construction is shown in fig. 3.29 A. Primers RVF1 and RVR1 were used to amplify a 953 bp fragment of the *cpcat2* genomic region containing parts of the promotor and 3' coding sequences of *cpcat2*. Both primers contained artificial *Bgl*II sites on their 5' ends so that, after introducing the PCR fragment into the TOPO-cloning vector, the fragment could be excised with *Bgl*II and cloned into the *Bgl*II site 138 bp downstream of the beginning of the phleomycin resistance gene promotor in the fungal transformation vector pAN8-1. Orientation of the fragment was determined by sequencing with REVERSE primer. Similarly, primers RVF3 and RVR2, containing an artificial and a natural *Xba*I site, respectively, amplified a 1052 bp fragment which was cloned via the TOPO vector into the *Xba*I site at the end of the phleomycin resistance terminator in pAN8-1. Orientation of the second flank was determined by restriction analysis (data not shown). Between primers RVR1 and RVF3 lies a 63 bp region which has been replaced by the 3313 bp phleomycin resistance cassette in the vector pRV-1. Digestion of pRV-1 with *Pst*I and *Pvu*I releases a 5449 bp fragment containing both *cpcat2*-derived PCR fragments flanking the phleomycin resistance gene, as well as 4 bp preceding and 127 bp following the fragments which represent the pAN8-1 sequences between *Pst*I and *Bgl*II as well as *Xba*I and *Pvu*I, respectively. This fragment, denominated RF-cpcat2, was used to transform the pathogenic *C. purpurea* strain 20-1.

3.2.5.2 Transformation and analysis of RF-*cpcat2* transformants with PCR

Aliquots of 10^7 protoplasts were transformed with 10 µg of RF-cpcat2, embedded in regeneration media and overlaid with phleomycin-containing agar after 4 h incubation at 28°C. Controls were carried out as described in 3.1.5.2. Transformants selected in the course of several transformation experiments were analysed with PCR for the presence of homologously integrated RF-cpcat2. The screening strategy is schematically represented in fig. 3.29 B. Should the replacement fragment integrate homologously via a double crossover, the genomic region spanned by sequences contained in the fragment would be lost and the fragment containing the phleomycin resistance would take its place

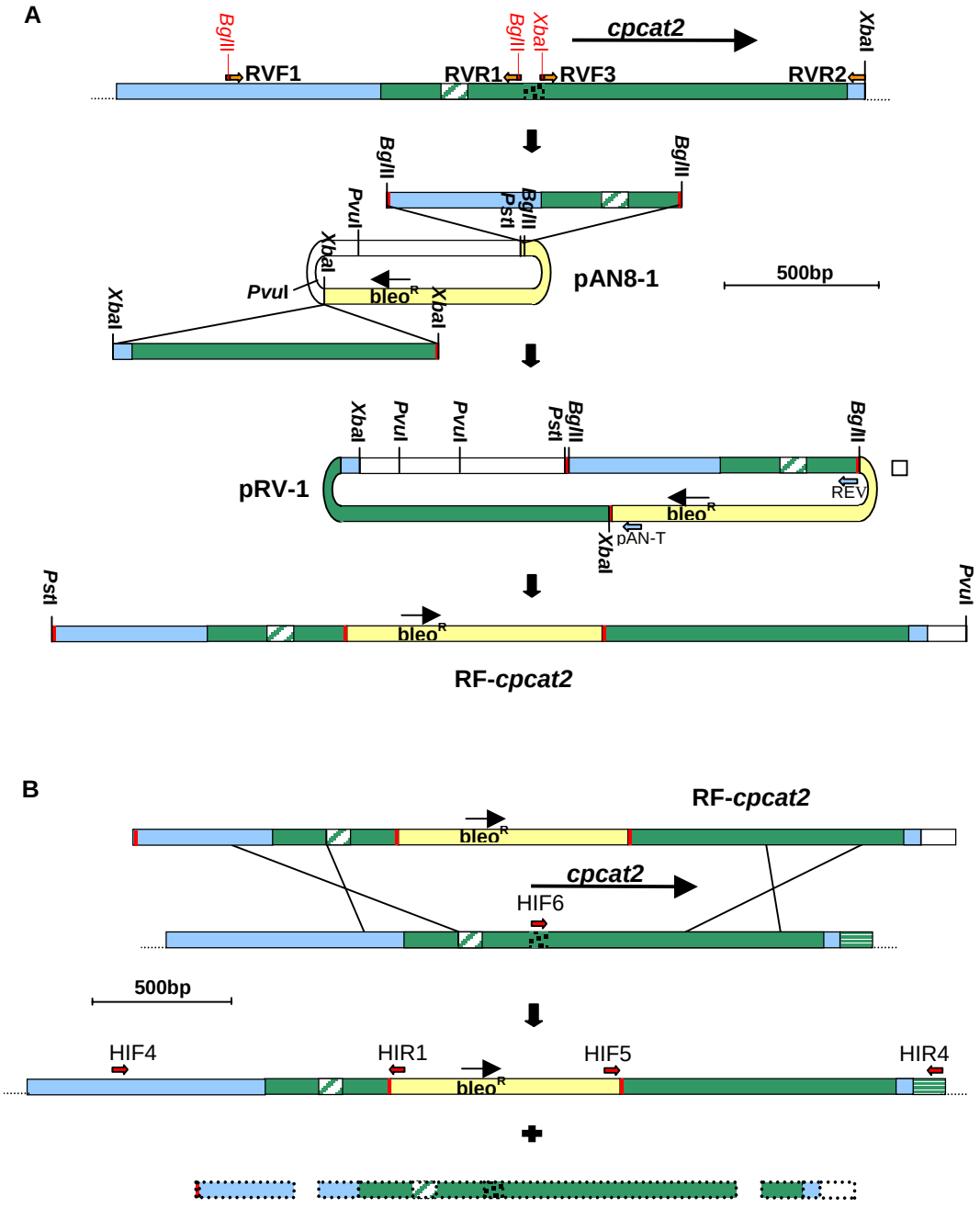

Fig. 3.29: Targeted inactivation of *cpcat2*. *Cpcat2* is depicted in green, exons are solid and introns are striped, surrounding genomic regions are blue. Red and blue arrows are PCR and sequencing primers, respectively; red regions indicate artificially induced restriction sites. Black arrows indicate direction of transcription; dotted lines indicate continuity of genomic DNA. The replacement vector is derived from pAN8-1 which contains the bleomycin resistance cassette (yellow) and pUC18 (white). All DNA is shown to scale with the exception of curved elements and those DNA regions derived from pAN8-1. Details are described in the text. **A. Construction of linear replacement fragment RF-cpcat2.** Primers RVF1 with RVR1 and RVF3 with RVR2 were used to amplify two flanks of the *cpcat2* genomic region which were cloned into the *Bgl*II and XbaI sites of pAN8-1, respectively, to create the replacement vector pRV-1. Orientation of the fragments was determined by sequencing with REVERSE and pAN-T primers (blue arrows). Digestion with *Pst*I and *Pvu*I releases the replacement fragment RF-cpcat2. The 63 bp sequence of genomic DNA which lies between the two amplified regions is depicted in black stipple. **B. Double crossover event which leads to gene replacement.** A double crossover event between the homologous regions of the replacement fragment RF-cpcat2 and the genomic region of *cpcat2* yields a coding region interrupted by the bleomycin resistance cassette as well as three DNA fragments destined for self-digestion (shown in stipple). Homologous integration was determined by screening of transformant DNA with either primers HIF4 and HIR1 or HIF5 and HIR4; of each primer pair, one binds in regions adjacent to those contained in the replacement fragment while the other binds within the bleomycin resistance gene. As all of the sequenced DNA downstream of the *cpcat2* gene is contained in RF-cpcat2, 116 bp of adjacent sequence was obtained from T. Correia (shown in pale green). The presence of the wild-type gene copy was determined by PCR with primers HIF6, which binds to DNA not contained in the replacement vector (black stipple), and HIR4.

in the genome. Primer HIF4, which binds to regions upstream of RF-cpcat2, in combination with HIR1, which binds to upstream sequences of the phleomycin resistance promotor, would amplify a fragment of 1028 bp. Similarly, the combination of primers HIF5 and HIR4, binding within the phleomycin resistance terminator and downstream of regions contained in RF-cpcat2, respectively, would produce a fragment of 1229 bp. As its template lies between the two flanks amplified for RF-cpcat2, the primer HIF6 was used in combination with HIR4 to detect the presence of the wild-type gene copy; these two primers would give rise to a 1226 bp fragment. Of the 480 transformants which were screened using PCR with all three primer pairs, only two, T2-36 and T8-20, showed a homologous integration. Although the genomic DNA of T2-36 gave rise to both homologous integration fragments in PCR, it also contained the wild type gene copy. Despite several rounds of single spore isolation, this transformant was unable to be purified. The presence of the wild-type copy of *cpcat2*, as well as a second copy containing the phleomycin gene cassette, was confirmed via Southern analysis in the original transformant along with several descendants (data not shown). In contrast, no purification of the transformant T8-20 was necessary, as the genomic DNA of the original transformant showed no contamination with the wildtype gene. The PCR analysis of the strain T8-20 is shown in fig. 3.30. Primer combination A (HIF4 and HIR1) and B (HIF5 and HIR4), which indicate homologous integration, amplify fragments of the correct size while the primer combination C (HIF6 and HIR4), which detects the presence of even small amounts of the wild-type gene, does not amplify a fragment. Identical PCR with the recipient strain 20-1 (WT) serves as a control; here, only the primer combination C gives rise to a fragment of the expected size. The identity of the PCR fragments indicating homologous integration in T8-20 was confirmed by sequencing (data not shown).

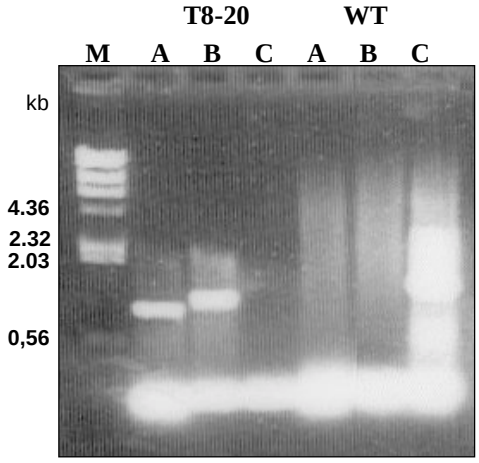

Fig. 3.30:Analytical PCR of transformant T8-20 and recipient strain 20-1 (WT). DNA strains are listed at top of picture. Lane M shows the DNA marker λ x *Hin*dIII; sizes are indicated on the far left in kb. The PCR was performed with three different primer combinations; A: HIF1 and HIR1 (shows homologous integration, 3' side). B: HIF5 and HIR4 (shows homologous integration, 5' side) and C: HIF6 and HIR4 (shows wild type gene copy).

In order to be ensure that only one copy of the replacement fragment has integrated into the genome of T8-20, as well as to confirm the deletion of *cpcat2*, Southern analysis was performed. *Eco*RI digested genomic DNA of strains 20-1 and T8-20 were probed with *cpcat2*; as *Eco*RI does not cut within the replacement fragment RF-cpcat2, a homologous integration would shift the wild-type fragment of 2.9 kb to a new fragment which contains an additional 3.4 kb. Fig. 3.31 shows that the wild type fragment has been replaced with a hybridising fragment at ca. 6.3 kb, and that no other fragment hybridises with the *cpcat2* probe. This

indicates that *cpcat2* has been inactivated and that only single copy of the replacement fragment has integrated into the genome of T8-20; this mutant will hereafter be referred to as Δcpcat2.

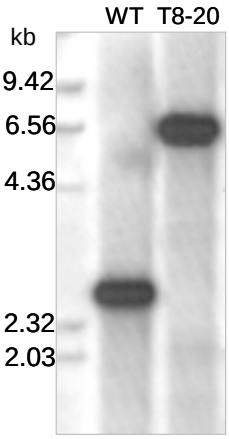

Fig. 3.31: Southern analysis of T8-20. Strains 20-1 and T8-20 were restricted with *Eco*RI and hybridised with a 1,6 kb *Eco*RI/SalI fragment of p25*Sac*IS4, which contains part of the *cpcat2* genomic region, at 65°C. Size marker fragments are indicated on the left in kb.

3.2.5.3 Protein analysis of Δcpcat2 in axenic culture

To ascertain the effect of the *cpcat2* deletion on the activity of other known catalases, protein extracts from mycelia of axenic cultures of both Δcpcat2 and the wildtype strain 20-1 were separated using isoelectric focussing and then stained for catalase activity. Cultures were grown both in sporulation media, in which the catalases A, B and C/D are expressed (Garre et al., 1998a), and in the alkaloid production media T25N (0.5 g phosphate/l), in which the *cpcat2* transcript was detected in northern analysis of the *C. purpurea* strain P1 (see 3.2.4.1). The results, shown in fig. 3.32, were surprising. The catalase activities in sporulation media (two left lanes) corresponded to those described in Garre et al. (1998a). A strong activity in the basic region of the gel represents the CATC/D (pI 7-8) encoded by *cpcat1*, while two acidic activities correspond to the putative peroxisomal catalase CATA and putative cell-wall associated catalase CATB (pI 5.0 and 5.2, respectively). The CATA activity seems to be slightly induced in the *cpcat2* deletion mutant. When the cultures were grown in alkaloid production media and harvested after 8 d (two right lanes), a new catalase activity appeared which is highly induced in Δcpcat2. IEF of gels pI 3-10 which include a pI marker protein show that CATE has a pI of 6.4 (E. Nathues, pers. comm.). As the *cpcat2* deletion mutant does not lack the activities corresponding to CATA or CATB which appears in the wild-type strain under the same conditions, it can be confirmed that this gene does not encode either of these two proteins. This was already indicated from expression analyses of *cpcat2*; the *cpcat2* transcript could not be detected in northern analysis under conditions in

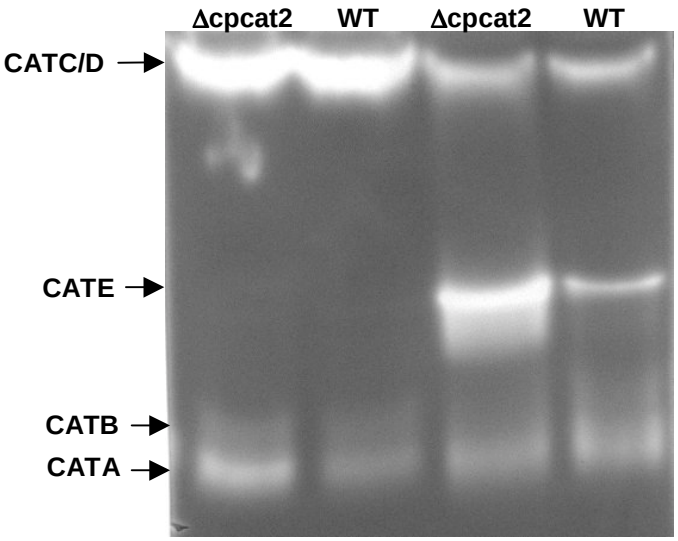

Fig. 3.32:Analysis of catalase activity in Δcpcat2 and the wildtype strain 20-1. Strains were cultivated in MA (sporulation media) and in T25N (alkaloid production media) for 4 and 8 d, respectively. Protein extracts corresponding to 10 mg ground lyophilised mycelia were separated on an IEF gel, pI 5 (bottom) to 8 (top) and then stained for catalase activity. Strains and media are indicated above.

which the activities of these two proteins were present. The induction of a new catalase activity in the *cpcat2* deletion mutant provides further (albeit indirect) support for the identity of Δcpcat2 as a functional catalase.

3.2.6 Pathogenicity assays with Δcpcat2

During pathogenesis of strain 20-1 on rye, the *cpcat2* messenger could be detected in phases III and IV, which encompass the differentiation of sphacelial to sclerotial mycelia as well as sclerotial ripening (see 1.3.1). After inoculation of blooming rye ears with conidia of the *cpcat2* deletion mutant and the wildtype strain 20-1, the course of infection caused by both strains, as detected by production of honeydew and sclerotia, were compared. This not only helps to determine the importance of the *cpcat2* gene product during parasitic growth but also provides sclerotia from both strains, which can be analysed for alkaloid content. The location of *cpcat2* in the alkaloid gene cluster and the evidence of co-regulation with other genes of the cluster in strain P1 suggests that this putative catalase may play a role in the biosynthesis of alkaloids.

Individual florets of male-sterile rye ears of cultivar CMS (ca. 80 florets/ear) were inoculated with conidia of each strain and graded as described in 3.1.6.2. There was no significant difference between the course of pathogenesis as observed in 7 ears infected with each strain. On all 14 ears, comparable amounts of honeydew appeared between 6 and 8 dpi and increased until about 10 dpi. Sclerotial tissue emerged from the floret between 17 and 20 dpi in both strains and no macroscopic differences in the ripening or ripe sclerotia were observed (data not shown). These results show that *cpcat2* is not essential for parasitic growth on rye.

Ripe sclerotia of both strains were harvested after about one month and sent to the laboratory of Dr. J. Wolff (BBA, Institut für Getreidechemie, Detmold, Germany) for analysis of alkaloid content. Here, the amounts of the individual alkaloids ergometrine, ergotamine and ergocryptine, as well as the total alkaloid content, was determined.

Strain	E-mitrine (µg/kg)	E-tamine (µg/kg)	E-cryptine (µg/kg)	Total alkaloids (µg/kg) (average)
20-1 (WT)	71	368	2649	8243
	109	511	2692	
Δcpcat2	n.d.	n.d.	n.d.	692
	n.d.	n.d.	n.d.	

Table 3.2: Alkaloid content analysis of sclerotia derived from infection with the wildtype 20-1 and the deletion mutant Δcpcat2 (results kindly provided by T. Betsche). n.d. (not detectable)**.**

The results, summarised in table 3.2, show that all three of the individually tested alkaloids were below detection level in the *cpcat2* deletion mutant and that the total alkaloid content of mutant

sclerotia is only 8.4 % of that determined for wild-type sclerotia. This would seem to indicate that the deletion of *cpcat2* significantly impedes alkaloid production in this particular mutant. In order to be sure that this phenotype arises only from the lack of *cpcat2* and not from individual peculiarities of this transformant, the mutation must either be complemented or new mutants showing the same phenotype must be generated.

3.3 Searching for new genes involved in AOS detoxification: Differential cDNA screening with and without copper

Parallel to the investigations involving the well characterised AOS scavenging enzymes SOD and catalases, an attempt was made to find further components of the AOS detoxifying system in *C. purpurea.* As metal ions catalyse the formation of the hydroxyl-radical (which, on account of its extreme reactivity, can not be added directly to the cultures), and as metals are involved in the transcriptional induction of some AOS scavenging enzymes, the method of choice was a differential cDNA screening using mycelia cultivated with and without excess copper (see 1.1.1). For this, a copper-induced cDNA library was first synthesised to provide background clones for the differential screening. Clones which showed a differential expression were sequenced; the most interesting ones (as judged by comparative sequence homology) were characterised further.

3.3.1 Creation of a copper-induced cDNA library

Mycelia of the (putative) haploid pathogenic *C. purpurea* strain 20-1 was grown in shaken cultures for 4 d in a complete medium (MA with 10% sucrose) to which 50 µM of copper sulfate was added directly prior to inoculation (with 10^4 conidia/ml medium). These are conditions in which the *cpsod1* gene is highly expressed (see 3.1.1); the catalase activities A, B and C/D are also found under these conditions (data not shown). Details of the library synthesis are provided in experimental procedures, see 2.5.1. The results of the primary library titering are presented in table 3.3, which shows that the primary library consists of ca. 2.2 million plaques, 2.7% of which lack an insert.

Aliquot volume (µl)	**Σ pfu/plate**	**Σ blue pfu/plate**	**average: Σ pfu/blue pfu**	**primary library size**	**% non-recombinant phages**
1	n.c.	---	448/12	4480 pfu/µl x 500µl= 2.24×10^6 pfu	2.7 %
1	n.c.	---			
0.1	386	12			
0.1	580	16			
0.1	414	9			
0.1	412	10			

Table 3.3: Results of the primary library titering. Pfu: plaque forming units, n.c.: not countable.

A secondary library was created by the amplification of one million primary plaques. Excision of the phagemid vector from 48 phages of the secondary library, followed by restriction with *Eco*RI and *Xho*I, showed that 46 of them could be separated into the 4.5 kb pBK-CMV (vector) and inserts ranging in size from 250–2500 bp. The average insert size was calculated to be ca. 1.3 kb.

3.3.2 Differential screening of the copper-induced cDNA library.

The differential screening (DS) was undertaken several times but all experiments fall into one of two categories depending on the conditions used. The first category includes screenings in which the cultivation of induced and non-induced mycelia differed only in the addition of $CuSO_4$ to the former. As only a few (weakly) differentially expressed clones were found in these experiments, a second type of screening was initiated in which the stringency of the conditions were increased. This was achieved by chelating all copper ions in the media in which the non-induced mycelia was cultivated. In addition, the concentration of $CuSO_4$ in the induced cultures was increased.

3.3.2.1 Results of non-stringent differential screening

In these experiments, a total of 12 000 clones of the copper-induced cDNA bank were hybridised with mRNA from mycelia which had been cultivated as the mycelia of the cDNA library was (induced conditions: 50 µM $CuSO_4$ with inoculum), and with a non-induced mRNA population, which was isolated from mycelia cultivated identically with the exception of $CuSO_4$. In these non-induced conditions, the mycelia will have been exposed to a trace amount of copper ions present in water as well as in the yeast extract added to the media base; it was assumed that this amount would not cause significant oxidative stress.

After the first round of screening, about 84 clones were screened in a second round; all clones which showed even the faintest hint of differential expression were isolated and subjected to a third round of testing. For this, the phagemid vectors were isolated from the λ-clones, digested with *Eco*RI and *Xho*I to release the 4.5 kb pBK-CMV vector and their inserts, and subjected to Southern analysis. This was done twice with each set of clones; each membrane was hybridised with induced and non-induced mRNA.

Of a total of 21 clones tested, only four showed any difference after hybridisation with differential mRNA populations. The results are shown in fig. 3.33. Comparison of both sets of EtBr-stained DNA shows that each radioactively marked cDNA population (represented by 1 µg mRNA) has probed the same amount of plasmid DNA on each membrane. Therefore, differences in the signal intensity after hybridisation must be the result of different relative amounts of probe within each population. The most dramatic result was obtained with clone X21 (lane 3). The ca. 450 bp insert shows only weak hybridisation with non-induced mRNA (3-) but a very strong signal after hybridisation with induced mRNA populations (3+). Sequencing reveals a 438 bp clone which shows no homologies after database analysis with BlastN (DNA-DNA) and BlastX (DNA-protein) and which contains 9 $CT_{4\text{-}6}$ repeats. The other three clones show only a partial increase of signal after hybridisation with the induced cDNA: X22, although only very slightly upregulated (lane 2), is interesting because it was found four times in three different screenings. Convincing homologies to proteins of unknown functions from

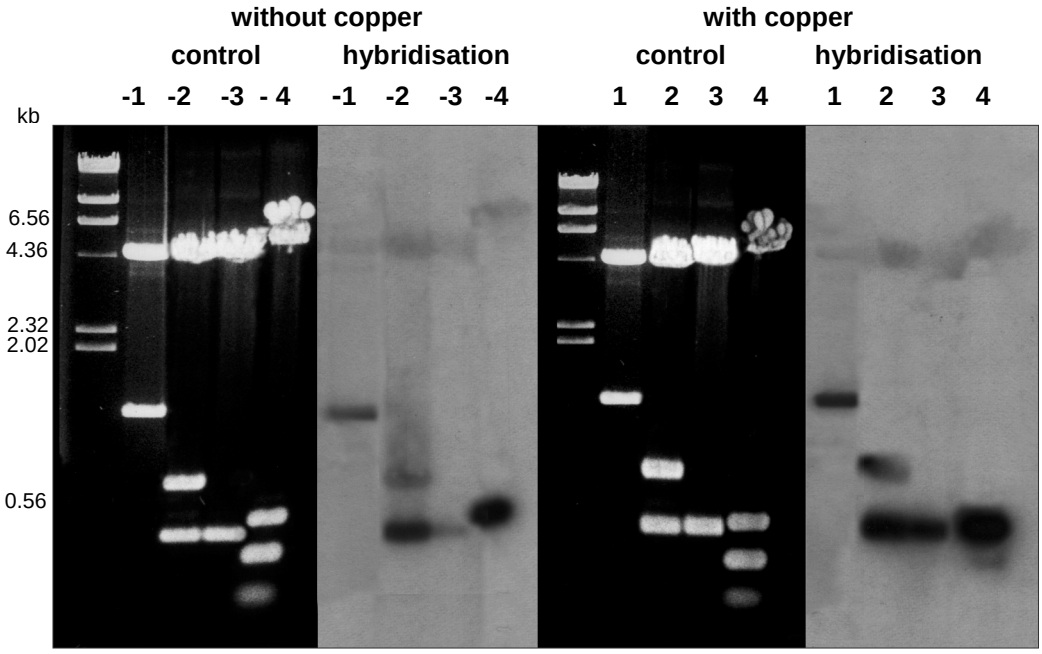

Fig. 3.33: Southern blots hybridised with differential mRNA populations (non-stringent conditions). Identical amounts of *Eco*RI/*Xho*I digested plasmid DNA (from clones isolated in the second round of differential cDNA screening) were separated twice via gel electrophoresis, blotted onto two nylon membranes, and hybridised with differential mRNA populations. mRNA used for hybridisation with the „minus lanes" (without copper: left half, -1 to -4) were isolated from mycelia grown without copper supplement while the „plus lanes" (with copper: right half, +1 to + 4) were hybridised with induced mRNA (mycelia was cultivated in media supplemented with 50 µM $CuSO_4$). In each case, a picture of the EtBr-stained DNA prior to blotting is shown to display insert size (sizes of marker λ DNA are shown on the far left) as well as to provide a quantity control. Lanes 1: XA2, 2: X22 , 3: X21 and 4: X46.

N. crassa and *Streptomyces coelicolor* were found when this clone was analysed with BlastX and BlastP (protein-protein). More information about this clone will be given in the next section, as it was found again during the stringent screening (clone X1, see 3.3.2.2.1). Interestingly, the other two clones (XA2 and X46) which show a slight, but definite, differential regulation (lanes 2 and 4, respectively) show homologies to enzymes which are involved in similar metabolic pathways. The top homologies provided by BlastP analysis of these two clones are shown in table 3.4.

Clone	**protein name**	**Acc.#**	**organism**	**high score**	**probability**
XA2	D-xylose reductase	AAF61912	*Aspergillus niger*	427	e^{-119}
	xylose reductase	AAD09330	*Pichia guilliermondii*	377	e^{-103}
	D-xylose reductase	BAA19476	*Candida tropicalis*	361	$4e^{-99}$
X46	probable Zn-binding dehydrogenase	CAB46402	*Streptomyces coelicolor* *Candida* sp. HA167	200	e^{-50}
	xylitol dehydrogenase	AAC24597	*Bacillus subtilis*	152	$6e^{-36}$
	sorbitol dehydrogenase	Q06004		148	$2e^{-34}$

Table 3.4.: Top homologies of clone XA2 and X46 in BlastP analysis.

The 1203 bp insert of XA2 shows strong homologies to the xylose reductase gene of *Aspergillus niger*. This gene encodes an enzyme which catalyses the first step in the metabolism of xylose, in which

xylose is converted to xylitol. The next step in the metabolic breakdown of xylose is catalysed by the xylitol dehydrogenase, which converts xylitol to xylulose. Xylulose can then be metabolised via the pentose phosphate pathway. Interestingly, the clone X46 shows homologies to xylitol dehydrogenases.

3.3.2.2 Results of stringent differential screening

Because the differential regulation of even the small number of clones found in the first screenings was only slight, the differences between non-induced and induced cultivations were made more extreme. As AOS scavenging genes such as the superoxide dismutase were regulated more by the metals which cause oxidative stress and less by the oxidative stress itself (see 3.1.4.1), it was decided that the next screening would target genes of the general copper metabolism. Once genes were found, their induction by metal excess alone as well as by more direct sources of AOS could be tested. The stringency of the conditions was raised by starving the non-induced mycelia of copper using ascorbic acid, which reduces all copper ions to their cuprous form (CuI), and bathocuproine disulfonic acid (BCA), which chelates Cu(I). Furthermore, induced mycelia was subjected to a twofold addition of 75 µM $CuSO_4$, once directly before inoculation and once four hours before harvesting. In this way the mycelia was subjected to long-term copper/oxidative stress while ensuring the expression of genes involved in the shorter term response to copper.

A total of ca. 7000 phages of the copper-induced cDNA library was differentially screened. In the first round, 101 clones were selected for further analysis. In order to determine if each of the isolated signals contained only one type of phage, the plasmids from a mixture of clones excised from each signal were isolated and subjected to gel electrophoresis. From each of the 46 clones which contained plasmids of different sizes, six individual colonies were isolated and their plasmids were analysed. To ensure that the clone which caused the differential signal could be identified, the different plasmids, dubbed a, b or c (a maxium of three different types were found), were then examined separately in the second round. The second round was done as a dot blot; ca. 1 µg of each plasmid was dropped in identical positions on two different membranes, which were then hybridised with induced and non-induced cDNA. The membranes were subsequently hybridised with the phagemid vector pBK-CMV to control the DNA quantity of each „dot“. The results are displayed in fig. 3.33 (pg. 92). Of the 101 original signals, 40 signals showing certain differential regulation were sequenced and the sequences subjected to BlastX analysis. Table 3.5 summarises the results of the stringent differential screening.

clone	diff. reg.	top homologies, high score, probability	notes
X1	+	-hypothetical protein B1D4.110 from *N. crassa*, 314, $4.0e^{-27}$ -probable secreted protein *from Streptomyces coelicolor*, 279, $2.0e^{-23}$	-found four times in three differential screenings despite low degree of differential regulation
X7 X12a X13 X16 X17 X18a X25 X27b X31 X36 X37 X42 X47 X49 X59b X70 X84 X93	++ - +++	-hydrophobin HFB1 from *Trichoderma reesei*, 58, $2e^{-8}$ -trihydrophobin CFTH1 from *Claviceps fusiformis*, 56, $9e^{-8}$	-found 18 times (single clones) and as part of three further mixed clones (X6, X8b and X23a) -X12a is a full length representational clone
X8b	+	-protein related to superoxide dismutase in *N. crassa*, 393, $1.7e^{-35}$ -superoxide dismutase of *Xenopus laevis*, 110, $8e^{-5}$	-homologies to REVERSE* sequences only -mixed clone, only detected here because it contains hydrophobin-sequences (see X7 and others)
X9 X20b X27b X30 X44 X82b X100	++	-Blast analysis (X, P and N) fails to produce significant homology to any known proteins or cDNAs	-found 7 times -small cystein-rich protein
X23a	++	-protein related to $Na^+/K^+/2Cl^-$cotransporters in *N. crassa*, 115, $6e^{-25}$ -probable membrane protein YBR235w in *S. cerevisiae*, 83, $2e^{-15}$	-homologies to REVERSE* sequences only -composite clone; UNIVERSE sequences show homology with the hydrophobin (see X7 and others)
X27a X68	+	-no homologies in BlastX analysis	-found twice
X34	(+)	-conserved hypothetical protein SPCC1450.14c from *S. pombe*, 74, $2e^{-12}$ -yeast ero1 homologue from *S. pombe*, 67, $1e^{-10}$	-although sequences obtained with UNIVERSE* and REVERSE* primers do not overlap, both show the same homologies (here: REVERSE*)
X43	+	-no homologies found with BlastX or BlastN	
X51a	+++	-related to cell surface ferroxidase of *N. crassa*, 703, 0.0 -ferro-0_2-oxidoreductase from *Arxula adeninivorans*, 623, e^{-177}	
X62	+	-probable glutamate-5-kinase from *S. pombe*, 805, $3.7e^{-79}$ -glutamate-5-kinase from *S. cerevisiae*, 780, $1.7e^{-76}$	
X65	+++	-proteasome component Y7 from *S. cerevisiae*, 337, $8e^{-92}$ -probable proteasome subunit alpha type 2 from *S. pombe*, 298, $4e^{-80}$	
X80c X98	++	-cystein-rich hair keratin associated proteins 90, 0.092	-found twice -homologies are extremely weak and only cover a ca. 300 bp of the 1.47 kb sequence -sequence is not good
X18b X22 X28	+ - ++	- not able to be sequenced	

Table 3.5: Results of the stringent differential cDNA screening (DS4). Clones with overlapping sequences are grouped together and their top homologies after BlastX analysis are shown (nucleotide query is translated in all six frames and compared to the contents of protein databases). The degree of differential regulation (diff. reg.) is indicated by + symbols: (+) represents minimal, and +++ maximal differential regulation. Where sequence quality allows the designation of ORFs, BlastP (protein-protein comparisons) has been employed to reveal possible conserved domains. Where multiple clones have been isolated which correspond to the same gene, the representational clone, used to probe northerns, Southerns or phage libraries, is depicted in red. **X1**, although only isolated once in the course of this experiment, was found three times during two previous screenings. * UNIVERSE and REVERSE refer to primers which bind to universal binding sites present on both sides of the cDNA insert of the vector pBK-CMV; both primers were used for insert sequencing. Usually, sequences obtained with UNIVERSE correspond to the C-terminus (poly-A), while REVERSE sequences correspond to the N-terminus of the protein.

3.3.2.2.1 Descriptions of the sequenced clones and their homologies

- **Clone X12a**

The most striking result of this experiment is that 18 of the 40 sequenced cDNA clones (represented by clone X12a) contain overlapping sequences which correspond to the same gene. The open reading frame of 288 bp translates into a protein of 96 aa which shows homology to hydrophobins. Hydrophobins are small secreted proteins, ubiquitous among fungi, which are able to form highly stable amphipathic polymers; their meaning is thought to lie in the coating of aerial structures, such as spores and fruiting bodies, which renders them hydrophobic (reviewed in Wessels, 1997). Although the overall sequence homology among hydrophobins is low, they are characterised by a fixed pattern of cystein residues. The protein derived from this species of cDNA, which was first discovered in the course of an *in planta* EST analysis (Oeser et al., 2002), shows the cystein pattern typical for hydrophobins (fig. 3.34).

$$X_{2\text{-}38}\text{-C-}X_{5\text{-}9}\text{-C-C-}X_{11\text{-}39}\text{-C-}X_{8\text{-}23}\text{-C-}X_{5\text{-}9}\text{-C-C-}X_{6\text{-}18}\text{-C-}X_{2\text{-}13}$$
$$X_{30}\ \text{-C-}X_{9}\ \text{-C-C-}X_{11}\ \ \text{-C-}X_{15}\ \ \text{-C-}X_{8}\ \ \text{-C-C-}X_{10}\ \ \text{-C-}X_{4}$$

Fig.3.34: Conserved cystein pattern in the primary structure of hydrophobins (top) and the putative hydrophobin represented by clone X12a (bottom).

The top homologies are to the HFB1 hydrophobin of the fungal hyperparasite *Trichoderma reesei* and to the trihydrophobin (containing three hydrophobin units) of *Claviceps fusiformis*. These are both class II hydrophobins (which form less stable polymers than the hot-SDS resistant class I polymers) of parasites. Although hydrophobins have often been found in the course of differential screenings as they tend to be strongly induced when switching from one developmental stage into another (Talbot et al., 1993, Lora et al., 1993, Arntz and Tudzynski, 1997), the connection to copper is as mysterious as it is intriguing. Hydrophobins are cystein-rich proteins; cysteinyl residues are typical ligands of metals as in the metal thiolate clusters of metallothioneins. Furthermore, hydrophobins are associated with aerial structures which are exposed to more oxidative stress than are submerged ones. The strength and novelty of the copper induction of this hydrophobin, dubbed *cph1*, justified sequencing of the entire gene.

- **Clone X9**

The other clone which was isolated several times in the course of this screening was the clone type represented by X9. Isolated seven times, it refused to show homologies with any other gene or EST-sequence in the EMBL/GenBank databases after BlastX and BlastN analysis. The sequences of the seven clones form a contig containing an open reading frame of 216 bp which translates into a protein of 72 aa. BlastP analysis of the putative protein (dubbed X9p) also fails to reveal homologies to other

known proteins; no conserved domains were found in Blast or PROSITE analysis. With a putative molecular weight of 7.3 kDa and a calculated pI of 8.52, X9p is a very small and basic protein. Furthermore, 6 of its 72 aa are cysteins, which puts it into the category of small cystein-rich proteins; this, together with its diminutive size and unique sequence, is shared by other proteins interesting for pathogenicity, such as the products of avirulence genes (Laugé and De Wit, 1998).

- **Clone X1**

Table 3.5 shows also a number of other clones whose expression is less dramatically induced by copper, some of which have also been found more than once. Clones of the type X1 were found three times during the non-stringent screenings (see 3.3.2.1) and once during the stringent screening, a fact which indicates that addition of copper alone induces a detectable expression increase of this gene. Although comparison of the induction obtained by non-stringent vs. stringent conditions shows that the background expression decreases under conditions of copper starvation (compare fig. 3.33, lane 1 with fig. 3.35, X1), the expression of this gene remains low in comparison to many of the other clones isolated in the course of stringent differential screening. Sequence analysis shows that all sequences build one contig 1103 bp in length, containing one open reading frame of 630 bp which translates into a protein of 210 aa. Blast analysis shows convincing homologies to putative proteins from *Neurospora crassa* and *Streptomyces coelicolor*. Unfortunately, as both ORFs were discovered in the course of genome sequencing, nothing is known about the possible functions or expression patterns of these proteins. Although three of the four most homologous proteins are estimated as secreted or membrane proteins (data not shown), analysis of the X1 consensus sequence with PSORT, which predicts cell localisation on the basis of sequence comparison with conserved protein targeting signals (Nakai and Kanehisa, 1992), revealed no signal sequence for secretion. This may only indicate that some of the 280 bp of sequence prior to the start of the predicted ORF (an uncomfortably large amount) is actually part of the putative protein, although it contains no detectable homology to other proteins.

- **Clones X27a/X68 and X98/X80c**

Two further cDNAs were each found twice. X27a (putatively) overlaps with X68 to form a contig of 1534 bp, while X98a and X80c unite into a single contig of 1474 bp. Both messenger types are barely detectable under conditions of copper starvation; bombardment with copper results in a modest expression only. Furthermore, no putative function can be assigned to either clone by Blast analysis. Translation the X98a/X80c sequence (between 430 and 575 bp) shows a putative protein sequence which displays slight homology to a cystein rich, keratin-associated protein. The homology is very slight, and further interpretation of this clone must await more sequence data.

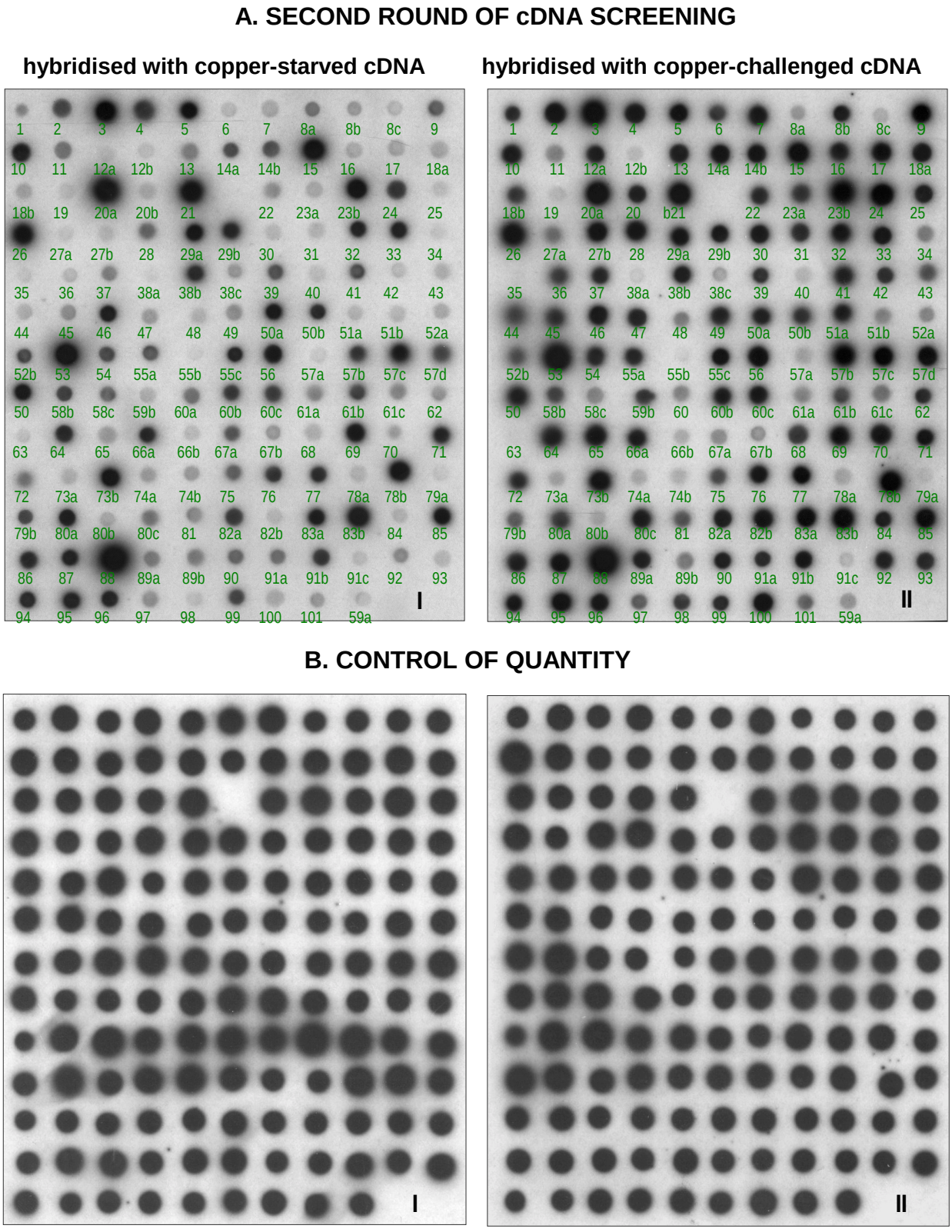

Fig. 3.35: Second round of stringent differential screening. A. Identical amounts of DNA were dropped on two membranes and hybridised with the 1µg of radiolabelled cDNA from copper starved (I) and copper-challenged (II) mycelia. B. Both membranes were hybridised with vector pBK-CMW common to all excised clones as a quantitiy control. Green numbers, shown only in A, correspond to clone name; letters indicate purified clones originating from mixed phages which gave rise to one signal in the first round.

- **Clone X8b**

Another attractive set of homologies unveiled in the course of this screening is provided by the clone X8b. BlastX analysis of its reverse sequence (corresponding to the N-terminus of the derived protein) shows a slew of homologies to the Cu,Zn superoxide dismutases of a number of outlandish organisms. Some homologies are even quite convincing, such as that to the enzyme from the African clawed frog, *Xenopus laevis*, which scores 110 by a probability of $8e^{-5}$. These homologies led to the denomination of this clone as *cpsod-ish*. Closer investigation of this clone yielded a number of dampening discoveries. First, the increased hybridisation of this clone with copper-challenged cDNA is due not to sequences originating from *cpsod-ish*, but to *cph1* (hydrophobin), which was revealed after the sequencing of the insert from the opposite side. (Later experiments showed that the expression of *cpsod-ish* under the conditions of the copper-induced cDNA library is non-detectable). The clone X8b is therefore a mixed clone, composed of messengers originating from two separate genes. Secondly, although the homology to Cu,ZnSOD looks convincing, it contains neither of the two annotated domains which are found in functional Cu,ZnSODs (PROSITE signature 1 and 2), even though the homologous regions in the true SODs do span signature 1. Furthermore, although the reverse sequence of 944 bp offers an 193 aa ORF in the same frame which corresponds to the region between 365 and 944 bp, the homologies to this highly conserved enzyme only range from 515-871 bp. Finally, the top homology (between 440 and 907 bp) is to a protein from *Neurospora crassa* which is deemed „similar to Cu,ZnSODs“, presumably because of similarly striking, but inconclusive sequence homologies.

- **Clone X23a**

Another such composite clone is X23a, whose reverse sequence shows good homologies with a protein of *N. crassa* related to a symporter which takes up sodium and potassium cations while expelling chloride anions. Again, the universe sequence is derived from *cph1*; later, experiments in which northern blots were probed with a PCR fragment amplified from the symporter-homologous region of this clone failed to reveal any transcription of the corresponding gene under conditions of copper excess. Unlike the clone X8b, the homologies of the „silent“ messenger fragment were not interesting enough to warrant further analysis, although there is evidence that K^+ transporters are regulated by active oxygen species (Taglialatela et al., 1997).

- **Clone X51a**

The clone X51a is of interest because of both its strong differential regulation and its very high homologies with the multicopper oxidases (FET3 homologues) of yeast and *Neurospora crassa*. Sequencing of the entire insert uncovered an ORF which translates into a protein of 625 aa containing two PROSITE signatures for multicopper oxidases and a predicted signal peptide for secretion as defined by von Heijne (1986). Protein homologies span the entire putative *S. cerevisiae* FET3 homo-

logues of *N. crassa*, *Arxula adeninivorans* and *Pichia pastoria* (to name the top three). FET3 of *S. cerevisiae* is a copper-containing ferrooxidase which forms part of a high-affinity iron uptake system. It uses molecular oxygen to oxidise ferrous to ferric iron, which is then transported into the cell by an associated permease, FTR1 (Akswith et al., 1996). *In S. cerevisiae*, the transcription of both genes is increased by addition of 100 µM copper (Gross et al., 2000).

- **Clones X62, X65 and X34**

Another clone showing strong homologies to proteins of a known function is **X62**, which is very likely a glutamate-5-kinase, the enzyme which catalyses the first step in the biosynthesis of proline (Li and Brandriss, 1992). The 786 bp sequence originating from the reverse primer shows an ORF of 240 aa which contains the PROSITE glutamate-5-kinase signature.

Insert sequences of the clone X65 unite to form a contig of 1074 bp, containing a single ORF which translates into a protein of 277 aa. The homologies indicate that this sequence encodes a full length proteasome α-subunit (homologous to one of 14 different kinds in mammals); furthermore, it contains a PROSITE signature typical for this protein.

The sequences of clone X34, which shows an extremely slight differential regulation, group into universe and reverse contigs. Although table 3.5 displays only the homologies obtained with the reverse sequence, both show respectable homology with the yeast ERO1-L. This protein is responsible for maintaining conditions favouring disulfide bond formation in the endoplasmatic reticulum (Cabibbo et al., 2000).

3.3.2.2.2 Summary: stringent differential screening

The increase of differential stringency resulted in the discovery of many differentially regulated messengers. Sequence analysis of 37 clones showing differential regulation in the second screening round resulted in the identification of twelve individual cDNAs; this involved the analysis of 92 single sequences encompassing more than 60 kb. Most of this work contributed to the isolation of one clone only: the type X12a which encodes the putative hydrophobin *cph1*. This illustrates both its massive differential regulation under the conditions of this screening and its high rate of expression under the induced conditions. The same conclusions (although in slightly milder form) can be made for the protein encoded by the gene corresponding to type X9 cDNA. Of the twelve cDNAs, 7 displayed significant homology with proteins of known functions, one clone (X1) showed homology to a protein of unknown function and four showed no significant homologies to genes registered in the EMBL/GenBank databanks. With the exception of X1, none of the cDNAs were identified in the non-stringent screening, suggesting that the regulatory element(s) responsible for increased transcription of the corresponding genes under induced conditions may not be controlled by copper excess alone.

3.3.2.3 Northern analysis of isolated cDNAs

The goal of the differential screening experiments was to find genes involved in the response to oxidative stress. Although the increase of stringency in the conditions of the last differential screening led to the identification of many candidates for such genes, it also increased the complexity of the differential factors, resulting in the isolation of genes responding to different physiological stimuli. The fact that the non-induced conditions involved copper starvation could lead to genes which are repressed by copper deprivation rather than activated by copper excess. Although, given the interplay between AOS and metals, this does not bar their importance for survival under oxidative insult; their involvement is unlikely to be direct. Furthermore, ascorbic acid was used to reduce the copper ions to a form which is bound by the chelator. As this substance is an efficient quencher of oxidative stress, it was not included in the induced conditions. This could lead to the isolation of genes repressed by ascorbic acid. Finally, genes which are upregulated by copper could be part of an AOS-independent copper housekeeping system, rendering them less interesting for further investigation.

The first step which was taken to classify the regulatory response of the isolated genes, was to determine which of those could be upregulated by simple addition of copper. Secondly, in order to determine which of these genes are likely

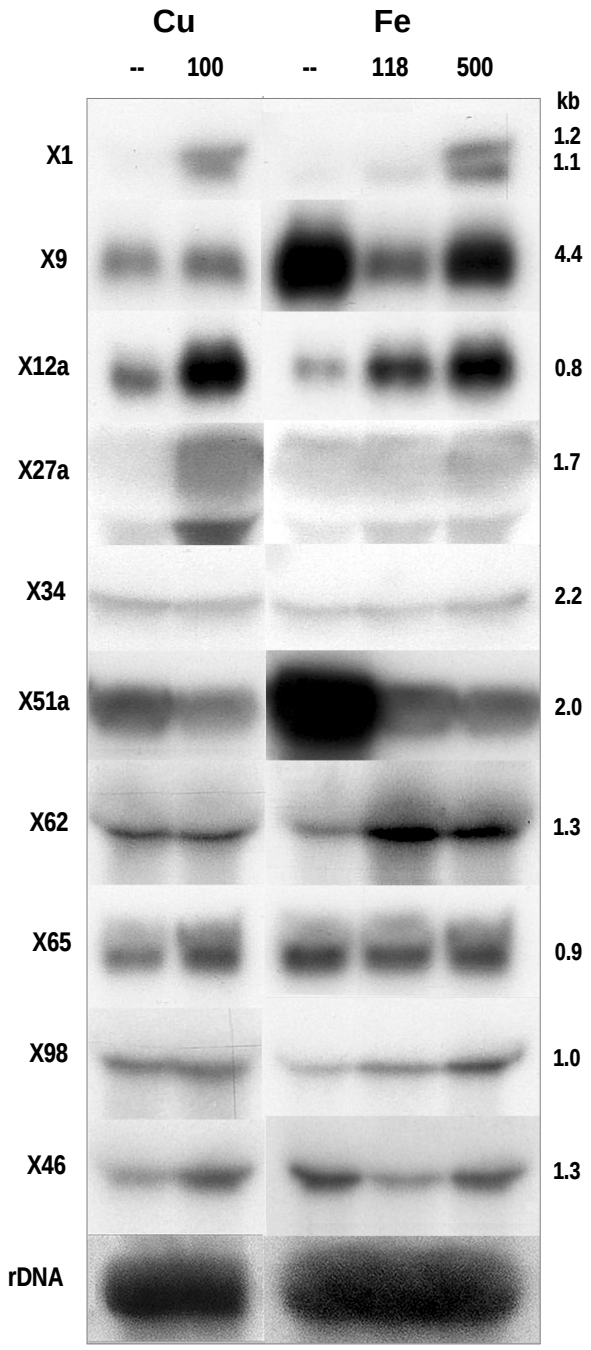

Fig. 3.36: Effect of excess copper and iron on the expression of genes isolated in the course of differential cDNA screening. In separate experiments, the induction of genes by Cu and Fe were tested. To create excess conditions, either 100 µM $CuSO_4$ or 118 and 500 µM $FeSO_4$ were added to a complete medium (MA) directly prior to inoculation. Cultivation of both controls (--) was done in MA to which no metals had been added. 25 µg of total RNA were loaded on each lane and probed with the cDNA insert of the clone indicated on the left. A total of six northern blots were made for each metal (CuI-CuVI and FeI-FeVI). Although each blot was hybridised separately with rDNA from *Giberella fujikuroi* as a control of quantity, showing no significant differences in the amount of RNA in the lanes of all blots, only one of each type (CuI and FeI) is shown here as an example (bottom). All probes are cDNAs isolated in the course of stringent differential screening with the exception of X46, which was found during the non-stringent screening. The transcript size is indicated on the far right.

candidates for the oxidative stress response, two further sets of experiments were implemented. The first approach draws again on Fenton chemistry as a source of AOS, arguing that genes induced as by excess copper as part of the metal-mediated oxidative stress response should also be induced by excess iron. The second approach, carried out by S. Joshi, investigated the ability of some of the isolated genes to respond to a direct source of oxidative stress in the form of hydrogen peroxide.

In order to test the induction with copper and iron, cultures grown in media to which no metal had been added were compared to cultures in which the sulfate salt was added directly prior to inoculation. Induction with 100 µM $CuSO_4$, 118 µM (the routine $FeSO_4$ concentration of the base medium) and 500 µM $FeSO_4$ were tested; the results are depicted in fig. 3.36 (see above). As the original cDNA inserts of both "silent" clones X8b and X23a combined sequences that were identical to regions of *cph1* (X12a) with sequences showing homologies to Cu,Zn SODs (X8b) and ion symporters (X23a), regions corresponding to the latter were amplified with PCR for use as probes (data not shown). The transcripts of the two genes could not be detected at all; this indicates that the expression of both genes under these conditions is, at best, very low. The appearance of these two clones in the cDNA bank must be regarded as coincidental. A look at the effect of the addition of H_2O_2 on the transcription of some of the cDNA clones, carried out by S. Joshi, shows that some respond with increased expression (fig. 3.37). Mycelia was challenged for three hours with 0.1, 0.5 and 1 mM H_2O_2; the expression of a variety of genes was compared to mycelia to which water had been added. The top lane shows the expression of *cpcat1* after oxidative challenge; as this gene is known to be induced by H_2O_2 (Joshi et al., 2002b), this served as a positive control for the other experiments. As expected, the expression of *cpcat1* increased after addition of 0.1 and 1 mM H_2O_2. The results of the northern analyses are summarised in table 3.6.

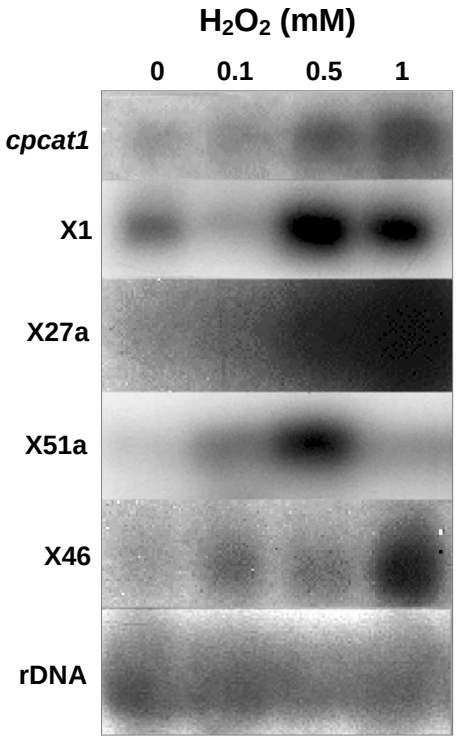

Fig. 3.37: H_2O_2 induction of isolated cDNA clones (results kindly provided by S. Joshi). The top indicates the amount of H_2O_2 added (in mM) 3 h before harvesting. The probes are listed on the left. The experiments were carried out with a number of filters, although they were all hybridised with rDNA of *G. fujikuroi* to check quantity, and showed no differences significant for the results shown here, only one such control has been included.

Clone	Cu	Fe	H_2O_2*
X1	+++	+++	++
X9	no effect	---/++†	n.a.
X12a	+++	+++	no effect
X27a	++	no effect	++
X34	no effect	no effect	n.a.
X51a	-	---	++
X62	no effect	++	n.a.
X65	+	no effect	n.a.
X98	(+)	+	no effect
X46	++	--/++†	++

Tab. 3.6: Summary of northern analyses with some of the cDNA clones obtained by differential screening. The effect of each substance on transcript levels is indicated by + (induced) or – (repressed). Clones X9 and X46 are both induced in media containing low iron amounts and in media containing high amounts of iron. *Effect of H_2O_2 on gene expression was carried out by S. Joshi. n.a.: not analysed.

3.3.2.3.1 Clones which are not induced by copper

Of the nine (non-silent) cDNAs isolated in the course of the stringent differential screening which were subjected to northern analysis, four (X9, X34, X51a and X62) showed no increase of expression when challenged with excess copper. While the expression of X9 (novel protein), X34 (similar to ERO-1) and X62 (glutamyl kinase) remains unchanged after the addition of copper, the expression of X51a (multicopper oxidase) actually shows a slight decrease in conditions of copper excess; this differs from reports of *S. cerevisiae* FET3 which is upregulated by addition of copper (Gross et al., 2000). The differential regulation of all four of these clones which led to their isolation must then originate from factors other than long-term copper excess. The dramatic decrease of X51a transcript after addition of iron is to be expected in a putative high-affinity iron transporter. More baffling is the behaviour of X9 in the experiments with iron; it seems to be upregulated when both no or excess iron has been added. Neither X9, X34 nor X51a show increased transcription with increasing iron concentrations, while X62 is only very slightly induced by iron. Of these clones, only the H_2O_2 induction of X51a, was tested; it is clearly induced by 0.5 mM H_2O_2.

3.3.2.3.2 Clones induced by copper: could induction be Fenton-mediated?

The remaining five clones show at least a slight induction with 100 µM copper. While the transcripts of X1, X12a and X27a show a substantial upregulation under conditions of copper excess, the clones X65 and X98 show only a minimal induction. The clone X46 also showed a moderate induction after addition of copper; this, along with the induction of X1, was to be expected as both clones were isolated in the course of non-stringent screening.

The clone X1 seems to be a beautiful example of a clone responding to Fenton-mediated oxidative stress as it is almost exclusively expressed when exposed to high concentrations of both metals and is induced by 0.5 mM H_2O_2. The clone X46, which was induced by copper and iron, also responded to H_2O_2 challenge (0.1 and 1 mM, respectively) with increased transcription. However, interpretation of

this is complicated by the fact that transcript concentrations increase under conditions of low iron. (The response to iron is similar to that of clone X9; this is not an effect of varying RNA concentrations as different northern blots were used for each hybridisation; data not shown.)

The putative hydrophobin (X12a) is also convincingly upregulated with both increasing iron and copper concentrations as is clone X98, which, while showing only a very slight increase of expression after addition of copper, seems to be more responsive to iron. Disppointingly, both clones show no induction after addition of H_2O_2 (data not shown), so that direct evidence linking these clones to the AOS-response is still lacking.

The very low basal expression of another clone, X27a, is unaffected by excess iron and increases only when the mycelia is exposed to excess copper. Interestingly, this clone is highly induced by 0.5 and 1 mM H_2O_2. However, the failure of iron to induce transcription suggests that the response to both stimuli is mediated by separate pathways rather than one common induction pathway which includes Fenton-driven AOS. The expression of the putative proteasome subunit X65 is similarly indifferent to an increase in medium iron. This clone showed so little response to copper and iron that the induction by H_2O_2 was not tested.

The results of the northern analyses show that 6 of 9 clones isolated by differential screening are upregulated by simple addition of copper to the medium, albeit to different extents. Testing of five genes which are induced by copper showed that three are also induced by H_2O_2. These results indicate that the metal/AOS response does, to some degree, overlap. However, as only one clone (X1) is induced by all three factors (and repressed by none), it can be concluded that the cellular response to high concentrations of metal ions is not generally transduced by pathways involved in H_2O_2-mediated gene induction.

3.3.3 Further characterisation of some of the clones which emerged in the differential screening

Of the genes isolated in the course of differential screening, the most promising candidates for new AOS-scavenging enzymes are either those which show increased transcription under conditions of both iron and copper excess, those which are upregulated by H_2O_2, or both. Only two clones, X1 and X46, show induction with excess copper, excess iron and H_2O_2.

Although X1 is one of the most promising clones, it fails to show any homologies with proteins of known function in the EMBL and GenBank databases, and was thus passed over in the selection of genes for further characterisation for X46. This clone shows clear homologies to sugar alcohol dehydrogenases. In conjunction with the AOS-response, these genes could represent a source of reductive power.

The putative hydrophobin X12a was also chosen for further characterisation as it shows a very

strong induction to both iron and copper. Although this gene does not seem to respond to more direct sources of AOS, it can not be concluded that it is not an important component of the AOS defence system as the Cu,ZnSOD shows response pattern to all three stimuli (see 3.1.4.1). Furthermore, this protein is thought to be involved in the formation of aerial structures which provides an obvious link to oxidative stress.

Of the two clones which were upregulated after oxidative insult with H_2O_2, the clone X51a, which shows homology with components of the high affinity iron-transport system, was characterised further by S. Joshi. The second clone, X27a, did not show any homologies with Blast analysis.

One other clone was investigated in greater depth: X8b (*cpsod-ish*). Although this clone is not expressed under the conditions of the cDNA bank, the homologies to Cu,Zn SODs shown by the cDNA fragment are strong enough to justify further investigation.

In all cases the genomic copy of the cDNA clones were isolated and sequenced. This allowed a more accurate investigation of their homologies as well as promotor analyses. The determination of the exon/intron pattern enabled an investigation of the *in planta* expression of these genes to be undertaken with RT-PCR.

3.3.3.1 Isolation and sequencing of genomic regions corresponding to the cDNA clones

The genomic copies of cDNAs isolated in the course of differential screening were isolated in separate experiments; each involved the screening of ca. 60 000 lambda phages from the genomic library of *C. purpurea* strain T5 with the corresponding cDNA fragment. Hybridising signals were diluted, replated to produce single plaques, and subjected to a second screening round. The DNA of purified phages was digested with a variety of restriction enzymes; hybridising fragments, detected by Southern analysis, were cloned. After further subcloning of the first generation clones, the clones were sequenced.

3.3.3.1.1 X12a, the putative hydrophobin (*cph1)*

The entire 0.8 kb *Eco*RI/*Xho*I cDNA fragment of X12a was used as a probe in the genomic library screening (S9). Of the eleven signals isolated in the first round, seven were purified in the second round. Of these six λ-clones (1-1, 3-1, 5-3, 7-1, 8-3 and 11-1) were analysed further as described above. Two fragments, a 7 kb *Hin*dIII and a 6 kb *Eco*RI fragment, which hybridised repeatedly in different lambdas, were selected for subcloning and sequencing. The cloning strategy is shown in fig. 3.38; all listed subclones, with the exception of S96EK1 (which contains the 6 kb *Eco*RI fragment from λ S95-3), are derived from the S97HK1 clone which contains the 7 kb *Hin*dIII fragment from λ S97-1. The sequenced genomic region of 2144 bp contains the coding region of *cph1* including 1463 bp upstream of the start codon and 305 bp downstream of the stop codon. The coding regions span only 376 bp and contain a single intron of 89 bp. The coding regions, which show 100 % homol-

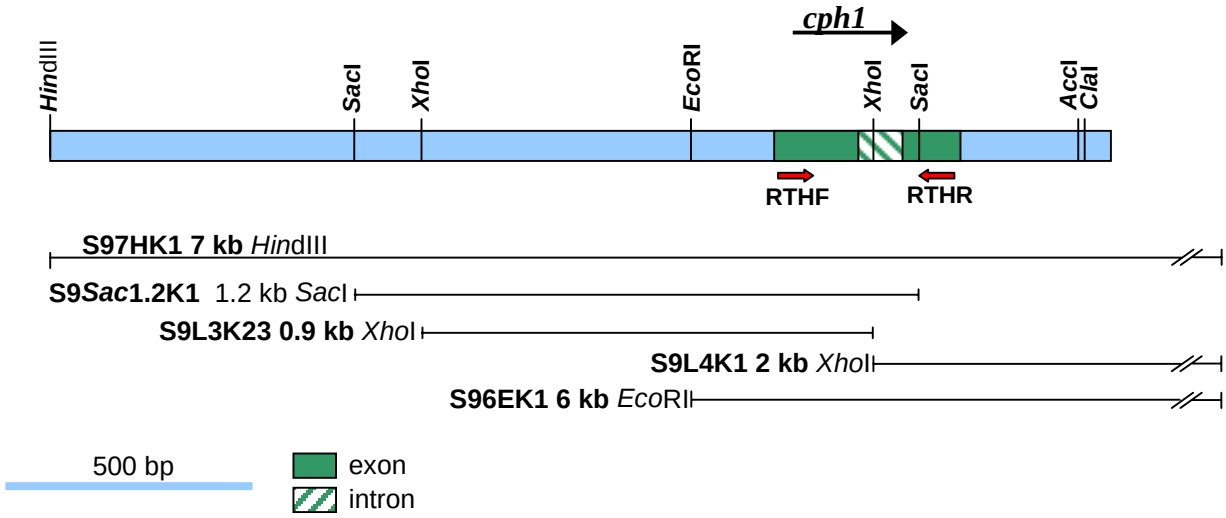

Fig. 3.38: Restriction map and subcloning strategy of the *cph1* genomic region. All subclones were derived from a 7 kb *Hin*dIII subclone from λS97-1 of screening S9 with the exception of S9EK1, which is derived from λS95-3. All fragments were cloned into the vector pBSKS-; sequencing was done with universe and reverse primers. Intron and exon pattern was obtained by comparison with the cDNA consensus sequence of the X12a-type DS4 clones. All DNA is shown to scale; non-coding regions are in blue, exons are solid green, while introns are striped green. Red arrows indicate RT-PCR primers.

ogy with the consensus sequence of the type X12a clones, encode a putative hydrophobin of 96 aa. Analysis of protein targeting signals with PSORT (Nakai and Kanehisa, 1992) predicts that the first 17 aa are a signal sequence for secretion as defined by von Heijne, 1986. As the entire putative protein sequence was already unveiled in the course of the differential cDNA screening, no further homology analyses are presented here. The sequence, including 1000 bp of promotor region, is presented in appendix A.3.

3.3.3.1.2 X46, the putative Zn-binding dehydrogenase (*cpdh1*)

The isolation of the genomic region corresponding to the X46 cDNA involved two separate screenings. In the first screening (S6) the largest fragment released by *Eco*RI/*Xho*I-digestion of X46 was used as a probe. This 456 bp *Xho*I fragment spans the 3' region of the cDNA, corresponding to the C-terminus of the protein. After purification of four lambda clones (λB1-B4), from the second round of screening, Southern analysis revealed that the inserts of all four were identical. A 0.8 kb *Sal*I fragment and a 6.5 kb *Hin*dIII fragment (containing 4 kb of λ-arm) were selected for further analysis. The 2.5 kb fragment of the *C. purpurea* genome, starting with the λ-derived *Sal*I which cleaves the arm), was subcloned and sequenced (fig. 3.39, right side). Comparison of the 2525 bp sequence with the cDNA showed that only the first 451 bp overlapped with the 3' end of the cDNA; as the insert begins at this point in all four lambda clones, a new screening was necessary to isolate the rest of the gene.

The probe used in the second screening (S6-2), a mixture of a 283 bp site *Eco*RI/*Xho*I and a 279 bp *Xho*I fragment, comprised upstream regions of the X46 cDNA only. Six of twelve first round signals were purified and analysed. Four hybridising fragments of λS62-4 were selected for subcloning and

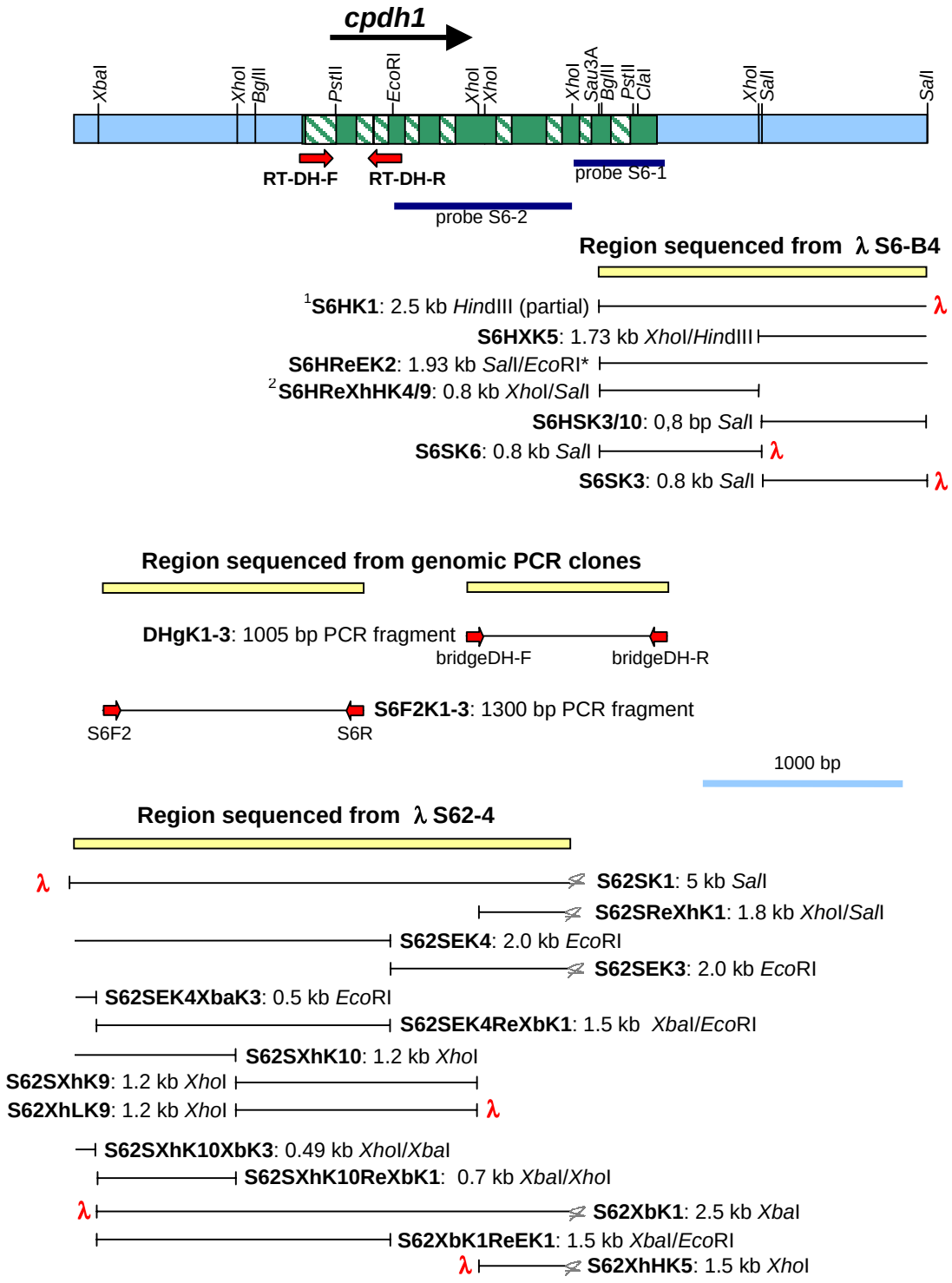

Fig.3.39: Subcloning and sequencing of *cpdh1*. Non-coding genomic regions are depicted in blue, coding regions in green. Primers are indicated by red arrows; a black arrow indicates direction of transcription. Yellow bars denote the origin of subclones, while dark blue bars indicate the area covered by probes used in the first (S6) and in the second (S6-2) screening. The grey scribble shows the start of recombined DNA sequence from λS62 which lacks introns; this region was not used for sequence verification. All fragments were cloned into pBSKS- with the exception of PCR fragments, which were cloned into the TOPO-vector. Sequencing was done with universe and reverse primers. Red lambda symbols denote first generation λ-subclones, while the origin of sub-subclones are indicated in the name. [1]This clone is a partial *Hin*d III fragment, originating from a 6.5 kb *Hin*dIII fragment which recombined in *E.coli* to delete 4 kb of the insert derived from the 3' λ arm, along with the universe primer binding site. The 5' sequence begins with a λ-derived *Sal*I site. [2]This clone was made by religating blunt-ended *Xho*I and *Hin*dIII sites of S6HK1.

sequencing. Sequencing of the subclones from the second screening resulted in a continuous sequence of 3393 bp which showed homology to the upstream regions of the cDNA sequence (fig 3.39, left side). In order to unite the sequences obtained from both screenings, primers from regions of both sequences showing homology to the X46 cDNA were used to amplify genomic DNA and the resulting 1 kb fragment was cloned and sequenced (fig. 3.39, middle). Comparison of PCR and λ-insert sequences indicated that λS62-4 was recombined. After discarding all regions not covered by PCR fragments of genomic DNA or cDNA, the remaining sequences could be assembled into a continuous DNA sequence of 4261 bp containing the entire coding regions as well as 1141 bp upstream of the start codon and 1335 bp downstream of the stop codon.

In order to resolve conflicts which arose during sequencing, and to decipher the intron-exon pattern of the gene, a full length cDNA clone was needed. Comparison of the cDNA clone X46 to the coding sequences of similar genes revealed that the putative protein derived from the 1.1 kb sequence was missing at least 50 aa; northern analysis also showed a transcript size of ca. 1.3 kb. About 60 000 clones of the Cu-induced cDNA library were screened (S11) with the S6-2 probe covering the upstream coding sequences; 12 of 41 signals were purified in a second screening round. Analysis of the excised phagemids using gel electrophoresis showed that only one (S11K12) was larger than X46; this was sequenced. The cDNA sequences overlap to form a single sequence of 1.33 kb containing a 1023 bp ORF. This ORF translates into a protein of 341 aa which shows homology with similar-sized alcohol dehydrogenases over their entire length.

Comparison of cDNA and DNA sequences showed that the coding sequences of the gene, spanning a region of 1783 bp, is interrupted by nine introns, ranging in length from 60-153 bp, which make up 752 bp or 42% of the coding region (see fig. 3.39). The DNA and putative protein sequences of the dehydrogenase, including 1000 bp upstream of the start codon and 20 bp downstream of the stop codon, is shown in Appendix A.4.

Homology analysis (BlastP) of the entire putative protein produced similar homologies as those found with the partial protein (see table 3.4); as expected, the statistical significance of these homologies increased. Although one of the top homologies is to a yeast xylitol dehydrogenase, most of the high scoring proteins are Zn-binding alcohol or sugar-alcohol dehydrogenases of bacteria. Analysis of the putative protein with PROSITE shows a signature sequence for Zn-containing alcohol dehydrogenases at 57-71; this led to the denomination of the gene as *cpdh1*. Alcohol dehydrogenases catalyse the oxidation of an alcohol to an aldehyde with the concomitant reduction of NAD or NADP. Analysis of 47 members of the Zn-containing alcohol dehydrogenase family (Sun and Plapp, 1992) shows that only a few residues are strictly conserved, most of which are glycine; these are probably of structural importance for their lack of bulky side chains. Eight of nine conserved glycines are also conserved in *cpdh1* (not shown in the sequence). Almost all other highly conserved residues interact with the cata-

lytic Zn atom (see A.4; conserved amino acids are in red; numbers correspond to the protein sequence derived from *cpdh1*); C_{37}, and H_{58} are direct ligands, while the charged residues of D_{40} and E_{59} are important for the redox status of its environment. The alcohol group of either serine or threonine (T_{39}), which functions as proton acceptor, is also conserved among Zn-binding alcohol dehydrogenases. The sorbitol dehydrogenases tend to have only one Zn atom (the catalytic Zn), while other members of this enzyme family have two, one catalytic and one non-catalytic (probably important for enzyme structure), which is ligated to four highly conserved cysteins. These four cysteine residues are also present in CPDH1 ($C_{88, 92, 94, 102}$). The presence of most catalytically important residues, as well as the conservation of the non-catalytic Zn ligands, suggests that this enzyme is functional and contains two Zn atoms. Another highly conserved residue is a glutamate thought to be involved in coenzyme specifity; of the 47 enzymes examined, 45 have this glutamate and only two enzymes, both of which use NADP instead of NAD as a coenzyme, have either an alanine or a glycine in the corresponding position (Sun and Plapp, 1992). CPDH1 has an alanine (A_{190}) in this position, indicating that it may also generate NADPH instead of NADH.

Alcohol dehydrogenases build a large super-family of enzymes, which are classified into three groups according to their structural and catalytical qualities: the zinc-containing 'long-chain' alcohol dehydrogenases, the short-chain alcohol dehydrogenases, and the iron-containing alcohol dehydrogenases. Zn-containing alcohol dehydrogenase enzymes, to which both homologies and PROSITE analysis group *cpdh1*, are either dimeric (plant and animal forms) or tetrameric (fungal forms) and contain one catalytic and one non-catalytic atom of Zn per subunit (Jornvall et al., 1987). Although sorbitol (and other sugar-alcohol) dehydrogenases are loosely grouped with the long-chain dehydrogenases, some types of sorbitol and xylitol dehydrogenases build a separate subgroup which, missing much of a loop structure, are denominated "medium-chain dehydrogenases" (Persson et al., 1993). The subdivision of the alcohol dehydrogenase family is complicated by the fact that groupings according to structure do not always correspond to substrate specifity; for instance, the yeast *Pichia stipitis* has at least two xylitol dehydrogenases, one of which belongs to the medium chain type dehydrogenase group, while the other shows more structural similarities with the short-chain dehydrogenases (Persson et al., 1993). Thus, analysis of structure by homology comparison can not supply any concrete information about substrate specifity.

In order to gain more information about the substrate of the putative dehydrogenase, the ability of different sugar-alcohols to induce transcription of the putative dehydrogenase was tested in northern analysis. After 5 d cultivation in a complete medium, mycelia was shifted to media containing either sorbitol, mannitol or xylitol; sucrose was used as a control. After incubation for 5 and 24 h, the gene showed no induction with any of the substances (data not shown). As the substrate-induction of sugar-alcohol dehydrogenases is well documented in yeasts and filamentous fungi (Sarthy et al., 1994, Kern

et al., 1991, Singh and Schugerl, 1992), this result, combined with the general nature of the homologies, suggests that this enzyme may represent a yet uncharacterised type of dehydrogenase.

3.3.3.1.3 X8b, the Cu,Zn SOD-like protein (*cpsod-ish*)

The separate homologies of universe and reverse sequences from the ca. 2 kb insert of cDNA clone X8b indicated that it was derived from at least two separate transcripts. Of the 944 bp reverse consensus sequence (from which the *Eco*RI site, separating vector from insert, was missing), only a 200 bp region showed homologies to Cu,ZnSODs. In order to determine if the missing homologies were due to a recombination in the area of the reverse sequence, a cDNA screening was undertaken using a 181 bp PCR fragment of the Cu,Zn SOD-homologous region as a probe. After screening 60 000 cDNA clones of the Cu-induced cDNA library and 60 000 of the alkaloid-induced cDNA library without finding a single positive clone, it was concluded that this gene is not significantly transcribed under these conditions in axenic culture. This result is supported by the lack of hybridising transcripts in northern analyses (see 3.3.2.3). PCR with the primers used to amplify the 181 bp cDNA probe and genomic DNA as a template produced a 283 bp fragment, which sequencing revealed as the Cu,ZnSOD-like cDNA interrupted by a 102 bp intron. RT-PCR experiments with the same primers indicated that the gene was expressed *in planta* (see 3.3.3.3.3.), genomic screening was initiated to clarify the identity of this gene.

The first round of screening was done together with S. Joshi using two probes (X51a, the putative multicopper oxidase, and the 181 bp cDNA fragment from X8b); four clones of the first round which hybridised only with the *cpsod-ish* probe in the second round were analysed further. Of these, the clone S8λ2-1 containing two hybridising fragments, a 5.5 kb *Eco*RI fragment and a 2.0 kb *Sal*I fragment, was selected for subcloning and sequencing. Sequences were elongated and double-checked using the sequencing primers S8R and S8M, respectively. The sequences were resolved into a continuous DNA sequence consisting of 2257 bp including 639 bp upstream and 460 bp downstream of the putative coding sequences. The sequence shows only one intron, but as only a recombined cDNA clone is available for the determination of coding regions, the exon is putative. The methionine immediately preceding the regions showing homology with other proteins was deemed the start codon; this choice was supported by the lack of upstream ORFs. The putative coding regions and subcloning strategy of *cpsod-ish* is shown in fig. 3.40.

Comparison of the genomic sequence to the 944 bp reverse sequence of clone X8b shows that both are identical with the exception of one 102 bp intron; after removal of the intron the remaining sequence forms an ORF of 1056 bp which translates into a protein of 351 aa. BlastX of the coding sequences shows some interesting homologies, the highest of which is to the Cu,Zn SOD-like protein of *N. crassa* (high score 425, probability $6.8e^{-39}$). Homologies cover a corresponding area of the putative protein (the first 241 aa of the *Neurospora* protein shows homology to the first 234 aa of the *Claviceps*

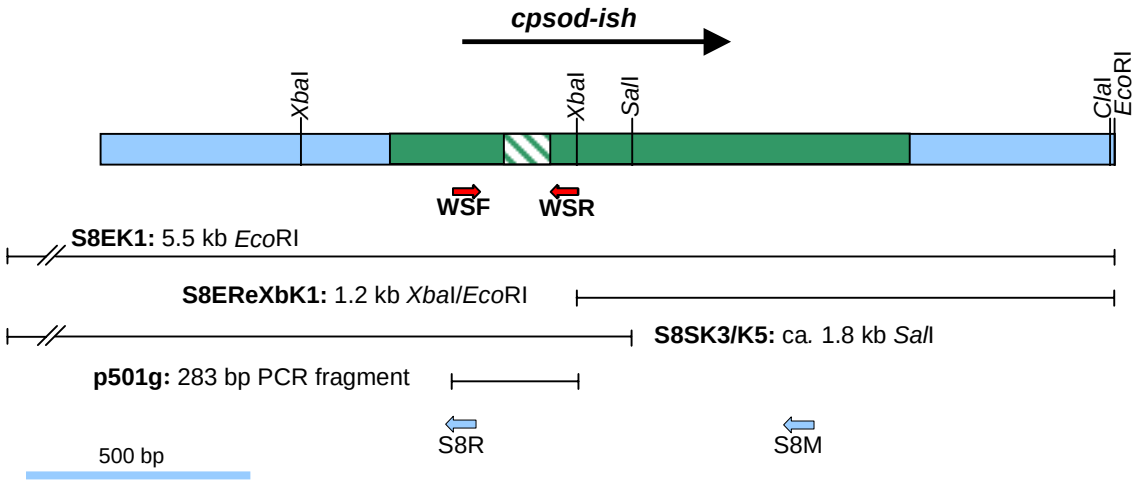

Fig. 3.40: Restriction map and subcloning strategy of the *cpsodish* genomic region. A 181 bp PCR fragment of X8b comprising the region homologous to Cu,ZnSODs was used as a probe (screening S8). Subclones were derived from a 5.5 kb *Eco*RI or a 1.7 kb *Sal*I fragment from λS82-1 of with the exception of p501g which is a genomic PCR clone with primers WSF and WSR. With the exception of the PCR fragment which was cloned into the TOPO vector, all fragments were cloned into the vector pBS. Sequencing was done with UNIVERSE and REVERSE primers. Intron and exon pattern is putative, and obtained by comparison with the cDNA consensus sequence (where available) as well as by comparison to the homologuous protein of *N. crassa*. All DNA is shown to scale; non-coding regions are in blue, exons are solid green while introns are striped green. Red arrows indicate RT-PCR primers while blue arrows indicate sequencing primers.

protein), although the putative protein in *Claviceps* is longer (351 as opposed to 248 aa). Although homologies to exotic Cu,Zn SODs are still there (for instance to that of *Xenopus laevis* with 116 high score and $2.2e^{-5}$ probability), the PROSITE signatures for Cu,Zn SODs do not appear in the putative protein; the cDNA fragment of X8b appears to have been colinear with the genomic gene copy (excepting the intron). Therefore, it can be concluded that this protein is not a true Cu,ZnSOD.

Some interesting new homologies to the C-terminal part of the *Claviceps* protein appear. These homologies involve serine and threonine-rich cell surface proteins such as yeast Muc1p and human mucins, and although the homologies look quite high (Muc1p: 147, $6.3e^{-8}$), closer examination shows that the matches are rather unspecific and based almost entirely on threonines and serines; furthermore Muc1 is quite large (1367 aa) and is richer in these two amino acids than is *cpsod-ish*. The *Claviceps* protein contains a putative signal peptide for secretion (1-19), as well as a possible trans-membrane segment at its C-terminus (334-350), which suggests that this protein may be localised at the cell surface.

It is important to note that, as only the one composite cDNA clone could be isolated, the C-terminal end of this protein is still speculative; although the 609 bp region downstream of the putative stop codon shows no large ORFs, RT-PCR with RNA from parasitic cultures will be needed to confirm this.

3.3.3.2 Promotor analysis of the sequenced cDNA clones

In each case the sequence (maximum 1000 bp) directly preceding the start codons was analysed for the presence of putative promotor elements. All sequences were examined for copper and iron re-

sponse elements (CuREs, FeREs, and ACE), general metal response elements (MRE), AP-1 binding consensus sequences (general and oxidative stress in yeast and mammals), and the fungal stress element STRE, as well as the binding consensus sequence of the yeast transcription factor ATF1, a homologue of which (*cpft1*) is induced by H_2O_2 in *Claviceps purpurea* (Joshi et al., 2002b). Furthermore, a general search was done by scanning the promotor against a database of transcription factor binding sites (TRANSFAC) via MatInspector (Quandt et al., 1995). The putative transcription factor binding sites described here are highlighted in the sequences which are depicted in App. A.

3.3.3.2.1 Promotor analysis of *cph1*

The designated promotor region contains three putative stress response elements (STRE) which are reported to induce transcription of yeast genes involved in the response to a variety of stress types, such as heat shock, osmotic- and oxidative-stress (Causton et al., 2001). First found in the promotor of the *S. cerevisiae* cytosolic catalase CATT (Marchler et al., 1993), these elements are bound by the Zn-finger transcription factors MSN2 and MSN4, which relocate from the cytoplasm to the nucleus when the cell is subjected to stress (Gorner et al., 1998). Typically, functional STRE are found twice within 60 bp (Moskvina et al., 1998); this renders the finding of STRE consensus sequences at –473 and –484 bp more convincing. A third is present at –956 bp.

A search for putative copper responsive elements revealed two sequences which correspond perfectly to the binding site consensus of the copper-sensing transcription factor MAC1 of *S. cerevisiae*, TTTGCKCR. Although in yeast these CuRE are important for conditions of copper starvation and not copper excess, the discovery of two perfect putative CuREs at –702 (TTTGCGCA) and –686 bp (TTTGCTCG) in a gene so responsive to copper concentrations is intriguing, especially as CuREs are thought to function synergistically; highly induced genes tend to have at least two CuREs within 100 bp of each other (Jensen et al., 1998).

Also interesting is the presence of two putative iron response elements in the *cph1* promotor. Although in both cases they fall slightly short of the yeast consensus sequence YRCACCCR (Hassett et al., 1998), they are perhaps relevant as this gene does respond to changes in iron concentrations; Furthermore, the mismatch is one of the less specific outer bases: at –961 bp CACACCCC*C* and at -494 bp T*T*CACCCA. Although the significance of promotor elements located almost 1000 bp preceding the start codon is questionable, promotors of some iron-responsive yeast genes contain only a single FeRE. In yeast, these elements are bound by the AFT1 factor, which, in analogy to MAC1, activates genes under Fe starvation (Yamaguchi-Iwai et al., 1995).

Finally, there is a putative binding site for the fungal regulator PACC at –407 bp; the activation of this constitutively expressed transcription factor is pH-dependent. The low *re*-value (0.05), which defines the amount of times these elements will appear within 1000 bp of random DNA sequence, together with the fact that one PACC-binding site can be enough for pH-dependent regulation (Schmidt

et al., 2001, Then Bergh and Brakhage, 1998), gives this match significance.

3.3.3.2.2 Promotor analysis of *cpdh1*

Screening of the designated promotor sequence of *cpdh1* showed two putative fungal STREs (see 3.3.3.2.1) at –658 and -669 bp.

Of the promotor elements which respond to metals, a CuRE is found at –152 and a putative FeRE is found at –850 bp. Although promotors under the control of copper usually contain two CuREs, recent experiments have uncovered two genes (of unknown function) in yeast whose promotors are influenced by copper concentration but contain only single CuRE consensus elements (Gross et al., 2000).

3.3.3.2.3 Promotor analysis of *cpsod-ish*

The promotor of the *cpsod-ish* gene is interesting both because of its lack of expression in axenic culture (at least under the tested conditions) and because of its early-phase *in planta* regulation (see below). The 639 bp upstream of the putative start codon which have been sequenced were subjected to promotor analysis as described above.

This promotor contains four putative binding sites for fungal heat shock factors, two for HSP1 (-173 and –300), and one each for HSP2 and HSP3 at positions –72 and –519, respectively. Heat shock factors acquire DNA-binding ability in response to variety of stress including elevated temperatures, oxidants and heavy metals (Pirkkala et al., 2001).

Interestingly, two putative binding elements for the yeast factor RLM1 (re<0.01) can be found at positions –381 and –420. RLM1, which belongs to the highly conserved MADS-box family of transcription factors, is a positive-acting regulator which is under the control of MAPK1 and involved in cell wall biosynthesis (Dodou and Treisman, 1997). One of the genes underlying control of RLM1 is the flocculation gene Flo1p (Dodou and Treisman, 1997), which encodes a serine-threonine-rich protein involved in cell-cell adhesion as is Muc1p (see 3.3.3.1.3).

Finally, overlapping with the putative ACE-binding region at -109 bp is a perfect consensus sequence for ATF-1 binding; the *C. purpurea* homologue (CpTF1) is induced by H_2O_2.

3.3.3.3 *In planta* expression analysis of the sequenced cDNA clones

The method of RT-PCR was used in order to investigate the expression of the sequenced cDNA clones during parasitic culture. Total RNA from rye infected with *Claviceps purpurea*, strain T5 (the diploid version of 20-1), was used as a template. The RNA template originates from phases I-IV of infection as described in 3.1.4.2. Primers were chosen from both sides of the intron-containing sequence, so that the difference between PCR products originating from RNA and DNA would be clearly visible on a gel. As a DNA control, genomic DNA was used; when possible, a cDNA clone served as a con-

trol of the RNA-based fragment. Stringent hybridisation of the PCR products with specific probes was used to differentiate specific from unspecific amplificons.

3.3.3.3.1 cph1

The RT-PCR primers RTHF and RTHR, which span the only intron of *cph1*, are shown in fig.3.38. With genomic DNA template, these primers amplify a 360 bp fragment; amplification of cDNA template produces a fragment of 271 bp. The result, depicted in fig. 3.41, shows a fragment of the expected size in the cDNA control lane, as well as a larger fragment in the DNA control. PCR with the mRNA from phases I-IV as a template shows strong amplification of the 271 bp cDNA fragment in all phases (A) which hybridises with the *cph1* cDNA probe (B), indicating that *cph1* is expressed in all four phases of infection. Small phase-dependent variation of expression can not be detected with this non-quantitative PCR method; the slightly smaller amount of product in phase I is, as always, probably due to the low amount of fungal RNA template in this phase.

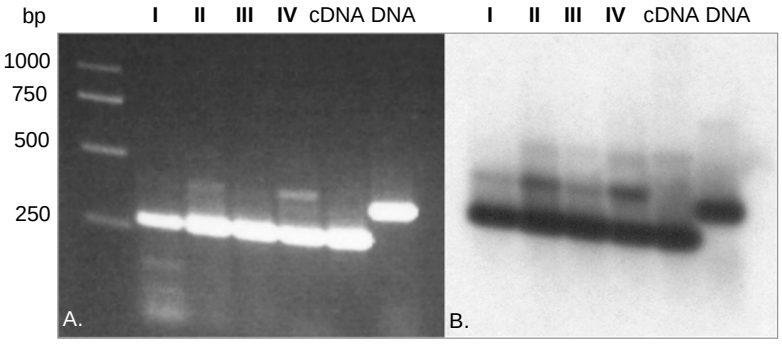

Fig. 3.41: *In planta* expression of *cph1* A. RT-PCR products. Template for the PCR: Phase I-IV mRNA, cDNA clone X12a, genomic 20-1 DNA. **B. Southern analysis.** The gel shown in A was blotted and probed with the 0.8 kb *cph1* cDNA insert. Size marker fragments (from the 1 kb ladder) are indicated on the far right.

3.3.3.3.2 *cpdh1*

For the *in planta* expression analysis of *cpdh1*, the primers RT-DH-F and RT-DH-R (see 3.39) were used to amplify a 205 bp cDNA fragment. The results, shown in fig. 3.42 (A), show that a PCR product of about the correct size is present in all stages of infection (I-IV); in a control with the full length *cpdh1* cDNA clone S11K12 a fragment of the same length is amplified. The same primers amplify a 514 bp product from DNA template which contains three introns. The specifity of primer binding was confirmed by Southern analysis (B). Although the method of RT-PCR is only semi-quantitative, clear differences in product amount are seen in each stage. As this experiment was done together with that for *cph1*

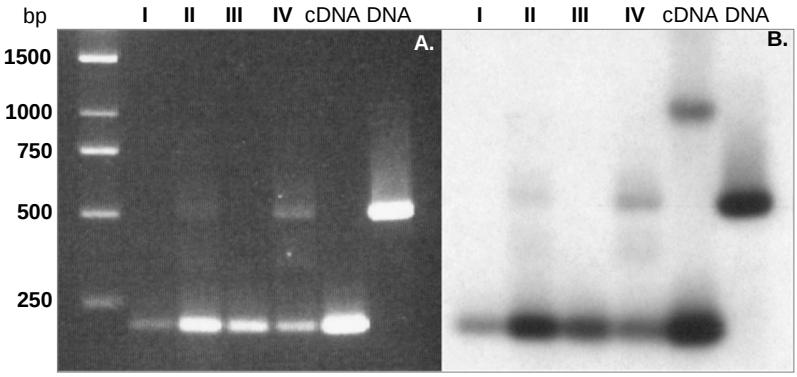

Fig. 3.42: *In planta* expression of *cpdh1* A. RT-PCR products. Template for the PCR: Phase I-IV mRNA, cDNA clone S11K12, genomic 20-1 DNA. **B. Southern analysis.** The gel shown in A was blotted and probed with the *cpdh1* cDNA fragment mixture used in S6-2 (see 3.3.3.1.2). Size marker fragments (from the 1 kb ladder) are indicated on the far right.

(see 3.41) using aliquots of the same RNA template, these differences can be considered significant, as the amount of *cph1*-product does not vary in a stage-specific fashion. The expression of the putative dehydrogenase seems to peak at phase II (ca. 10 dpi) when the mycelia is still in its sphacelial, honey-dew-producing form. Later, during the formation and ripening of sclerotia (15-20 dpi), the expression seems to peter out again.

3.3.3.3.3 *cpsod-ish*

The primers WSF and WSR (see fig. 3.40) were used to amplify a cDNA fragment 181 bp in length, while the corresponding PCR product from genomic template, containing the 102 bp intron, consists of 283 bp. The results of the *in planta* expression analysis, shown in fig. 3.43, are intriguing. Although infection phases I-IV all show the 181 bp cDNA fragment (also present in the control lane using X8b as cDNA template), indicating expression of the Cu,ZnSOD-like protein, the highest amount of product is to be found after PCR with phase I template (A). Considering that not only is the RT-PCR method semi-quantitative, showing only dramatic differences in expression, but that the phase I RNA contains a high proportion of rye-derived transcript in comparison to the template of the other phases, the expression of this gene in this earliest infection phase must be much higher than that in the following phases. Hybridisation (B) confirms that the product is not the result of unspecific amplification. The expression seems to steadily decrease from phase II to phase IV. Genes with this sort of expression pattern are particularly interesting for the study of disease establishment, especially when there is, as in the case of the Cu,Zn SOD-like protein, as of yet no indication of expression in axenic culture.

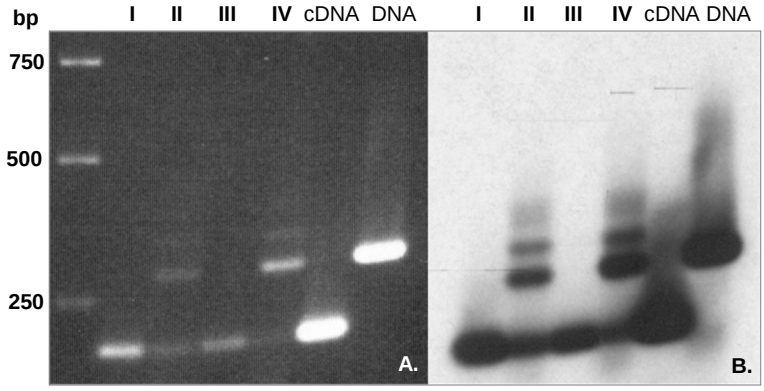

Fig. 3.43: *In planta* expression of *cpsoddish* A. RT-PCR products. Template for the PCR: Phase I-IV mRNA, X8b (cDNA fragment), genomic 20-1 DNA. **B. Southern analysis.** The gel shown in A was blotted and probed with a 181 bp cDNA fragment of the Cu,Zn-like protein. Size marker fragments (from the 1 kb ladder) are indicated on the far right.

4 Discussion

The discovery of a putative cell wall-associated SOD in the pathogenic fungus *Claviceps fusiformis* provided support for the theory that scavenging of oxygen toxins played some role in the pathogenesis of *Claviceps*, which was postulated when abundant secreted catalase activity was found in parasitically growing *C. purpurea* (Garre et al., 1998a). At that time, the oxidative burst was a focal point of plant defense research, as a growing number of researchers discovered the phenomenon in their systems; AOS were thought to be involved in almost every aspect of plant defence. The emerging correlation between generation of AOS and the hypersensitive response of the attacked cells raised the possibility that the ability of *Claviceps* to evade such a response could be attributed (at least in part) to its secretion of AOS scavengers. While the hypersensitive response is an important component of the defense arsenal of related cereals such as wheat and barley (Tiburzy et al., 1991, Hückelhoven and Kogel, 1998), very little is known about the HR of rye. The HR aside, secretion of AOS scavengers by the pathogen could reduce pathogen-induced phenolic crosslinking of the type observed at the ovary base, which represents the limit of fungal colonisation (see 1.3.1). Fungal mechanisms which protect against the abundant AOS found in the developing rye ovary (see fig. 1.9) may be a prerequisite of its colonisation. In addition, AOS are proposed to be involved in the transduction of signals in plant and animal systems, either directly as second messengers or indirectly by altering the redox state of the cell (see 1.2.3.3). H_2O_2 generated in the ovary is able to cross membranes into the fungal cytoplasm, where it may take part in the complex exchange of signals necessary for the establishment and maintenance of a biotrophic interaction. Finally, the very foundation of this research is anchored in a fierce belief in the economy of the proteome; this dictates that behind the expression of a gene there lies a function which is relevant for the survival of the organism.

The following sections will attempt to order the results into the context of existing data and to discuss their implications for fungal biology and pathogenesis.

4.1 The Cu,Zn SOD of *C. purpurea*

To date, very little is known about the superoxide dismutases in filamentous fungi. The Mn SOD of *Aspergillus fumigatus* is the only protein sequence of this kind which is listed in databases accessible to the public; of the Cu,Zn SODs, only the sequences from *Neurospora crassa, Aspergillus fumigatus* and *Glomerella cingulata* are available. The *N. crassa* enzyme is the sole Cu,Zn SOD to have been functionally classified by gene deletion (Lerch and Schenk, 1985, Chary et al., 1994).

As apoplastic superoxide produced in the course of a hypothetical oxidative burst is not easily able to penetrate membranes, at least a part of the oxidative battle is rendered extracellular. This generates special interest in secreted superoxide scavengers. Research in other organisms indicates that an extracellular SOD is likely to be of the Cu,Zn-type (see below) while homology analysis of the cell wall-associated SOD in *Claviceps fusiformis* classifies it with the Cu,Zn-type enzymes. Therefore, the Cu,Zn SOD has been the main focus of attention during the investigation of possible pathogenesis-relevant SODs.

4.1.1 Localisation of CpSOD1

Analyses of protein extracts derived from the culture filtrate, cell wall and mycelia of axenic cultures of *C. purpurea* have shown that all three contain SOD activity. Most activity seen in IEF-gels after SOD activity staining is represented by one band at pI 5.3 which appears in all three protein fractions. Similarly, western analysis shows that the 16-18 kDa protein which cross-reacts with the antibody directed against the cell-wall associated Cu,Zn SOD in *C. fusiformis* is also present in all three protein fractions. Comparative analyses of wild-type and *cpsod1*-deleted strains show that the main signal obtained with both enzymatic and immunological methods is the product of one gene, *cpsod1*. Although CpSOD1 is most abundant in the mycelial fractions, the results indicate that this protein is also secreted, as large amounts are associated with the cell wall, and it can be detected in the media. Measurement of cytoplasmatic contamination in the cell wall fractions excluded the possibility that activity in the cell wall was derived from leakage of this small protein from the intact but lyophilised mycelia. Thus, protein data indicates that this Cu,Zn SOD is both cytosolic and secreted.

Although investigations of superoxide dismutases have shown that most eucaryotes possess multiple Cu,Zn SODs, yeast and fungi do not seem to have more than one Cu,Zn SOD. Experiments in yeast show that mutation of the gene encoding the Cu,Zn SOD results in the loss of all Cu,Zn SOD activity (Bilinski et al., 1985). The Cu,Zn SOD of *Neurospora crassa*, encoded by *sod1,* is reported to constitute 90% of the SOD activity in axenic culture (Lerch and Schenk, 1985), and 100 % of the Cu,Zn SOD activity (Chary et al., 1994). Similarly, investigations of various species of *Cryptococcus* and *Aspergillus* have unveiled only one Cu,Zn SOD, which is responsible for almost all of the activity in axenic culture (Holdom et al., 1996, Hamilton and Holdom, 1997). This tendency continues in *C. purpurea*, where the Cu,Zn SOD protein derived from *cpsod1* produces the only major band of SOD activity in both axenic and parasitic cultures. Although in axenic culture many other and fainter bands of activity can be detected, none are inhibited by the copper chelator DDC. The second, more basic band of activity seen in proteins derived from parasitically growing *C. purpurea,* which shows a similar lack of response to DDC, is probably a Mn SOD. Furthermore, non-stringent Southern analysis shows that *cpsod1* encodes the only Cu,Zn SOD in *C. purpurea*, as the highly conserved nature of

these proteins renders the detection of similar genes very likely.

The evidence for the occurance of a single Cu,Zn SOD in fungi is difficult to resolve with tentative reports of extracellular SOD activity. Extracellular superoxide dismutase activity has been observed in cultures of both *N. crassa* and *S. cerevisiae* (Munkres, 1985, Munkres, 1990). Similar activity has been found in the culture filtrates of *C. neoformans* and several types of *Aspergillus* (Hamilton and Holdom, 1997, Holdom et al., 1996, respectively). This activity has been traced to a Cu,Zn SOD in *A. fumigatus*, where an antibody directed against the Cu,Zn SOD caused the intense staining of conidial and hyphal cell walls as well as cytoplasma (Hamilton et al., 1996). In all cases, the authors have refrained from concluding that extracellular SODs exist in fungi.

In higher mammals, reports of extracellular SODs (EC-SOD) are abundant, but these enzymes, while also of the Cu,Zn type, are structurally distinct and contain an N-terminal peptide for secretion (see 1.1.4.1). Similarly, the periplasmatic Cu,Zn SODs of bacteria also contain a hydrophobic leader peptide for secretion into the extracellular space (Fang et al., 1999). In contrast, none of the putative proteins derived from fungal Cu,Zn SODs sequences, including *cpsod1*, contain any detectable signal peptide for secretion; in size, they correspond to the smaller cytosolic enzyme type and lack the typical positively charged carboxy-terminus which is thought to mediate binding to the cell surface (Sandstrom et al., 1994). While some EC-SODs from nematodes are reported to lack the positively charged C-terminus, they do have a typical signal peptide for secretion (Liddell and Knox, 1997).

The phylogenetic tree shown in fig. 4.1 offers a broad overview of the homologies among Cu,Zn SODs ranging from bacterial to human. The tree groups primarily into procaryotic and eucaryotic enzymes. The complex topology of the eucaryotic Cu,Zn SODs includes several subgroups. The cytosolic (SOD or SODE) and extracellular (EC-SOD) enzymes of higher eucaryotes do not cluster together, a fact which suggests that the extracellular protein evolved before the divergence of higher eucaryotes. EC-SOD has also been found in many parasitic nematodes; here they tend to be more similar to the cytosolic forms. The two Cu,Zn SODs from rice, representing the plant enzymes, build a distinct group; plants tend to have multiple Cu,Zn SODs which cluster into plastid and cytoplasmatic forms. The fungal Cu,Zn SODs cluster together in a single group (with the exception of the *S. pombe* and *F. neoformans* proteins, which build a closely related subgroup), and surprisingly, are associated with the group of extracellular proteins (EC-SOD) from higher eucaryotes. The fact that fungal Cu,Zn SODs show more structural similarity with the only distinct group of extracellular Cu,Zn SODs than with the intracellular forms of the same organisms would seem to support the hypothesis that this enzyme could be at least partially extracellular.

Secreted forms of SOD have been well documented in bacteria, nematodes and mammals. Recently, evidence for a distinct extracellular SOD in plants has also been presented (Karpinska et al., 2001). This broad occurrence across the ranks of phylogeny suggests that the requirement for such an enzyme is universal; it is unlikely that fungi alone are exempt from the advantages conveyed by a secreted SOD. With the exception of bacteria, which contain Mn or Fe SOD in their cytoplasma, all of the organisms which have an EC-SOD also have a second distinct cytosolic form of Cu,Zn SOD. Could the requirement of an extracellular and cytosolic SOD in fungi be fulfilled by one enzyme? The results of this thesis would seem to indicate that this is the case, as deletion of the one enzyme in *C. purpurea* results in the disappearance of both cell wall-associated and mycelial activities. The lack of a typical signal peptide for secretion would support such an assumption, as a protein which was localised in more than one cellular compartment could not be properly targeted by an address leading exclusively to one location. In eucaryotes, research of secretion pathways deals almost exclusively with the classical vesicle sorting system, which requires that the secreted protein has a leader sequence to secure escort to the ER by signal recognition proteins. Although reports of proteins arriving at the cell surface without the help of the ER or N-terminal signal peptides do exist (Kuchler and Thorner, 1990, Parmer et al., 1993, Baier et al., 1997, Wiser et al., 1999), the mechanisms of alternative secretion pathways have yet to be researched in detail. In bacteria, at least four types of secretion signal

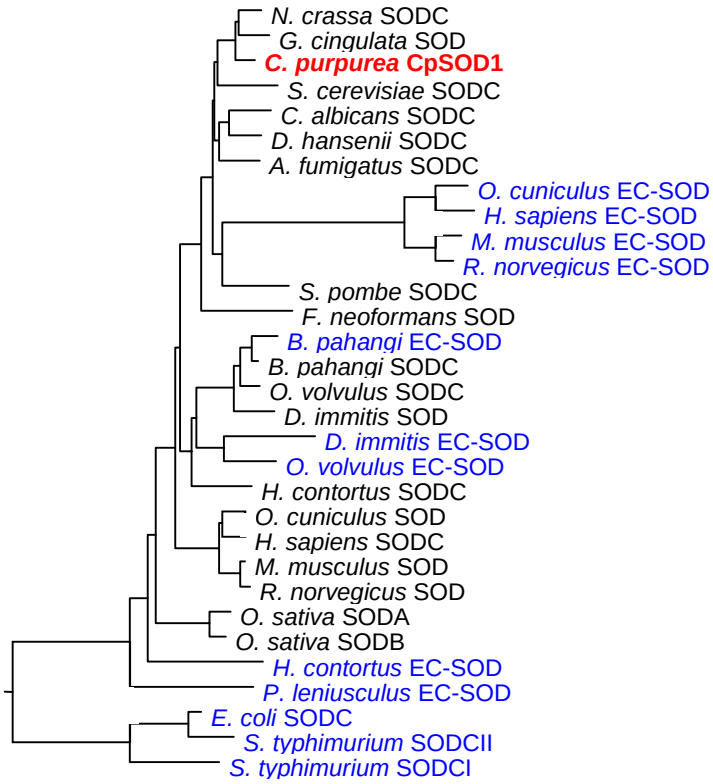

Fig. 4.1: Phylogenetic tree of Cu,Zn SODs including the *cpsod1* gene product (CpSOD1). EC-SODE are extracellular SODs, while SOD or SODC are typically cytosolic, with the exception of the bacterial enzymes which are periplasmatic. The GenBank accession numbers are as follows: *Neurospora crassa* P07509, *Glomerella cingulata* AAD19338, *Saccharomyces cerevisiae* P00445, *Candida albicans* O59924, *Debaryomyces hansenii* O42724, *Aspergillus fumigatus* Q9Y8D9, *Oryctolagus cuniculus* EC-SODE (rabbit) P41975, *Homo sapiens* EC-SOD DSHUEC, *Mus musculus* EC-SODE O09164, *Rattus norvegicus* EC-SODE Q08420, *Schizosaccharomyces pombe* SODC P28758, *Filobasidiella neoformans* SOD AAK01665, *Brugia pahangi* SODC P41962, *B. pahangi* EC-SODE P41963, *Onchocerca volvulus* SODC P24706, *Dirofilaria immitis* SOD AAB61472, *D. immitis* EC-SODE P41974, *O. volvulus* EC-SODE Q07449, *Haemonchus contortus* SODC Q27666, *O cuniculus* SOD S01134, *H. sapiens* SODC P00441, *M. musculus* SOD CAA29880, *R norvegicus* SOD CAA79925, *Oryza sativa* SODA S22508, *O. sativa* SODB S21136, *H. contortus* EC-SODE P51547, *Pacifastacus leniusculus* (crayfish) EC-SOD AAD25400, *Escherichia coli* SODC P53635, *Salmonella typhimurium* SODCII AF056931, *S. typhimurium* SODCI AAB62385. The phylogram was constructed using the clustal analysis program (based on distance) included in MEGALIGN, DNA Star. Secreted SOD forms are shown in blue type.

pathways are known, one of which does not seem to require an N-terminal leader peptide. This type I secretion system, found in gram-negative bacteria, involves ATP-binding cassette (ABC) transporters, which can translocate small proteins (up to 50 kDa) from the cytoplasm into the extracellular space (Binet et al., 1997). Similar protein targeting mechanisms are proposed to exist in eucaryotic cells (Kuchler and Thorner, 1992).

However, irrevocable conclusions as to the localisation of CpSOD1 must await morphological data. Although comparative immuno-analysis of the wild type and *cpsod1*-deletion mutant have been attempted with the anti-CfSOD1 antibodies, results are still lacking due to the high unspecific cross-reactivity of the polyserum (M. von den Driesch, pers. comm.). The generation of new monoclonal antibodies based on peptide sequences lacking in the deletion mutant promises new data in the near future.

4.1.2 Regulation of *cpsod1*

In many systems, expression of mitochondrial Mn SOD seems to be more affected by species of active oxygen than the Cu,Zn SOD, whose expression level is generally not influenced by the presence of AOS (Shull et al., 1991, Gralla and Kosman, 1992, Strålin and Marklund, 1994, Strohmeier-Gort et al., 1999). The *C. purpurea* Cu,Zn SOD transcript shows a similar lack of response to AOS such as hydrogen peroxide, and the superoxide generators paraquat and xanthine/xanthine oxidase. Instead, it shows a strong induction by copper as well as a weaker induction by iron. Induction of Cu,Zn SOD by copper has been described in detail for yeast (Gralla et al., 1991, Carri et al., 1991), and the rat protein is induced by copper, cadmium and zinc (Yoo et al., 1999). Although the gene encoding the Cu,Zn SOD of *E. coli* is not directly induced by medium copper, addition of a Cu-chelator decreased its transcription (Strohmeier-Gort et al., 1999). Not only does this protein contain copper in its catalytic centre, rendering the synthesis of the apoprotein under copper limiting conditions uneconomical, but the ability of the Cu,Zn SOD to sequester free copper ions can prevent Fenton-mediated oxidative damage (see 1.1.1). In yeast it has been shown that over-expression of the copper metallothionein CUP1 can compensate for lack of the Cu,Zn SOD (Culotta et al., 1995) and vice versa (Tamai et al., 1993). It is even postulated that the Cu,Zn SOD, which is the phylogenetically younger form of superoxide dismutase, evolved from a simple copper-binding protein in bacteria (Gralla and Kosman, 1992), probably in response to extracellular sources of superoxide (Imlay and Imlay, 1996). The copper-induced increase of *sod1* transcription seen in *C. purpurea* and other organisms thus seems to have a simple physiological basis.

In yeast, copper sensing by the SOD1 promotor is mediated via the ACE protein (Carri et al., 1991, Gralla et al., 1991). This constitutively expressed transcription factor binds the Cu(I) ion; in its copper-containing form it can bind to specific promotor sequences and activate transcription of neighbouring

genes (Thiele, 1988). Yeast SOD1 contains a single ACE-binding element in its promotor, and is activated 2-3 fold by 50 µM $CuSO_4$. These elements are thought to function co-operatively as similar concentrations of copper activate transcription of the gene encoding the copper metallothionein CUP1, which contains four ACE-binding regions in its promotor, 10-50 fold (Gralla et al., 1991). Promotor analysis of the *C. purpurea* enzyme reveals only one putative ACE –binding site, consistent with the ca. 2-fold induction of the gene after addition of copper salt.

As of yet, induction of Cu,Zn SODs by iron has not been reported. Oxidative stress in the form of superoxide is thought to cause an increase of intracellular iron by oxidative inactivation of [4Fe-4S] containing enzymes (Fridovich, 1995, Srinivasan et al., 2000); it would be conceivable that iron released from the damaged proteins could mediate increased transcription of a superoxide scavenging enzyme.

Specific promotor elements involving the induction of gene transcription under high iron conditions have not yet been described in fungi; in mammalian systems, iron-mediated gene activation is under post-transcriptional control. Binding of iron regulatory proteins to iron response elements (IREs) in the 5' untranslated regions of the mRNA is postulated to lead to increased mRNA stability (Thomson et al., 1999). Although a similar extension of mRNA half-life could lead to increased concentrations of *cpsod1* transcript, no sequence corresponding to the IRE consensus was found in the cDNA.

The *cpsod1* promotor contains two putative metal response elements (MREs). These elements are found in the promotors of metallothioneins from *Drosophila* to mammals, where they activate transcription in response to heavy metals such as Cd, Zn and Cu (Culotta and Hamer, 1989). The binding of mammalian metal-responsive transcription factor 1 to MREs requires Zn, which is proposed to act as a second messenger for several types of metals (Palmiter, 1994). The induction of Cu,Zn SOD gene transcription in rat by copper, cadmium and zinc is mediated by a single MRE (Yoo et al., 1999). No interaction between iron and MREs has yet been described.

The lack of information pertaining to metal-mediated activation of gene transcription in filamentous fungi renders the analysis of putative promotor elements highly speculative. Most information is derived from yeast systems and the degree of conservation among different organisms is unknown. Even among different yeast, homologues of transcriptional regulators involved in copper sensing differ in function (see 4.3.2.1.2). Ultimately, promotor mutation experiments and band shift assays will be necessary to conclude which elements are responsible for copper- and iron-mediated gene activation.

Furthermore, the significance of metal regulation *in planta* is unclear. RT-PCR experiments show that *cpsod1* is expressed during all infection phases. This "constitutive" expression is disappointing for a gene which was proposed to be important for initial ovary colonisation and establishment of the

host-parasite interface. However, the fact that *cpsod1* seems to be the only Cu,Zn SOD in *C. purpurea*, and that it is responsible for most of the superoxide dismutase activity (as ascertained by reduction of NBT) in axenic culture and *in planta* both inside and outside of the cell, suggests that it may be required in several contexts.

It is tempting to speculate that the juxtaposition of the *cpsod1* gene product with the site of oxidative stress could be achieved by regulation of its cellular localisation. This sort of regulation has been described for transcription factors which are transported to the nucleus when the cell is in need of their target genes (Kuge et al., 1997, Gorner et al., 1998). Perhaps similar mechanisms have evolved on a protein level. There are other examples of differential protein distribution; for instance, the catalase cta1p of *Candida boidinii* is bimodally distributed between the cytoplasma and the peroxisome during growth on methanol, but growth on oleate, which is accompanied by an increase in peroxisomal H_2O_2 production, relocates this protein exclusively to the peroxisome (Horiguchi et al., 2001).

4.1.3 The importance of *cpsod1* in axenic culture

Deletion of *cpsod1* in *C. purpurea* had only minimal effects on its ability to grow in axenic culture. Light microscopic analysis of submerged and plate cultures revealed no morphological differences in strains with and without *cpsod1* (data not shown). Mutants were not affected in sporulation, and germination rates of mutant spores were comparable to those of the wild type. Comparison of dry weight yields after growth in shaken culture showed that the deletion mutant tended to grow more slowly than the wild type; quantification by measuring colony diameters on plates indicated that the lack of *cpsod1* resulted in a 30% reduction in growth rate, which could be restored by ectopic complementation with the *cpsod1* gene. Although reduced growth rates are reported for yeast lacking Cu,Zn SOD (Bilinski et al., 1985), no mention is made of this phenotype in a report concerning phenotypes of SOD1 deletion mutants of *N. crassa* (Chary et al., 1994). Similarly, analysis of *E. coli* strains lacking the periplasmatic Cu,Zn SOD shows that this gene is not required for aerobic growth (Strohmeier-Gort et al., 1999). Therefore, the ability of *C. purpurea* to survive without its major cytosolic and cell wall-associated superoxide scavenging enzyme is not surprising.

In contrast to Cu,Zn SOD deletion mutants in yeast and *N. crassa*, which show increased sensitivity to the intercellular superoxide generator paraquat (Gralla et al., 1991, and Chary et al., 1994), the *cpsod1* deletion mutant is not more sensitive to this redox cycler than the wild type. For instance, although the *N. crassa* strains lacking *sod1* were completely unable to germinate on 25 µM paraquat, concentrations as high as 100 µM did not significantly affect the conidial survival of Δcpsod1. Despite the fact that wild-type growth on paraquat-containing plates was already reduced by 40%, indicating that this substance is toxic to *C. purpurea*, the deletion of *cpsod1* did not result in

further decrease of growth rates as reported to be the case in the *N. crassa* mutants. The inability of paraquat to induce the transcription of *cpsod1* supports the conclusion that mechanisms other than SODs must be responsible for responding to this type of oxidative stress. Although it would be tempting to link the greater redundancy of AOS detoxifying systems in *C. purpurea* with the evolution of a pathogen in an AOS-rich environment, as of yet too little is known about the significance of SODs in other pathogenic and non-pathogenic fungi to allow such conclusions.

The universal conservation of cytosolic and extracellular Cu,Zn SODs across all kingdoms testifies to the importance of superoxide scavenging. As deletion of Cu,Zn SODs does not generally impede survival, other superoxide-detoxification mechanisms must be able to compensate for lack of this enzyme. The question arises as to what sort of complementary mechanisms enable the growth of *C. purpurea* which is lacking the only major intra- and extracellular SOD activity. Analysis of the SOD activities in axenically cultivated Δcpsod1 fails to show the induction of alternative enzymes even under oxidative stress generated by paraquat and excess copper (data not shown). Although the entirety of eucaryotic evolution has been accompanied by oxidative stress, giving rise to a great redundancy in AOS-detoxifying systems, most of the classical AOS detoxifying enzymes are involved in the breakdown of hydrogen peroxide rather than superoxide. The ability of superoxide to dismutate non-enzymatically underlies the basic simplicity of this enzyme; indeed, a large group of molecules, called SOD-mimics, are also able to dismutate superoxide. Many of these are simple porphyrines liganded to Mn or Fe (Batinic-Haberle et al., 1999).

Support for the compensation of SOD by other metal-containing substances is provided by research in yeast; addition of medium iron ameliorates difficulties in respiratory growth observed in Cu,Zn SOD-deficient mutants. These mutants also show increased transcription of the *fet3* gene which is involved in iron transport (De Freitas et al., 2000). Similarly, a mutation leading to manganese accumulation helps to suppress oxidative damage in yeast lacking Cu,Zn SOD (Lapinskas et al., 1995). Furthermore, the ability of metallothioneins such as *cup1* to compensate for *sod1* deficiency has already been mentioned (see 4.1.2), although this may be more important for the prevention of oxidative damage rather than for the detoxification of superoxide. Finally, compensatory superoxide dismutation could also involve non-soluble compounds such as melanin; this polymer has the ability to scavenge free radicals and has been shown to compensate for lack of Cu,Zn SOD in frog (Sichel et al., 1991). The identification of factors which compensate for lack of the major Cu,Zn SOD in *C. purpurea* requires further analysis.

4.1.4 Role of *cpsod1* during pathogenesis

Comparative pathogenicity assays on rye were used to investigate the importance of CpSOD1 for the parasitic growth of *C. purpurea*. Disappointingly, it was found that the deletion mutant Δcpsod1

can infect rye as well as the wild type can. The slight lag which was observed in the initial production of honeydew disappears within 10 dpi and both quantity and quality of honeydew are comparable to those produced by infection with the wild type. No difference was observed in the development and morphology of sclerotia. Light microscopical comparison of infected rye ovaries also fails to reveal differences in the pathogenesis of strains with and without *cpsod1* (M. von den Driesch, pers. comm.). Thus, it can be concluded that *cpsod1* is not essential for the pathogenesis of *C. purpurea*. Growth of *C. purpurea* lacking *cpsod1* is slower in axenic culture; this could be responsible for the initial delay in honeydew production observed in the pathogenicity assays. Although this does not significantly affect the ability of this fungus to complete its parasitic cycle during these controlled conditions, a slight lag in growth could be of importance in the natural environment, as it has been reported that some strains of *C. purpurea* are able to form sclerotia on ovaries already infected by other, less virulent strains of the same fungus (Swan and Mantle, 1991).

The results obtained in the *C. purpurea*/rye interaction can not be put into the context of similar experiments in other systems, as this represents the first report concerning the deletion of a SOD in a fungal plant pathogen. As H_2O_2 is considered to be the major product of the defensive oxidative burst, most investigators have focussed on the role of catalases in their interaction systems. However, the role of SODs in bacterial plant pathogens has been investigated. A similar lack of phenotype has been found in mutants of *Pseudomonas syringae* lacking cytoplasmatic SOD; these mutants are still able to cause bacterial brown spot disease on bean (Kim et al., 1999). Unfortunately, no information has been offered about the existence of a periplasmatic Cu,Zn SOD in *Pseudomonas*, which would seem to be of more potential importance for the interaction. On the other hand, the cytosolic SOD of the necrotrophic pathogen *Erwinia chrysanthemi* is required for successful infection of African violets (Santos et al., 2001). Generally, the involvement of AOS in infection strategies of necrotrophs may be very different than those of pathogens which colonise living tissue. An oxidative burst inducing tissue death via the HR, designed to discourage biotrophic growth, will only set the table for a necrotroph. In bacterial pathogens of animals, correlation between virulence and the activity of periplasmatic SODs has been observed. The periplasmatic SODCII of *Salmonella typhimurium* was shown to contribute to virulence in mice (Fang et al., 1999.) The significance of similar enzymes for plant pathogens is questionable, as the toxic effect of AOS on the attacker may be greatly amplified by accumulation during phagocytosis (see 1.2.3.1).

As the deletion of *cpsod1*, which gives rise to the only major secreted SOD activity of *C. purpurea*, does not significantly impede pathogenesis, the hypothesis that the production of secreted AOS scavengers contributes decisively to the early establishment of infection must be re-examined. SOD activity secreted by the fungus is of particular interest, as proposed sources of AOS produced in the oxidative burst probably originate from superoxide. However, as previously mentioned, the pathogen-

induced generation of AOS in the rye ovary has yet to be demonstrated. Either compensatory mechanisms are able to deal with such toxins, or this organ does not respond to infection with an oxidative burst. Analysis of SOD activity in the early phases of infection by Δcpsod1 fails to reveal another activity which could compensate for lack of the first. As the acidic nature of the apoplast would favour the spontaneous dismutation of superoxide, the enzyme-catalysed reaction may be only of secondary importance for an extracellular oxidative skirmish. However, the fact that deletion of the major secreted catalase activity (*cpcat1*) shows a similar lack of effect on the ability of *C. purpurea* to infect rye (Garre et al., 1998b) would seem to support the lesser importance of extracellular AOS detoxification mechanisms during ovary colonisation. To add oxidative insult to injury, mutants simultaneously lacking both *cpsod1* and *cpcat1* are also able to cause normal infection (Joshi et al., 2002a). Yet, the high redundancy of AOS detoxifying enzymes must prevent complete discardal of this theory. Enzymes such as the cell-wall associated CATB are still active in the *C. purpurea* mutants. Although *Claviceps* may not be confronted with a classical oxidative burst, staining of rye ovaries for hydrogen peroxide (see fig. 1.9) indicates that the fungus must deal with considerable oxidative stress. As H_2O_2, in contrast to superoxide, is easily able to diffuse across membranes, intercellular components of the AOS detoxification system may also be of interest.

4.2 Yet more catalases: role in parasitic growth and biosynthesis of ergot alkaloids

Previous work had shown that *C. purpurea* expresses at least three catalases during parasitic growth: CATC/D, a (putatively) cell-wall associated CATB and the mycelial CATA, presumed to be peroxisomal (Garre et al., 1998a). The second putative catalase gene to be sequenced, *cpcat2*, encodes a protein which shows homology to the smaller, peroxisomal type of catalases. Expression analyses revealed that *cpcat2* did not correspond to either CATA or CATB, as *cpcat2* transcripts could only be found in parasitic culture, while the activities of CATA and CATB were present in axenic culture. In order to ascertain the importance of this new putative catalase for the parasitic survival of *C. purpurea*, this gene was subjected to functional analysis via gene inactivation. Parallel to the investigation of *cpcat2*, sequencing of genes involved in alkaloid biosynthesis showed that this gene is located within a cluster of genes involved in the biosynthetic pathway (Tudzynski et al., 1999). Furthermore, catalase activity analyses of strain 20-1 grown in alkaloid production media revealed the presence of yet another catalase isoform, denominated CATE.

4.2.1 The putative protein of *cpcat2*

The protein sequence derived from *cpcat2* encodes a putative catalase of 473 aa, which contains residues important for heme binding and catalysis; this indicates that the gene product is functional. Although no direct experimental evidence has been provided for the identity of *cpcat2* as a catalase, indirect evidence is provided by the increase of another catalase activity in one *cpcat2*-deletion mutant as well as the (tentative) correlation of *cpcat2* expression with a faint band of catalase activity in the alkaloid production strain P1. The fact that this gene seems to encode a small-subunit catalase could impede visualisation of the corresponding activity, as small-subunit enzymes are less stable than the larger proteins (see below). Final confirmation of the identity of *cpcat2* as an active catalase must await heterologous expression experiments.

The conceptual protein sequence does not contain a signal peptide for secretion, but does contain an in-frame peroxisomal targeting signal (PTS) type 1 (SKL) followed by a stop codon two residues after the putative stop codon (see A.2). Although this suggests that a mutation in CpCAT2 has severed the PTS1 from the rest of the protein, this may not affect the transport into the peroxisome as the alternative targeting signal PTS2 alone is sufficient for peroxisomal localisation of CTA1 in yeast (Binder et al., 1991).

Many fungal catalases have been sequenced. Filamentous fungi usually have at least three distinct catalases; when multiple catalases have been genetically characterised there are typically at least two large-subunit catalases (>700 aa), containing the extra C-terminal "flavodoxin-like" domain (see 1.1.4.2), and one small subunit enzyme (450-600 aa). Many of the small subunit enzymes are deemed peroxisomal by homologies to established peroxisomal enzymes and because of the presence of putative peroxisomal targeting sequences. A phylogenetic tree of fungal catalase cores comprising the most conserved regions of these enzymes is shown in fig. 4.2. The phylogram divides fungal catalases into two major groups: the large-subunit catalases, which are subdivided into the similar type I and type II groups, and the small-subunit group. The *C. purpurea* CATC/D groups with the type II enzymes which includes other secreted catalases. Interestingly, yeast (and higher eucaryotes) do not seem to have developed the large-subunit enzymes, which until now have only been documented in filamentous fungi and bacteria (Klotz et al., 1997, Kawasaki and Aguirre, 2001). Although the significance of these large catalases are not fully understood, the difference to small-subunit sequences consist of additional protein regions in the N- and C-terminal areas, rather than changes in the catalytically active core; these additional sequences result in an increase of enzyme stability (Klotz et al., 1997). As all known secreted catalases belong to the group of large catalases, increased stability may be important for an enzyme exposed to the unpredictability of the extracellular environment. However, some fungal catalases belonging to the large subunit type lack a signal peptide for secretion (Bussink and Oliver, 2001). As of yet, no extracellular form of catalase seems to have been

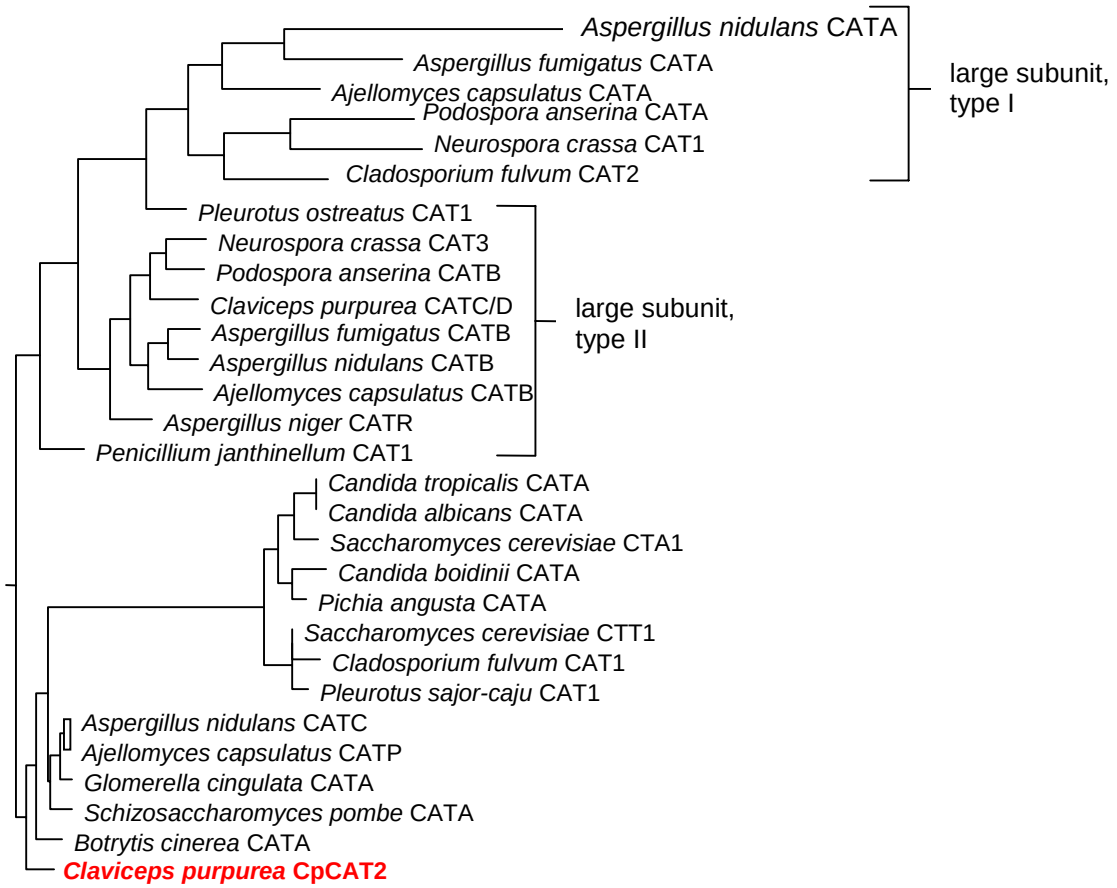

Fig.4.2: Phylogram of fungal catalases, including the putative protein of *cpcat2*. The phylogram was created using the Jotun-Hein parsiomony method of Megalign, DNA-Star. The GenBank accession numbers are as follows: *Aspergillus nidulans* CATA P55305, *Aspergillus fumigatus* CATA P78574, *Ajellomyces capsulatus* CATA AAF01462, *Podospora anserina* CATA CAC20748, *Neurospora crassa* CAT1 P15937, *Cladosporium fulvum* CAT2 AAG53519, *Pleurotus ostreatus* CAT1 AAD09575, *N. crassa* CAT3 AAK15807, *P. anserina* CATB CAC20749, *Claviceps purpurea* CATC/D CAA04716, *A. fumigatus* CATB Q92405, *A. nidulans* CATB P78619, *A. capsulatus* CATB AAD33062, *Aspergillus niger* CATR P55303, *Penicillium janthinellum* CAT1 P81138, *Candida tropicalis* CATA P07820, *Candida albicans* CATA O13289, *Saccharomyces cerevisiae* CTA1 CAA31443, *Candida boidinii* CATA BAB69893, *Pichia angusta* CATA P30263, *S. cerevisiae* CTT1 AAA34540, *C. fulvum* CAT1 AAG53518, *Pleurotus sajor-caju* CAT1 AAK15159, *A. nidulans* CATC AAG45152, *A. capsulatus* CATP AAF01463, *Glomerella cingulata* CATA CAC35154, *Schizosaccharomyces pombe* CATA P55306, *Botrytis cinerea* CATA P55304. Explanations are provided in the text.

documented for plants or higher mammals.

The group of small subunit enzymes tends to subdivide into yeast and filamentous fungal proteins, with a few exceptions. For instance, the cytosolic enzyme of *S. cerevisiae* (CTT1) groups with two non-yeast proteins. The putative CpCAT2 groups only loosely with other small-subunit catalases using both parsimony and distance methods (Jotun-Hein and Clustal analysis, respectively). Many of these small subunit enzymes are thought to be peroxisomal because of the presence of putative peroxisomal targeting sequences. In most cases this has yet to be proven, and at least one enzyme, Ctap of *Candida boidinii*, is thought to be both cytosolic and peroxisomal (see 4.1.2). Thus, small-subunit catalases, even if they possess the well-defined PTS1 at their carboxy-termini, are not necessarily purely

peroxisomal. As, in *C. purpurea*, deletion of CpCAT2 does not affect the mycelia-associated catalase CATA, it is possible that the latter is the peroxisomal enzyme and that the function of CpCAT2 may have evolved beyond the scavenging of peroxisomal hydrogen peroxide. As non-stringent Southern analysis indicates that only one such gene is present in the *C. purpurea* genome (data not shown), it is unlikely that *cpcat2* evolved from a peroxisomal ancestor within *Claviceps*; this is supported by its unique grouping in the phylogenetic analyses, which deals only with the enzyme core.

4.2.2 Significance of *cpcat2* for axenic and parasitic growth

4.2.2.1 Catalase: phase-specific expression and redundancy

The expression of many fungal catalases is reported to be tissue-specific, emerging or peaking at a distinct developmental stage which gives rise to a certain type of fungal structure. Typically, spores and vegetative mycelia have distinct catalases (*C. fulvum:* Bussink and Oliver, 2001, *A. nidulans:* Navarro et al., 1996, Kawasaki et al., 1997, *N. crassa*: Chary and Natvig, 1989). Some catalases are also reported to be expressed specifically in the stationary phase of axenic culture (*A. nidulans*: Kawasaki and Aguirre, 2001, *N. crassa*: Chary and Natvig, 1989). Regulation according to cell morphology (mycelial versus yeast phase) has been reported for the human pathogen *Ajellomyces capsulatus* (*Histoplasma capsulatum*) catalases (Johnson et al., 2002), and the expression of a small-subunit catalase is reported to be very much increased in the later, necrotrophic stage in comparison to the earlier, biotrophic stage of *Colletotrichum gloeosporioides* (*Glomerella cingulata*) infecting round-leafed mallow (Goodwin et al., 2001). In parasitically growing *Claviceps purpurea*, the activity of CATC/D peaks at phase II, in which the fungus produces the conidiospore-containing honeydew; isolation and analysis of honeydew shows only CATC/D activity (Garre et al., 1998b). The activity of CATB and CATA (putatively peroxisomal) did not clearly correlate with a specific infection stage (Garre et al., 1998b). It is perhaps not surprising that a peroxisomal catalase shows a constant basal expression; the expression of *Aspergillus nidulans* CATC, thought to be peroxisomal, is reported to be constitutive (Kawasaki and Aguirre, 2001).

Although expression of the *cpcat2*-gene could not be shown for mycelia derived from axenic culture, RT-PCR analysis indicated that this gene was expressed *in planta*. Expression was almost completely confined to phases III and IV of infection, which correlates with the differentiation and ripening of sclerotia. One major difference of sclerotial mycelium to the sphacelial mycelium of earlier infection phases is the respiration of lipids instead of sugars (Nisbet et al., 1977, Taber et al., 1985). As the β-oxidation of fatty acids involves production of H_2O_2 via acyl-coA oxidase, it is to be expected that sclerotial tissue requires a higher activity of H_2O_2-degrading enzymes. Although much of this oxidative stress is probably scavenged by the peroxisomal catalase, an excess of H_2O_2 could

diffuse into other areas of the cell, rendering production of additional catalases (such as CpCAT2 or CATE) a necessity.

The universal occurrence and high conservation of catalases among aerobes would seem to suggest its importance for some cellular processes, presumably those involved in aerobic survival. Yet, many different authors have documented a similar non-essential role of catalases for normal growth rates, sporulation and spore germination in bacteria (Xu and Pan, 2000), yeast (Izawa et al., 1996, Wysong et al., 1998) and filamentous fungi (Chang et al., 1998, Calera et al., 1997, Bussink and Oliver, 2001). Similarly, no difference was seen in the ability of Δcpcat2 to grow or sporulate in axenic culture, although the lack of expression under these conditions renders this unsurprising.

Although this could be explained by the presence of multiple catalases, even mutants which totally lack catalase activity show a similar lack of phenotype regarding the oxidative challenges of normal growth (Wysong et al., 1998, Izawa et al., 1996). Furthermore, many catalases show a strong differential regulation which may prevent them from compensating for the lack of a similar enzyme (see above). The conclusion that degradation of H_2O_2 which arises in the course of normal growth falls to the lot of alternative AOS scavengers such as peroxidases is confirmed by experimental evidence (Inoue et al., 1999). The physiological reason behind this could lie in the high K_m of catalases (Baker et al., 1997), which reflects a low affinity to its substrate, making it unsuitable for efficient antioxidant protection at the relatively moderate concentrations of H_2O_2 one would expect to find during normal growth. Catalases may be of importance in peroxisomes, as they contain many H_2O_2-generating enzymes confined within the peroxisomal membrane. Mutants with no or less catalase activity show increased sensitivity to high concentrations of H_2O_2 (Xu and Pan, 2000, Mutoh et al., 1999, Wysong et al., 1998, Navarro et al., 1996). Although some catalase-deficient strains did not show this phenotype, (Bussink and Oliver, 2001, Calera et al., 1997), this could be explained by the simultaneous expression of another catalase.

4.2.2.2 *Cpcat2* is not required for pathogenicity

The lack of expression (as detected by RT-PCR) in the early phases of infection belied a role in both degradation of oxidative-burst H_2O_2 and in coping with the oxidative stress involved in early ovary colonisation. Although even a catalase expressed only in late infection is a potential pathogenicity factor, as it may influence sclerotial differentiation and thus the completion of the parasitic life cycle, targeted inactivation of this enzyme does not impede *C. purpurea* in any stage of infection on rye ovaries. The lack of phenotype regarding the production of honeydew was predictable, but even the appearance of developing and mature sclerotia formed by strains of Δcpcat2 did not differ macroscopically from those formed by the wild type.

It is conceivable that catalases, with their relatively high K_m, could be of importance for phytopathogens exposed to the abundant H_2O_2 produced in the plant oxidative burst. However,

deletion mutants have shown that the major secreted catalase of *Claviceps purpurea*, as well as a large-subunit catalase in *Cladosporium fulvum* are not necessary for infection of rye and tomato, respectively (Garre et al., 1998b, Bussink and Oliver, 2001). In both cases, simultaneously expressed second catalases are proposed to compensate for the lack of the first. In contrast, *Agrobacterium tumifaciens* is unable to cause crown gall tumours on *Kalanchoe sp.* without its large-subunit catalase KATA despite still being in possession of at least one further catalase (Xu and Pan, 2000). To date, this remains the single example of a catalase playing a decisive role in plant pathogenesis, although a mutant of *Botrytis cinerea* lacking a secreted catalase is reported to be somewhat reduced in virulence (Schouten et al., in press). As the infection modus of *Agrobacterium* differs widely from those known by most phytopathogenic bacteria, this may not be comparable to more classical pathogens. The second example deals with a necrotrophic pathogen, which may have completely different mechanisms in respect to AOS (see 4.1.4). Catalases have been shown to be important for animal pathogens (Wysong et al., 1998, Wilson et al., 1995, Day et al., 2000); this may be expected as the antimicrobial activity of AOS may play a more significant role in phagocyte defence systems (see 1.2.3.1). Seen in this context, it is not surprising that the *cpcat2* deletion mutant of the biotrophic pathogen *C. purpurea*, expressed only after the initial colonisation of the ovary is complete, shows no apparent lack of ability to survive *in planta*. Analysis of phase IV protein extracts shows that CATE is still expressed under these conditions, although no increased activity could be shown *in planta* (E. Nathues, pers. comm.). Thus, the compensatory activity of other concomitantly expressed catalases can (as usual) explain the dispensability of *cpcat2* for survival during pathogenesis.

4.2.2.3 A role for catalase in morphogenetic differentiation?

In *N. crassa*, it has been shown that initiation of each of the three morphogenetic differentiation stages involved in conidiation (hyphal adhesion, formation of aerial hyphae and production of conidia) correlates with a hyperoxidant cellular state (Toledo et al., 1991, Toledo et al., 1995) Addition of membrane-permeable antioxidants reduced, while oxidants increased the formation of conidia (Hansberg et al., 1993). This supports the theory, formulated by Hansberg and Aguirre (1990), that a hyperoxidant state is a key factor in triggering microbial cell differentiation. Oxidation of diverse proteins, which results in accelerated proteolytic degradation, is thought to be crucial in the remodelling of protein profiles which is necessary for the transition from one morphogenetic state into the next (Dean et al., 1997). However, the increase of oxidatively damaged proteins observed at the initiation of the three conidiation states (Toledo et al., 1994) may be the result of, and not the cause of increased exposure of mycelia to oxygen or light (which can cause photosensitiser-mediated generation of singlet oxygen). Both CAT3 and CAT1 from *N. crassa* were discovered to be modified, but not inactivated by singlet oxygen; furthermore, intense light and sources of singlet oxygen induced catalase transcription (Lledías et al., 1999, Diaz et al., 2001). Causal involvement of AOS in conidial

differentiation was cemented by the discovery that deletion of the large secreted catalase CAT3 of *N. crassa* resulted in enhanced conidiation (Hansberg et al., 2002). As of yet, no explanation is offered for the mechanisms responsible for this effect. It can only be concluded that, by contributing to the lowering of cellular redox status, catalases can influence developmental processes.

Interestingly, similar results have been documented for the fungi *Sclerotinia sclerotiorum* and *Rhizoctonia solani*, where hydroxyl radical scavengers are reported to inhibit sclerotial differentiation (Georgiou et al., 2000). Experiments with other AOS scavenging compounds such as ascorbate acid and the singlet oxygen scavenger β-carotene further support the role of AOS in the differentiation of sclerotia in *S. sclerotiorum* (Georgiou and Petropoulou, 2001, Georgiou et al., 2001). The authors propose that the increase of oxidative stress mediated by exhaustion of carbon source (analogue to increase of oxidative stress in stationary phase) initiates differentiation of sclerotia as a survival mechanism (Georgiou et al., 2001). This provides support for the hyperoxidant-mediated differentiation described above, and indicates that this theory can be extended to sclerotial differentiation.

It is interesting to consider the expression of both *cpcat2* and the presence of CATE in this context for the sclerotial differentiation of *C. purpurea*. Expression of *cpcat2* is confined to the differentiation of sclerotia. Should sclerotial differentiation be triggered by oxidative stress, induction of *cpcat2* expression could be an indirect effect of this, designed to keep the lid on oxidative damage. Many catalases are reported to be induced by oxidative stress (yeast: Marchler et al., 1993, *N. crassa*: Chary and Natvig, 1989, *A. nidulans*: Kawasaki et al., 1997, *Agrobacterium*: Xu and Pan, 2000, *C. fulvum*: Bussink and Oliver, 2001). Although the refusal of *cpcat2* to be transcribed at all in axenic culture of the pathogenic strain (under the tested conditions) prevented the investigation of induction by AOS, the promotor of this gene does contain a putative binding site for CPTF1, a putative transcription factor (homologous to yeast ATF-1) which is itself induced by H_2O_2 in *C. purpurea* (Joshi et al., 2002b). Furthermore, an identical binding site was found in the promotor of *cpcat1*, a gene which is induced by H_2O_2 in axenic culture (Joshi et al., 2002b). However, in contrast to CAT3 of *N. crassa* during conidiation, the importance of the *cpcat2* gene product for successful sclerotial differentiation seems to be minimal, although this was only investigated macroscopically. The discovery that strains lacking *cpcat2* had only a fraction of the alkaloid content seen in the wild type does indicate that this catalase is significant for physiological processes. Perhaps a closer examination of the structure and physiology of sclerotia from both strains will reveal more differences. Increased oxidative stress during sclerotial differentiation could also give rise to CATE. In *N. crassa*, oxidative stress accompanying conidiation produces both increased activity and oxidatively altered forms of CAT1, which still retain their activity (Lledías et al., 1999). Therefore, CATE could represent a new isoform of an old catalase.

4.2.3 *Cpcat2* and the biosynthesis of ergot alkaloids

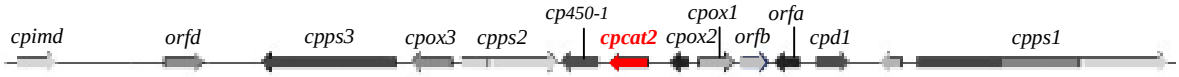

Fig. 4.3: Cluster of genes involved in the alkaloid biosynthetic pathway. All genes begin with cp which refers to *Claviceps purpurea*. imd: isopropyl malate dehydrogenase1, ps: peptide synthase, ox: oxidase, cpd1: dimethylallyltryptophan synthase (also known as DMATS), orf: open reading frame (showing no homology to known proteins). Gene schema kindly provided by T. Correia.

The discovery that *cpcat2* was located within the cluster of alkaloid biosynthesis genes (see fig. 4.3) had strong implications for the sclerotial expression of this catalase, as alkaloid biosynthesis is also confined strictly to sclerotial tissue. Pathogenic field isolates of *C. purpurea*, such as T5 (the parent strain of 20-1), do not express genes of the alkaloid biosynthetic pathway in axenic culture, although they can be induced to undergo a morphogenetic switch to sclerotial-like hyphae which accumulate lipids (see 1.3.2). Growth of the pathogenic strain 20-1 in an alkaloid production medium did induce the bulbous morphology associated with sclerotial-type mycelia, but northern analysis of this mycelium did not reveal expression of the *cpcat2* gene (data not shown). This is supported by lack of *cpcat2*-derived activity in protein extracts from similarly cultivated mycelia. *Cpcat2* is co-regulated with genes involved in alkaloid biosynthesis not only in the pathogenic strain 20-1, but also in the alkaloid production strain P1. This "crippled" strain is not pathogenic and does not form spores, but does produce alkaloids in axenic culture. Not only is *cpcat2* expressed in axenic culture of P1, but it shows the de-repression when phosphate-starved which is typical for alkaloid biosynthetic genes, despite the lack of putative binding sites for phosphate-sensitive regulation factors such as NUC1 in the promotor of *cpcat2*. A putative binding site for a NUC1-homologue can be found in the promotor of the alkaloid cluster gene *cpd1* (Lübbe, 2001); NUC1 is responsible for phosphate starvation-mediated transcriptional de-repression in *N. crassa* (Peleg and Metzenberg, 1994).

Of course, the final and most convincing evidence for the importance of this catalase in the biosynthesis of alkaloids is supplied by Δcpcat2, which produces sclerotia containing only 8% of the alkaloids found in sclerotia of the wild type. The fact that inactivation of this gene in the strain P1 leads to a similar reduction in the amount of alkaloids produced in axenic culture (E. Nathues, pers. comm.) shows that the phenotype of the 20-1-derived mutant is not a peculiarity of a single mutant arising from transformation-induced genomic rearrangement. In both cases, sequencing of genomic regions flanking the integration site of the replacement vector show that adjacent genes have not been disturbed by the integration event (E. Nathues pers. comm.).

The presence of a catalase in a gene cluster for the biosynthesis of secondary metabolites in fungus is a novel discovery. Mechanisms behind the dramatic effect of *cpcat2* deletion on alkaloid

biosynthesis remain, for the present, a matter of speculation. The simplest explanation would be that lack of *cpcat2* leads to oxidative damage of one or more enzymes in the biosynthetic pathway. Although genes encoding oxidases which incorporate molecular oxygen into their substrates (such as P_{450}-monooxygenases) could be a source of superoxide (see 1.1.2) and, through spontaneous dismutation, hydrogen peroxide, these types of molecules are found in other biosynthetic pathways which do not include a catalase in the corresponding gene cluster (Tudzynski and Hölter, 1998, Keller and Hohn, 1997). At least four genes (orfa-d) are present in the cluster which show no homology to known genes; better classification of these genes could shed more light on the involvement of *cpcat2*. To date, nothing is known about the compartementalisation of alkaloid biosynthesis in *Claviceps*. Enzymes involved in the fungal synthesis of β-lactam antibiotics are thought to be located in both microbodies and the cytoplasma (van de Kamp et al., 1999). Putative membrane-localisation segments of the *C. purpurea* peptide synthases indicate that they may be associated with microbodies (T. Correia, pers. comm.). Co-localisation of a redox-sensitive enzyme with a monooxygenase in a microbody could concentrate oxidative stress and require a specific AOS- scavenger. In this case, an intermediate product of the pathway should accumulate in Δcpcat2 strains. On the other hand, the role of *cpcat2* could be more indirect. Changes of cellular redox status caused by lack of *cpcat2* could influence transcription factors required for alkaloid biosynthesis; in this case, at least some of the biosynthetic genes should be transcriptionally repressed. Preliminary results showing that *cpd1*, the gene encoding the enzyme which catalyses the first specific step in the pathway, is transcriptionally repressed in Δcpcat2 strains of both P1 and 20-1 (E. Nathues, pers. comm.) indicate that this may indeed be the case. This would suggest both that deletion of other intracellular catalases may have a similar effect, and that other regulatory pathways are likely to be altered as a result of *cpcat2*-deletion. It would be interesting to see if exogenous, membrane-permeable antioxidants could restore alkaloid production in *cpcat2*-deletion strains of P1.

4.2.3.1 Putative trans-acting factors

The ability of *Claviceps* to produce alkaloids is exploited by the pharmaceutical industry. Most industrial alkaloid production is done in fermentative cultures with special production strains. These strains, arising from random mutagenesis and repeated selection, have been induced to produce alkaloids in axenic culture (Keller and Tudzynski, 2002). The lack of understanding concerning the underlying mechanisms prevents improvement of production strains using targeted genetic modification. Similarly, the factors which induce sclerotial differentiation during growth *in planta* are poorly understood. As alkaloid biosynthesis is confined to sclerotial tissue during parasitic growth, it is likely that both phenomena share regulatory pathways. However, the highly variable alkaloid content of sclerotia indicates that genes controlling the biosynthesis of alkaloids probably require the action of one specific (or more than one less specific) regulatory factor(s) for strong expression. As

cpcat2 seems to be co-regulated with genes of the alkaloid biosynthesis, a look at the promotor of this gene may provide possible candidates for such trans-acting factors.

In this context, the putative binding sites for the oxygen sensor HAP-1 (heme-activating-protein) of yeast are of interest. HAP-1 is a positive regulatory factor which increases the transcription of genes involved directly or indirectly in aerobic metabolism (such as cytochromes involved in electron transfer in respiration and cytosolic catalase) (Kwast et al., 1998). Oxygen sensing of HAP-1 occurs through direct association with heme, as heme biosynthesis is dependent on molecular oxygen (Zitomer and Lowry, 1992); furthermore, heme may act as a redox-sensor (Kwast et al., 1998). In some yeast genes, HAP-1 activation requires the activity of a protein complex composed of HAP-2, HAP-3, HAP-4, and HAP-5 (Ramil et al., 2000). This HAP-2345 complex (hereafter referred to as the HAP-complex) is responsible for carbon source-dependent regulation of a number of aerobic genes and acts upstream of oxygen sensors. In yeast, many genes controlled by the HAP-complex, such as enzymes of the citric acid cycle, are activated by non-fermentable carbon sources independent of the presence or absence of oxygen (Kwast et al., 1998). Homologues of components of the HAP-complex are highly conserved and have been found in mammals and filamentous fungi; in all cases these proteins assemble to a complex which binds CCAAT boxes (Brakhage et al., 1999). Several experiments indicate that the mechanism of activation by the HAP-complex involves remodelling of chromatin structure through modification of histones (Gancedo, 1998, Faniello et al., 1999, Narendja et al., 1999); in some cases, this is postulated to be mediated by interaction with a repressor (binding to an upstream repressing sequence URS) such as CAR1 (Lodi and Guiard, 1991, Ramil et al., 2000). Consistent with a function in the activation of pathways involved in the metabolism of non-fermentable carbons in yeast, mutants deficient in the HAP-complex components are unable to grow on non-fermentable carbon sources in yeast, such as ethanol (Pinkham and Guarente, 1985). In filamentous fungi, which are obligate aerobes, HAP-complex components are not required for the induction of genes involved in oxidative phosphorylation; mutants lacking homologues of the HAP proteins show decreased growth rates and poor conidiation (Brakhage et al., 1999). Interestingly, many biotechnologically important genes, including some involved in the regulation of penicillin biosynthesis, underlie control of HAP-complex homologues (Brakhage et al., 1999). In penicillin biosynthesis of *A. nidulans*, the HAP-234-homologue (AnCF) is required for activation by the pathway specific regulatory gene (Steidl et al., 1999) and similar protein complexes are involved in the regulation of penicillin and cephalosporin biosynthesis in *Penicillium* and *Acremonium* species (Litzka et al., 1999).

In the *cpcat2* promotor, four putative HAP-1 binding sites and one putative HAP-complex-binding region can be found. Furthermore, a putative binding site for a general yeast repressor CAR1 (Luche et al., 1990) is also present. Information provided by analysis of the cis and trans factors involved in

HAP-dependent transcription in yeast, along with the fact that two putative HAP-1-binding sites and a putative HAP-complex binding site are found 260 bp upstream of the proposed start codon, suggest that HAP-1 may be a positive regulator of *cpcat2* which can only be induced in the presence of active HAP-complex. Lack of activated HAP-complex could be reflected in a highly condensed chromatin structure in the region of the alkaloid biosynthesis genes, offering an explanation for the very low rate of homologous integration (0.4%) of the Δcpcat2 replacement vector in the pathogenic strain 20-1.

Although no occurrence of HAP-1 homologues has been documented in filamentous fungi until now, the discovery of a putative HAP-1 binding site in the promotor of *cpcat2* is rendered more significant by the fact that the cytosolic catalase of yeast underlies control of HAP-1 (Spevak et al., 1986, Winkler et al.,1988). While oxygen-dependent regulation of an AOS-scavenging enzyme seems meaningful, the connection between oxygen and alkaloid production is less obvious. That oxygen concentration does influence alkaloid production is shown by experiments in which addition of oxygen vectors (perfluorocarbons) to production media leads to a five-fold increase in alkaloid yields (Menge et al., 2001). Of two further promotors of genes involved in alkaloid biosynthesis (*cpd1* and *cpps1*), only one (*cpps1*) contains putative binding sites for HAP-1; this indicates that not all individual promotors can be regulated by a HAP-1 homologue. The decrease of *cpd1* transcript in the altered redox environment of *cpcat2*-deletion mutants is therefore unlikely to be the direct result of abberant HAP-1 activity but may reflect more complex cross-talk mechanisms.

The high amount of putative ABA response elements (ABAREs) in the *cpcat2* promotor should also be noted. The phytohormone abscisic acid (ABA) is involved in manifold aspects of plant regulation including stress management (Giraudat, 1995) and the co-ordination of a variety of processes in seeds (McCarty, 1995). ABA-mediated gene regulation via ABAREs is involved in the co-ordination of physiological processes in response to osmotic stress (Guan et al., 2000). Alkaloid production media contains very high amounts of sugar (30%), which may induce osmotic stress pathways in producing cultures. Exogenous ABA induces production of AOS in maize (Jiang and Zhang, 2001) and the transcription of the maize CAT-1 gene via an ABARE (Guan et al., 2000). Interestingly, the enzyme which catalyses the first specific step in alkaloid biosynthesis (*cpd1*) has two ABAREs. Although some plant pathogenic fungi are themselves capable of ABA production (Hirai et al., 2000, Tudzynski and Sharon, 2002), until now no ABA-dependent promotors have been identified in fungi.

In an attempt to clarify the trans-acting factors involved in the regulation of the alkaloid biosynthetic cluster, extracts of rye ovaries are being tested for their ability to induce the transcription of alkaloid pathway genes in the phytopathogenic strain 20-1 (T. Haarman, pers. comm). The fact that even alkaloid content of different sclerotia on the same ear of rye can vary up to 50-fold in alkaloid content, points to a complex regulation possibly involving abiotic factors (light, oxygen availability

etc.). Detailed and comparative analysis of all gene promotors in the cluster should be the first step towards pinpointing and testing the effect of possible regulatory factors.

4.2.4 Conclusions: *cpcat2*

The gene encoding the putative small subunit-type catalase *cpcat2*, probably either a peroxisomal or cytosolic enzyme, is not required for pathogenicity, but is essential for the production of alkaloids. Deletion experiments in other phytopathogens show that catalases are generally not pathogenicity factors, although the abundance of multiple catalase isoforms and other enzymes which can degrade H_2O_2 (such as catalase-peroxidases and peroxidases) prevent conclusions as to the importance of AOS detoxifying enzymes for survival of plant pathogens. *C. purpurea* is no exception; both catalase genes which have been classified as not essential after deletion experiments (CATC/D, CpCAT2) exhibit co-expression with other catalase activities (CATB and CATE, respectively). Some of these catalase activities may correspond to catalase-peroxidases, which have also been identified in fungi (Levy et al., 1992, Fraaije et al., 1996). As of yet, no classification of either peroxidases or catalase-peroxidase has been undertaken in *C. purpurea*.

The reason for multiple catalase isoforms underlying complex differential regulation in fungi is far from clear. The large subunit-type enzymes are particularly interesting as their occurance seems to be confined to bacteria and fungi. Perhaps organisms which do not form real tissue are more exposed to AOS as the intersection of individual cells with the atmosphere is greater. The function of this enzyme may extend beyond the detoxification of H_2O_2 for cellular protection. The theory that hyperoxidant states are key mediators of morphogenetic differentiation would grant those enzymes which regulate AOS concentrations a more complex role in cellular processes. The possibility that the NADPH-binding domain of catalases may be able to bind mRNA, suggested by Clerch et al. (1996), is intriguing in this context.

Comparison of *cpcat2* to other fungal catalases shows a unique grouping among other small-subunit type catalases which may reflect the novel role of this protein in the synthesis of secondary metabolites. The activity of *cpat2* may be highly unstable, as indicated by the failure to visualise catalase activity of its gene product; this, along with its decreased homology to other fungal catalases may explain the lack of reports describing similar enzymes in other fungi. Although the mechanism of *cpcat2* involvement in alkaloid biosynthesis is unclear, preliminary results indicate that the transcripts of other genes in the same cluster are down-regulated in the deletion mutants. This indicates a regulatory, rather than a structural, role in alkaloid biosynthesis. Redox-dependent alteration in the activity of transcription factors such as HAP-1 could provide an explanation for the Δcpcat2-phenotype.

As is the case for many complex secondary metabolites, the actual function of alkaloids in the

biology of *Claviceps* remains a mystery. It has been suggested that alkaloids are the products of detoxification (Řeháček, 1984) and toxic alkaloids may mediate a symbiotic-type relationship with the host plant by providing protection against grazing (Parbery, 1996). The latter is supported by the occurrence of symbiotic alkaloid-producing grass endophytes among the *Clavicipitaceae* (Schardl et al., 1991). The plant seems to mount very little protest against invasion by *Claviceps*, and, in most cases, is not materially damaged by infection as it is still able to survive and produce seed. However, other non-pathogenic and non-symbiotic fungi belonging to the genera of *Aspergillus* and *Penicillium* produce similar alkaloids (Vining, 1973), weakening both an exclusive significance of ergot alkaloids in the give and take of symbiosis as well as any specificity of function in *Claviceps.* Alkaloids are certainly not required for the parasitic growth of *C. purpurea*, as illustrated both by pathotests with Δcpcat2 and the fact that many naturally occurring field isolates are also almost completely devoid of alkaloids (Mantle and Tonolo, 1968).

However, pharmaceutical interest in this fungal metabolite pathway, as well as the novelty of catalase-dependent secondary metabolite production, justifies a more detailed investigation into the physiological interactions of this catalase. Indications that an alteration in cellular redox status may be able to influence the regulation of genes which seem to be completely detached from direct pathways of AOS scavenging awakens interest in other intercellular components of the AOS-response.

4.3 From metals to the oxidative stress response

In order to identify other genes which may be involved in the response of *C. purpurea* to oxidative stress, a differential screening approach was taken to isolate genes which were induced in response to high concentrations of copper.

Transition metals such as copper and iron can easily undergo one-electron redox reactions (Hippeli and Elstner, 1999). This ability renders them useful cofactors for enzymatic redox reactions, making them essential for normal cellular processes. At the same time, one-electron-transfer mediated by transition metals can catalyse the production of the hydroxyl-radical (see 1.1.1.), rendering them highly toxic (Halliwell and Gutteridge, 1990, Stohs and Bagchi, 1995).

This basic dilemma of cell physiology is reflected in a tightly controlled regulation of intracellular metal ion concentrations, including reduction of uptake, enhanced exportation and sequestration mechanisms (Dameron and Harrison, 1998). In yeast, excess copper induces the transcription of Cu-metallothionein (Carri et al., 1991), AOS scavengers such as catalase (Lapinskas et al., 1993) and Cu,Zn SOD (Gralla et al., 1991, Carri et al., 1991), and represses the transcription of high-affinity copper transporters (Graden and Winge, 1997). At the same time, a variety of chaperones escort copper ions from storage proteins to the enzymes which require them (Pena et al., 1999), effectively

rendering the concentration of free copper ions to less than one per cell (Rae et al., 1999).

Damage caused by copper overload of yeast cells, manifesting as an increase of insoluble proteins, a loss of enzyme activity and a decrease in RNA, is oxygen-dependent (Greco et al., 1990). The induction of AOS scavenging enzymes by copper, as well as the ability of Cu-metallothionein (CUP1) to ameliorate oxidative stress in yeast mutants lacking Cu,Zn SOD (Culotta et al., 1995) and Cu,Zn SOD to compensate for CUP1 deficiency (Tamai et al., 1993), further underlines the common elements of copper homeostasis and AOS detoxification.

The ability of copper to produce the hydroxyl-radical, whose instability prevents it from being added directly, and to induce proteins of the AOS-response, was implemented in the search for genes involved in the interaction with AOS in *Claviceps purpurea*. However, as it is to be expected that many of the genes involved in copper homeostasis may not be of direct importance for AOS detoxification or AOS-mediated signal transduction, the genes isolated in the course of differential cDNA screening were further screened for induction by excess iron and H_2O_2 via northern analyses.

4.3.1 Implications of the transcriptional response to copper, iron and H_2O_2

Northern analyses of clones obtained in the differential screening indicate that mechanisms involved in the induction of genes in response to metal excess and to classical AOS such as hydrogen peroxide are generally distinct. Only two clones (X1 and X46) were found whose transcription is clearly upregulated by all three stimuli. The oxidative toxicity of transition metal ions is thought to lie in the production of the hydroxyl radical, which has a half-life of approximately 1 µs (Hippeli and Elstner, 1999). The exceedingly high instability of this compound makes it an unlikely candidate for a direct mediator of cellular protectant systems. The ability of the hydroxyl radical to rapidly initiate radical chain reactions renders it exceedingly dangerous in even small concentrations; less than 50 molecules/cell can already have enormous biological consequences (Stohs and Bagchi, 1995). As the presence of the hydroxyl radical alone is tantamount to severe oxidative damage, it would be more economic for the cell to prevent the formation of these molecules by responding to the metals directly. Therefore, genes which are induced by both copper and iron excess could be involved in AOS pathways, even if they are not induced by more direct sources of AOS. In *C. purpurea*, the AOS-scavenging enzyme *cpsod1* is also induced by both metals, while transcript concentration is unaffected by superoxide and H_2O_2. In the course of the differential screening, four genes (X1, X12a, X46 and X98) were found which were induced by an excess of both metals. A general transcriptional response to metals could be mediated by a MTF-1 (metal-responsive transcription factor) homologue. Recent results implicate MTF-1 in the oxidative stress response of mammals (Giedroc et al., 2001) and MTF-1 is thought to be the trans-acting element in the induction of rat Cu,Zn SOD by a variety of

metals (Yoo et al., 1999). While a putative MRE (the cis-element of MTF-1) is found in the promotor of the Cu,Zn SOD, the promotors of X12a and X46 which are induced by both excess copper and iron, do not contain putative MREs. Instead, both promotors contain putative elements which respond individually to copper and iron, although homologues which bind these elements in yeast activate genes in response to metal starvation rather than under conditions of excess metal (see 4.3.2.1.2). Iron and copper homeostases of yeast are also linked by the high affinity transporter system for iron, one of the components of which is induced by copper (FET3, the homologue of *C. purpurea* X51a); this system has also been implicated in the AOS response, as it is upregulated in SOD-deficient strains (De Freitas et al., 2000).

As Fenton-generated hydroxyl radical production also involves H_2O_2, it is conceivable that genes involved in protection against metal-mediated AOS are also induced by H_2O_2 directly. Of the genes isolated during differential screening, four (X1, X46, X51a and X27a) have been shown to be induced by hydrogen peroxide. Sequencing of two of these genes (X46 and X51a) fails to show putative binding sites for the H_2O_2-induced transcription factor CpTF-1 in *C. purpurea*, or similar sites which bind AP-1, the major transcription factor which responds to oxidative stress in yeast and mammals (Toone et al., 2001).

The results obtained by northern analysis of the differential cDNA clones can not yet be interpreted further in any general context. Firstly, as neither the Cu,Zn SOD nor genes with high homologies to metallothioneins were found, it is obvious that the screening is far from saturated. The inherent problem of this method of differential screening lies in the fact that the differentially hybridised membranes contain different amounts of DNA (see 2.5.2). Secondly, the low amount of analysed clones prevents a reliable interpretation of the overlap in the transcriptional responses to these stimuli which could be provided by large scale analyses (for example, by microchip technology). Thirdly, experimental promotor analysis must be done before conclusions about possible cis-acting elements can be made. Finally, the scarcity of data concerning metal homeostasis in filamentous fungi and even yeast renders interpretation of the results mostly speculative. The fact that many of the most interesting genes induced by either copper or iron (X1, X9, X27a and X98) show no significant homologues to any sequenced proteins reflects the lack of knowledge about this aspect of fungal biology. The fact that the differential screening with and without copper led to the isolation of genes induced by H_2O_2 indicates that the response to metals and oxidative stress does overlap to some extent in *Claviceps purpurea* but elucidation of the underlying mechanisms must await further research.

4.3.2 Preliminary analysis of selected genes isolated in the course of differential cDNA screening

It was reasoned that genes, which are either induced by both excess iron *and* copper or, by more direct sources of AOS, could be of interest for the investigation of AOS pathways in *C. purpurea*. Further characterisation of these genes involved the sequencing of the entire gene and its promotor region, which allowed a more detailed analysis of the protein homologies, a look at putative cis-acting elements in the promotor and *in planta* expression analysis using RT-PCR. In the research presented in this thesis, only genes were investigated whose products showed significant homology to characterised proteins. The putative hydrophobin was selected for its strong (and hitherto unreported) response to both copper and iron, while the putative polyol dehydrogenase was of interest for its upregulation under excess copper and iron as well as after oxidative insult with H_2O_2. The gene encoding a Cu,Zn SOD-like protein was also examined because of its similarities to a classical AOS-scavenging enzyme.

4.3.2.1 *cph1*: a metal-responsive hydrophobin?

Conceptual translation of clones of the type X12a reveals a protein with all the sequence characteristics of typical (mono)hydrophobins: it is about 100 aa in size, carries a signal peptide for secretion and contains the conserved cystein pattern which defines this type of protein. This cystein pattern allows assembly of monomers into amphipathic polymer, which coats aerial fungal structures such as conidia, conidiophores and fruiting bodies, rendering them hydrophobic. Hydrophobic surfaces are thought to ease spore dispersal, facilitate attachment to hydrophobic surfaces (Wösten et al., 1994b), enable mycelia to free itself from aqueous environments by lowering of surface tension (Wösten et al., 1999) and to assist diffusion of gases in fruiting bodies (Lugones et al., 1999).

Hydrophobins (putative and otherwise) have as of yet only been discovered in filamentous fungi; excepting the rigid pattern of cysteins, which are essential for polymer formation, the degree of overall conservation in their protein sequences is low. The abundance of different hydrophobins among filamentous fungi suggests that the ability to form amphipathic polymers confers a strong selective advantage, but it is not obvious why this should be the case. It is conceivable that many other types of proteins could fulfil the simple conferral of hydrophobicity to outer surfaces. Furthermore, it seems strange that large numbers of meticulously regulated, distinct hydrophobins are produced within the life cycle of a single fungal species to fulfil such a simple function. This would seem to indicate a more complex role in fungal biology than providing a hydrophobic coating. Several tangent functions have been proposed for hydrophobins; they include acting as toxins, influencing the composition of cell walls, protection against adverse environmental conditions or bacterial infection and signal transduction (reviewed by Wösten, 2001). As of yet, only one hydrophobin has been shown to be of

importance for infection by a phytopathogen; deletion of the hydrophobin MPG1 in *Magnaporthe grisea* reduced the ability to differentiate appressoria (specialised infection structures) rendering the mutant less virulent (Talbot et al., 1993). Interestingly, the lack of MPG1 can be bypassed by exogenous cAMP, indicating a role in signal transduction (Talbot et al., 1996). The induction of a hydrophobin by metals is a novel finding, and adds yet another aspect to an already heterogenous mixture. As *cph1* is not induced by H_2O_2, it is not clear if this protein is involved in the response to metal-mediated oxidative stress or in other aspects of transition metal homeostasis.

4.3.2.1.1 Hydrophobins, oxidative stress and metals

Hydrophobins are associated with aerial structures which are exposed to more oxidative stress than are submerged ones. The simplest explanation would be that hydrophobins could contribute to a decrease in oxidative stress by reducing the contact zone of other, less stable fungal structures to the atmosphere. However, analysis of the rodlet layers formed by the polymers of the class I hydrophobin SC3 shows a high degree of porosity (Wösten et al., 1994a). Although the class II hydrophobins (such as the putative *cph1*, see 3.3.2.2.1) are also thought to coat aerial surfaces, rodlet layers have not yet been observed (Wessels, 1997, Wösten, 2001). Generally, the differential expression of hydrophobins tends to reflect changes in morphogenetic stages. Perhaps a link may be forged to the proposed role of AOS as a key factor in triggering microbial cell differentiation (see 4.2.2.3).

Hydrophobins are characterised by a distinct pattern of cystein, the thiol group of which is a typical ligand of metals as seen for instance in the copper thiolate clusters of metallothioneins (Kagi et al., 1984) and copper chaperones (Harrison et al., 1999). As of yet, it is not known if hydrophobins are able to bind metals, or if the presence of copper influences the state of thiol residues. Self-assembly of hydrophobin monomers in the absence of a hydrophilic/hydrophobic interface is prevented by the formation of cystein bridges; *in vitro* experiments show that reduction of the sulfhydryl groups induce polymer formation in water (Wösten, 2001). Therefore, oxidative conditions (albeit in the ER) which supress polymer formation might be necessary for the synthesis and secretion of monomers. Redox-sensitive cystein thiols whose alteration could lead to dramatic conformational changes could be important for the transduction and potentiation of signals.

The rodlets formed by polymers of class I hydrophobins have been compared to the fibrils formed by amyloid proteins (Wösten, 2001). This parallel is especially intriguing with respect to a possible role in metal-mediated oxidative stress, as β-amyloid is a pro-oxidant, binding to copper and other transition metals and promoting metal-mediated hydroxyl-radical formation (White et al., 1999, Kontush, 2001). Furthermore, interaction with copper, possibly mediated by oxidative stress, is thought to contribute to the tendency of β-amyloid to form fibrils (Gjnec et al., 2002).

4.3.2.1.2 Aspects of *cph1* regulation

Northern analysis shows that transcript concentrations of *cph1* are very much higher in medium containing excess copper than in medium to which no copper had been added, while copper chelation reduces the transcript concentration even further (data not shown). Although the increase of stringency in the differential conditions amplified the differential expression of *cph1*, it should have also been found during the non-stringent screening. In order to be isolated by this method, the degree of differential expression must be able to emerge despite the fact that membranes hybridised with induced cDNA have lower template concentrations (see 2.5.2); only clones whose expression under the negative screening conditions is very low (such as X1) are easily isolated. The fairly strong basal expression of clones such as *cpsod1* or *cph1* in medium to which no copper had been added impedes their isolation in such a screening.

Two putative copper-responsive elements (CuREs), separated only by 8 bp, are found in the promotor of *cph1*. In *Saccharomyces cerevisiae*, CuREs are bound by the MAC1 (metal activation) protein, which is responsible for the activation of genes under copper deprivation (Labbe et al., 1997). MAC1 contains a DNA binding domain and a copper-sensing transactivation domain; when copper is sufficient, MAC1 releases the CuRe (Labbe et al., 1997) and is rapidly degraded (Zhu et al., 1998). A MAC1 orthologue, GRISEA, has also been found in the filamentous fungus *Podospora anserina* (Borghouts and Osiewacz, 1998). In *Schizosaccharomyces pombe*, cis-acting elements are bound by the CUF1 protein which can both activate and repress gene transcription under conditions of copper deprivation (Labbe et al., 1999). Increase of transcript concentration which follows after addition of copper is the result of de-repression (Labbe et al., 1999). The DNA-binding domain of CUF1 shows homology to the ACE-binding protein (responsible for the activation of genes under excess copper) while the transactivation domain is homologous to the copper-sensing domain of Mac1, merging two distinct classes of copper metalloregulatory transcription factors (Labbe et al., 1999) Therefore, upregulation of *cph1* during conditions of excess copper could be the result of de-repression mediated by a transcription factor similar to CUF1; alternatively, it could be the result of activation via a new type of copper-sensing transcription factor which combines a DNA-binding domain similar to CUF1 and MAC1 but a copper-sensing trans-activation domain more similar to ACE-1.

Post-transcriptional mechanisms such as a metal-mediated extension of mRNA half-life could also contribute to increased transcript concentrations. It is important to note that the expression of the pentahydrophobin of *C. purpurea* (see 1.3.3.1) is not induced by copper (G. Mey, pers. comm.), indicating that interactions with metals may be a specific, rather than a general, phenomenon. Analogue to the CuREs, the putative FeREs present in the promotor of *cph1* are typically found in promotors of genes activated under iron starvation, such as high affinity iron transporters. Sequencing of the promotor region of clone X51a (done by S. Joshi) encoding the Fet3-homologue, shows that it

lacks elements having any similarity to FeREs, despite being highly activated under conditions of iron starvation. This provides further evidence for regulatory mechanisms in *C. purpurea* differing from those described in yeast.

The regulation of *cpsod1* and *cph1* shows many similarities: both genes have a strong basal expression, are induced by iron and copper, are unaffected by H_2O_2 and seem to be expressed during all phases of infection. The presence of *cph1* during all phases of infection would seem to rule out a role in a single process such as penetration, conidiation or sclerotial differentiation; this indicates a function which transcends the hydrophobic rendering of specific aerial structures.

4.3.2.2 *cpdh1*: a putative polyol dehydrogenase

The clone *cpdh1* shows convincing homologies to Zn-binding polyol dehydrogenases of bacteria, while analysis of conserved residues seems to indicate that this enzyme could be functional. Both the lack of strong homologies to fungal sorbitol and mannitol dehydrogenases, as well as the bewildering amount of introns (should they even be partially conserved), which would impede recognition by a genomics approach, may explain why no homologues have been reported for fungi or other eukaryotes.

Polyols, which are widely distributed in fungi, are important in many aspects of cell physiology. They are a storage form for energy and reduction power, are involved in the response to osmotic stress, in pH buffering, and in the stabilising of enzymes (Jennings, 1985). Some polyols, such as mannitol and sorbitol have been implicated in the AOS response as they are efficient quenchers of the hydroxyl radical (Smirnoff and Cumbes, 1989, Hunt and Wolff, 1991). They may also be involved in complexing metals (Dolezal et al., 1973, Hamalainen and Makinen,1989).

There is some evidence that the hydroxyl-radical scavenging ability of mannitol is of significance for host-pathogen interactions. Mutants of the yeast *Cryptococcus neoformans* which are unable to accumulate mannitol are more sensitive to oxidative killing by human neutrophils and cell free oxidants and are less virulent in mice (Chaturvedi et al., 1996). The tobacco pathogen *Alternaria alternata* secretes mannitol during plant colonisation and induces the expression of mannitol dehydrogenase in tobacco, a plant which does not itself accumulate mannitol (Jennings et al., 1998).

Another interesting aspect of polyols for the AOS-response is their ability to store reduction equivalents. Many components of the oxidative stress system centre around glutathione (GSH) (see 1.1.3). GSH has been shown to be essential for the oxidative response in yeast (Izawa et al., 1995, Grant et al., 1996) and *Penicillium chrysogenum* (Emri et al., 1997). Restoration of sulfhydryl groups in oxidatively damaged proteins and donation of electrons to GPx or GST produces GSSG, which is replenished by NADPH via the glutathione reductase (GR) (Anderson, 1998). Other antioxidant thiols such as thioredoxin and glutaredoxin contribute to the constant depletion of NADPH in a similar fashion (Grant, 2001). Thus, a cell exposed to oxidative stress requires a constant source of electrons

to replenish NADPH. This is thought to be supplied by the glucose-6-phosphate dehydrogenase of the pentose-phosphate cycle (Slekar et al., 1996, Izawa et al., 1998). However, oxidative challenge of *P. chrysogenum* results in higher GR and GST activities, as well as an increase in *de novo* GSH synthesis, while the G6PDH activity remained unchanged (Emri et al., 1999), indicating that some systems may require alternative sources of reducing power. It is conceivable that polyols could represent another source of reduction equivalents. Evidence for this is supplied by experiments with sorbitol dehydrogenase (SDH); it was found that GSSG is directly involved in mediating the transfer of Zn from metallothionein to apo-SDH, resulting in the activation of this enzyme (Jiang et al., 1998). Northern analysis with the putative dehydrogenase of *C. purpurea* shows that it can be induced by H_2O_2; the strongest homologies are to Zn-binding enzymes, and analysis of the conceptual protein shows the conservation of Zn-binding residues.

Although these results render *cpdh1* a good candidate for direct involvement in the AOS response, many things must be established before this is anything but speculation. At present, neither the substrate nor the co-factor of *cpdh1* is clear, as conserved residues only provide the possibility of NADP binding, while none of the tested polyols were able to induce *cpdh1* expression in northern analysis. Furthermore, the transcriptional induction of this enzyme after H_2O_2 treatment is highly variant (S. Joshi, pers. comm.), which indicates that other (as of yet unknown) factors must play a decisive role in its regulation. This gene is also induced by high amounts of copper and iron, a phenomenon which could be part of a metal-mediated AOS response. However, the strong induction under conditions of minimal iron concentrations fits less neatly into the picture. A putative CuRE is found at -152 bp preceding the designated start codon; this could correspond to the induction (or de-repression) by copper as seen in the putative hydrophobin (see previous section). The increased transcript concentrations under conditions of very low and very high iron concentrations (a phenomenon also observed in the clone X9) remains a complete mystery. This kind of biphasic regulation, perhaps conceivable for diffusion-based transporters or the components of transcription factor complexes, is baffling in a putative dehydrogenase.

The *in planta* expression pattern of this gene, which shows transcription peaking during phase II, in which the host-parasite interface is being established, fits with its identity of a gene induced by AOS, as cross linking of phenolic compound in the area of the host-parasite interface indicates that AOS may be involved in its formation. This phase also coincides with the production of honeydew, which contains a variety of polyols (Mower and Hancock, 1975a). Only biochemical characterisation and functional analysis of this novel putative dehydrogenase can provide more information as to its function and importance for pathogenesis.

4.3.2.3 *cpsod-ish*: encodes a protein similar to Cu,Zn SODs

As this gene could not be isolated from either the copper-induced cDNA library from strain 20-1 or the alkaloid production library of strain P1, the genomic region corresponding to the cDNA fragment of clone X8b, which showed similarities to Cu,Zn SOD, was sequenced. Conceptual translation of the putative protein revealed that residues important for metal binding and catalysis in Cu,Zn SODs were lacking in *cpsod-ish*, and that the homology was confined to 127 bp in the N-terminal half of the protein. Although the copper chaperone for Cu,Zn SOD is reported to have a similar degree of homology with Cu,Zn SODs (Schmidt et al., 1999), the putative protein lacks the Cys-X-X-Cys pattern typical for copper chaperones (Harrison et al., 1999). The C-terminal half of the protein shows an abundance of serine and threonine. These residues are typical sites of post-translational modifications such as O-glycosylsation and phosphorylation. Many secreted proteins are O-glycosylated; core proteins of proteoglycans such as mucin contain extensive clusters of serines and threonines which are attached to oligosaccharide chains. The serine and threonine-rich nature of *cpsod-ish*, in combination with the presence of a putative signal peptide for secretion, indicates that this protein may interact with cell wall components. Interestingly, promotor analysis shows two putative binding sites for a transcription factor in yeast involved in cell wall biosynthesis. As glycoproteins are often involved in intracellular communication, it is interesting that this protein seems to be most highly expressed during the earliest phase of infection.

The appearance of a similar, as of yet unclassified protein in the non-pathogenic fungus *Neurospora crassa* indicates that *cpsod-ish* may have a function which is not only related to pathogenicity. The large amount of putative binding sites for heat shock factors (HSFs) in the *cpsod-ish* promotor may be relevant for stress-mediated gene induction; for instance, in one yeast strain, resistance to toxic metals is conferred by the constitutive activation of the yeast metallothionein *cup1* via HSF1 (Sewell et al., 1995). Heat shock factors may also be involved in transcriptional control during differentiation. In mammalian cells, some of these highly conserved factors, such as HSF2, are dispensable for the stress response but crucial for differentiation processes (Pirkkala et al., 2001). A link between the oxidative stress response and *cpsod-ish* is provided by the presence of a putative binding site for the H_2O_2-induced transcription factor CPTF-1 in the promotor.

4.3.3 Could the response to metals and metal-mediated oxidative stress be relevant for pathogenicity?

The differential screening with copper was initiated in order to isolate genes which respond to hydroxyl-radical mediated oxidative damage, and the significance of the transcriptional response to high amounts of transition metals *in vivo* is questionable. *In vivo* expression analysis of three genes which were induced by both iron and copper (*cpsod1*, *cph1* and *cpdh1*) do not show a common

induction during any specific phase which could be correlated with elevated exposure to these metals *in planta*. However, the study of three genes can hardly be conclusive; furthermore, a PCR-based expression analysis will not allow detection of induction from a strong basal expression (as seems to be the case for *cpsod1* and *cph1*).

Most research concerning the role of metals in host-pathogen interactions involves iron rather than copper. Whereas the enrichment of the atmosphere with oxygen led to a dramatic decrease of iron bioavailability, as oxidised iron (FeIII) is insoluble, the same phenomenon rendered copper soluble and more easily assimilated (Crichton and Pierre, 2001). Thus, competition for available iron is an important aspect of growth, and the focal point of research in this field (Howard, 1999). Although the ability of transition metals to potentiate oxidative stress in living tissue is well documented, it is not known if secretion of metals is a mechanism used to exacerbate AOS during pathogenic interactions. When the correlation between possession of a periplasmatic Cu,Zn SOD and increased virulence of *Salmonella typhimurium* species was drawn, the investigators suggested that increased susceptibility to phagocyte superoxide could lessen viability (Fang et al., 1999). Interestingly, bacteria lacking this enzyme were shown to be susceptible to H_2O_2 rather than superoxide, and only in combination with extracellular iron (Strohmeier-Gort et al., 1999). The relevance of this finding for virulence has yet to be shown. Deletion of a gene encoding an iron siderophore lessened the ability of the necrotrophic phytopathogen *Erwinia amylovora* to induce electrolyte leakage in host cells (Dellagi et al., 1998), suggesting that iron may be used by this pathogen to induce hydroxyl-radical production in its host. The evolution of multiple mechanisms for the rigid control of transition metal concentrations, as well as the metal-mediated induction of antioxidant defenses, suggests that metal toxicity is a universal threat to survival, and as thus may be employed in the battle between pathogens and their unwilling hosts.

4.4 Conclusions: AOS and beyond

General research into the role of AOS in pathogenesis indicates that these compounds can function as toxins, that they can contribute to the formation of physical barriers and that they may be involved in signal transduction.

Should the former two points be of importance in the *C. purpurea*-rye interaction, the possession of extracellular scavengers would seem to be required for rapid colonisation. The results suggest that increased concentrations of AOS in the apoplast do not damage or impede the fungus, as simultaneous deletion of both the major secreted catalase and the cell-wall associated SOD have no impact on virulence (see 4.1.4). The slight (ca. 1 d) increase in time until the first appearance of honeydew shown by strains lacking *cpsod1* (with or without additional deletion of *cpcat1*) can not be attributed

to mechanisms at work *in planta*, as axenic growth of these mutants was also slightly reduced. However, it can not be ruled out that other scavengers are able to compensate for the lack of these enzymes.

In general, the multiple nature of antioxidant pathways complicates research in this field; the targeted deletion of single enzymes rarely results in dramatic phenotypes. More promising is the simultaneous down-regulation of several enzymes by the deletion of activating transcription factors. The discovery of the H_2O_2–induced transcription factor CPTF-1 enables this approach in *C. purpurea*. Deletion of *cptf1* resulted in a significant reduction of virulence; honeydew, which was first observed 3-4 days later than on ears inoculated with the wild type, was less abundant. Furthermore, sclerotia formation was reduced and the sclerotial tissue was less firm (Joshi et al., 2002b). The downstream-acting factors which contribute to the reduction of virulence and the aberrant sclerotial morphology in these strains are not yet known. Although regulatory control via *cptf-1* has only been shown for *cpcat1*, the promotors of both *cpcat2* and *cpsod-ish* (both of which do not seem to be expressed in axenic culture) contain putative binding sites for this factor. The study of *cptf-1* deletion mutants which are complemented with single *cptf-1*-regulated genes under the control of alternative promotors could contribute to the understanding of the mechanisms behind the observed phenotypes.

Even the fact *C. purpurea* strains which lack functional CPTF-1 are still able to survive *in planta* does not necessarily indicate that AOS-scavenging is not essential for infection, as enzymes involved in the oxidative response may underlie alternative induction mechanisms. For instance, the putative multicopper oxidase, discovered in the course of differential cDNA screening, is still induced by H_2O_2 in the *cptf1* deletion mutant (Joshi et al., 2002b). Other genes, such as *cpsod1*, may respond to fluctuation in transition metal concentrations rather than oxidative toxins. Further analysis of clones such as X1 or X27a, which have metal-sensitive promotors with a low basal expression, may provide more information as to possible fluctuations of metal concentrations *in planta*.

Until now, most work involving the role of AOS in signal transduction of phytopathogen-host systems concerns the host cell only. In *C. purpurea*, the identification of an H_2O_2-induced transcriptional regulator as a virulence determinant suggests that AOS could influence the transcriptome of the pathogen as well. The effect of *cptf-1* deletion on the formation and consistency of sclerotia is interesting in conjunction with the theory of hyperoxidant-triggered morphogenetic differentiation, while deletion of *cpcat2* results in the aberrant regulation of genes involved in alkaloid production (see 4.2.3). Both results tentatively cast AOS in the role of signal effector, influencing fungal processes throughout the infection rather than just during initial colonisation.

The recent discovery that *C. purpurea* itself produces AOS in axenic culture and *in planta* (M. von den Driesch, pers. comm.) detracts still further from the oxidative burst-type hypothesis. It has been suggested that exacerbation of AOS by necrotrophic pathogens such as *Erwinia* and *Botrytis*

may ease colonisation of the host plant (Tiedemann, 1997 Dellagi et al., 1998). Although *Claviceps purpurea* is generally known as a biotroph of the rye plant, it can be seen as a necrotroph of the rye ovary, as it rapidly and completely destroys this tissue during the infection, replacing it with fungal structures. A possible hypothesis which better fits the obtained data would be that this fungus itself produces H_2O_2 in order to facilitate ovary colonisation, and produces cell wall-bound catalases (such as CATB) to protect itself from high concentrations of its own toxins. This theory would implicate secreted *cpsod1* more in the production of H_2O_2 rather than the detoxification of superoxide. In an acidic environment, the spontaneous dismutation of superoxide may render this enzyme a luxury, rather than a necessity. The relatively low substrate affinity of catalases would enable some H_2O_2 to diffuse back into the cell; there, it may be involved in triggering or modulating signal transduction pathways.

It seems puzzling that the lack of enzymes as abundantly produced as *cpcat1* and *cpsod1* should have so little effect on pathogenesis. The rye ovary represents a very specialised niche for *Claviceps*; this, along with the abundant source of nutrients supplied by the plant vascular tissue, may contribute to a high redundance of expressed proteins. The wide host range of this fungus may also result in the expression of genes which are not essential for the infection of one host, but important for infection of others. It may be that we must relinquish our belief in the indication of importance by expression, and in future research, start with phenotypes rather than genes.

5 Summary

The oxidative toxins superoxide, hydrogen peroxide and the hydroxyl radical are known as active oxygen species (AOS). As plants have harnessed the oxidative potential of these compounds to function as part of their defense arsenals (in what is known as the oxidative burst), it has been hypothesised that AOS scavenging by phytopathogens is necessary for successful pathogenesis.

The discovery that the fungal cereal pathogen *Claviceps purpurea* secretes catalases during colonisation of rye ovaries suggests that there may be AOS-mediated host defense reactions which these are designed to overcome. Furthermore, an abundance of hydrogen peroxide in the uninfected rye ovary, as well as the presence of pathogen-induced cross-linking of phenolic compounds at the ovary base (beyond which the fungus does not venture), indicates that AOS-scavengers may be essential for parasitic survival even in the absence of a typical oxidative burst.

The research presented in this thesis investigates proteins of *C. purpurea* which are involved in AOS scavenging and their significance for the pathogenesis of rye. The work is divided into three parts: the first part describes the isolation and characterisation of the *C. purpurea* homologue of a cell-wall associated Cu,Zn SOD found in the related pathogen *C. fusiformis*. The second part deals with the characterisation of a putative catalase gene. The third part describes the attempt to isolate new genes of the AOS response using copper to create oxidative stress via Fenton-mediated hydroxyl-radical production.

The existence of a cell-wall associated Cu,Zn SOD in the pathogenic *C. purpurea* strain 20-1 was determined by analyses of protein extracts from axenic cultures. The Cu,Zn SOD, forming the major SOD activity in all extracts, was present in the culture filtrate as well as in proteins extracted from the cell wall and mycelia, and could be increased by the addition of copper to the medium. Using degenerate primers directed against conserved regions of Cu,Zn SODs to amplify cDNA template, *cpsod1* was isolated. Although sequencing of the entire gene failed to uncover a signal peptide for secretion, analysis of cell-wall associated protein fractions for mycelial contamination confirmed that the Cu,Zn SOD was secreted. Northern analyses of axenic cultures indicated that this gene was induced by copper and iron, but not by direct sources of AOS, while *in planta* expression analysis showed that it was expressed throughout the course of infection. Targeted gene inactivation of *cpsod1* and analysis of the deletion mutant revealed that this gene, which corresponded to the major and cell-wall associated SOD activity of axenic cultures, was not essential for pathogenesis. A 30 % reduction of growth rate observed in axenic culture, which could be eradicated by complementation of the m

utant with *cpsod1*, correlated with a slight retardation of honeydew production observed during

parasitic growth. As no induction of complementary SOD activities could be observed in the deletion mutant either in parasitic or axenic culture, it was concluded that scavenging of superoxide via SODs is not a requirement for pathogenesis.

Sequence analysis of the putative catalase *cpcat2*, located within the gene cluster for alkaloid biosynthesis, suggested that this gene encoded a functional intracellular catalase. Analysis of axenic cultures of the pathogenic strain 20-1 failed to detect a transcript for *cpcat2*, although this gene was shown to be induced in the alkaloid production strain P1 under conditions which induced other alkaloid cluster genes. As *in planta* expression analysis of strain 20-1 indicated that *cpcat2* was expressed during pathogenesis, targeted gene inactivation was used to create a strain lacking functional *cpcat2*. Catalase activity analyses of the deletion mutant confirmed that this gene did not correspond to any of the previously identified catalases; in contrast, a new catalase isozyme was induced in the mutant strain. While pathogenicity assays showed that the *cpcat2* deletion mutant was not retarded in virulence in comparison to the wild type strain, analysis of sclerotial alkaloids showed an 8 % reduction of alkaloid content. These results indicated that while *cpcat2* is dispensable for pathogenesis it plays a novel role in the biosynthesis of alkaloids.

A search for new genes involved in the response to oxidative stress was initiated by isolating genes induced by the Fenton catalyst copper. A copper-induced cDNA library of the pathogenic strain 20-1 was differentially screened with mRNA isolated from induced and non-induced cultures. Sequencing of differentially regulated clones revealed that almost 50 % of all isolated clones contained sequences corresponding to a putative hydrophobin *cph1*. A further clone, isolated because it contained sequences of *cph1*, also contained sequences from a gene with homologies to Cu,Zn SODs. In order to differentiate clones involved in copper homeostasis from clones which could be involved in the AOS response, several clones were tested in northern analyses for induction by iron, which also functions as a Fenton catalyst, and hydrogen peroxide (the latter was done by S. Joshi). Of six clones which were induced by the inclusion of copper in the culture medium, four were also induced by iron, and three were induced by hydrogen peroxide. Three clones were selected for further characterisation: the putative hydrophobin, a putative polyol dehydrogenase, and the clone which showed homology to Cu,Zn SODs. Characterisation included sequencing of the corresponding gene, promotor analysis and *in planta* expression analysis.

In summary, while the inactivation of single AOS-scavenging enzymes did not seem to affect the ability of *C. purpurea* to infect rye, the results of this thesis suggests a broader and more complex role for AOS in the biology of phytopathogens than was originally assumed, and lay the groundwork for future investigations involving many different aspects of this intricate host-pathogen system.

6 References

- Agrios GS (1988). Plant Pathology, 3rd Edition. Academic Press, San Diego, CA.
- Akswith CC, de Silva D and Kaplan J (1996). Molecular biology of iron aquisition in *Saccharomyces cerevisiae*. Molecular Microbiology 20(1), 27-34.
- Alvarez ME (2000). Salicylic acid in the machinery of hypersensitive cell death and disease resistance. Plant Molecular Biology 44, 429-442.
- Anderson ME (1998). Glutathione: an overview of biosynthesis and modulation. Chemico-Biological Interactions 111-112, 1-14.
- Apostol I, Heinsten PF and Low PS (1989). Rapid stimulation of an oxidative burst during elicitation of cultured plant cells. Plant Physiology 90, 109-116.
- Arcamone F, Cassinelli G, Ferni G, Penco S and Pol C (1970). Ergotamine production and metabolism of *Claviceps purpurea* strain 275 FI in stirred fermentors. Canadian Journal of Microbiology 16, 923-931.
- Arntz C and Tudzynski P (1997). Identification of genes induced in alkaloid-producing cultures of *Claviceps* sp. Current Genetics 31, 357-360.
- Arthur JR (2000). The glutathione peroxidases. Cellular and Molecular Life Sciences 57, 1825-1835.
- Asada K, Kanematsu S, Okaka S and Hayakawa T (1980). Phylogenic distribution of three types of superoxide dismutase in organisms and in cell organelles. In: Chemical and Biochemical Aspects of Superoxide and Superoxide Dismutase (Bannister JV and Hill HAO, Eds.). Elsevier, New York. p.136-153.
- Augustin AJ, Hunt S, Breipohl W, Boker T and Spitznas M (1996). Influence of oxygen free radicals and free radical scavengers on the growth behaviour and oxidative tissue damage of bovine retinal pigment epithelium cells *in vitro*. Graefes Archives for Clinical and Experimental Ophthalmology 234(1), 58-63.
- Ausubel FM, Brent R, Kingston RE, Moore DD, Seidmann JG, Smith JA and Struhl K (1987). Current Protocols in Molecular Biology. John Wiley and Sons, New York, NY.
- Baier M, Bannert N, Werner A, Lang K and Kurth R (1997). Molecular cloning, sequence, expression, and processing of the interleukin 16 precursor. Proceedings of the National Academy of Science USA 94(10), 5273-5277.
- Bains KS, Bajwa GS and Singh Z (1999). Effects of indole-3-acetic acid, gibberellic acid and abscisic acid on abscission of mango fruitlets. Tropical Agriculture 76(2), 88-92.
- Baker CJ and Orlandi EW (1995). Active oxygen in plant pathogenesis. Annual Review of Phytopathology 33, 299-321.
- Baker CJ, Orlandi EW and Anderson AJ (1997). Oxygen metabolism in plant cell culture/bacteria interactions: role of bacterial concentration and H_2O_2-scavenging in survival under biological and artifical oxidative stress. Physiological and Molecular Plant Pathology 51, 401-415.
- Ballance DJ (1991). Transformation systems for filamentous fungi and an overview of fungal gene structure. In: Molecular industrial mycology: systems and applications for filamentous fungi (Leong SA and Berka RM, Eds.). Marcel Dekker, New York, NY. p.1-29.
- Bannister JV, Bannister WH and Rotilio G (1987). Aspects of the structure, function and applications of superoxide dimutase. Critical Reviews in Biochemistry and Molecular Biology 22, 111-180.
- Barra D, Bossa F, Marmocchi F, Martini F, Rigo A and Rotilio G (1979). Differential effects of urea on yeast and bovine copper, zinc superoxide dismutases, in relation to the extent of analogy of primary structure. Biochemical and Biophysical Research Communications 86, 1199-1205.
- Batinic-Haberle I, Stevens RD and Fridovich I (1999). Porphyrin-based SOD mimics. Electrospray mass spectroscopy of Mn(III) and Fe(III) isomeric tetrakis-(N-alkylpyridyl) porphyrins. Free Radical Biology & Medicine. 27(1), 18.
- Beauchamp C and Fridovich I (1971). Superoxide dismutase: improved assays and an assay applicable to acrylamide gels. Analytical Biochemistry 44, 276-287.

- Békésy N (1956). Über die vegetative und generative Übertragung von Mutterkorneigenschaften. Zeitschrift für Pflanzenzüchtung 23, 46-196.
- Belal R, Momenteau M and Meunier B (1989). Why an oxygen and not a nitrogen atom as proximal ligand in catalase? Hydrogen peroxide dismutation catalysed by synthetic iron and manganese porphyrins. New Journal of Chemistry 13, 853-862.
- Beligni MV and Lamattina L (1999). Nitric oxide counteracts cytotoxic processes mediated by reactive oxygen species in plant tissues. Planta 208, 337-344.
- Bilinski T, Krawiec Z, Liczmanski A and Litwinska J (1985). Is hydroxyl radical generated by the Fenton reaction in vivo? Biochemical and Biophysical Research Communications 130(2), 533-539.
- Binder M, Schanz M and Hartig A (1991). Vector-mediated overexpression of catalase A in the yeast *Saccharomyces cerevisiae* induces inclusion body formation. European Journal of Cell Biology 54(2), 305-312.
- Binet R, Letoffe S, Ghigo JM, Delepelaire P and Wandersman C (1997). Protein secretion by Gram-negative bacterial ABC exporters - a review. Gene 192(1), 7-11.
- Birnboim HC and Doly J (1979). A rapid alkaline extraction procedure for screening recombinant plasmid DNA. Nucleic Acids Research 7(6), 1513-1523.
- Blee KA, Jupe SC, Richard G, Zimmerlin A, Davies DR and Bolwell GP (2001). Molecular identification and expression of the peroxidase responsible for the oxidative burst in French bean (*Phaseolus vulgaris* L.) and related members of the gene family. Plant Molecular Biology 47(5), 607-620.
- Bliska J (1996). How pathogens exploit interactions mediated by SH3 domains. Chemical Biology 3(1), 7-11.
- Bolwell GP (1996). Free radical processes in plants (colloquium, 657th meeting Aberdeen). Biochemical Society Transactions 24(2), 438-442.
- Bolwell GP and Wojtaszek P (1997). Mechanisms for the generation of reactive oxygen species in plant defence - a broad perspective. Physiological and Molecular Plant Pathology 51, 347-366.
- Bolwell GP, Butt VS, Davies DR and Zimmerlin A (1995). The origin of the oxidative burst in plants. Free Radical Research 23(6), 517-532.
- Bordo D, Djinović K and Bolognesi M (1994). Conserved patterns in the Cu,Zn superoxide dismutase family. Journal of Molecular Biology 238, 366-386.
- Borghouts C and Osiewacz HD (1998). GRISEA, a copper-modulated transcription factor from *Podospora anserina* involved in senescence and morphogenesis, is an ortholog of MAC1 in *Saccharomyces cerevisiae*. Molecular and General Genetics 260(5), 492-502.
- Bove FJ (1970). The Story of Ergot. S. Karger, Basel.
- Boveris A and Chance B (1973). The mitochondrial generation of hydrogen peroxide. General properties and effect of hyperbaric oxygen. Biochemical Journal 134(3), 707-716.
- Bradley DJ, Kjellbom P and Lamb CJ (1992). Elicitor- and wound-induced oxidative cross-linking of a proline-rich plant cell wall protein: a novel, rapid defense response. Cell 70(1), 21-30.
- Brakhage AA, Andrianopoulos A, Kato M, Steidl S, Davis MA, Tsukagoshi N and Hynes MJ (1999). HAP-Like CCAAT-binding complexes in filamentous fungi: implications for biotechnology. Fungal Genetics and Biology 27(2-3), 243-252.
- Brisson LF, Tenhaken R and Lamb CJ (1994). Function of oxidatrive cross-linking of cell wall structural proteins in plant disease resistance. Plant Cell 6, 1703-1712.
- Brockman B, Smit R and Tudzynski P (1992). Characterization of an extracellular β-1,3-glucanase of *Claviceps purpurea*. Physiological and Molecular Plant Pathology 48, 251-275.
- Bucher P (1990). Weight matrix descriptions of four eukaryotic RNA polymerase II promoter elements derived from 502 unrelated promoter sequences. Journal of Molecular Biology 212(4), 563-578.
- Bucher P and Bairoch A (1994). A generalized profile syntax for biomolecular sequences motifs and its function in automatic sequence interpretation. In: ISMB-94; Proceedings 2nd International Conference on Intelligent Systems for Molecular Biology (Altman R, Brutlag D, Karp P, Lathrop R and Searls D, Eds.). AAAIPress, Menlo Park, CA. p.53-61.

- Buettner GR (1993). The pecking order of free radicals and antioxidants: lipdid peroxidation, α-tocopherol and ascorbate. Archives of Biochemistry and Biophysics 300, 535-543.
- Buonaurio R, Torre BD, and Montalbini P (1987). Soluble superoxide dismutase (SOD) in susceptible and resistant host-parasite complexes of *Phaseolus vulgaris* and *Uromyces phasioli*. Physiological and Molecular Plant Pathology 31, 173-184.
- Burge C and Karlin S (1997). Prediction of complete gene structures in human genomic DNA. Journal of Molecular Biology 268, 78-94.
- Bussink HJ and Oliver R (2001). Identification of two highly divergent catalase genes in the fungal tomato pathogen, *Cladosporium fulvum*. European Journal of Biochemistry 268(1), 15-24.
- Cabibbo A, Pagani M, Fabbri M, Rocchi M, Farmery MR, Bulleid NJ and Sitia R (2000). ERO1-L, a human protein that favors disulfide bond formation in the endoplasmic reticulum. Journal of Biological Chemistry 275(7), 4827-4833.
- Calera JA, Paris S, Monod M, Hamilton AJ, Debeaupuis JP, Diaquin M, Lopez-Medrano R, Leal F and Latge JP (1997). Cloning and disruption of the antigenic catalase gene of *Aspergillus fumigatus*. Infection and Immunity 65(11), 4718-4724.
- Cameron RK (2000). Salicylic acid and its role in plant defense responses: what do we really know? Physiological and Molecular Plant Pathology 56, 91-93.
- Carri MT, Galliazzo F., Ciriolo MR and Rotilio G (1991). Evidence for co-regulation of Cu,Zn superoxide dismutases and metallothionein gene expression in yeast through transcriptional control by copper via the ACE 1 factor. Federation of European Biochemical Societies (FEBS) Letters 278, 263-266.
- Carver TLW, Zhang L, Zeyen RJ and Robbins MP (1996). Phenolic biosynthesis inhibitors suppress adult plant resistance to *Erysiphe graminis* in oat at 20°C and 10°C. Physiological and Molecular Plant Pathology 49, 121-141.
- Causton HC, Ren B, Koh SS, Harbison CT, Kanin E, Jennings EG, Lee TI, True HL, Lander ES and Young RA (2001). Remodeling of yeast genome expression in response to environmental changes. Molecular Biology of the Cell 12(2), 323-337.
- Cenis JL (1992). Rapid extraction of fungal DNA for PCR amplification. Nucleic Acids Research 20, 2380.
- Chamnongpol S, Willekens H, Moeder W, Langebartels C, Sandermann H Jr, Van Montagu M, Inze D, Van Camp W (1998). Defense activation and enhanced pathogen tolerance induced by H_2O_2 in transgenic tobacco. Proceedings of the National Academy of Science USA 95(10), 5818-5823.
- Chang YC, Segal BH, Holland SM, Miller GF and Kwon-Chung KJ (1998). Virulence of catalase-deficient *Aspergillus nidulans* in p47(phox)-/- mice. Implications for fungal pathogenicity and host defense in chronic granulomatous disease. Journal of Clinical Investigations 101(9),1843-1850.
- Chary P and Natvig DO (1989). Evidence for three differentially regulated catalase genes in *Neurospora crassa*: effects of oxidative stress, heat shock and development. Journal of Bacteriology 171(5), 2646-2652.
- Chary P, Dillon D, Schroeder AL and Natvig DO (1994). Superoxide dismutase (sod-1) null mutants of *Neurospora crassa*: oxidative stress sensitivity, spontaneous mutation rate and response to mutagens. Genetics 137, 723-730.
- Chary P, Hallewell RA and Natvig DO (1990). Stucture, exon pattern and chromosome mapping of the gene for cytosolic copper-zinc superoxide dismutase (sod-1) from *Neurospora crassa*. Journal of Biological Chemistry 265, 18961-18967.
- Chaturvedi V, Wong B and Newman SL (1996). Oxidative killing of *Cryptococcus neoformans* by human neutrophils. Evidence that fungal mannitol protects by scavenging reactive oxygen intermediates. Journal of Immunology 156(10), 3836-3840.
- Chen SL, Wang SS, Huttermann A and Altman A (2002). Xylem abscisic acid accelerates leaf abscission by modulating polyamine and ethylene synthesis in water-stressed intact poplar. Trees - Structure and Function 16(1), 16-22.
- Chen Z, Silva H and Klessing DF (1993). Active oxygen species in the induction of plant systemic acquired resistance by salicylic acid. Science 262(5141), 1883-1886.

- Clare DA, Duong MN, Darr D, Archibald F and Fridovich I (1984). Effects of molecular oxygen on detection of superoxide radical with nitroblue tetrazolium and on activity stains for catalase. Analytical Biochemistry 140(2), 532-537.
- Clerch LB, Wright A and Massaro D (1996). Dinucleotide-binding site of bovine liver catalase mimics a catalase mRNA-binding protein domain. American Journal of Physiology 270, L790-L794.
- Clutton S (1997). The importance of oxidative stress in apoptosis. British Medical Bulletin 53(3), 662-668
- Cocco D, Calabrese L, Rigo A, Marmocchi F and Rotilio G (1981). Preparation of selectively metal-free and metal-substituted derivatives by reaction of Cu--Zn superoxide dismutase with diethyldithiocarbamate. Biochemical Journal 199(3), 675-680.
- Corbett K, Dickerson AG and Mantle PG (1974). Metabolic studies on *Claviceps purpurea* during parasitic development on rye. Journal of General Microbiology 84, 39-58.
- Crapo JD, Oury T, Rabouille C, Slot JW and Chang LY (1992). Copper,zinc superoxide dismutase is primarily a cytosolic protein in human cells. Proceedings of the National Academy of Science USA 89(21), 10405-10409.
- Crichton RR, Pierre JL (2001). Old iron, young copper: from Mars to Venus. Biometals 14(2), 99-112.
- Culotta VC and Hamer DH (1989). Fine mapping of a mouse metallothionein gene metal response element. Molecular and Cellular Biology 9(3), 1376-1380.
- Culotta VC, Joh HD, Lin SJ, Slekar KH and Strain J (1995). A physiological role for *Saccharomyces cerevisiae* copper/zinc superoxide dismutase in copper buffering. Journal of Biological Chemistry 270(50), 29991-29997.
- Czapski G (1984). On the use of $^{\cdot}OH$ scavengers in biological systems. Israel Journal of Chemistry 24, 29-32.
- Dameron CT and Harrison MD (1998). Mechanisms for protection against copper toxicity. American Journal of Clinical Nutrition 67(5), 1091S-1097S.
- Dangl JL, Dietrich RA and Richberg MH (1996). Death don't have no mercy: cell death programs in plant-microbe interactions. Plant Cell 8, 1793-1807.
- Daub ME and Ehrenshaft M (2000). The photoactivated *Cercospora* toxin cercosporin: contributions to plant disease and fundamental biology. Annual Review of Phytopathology 38, 461-490.
- Day WA Jr, Sajecki JL, Pitts TM and Joens LA (2000). Role of catalase in *Campylobacter jejuni* intracellular survival. Infection and Immunity 68(11), 6337-6345.
- De Freitas JM, Liba A, Meneghini R, Valentine JS and Gralla EB (2000). Yeast lacking Cu-Zn superoxide dismutase show altered iron homeostasis. Role of oxidative stress in iron metabolism. Journal of Biological Chemistry 275(16), 11645-11649.
- De Groote MA, Ochsner UA, Shiloh MU, Nathan C, McCord JM, Dinauer MC, Libby SJ, Vazquez-Torres A, Xu Y and Fang FC (1997). Periplasmic superoxide dismutase protects *Salmonella* from products of phagocyte NADPH-oxidase and nitric oxide synthase. Proceedings of the National Academy of Science USA 94(25), 13997-14001.
- De Vries OMH, Moore S, Arntz C, Wessels JG and Tudzynski P (1999). Identification and characterization of a tri-partite hydrophobin from *Claviceps fusiformis*. A novel type of class II hydrophobin. European Journal of Biochemistry 262(2), 377-385.
- Dean RT, Fu S, Stocker R and Davies MJ (1997). Biochemistry and pathology of radical-mediated protein oxidation. Biochemical Journal 324(1), 1-18.
- Degousee N, Triantaphylides C and Montillet JL (1994). Involvement of oxidative processes in the signaling mechanisms leading to the activation of glyceollin synthesis in soybean (*Glycine max*). Plant Physiology 104, 945-952.
- Dellagi A, Brisset MN, Paulin JP and Expert D (1998). Dual role of desferrioxamine in *Erwinia amylovora* pathogenicity. Molecular Plant Microbe Interactions 11(8), 734-742.
- Delledonne M, Zeier J, Marocco A, Lamb C (2001). Signal interactions between nitric oxide and reactive oxygen intermediates in the plant hypersensitive disease resistance response. Proceedings of the National Academy of Science USA 98(23), 13454-13459
- Devlin WS and Gustine DL (1992). Involvement of the oxidative burst in phytoalexin accumulation and the hypersensitive reaction. Plant Physiology 100, 1189-1195.

- Diaz A, Rangel P, Montes de Oca Y, Lledías F and Hansberg W (2001). Molecular and kinetic study of catalase-1, a durable large catalase of *Neurospora crassa*. Free Radicals in Biology and Medicine 31(11), 1323-1333.
- Dodou E and Treisman R (1997). The *Saccharomyces cerevisiae* MADS-box transcription factor Rlm1 is a target for the Mpk1 mitogen-activated protein kinase pathway. Molecular and Cellular Biology 17(4), 1848-1859.
- Doke N (1983). Generation of superoxide anion by potato tuber protoplasts during the hypersensitive response to hyphal wall components of *Phytophthora infestans* and specific inhibition of the reaction by suppressors of hypersensitivity. Physiological and Molecular Plant Pathology 23, 359-367.
- Dolezal J, Klausen KS and Langmyhr FJ (1973). Studies in the complex formation of metal ions with sugars. I. The complex formation of cobalt(II), cobalt(3), copper(II) and nickel(II) with mannitol. Analytica Chimica Acta 63(1), 71-77.
- Drauschke B (1999). Cytologische und cytochemische Analysen zur Bedeutung der Superoxiddismutase des Mutterkornpilzes *Claviceps purpurea* unter Berücksichtigung defizienter Mutanten. Schriftliche Hausarbeit in Rahmen der ersten Staatsprüfung. Westfälische Wilhems-Universität Münster.
- Dumas B, Freyssinet G and Pallett K (1995). Tissue-specific expression of germin-like oxalate oxidase during development and fungal infection of barley seedlings. Plant Physiology 107, 1091-1096.
- Düvell A, Hessberg-Stutzke H, Oeser B, Rogmann-Backwinkel P and Tudzynski P (1988). Structural and functional analysis of mitochondrial plasmids in *Claviceps purpurea*. Molecular and General Genetics 214(1), 128-134.
- Dwyer SC, Legendre L, Low PS and Leto TL (1996). Plant and human neutrophil oxidative burst complexes contain immunologically related proteins. Biochima et Biophysica Acta 1289(2), 231-237.
- Elstner EF, Osswald W and Schneider I (Eds.) (1996). Phytopathologie: allgemeine und biochemische Grundlagen. Spektrum, Akademischer Verlag, Heidelberg, Berlin, Oxford. p.218-220.
- Emri T, Pocsi I and Szentirmai A (1997). Glutathione metabolism and protection against oxidative stress caused by peroxides in *Penicillium chrysogenum*. Free Radical Biology and Medicine 23(5), 809-814.
- Emri T, Pocsi I and Szentirmai A (1999). Analysis of the oxidative stress response of *Penicillium chrysogenum* to menadione. Free Radical Research 30(2), 125-132.
- Esser K and Tudzynski P (1978). Genetics of the ergot fungus *Claviceps purpurea*. I. Proof of a monoecious life-cycle and segregation patterns for mycelial morphology and alkaloid production. Theoretical and Applied Genetics 53, 145-149.
- Falquet L, Pagni M, Bucher P, Hulo N, Sigrist CJ, Hofmann K and Bairoch A (2002). The PROSITE database, its status in 2002. Nucleic Acids Research 30, 235-238.
- Fang FC, De Groote MA, Foster JW, Bäumler AJ, Ochsner U, Testerman T, Bearson S, Giárd J, Xu Y, Cambell G, and Laessig T (1999). Virulent *Salmonella typhimurium* has two periplasmatic Cu,Zn-superoxide dismutases. Proceedings of the National Academy of Science USA 96, 7502-7507.
- Faniello MC, Bevilacqua MA, Condorelli G, de Crombrugghe B, Maity SN, Avvedimento VE, Cimino F and Costanzo F (1999). The B subunit of the CAAT-binding factor NFY binds the central segment of the co-activator p300. Journal of Biological Chemistry 274(12), 7623-7626.
- Fauth M, Merten A, Hahn MG, Jeblick W and Kauss H (1996). Competence for elicitation of H_2O_2 in hypocotyls of cucumber is induced by breaching the cuticle and is enhanced by salicylic acid. Plant Physiology 110, 347-354.
- Fenton HJH (1894). Oxidation of tartaric acid in the presence of iron. Journal of the Chemical Society 65, 899-905.
- Finkelstein RR, Tenbarge KM, Shumway JE and Crouch ML (1985). Role of ABA in maturation of rapeseed embryos. Plant Physiology 78, 630-636.
- Fita I and Rossmann MG (1985). The active centre of catalase. Journal of Molecular Biology 185(1), 21-37.
- Forsburg SL and Guarente L (1989). Identification and characterization of HAP4: a third component of the CCAAT-bound HAP2/HAP3 heteromer. Genes and Development 3(8), 1166-1178.

- Fowler T, Rey MW, Vaha-Vahe P, Power SD and Berka RM (1993). The catR gene encoding a catalase from *Aspergillus niger*: primary structure and elevated expression through increased gene copy number and use of a strong promoter. Molecular Microbiology 9(5), 989-998.
- Fraaije MW, Roubroeks HP, Hagen WR and Van Berkel WJ (1996). Purification and characterization of an intracellular catalase-peroxidase from *Penicillium simplicissimum*. European Journal of Biochemistry 235(1-2), 192-198.
- Freytag S, Arabatzis N, Hahlbrock K, and Schmelzer E (1994). Reversible cytoplasmic rearrangements precede wall apposition, hypersensitive cell death and defense-related gene activation in potato/*Phytophthora infestans* interactions. Planta 194, 123-135
- Fridovich I (1970). Quantitative aspects of the production of superoxide anion radical by milk xanthine oxidase. Journal of Biological Chemistry 245(16), 4053-4057.
- Fridovich I (1986). Overview: biological sources of $O_2^{\cdot-}$. Methods in Enzymology 105, 59-61.
- Fridovich I (1995). Superoxide radical and superoxide dismutases. Annual Review of Biochemistry 64, 97-112.
- Gaffney T, Friedrich L, Vernooij B, Negrotto D, Nye G, Uknes S, Ward E, Kessmann H and Ryals J (1993). Requirement of salicylic acid for the induction of systemic aquired resistance. Science 261, 754-756.
- Gancedo J (1998). Yeast carbon catabolite repression. Microbiology and Molecular Biology Reviews 62, 334-361.
- Gardner PR and Fridovich I (1991). Superoxide sensitivity of the *Escherichia coli* aconitase. Journal of Biological Chemistry 266(29), 19328-19333.
- Garre V, Müller U and Tudzynski P (1998b). Cloning, characterisation and targeted disruption of *cpcat1*, coding for an *in planta* secreted catalase of *Claviceps purpurea*. Molecular Plant Microbe Interactions 11(8), 772-783.
- Garre V, Tenberge KB and Tudzynski P (1998a). Secretion of a fungal extracellular catalase by *Claviceps purpurea* during infection of rye: putative role in pathogenicity and supression of host defense. Phytopathology 88(8), 744-753.
- Georgiou CD and Petropoulou KP (2001). Role of erythroascorbate and ascorbate in sclerotial differentiation in *Sclerotinia sclerotiorum*. Mycological Research 105(11), 1364-1370.
- Georgiou CD, Tairis N and Sotiropoulou A (2000). Hydroxyl radical scavengers inhibit sclerotial differentiation and growth in *Sclerotinia sclerotiorum* and *Rhizoctonia solani*. Mycological Research 104(10), 1191-1196.
- Georgiou CD, Zervoudakis G, Tairis N and Kornaros M (2001). Beta-carotene production and its role in sclerotial differentiation of *Sclerotium rolfsii*. Fungal Genetics and Biology 34(1), 11-20.
- Getzoff ED, Tainer JA, Stempien MM, Bell GI and Hallewell RA (1989). Evolution of copper zinc superoxide dismutase and the Greek key β-barrel structural motif. Protein 5, 322-336.
- Getzoff ED, Tainer JA, Weiner PK, Kollman PA, Richardson JS and Richardson DC (1983). Electrostatic recognition between superoxide and copper, zinc superoxide dismutases. Nature 306, 287-290.
- Giedroc DP, Chen X and Apuy JL (2001). Metal response element (MRE)-binding transcription factor-1 (MTF-1): structure, function, and regulation. Antioxidants and Redox Signaling 3(4), 577-596.
- Gilchrist DG (1998). Programmed cell death in plant disease: the purpose and promise of cellular suicide. Annual Review of Phytopathology 36, 393-414.
- Giraudat J (1995). Abscisic acid signaling. Current Opinion in Cell Biology 7(2), 232-238.
- Glazener JA, Orlandi EW and Baker CJ (1996). The active oxygen response of cell suspension to incompatible bacteria is not sufficient to cause hypersensitive cell death. Plant Physiology 110, 759-763.
- Gnjec A, Fonte JA, Atwood C and Martins RN (2002). Transition metal chelator therapy--a potential treatment for Alzheimer's disease? Frontiers in Bioscience 27, d1016-1023.
- Goodwin PH, Li J and Jin S (2001). A catalase gene of *Colletotrichum gloeosporioides* f. sp. malvae is highly expressed during the necrotrophic phase of infection of round-leaved mallow, *Malva pusilla*. Federation of European Microbiological Societies (FEMS) Microbiology Letters 202(1), 103-107.

- Gorner W, Durchschlag E, Martinez-Pastor MT, Estruch F, Ammerer G, Hamilton B, Ruis H and Schuller C (1998). Nuclear localization of the C_2H_2 zinc finger protein Msn2p is regulated by stress and protein kinase A activity. Genes and Development 12(4), 586-597.
- Graden JA and Winge DR (1997). Copper-mediated repression of the activation domain in the yeast Mac1p transcription factor. Proceedings of the National Academy of Science USA 94(11), 5550-5555.
- Gralla EB and Kosman DJ (1992). Molecular genetics of superoxide dismutases in yeast and related fungi. Advances in Genetics 30, 251-319.
- Gralla EB, Thiele DJ, Silar P and Valentine JS (1991). ACE, a copper-dependent transcription factor, activates expression of the yeast copper, zinc superoxide dismutase gene. Proceedings of the National Academy of Science USA 88, 8558-8562.
- Grant CM (2001). Role of the glutathione/glutaredoxin and thioredoxin systems in yeast growth and response to stress. Molecular Microbiology 39(3), 533-541.
- Grant CM, MacIver FH and Dawes IW (1996). Glutathione is an essential metabolite required for resistance to oxidative stress in the yeast *Saccharomyces cerevisiae*. Current Genetics 29(6), 511-515.
- Greco MA, Hrab DL, Magner W and Kosman DJ (1990). Cu,Zn superoxide dismutase and copper deprivation and toxicity in *Saccharomyces cerevisiae*. Journal of Bacteriology 172, 317-325.
- Greenberg JT, Monach P, Chou JH, Josephy PD and Demple B (1990). Positive control of a global antioxidant defense regulon activated by superoxide-generating agents in *Escherichia coli*. Proceedings of the National Acadamy of Science USA 87(16), 6181-6185.
- Gregersen PL, Thordal-Christensen H, Forster H and Collinge DB (1997). Differential gene transcript accumulation in barley leaf epidermis and mesophyll in response to attack by *Blumeria graminis* f.sp. hordei (Syn. *Erysiphe graminis* f.sp. hordei). Physiological and Molecular Plant Pathology 51, 85-97.
- Gross C, Kelleher M, Vishwanath RI, Brown PO and Winge DR (2000). Identification of the copper regulon in *Saccharomyces cerevisiae* by DNA microarrays. Journal of Biological Chemistry 275(41), 32310-32316.
- Grune T (2001). Oxidative stress, aging and the proteasomal system. Biogerontology 1(1), 31-40.
- Guan LM, Zhao J and Scandalios JG (2000). *Cis*-elements and *trans*-factors that regulate expression of the maize *Cat1* antioxidant gene in response to ABA and osmotic stress: H_2O_2 is the likely intermediary signaling molecule for the response. Plant Journal 22(2), 87-95.
- Haber F and Weiss J (1934). The catalytic decomposition of hydrogen peroxide by iron salts. Proceedings of the Royal Society of London, Series A 147, 332-351.
- Halliwell B (1978). Lignin synthesis: the generation of hydrogen peroxide and superoxide by horseradish peroxidase and its stimulation by manganese (II) and phenols. Planta 140, 81-88.
- Halliwell B and Gutteridge JM (1990). Role of free radicals and catalytic metal ions in human disease: an overview. Methods in Enzymology 186, 1-85.
- Halliwell B and Gutteridge JMC (1999). Free Radicals. In: Biology And Medicine, 3rd Edition. Oxford University Press, New York. p.134-140.
- Hamalainen MM and Makinen KK (1989). Relationship between mineral metabolism and peroral consumption of sugar alcohols. Mineral and Electrolyte Metabolism 15(6), 346-352.
- Hamilton AJ and Holdom MD (1997). Biochemical comparison of the Cu,Zn superoxide dismutases of *Cryptococcus neoformans* var. *neoformans* and *Cryptococcus neoformans* var. *gattii*. Infection and Immunity 65(2), 488-494.
- Hamilton AJ, Holdom MD and Jeavons L (1996). Expression of the Cu,Zn superoxide dismutase of *Aspergillus fumigatus* as determined by immunochemistry and immunoelectron microscopy. Federation of European Microbiological Societies (FEMS) Immunology and Medical Microbiology 14(2-3), 95-102.
- Hansberg W and Aguirre J (1990). Hyperoxidant states cause microbial cell differentiation by cell isolation from dioxygen. Journal of Theoretical Biology 142(2), 201-221.
- Hansberg W, de Groot H and Sies H (1993). Reactive oxygen species associated with cell differentiation in *Neurospora crassa*. Free Radicals in Biology and Medicine 14(3), 287-293.
- Hansberg W, Michán S and Lledías F (2002). Mutation of *Neurospora crassa* catalase-3 enhances conidiation. Abstract Book, 6th European Conference on Fungal Genetics. Biology and Development Io-9.

- Harrison MD, Jones CE and Dameron CT (1999). Copper chaperones: function, structure and copper-binding properties. Journal of Biological Inorganic Chemistry 4(2), 145-153.
- Hart PJ, Balbirnie MM, Ogihara NL, Nersissian AM, Weiss MS, Valentine JS and Eisenberg D (1999). A structure-based mechanism for copper-zinc superoxide dismutase. Biochemistry 38 (7), 2167-2178.
- Hassett RF, Romeo AM and Kosman DJ (1998). Regulation of high affinity iron uptake in the yeast *Saccharomyces cerevisiae*. Role of dioxygen and Fe. Journal of Biological Chemistry 273(13), 7628-76236.
- Hippeli S and Elstner EF (1999). Transition metal ion-catalyzed oxygen activation during pathogenic processes. Federation of European Biochemical Societies (FEBS) Letters 443(1), 1-7.
- Hirai N, Yoshida R, Todoroki Y and Ohigashi H (2000). Biosynthesis of abscisic acid by the non-mevalonate pathway in plants, and by the mevalonate pathway in fungi. Bioscience Biotechnology Biochemistry 64(7), 1448-1458.
- Hjalmarsson K, Marklund SL, Engstrom A, Edlund T (1987). Isolation and sequence of complementary DNA encoding human extracellular superoxide dismutase. Proceedings of the National Academy of Science USA 84, 6340-6344.
- Hoffman A (1972). Ergot - a rich source of pharmacologically active substances. In: Plants in the Development of Modern Medicine (Swain T, Ed.). Harvard University Press, Cambridge, MA. p.235-260.
- Holdom MD, Hay RJ and Hamilton AJ (1996). The Cu,Zn superoxide dismutases of *Aspergillus flavus*, *Aspergillus niger*, *Aspergillus nidulans* and *Aspergillus terreus*: purification and biochemical comparison with the *Aspergillus fumigatus* Cu,Zn superoxide dismutase. Infection and Immunity 64(8), 3326-3332.
- Holt MR and Koffer A (2001). Cell motility: proline-rich proteins promote protrusions. Trends in Cell Biology 11(1), 38-46.
- Horiguchi H, Yurimoto H, Goh T, Nakagawa T, Kato N and Sakai Y (2001). Peroxisomal catalase in the methylotrophic yeast *Candida boidinii*: transport efficiency and metabolic significance. Journal of Bacteriology 183(21), 6372-6383.
- Howard DH (1999). Acquisition, transport, and storage of iron by pathogenic fungi. Clinical Microbiology Reviews 12(3), 394-404.
- Hückelhoven R and Kogel K (1998). Tissue-specific superoxide generation at interaction sites in resistant and susceptible near-isogenic barely lines attacked by the powderey mildew fungus (*Erysiphe graminis f. sp. hordei*).Molecular Plant-Microbe Interactions 11(4), 292-300.
- Hunt JV and Wolff SP (1991). Oxidative glycation and free radical production: a causal mechanism of diabetic complications. Free Radical Research Communication 12-13(1), 115-123.
- Hunt MD, Neuenschwander UH, Delaney TP, Weymann KB, Friederich LB, Lawton KA, Steiner HY and Ryals JA (1996). Recent advances in systemic acquired resistance research - a review. Gene 179, 89-95.
- Hurkman WJ and Tanaka CK (1996) Germin gene expression is induced in wheat leaves by powdery mildew infection. Plant Physiology 111, 735-739.
- Iiyama K, Lam TBT and Stone BA (1994). Covalent cross-links in the cell wall. Plant Physiology 104, 315-320.
- Ikegawa T, Mayama S, Nakayashiki H and Kato H (1996). Accumulation of diferulic acid during the hypersensitive response of oat leaves to *Puccinia coronata* f. sp. *avenae* and its role in the resistance of oat leaves to cell wall degrading enzymes. Physiological and Molecular Plant Pathology 48, 245-255.
- Imlay KRC and Imlay JA (1996). Cloning and analysis of sodC, encoding the copper-zinc superoxide dismutase of *Escherichia coli*. Journal of Bacteriology 178(9), 2564-2571.
- Inoue Y, Matsuda T, Sugiyama K, Izawa S and Kimura A (1999). Genetic analysis of glutathione peroxidase in oxidative stress response of *Saccharomyces cerevisiae*. Journal of Biological Chemistry 274(38), 27002-27009.
- Iqbal J and Whitney P (1991). Use of cyanide and diethyldithiocarbamate in the assay of superoxide dismutases. Free Radicals in Biology and Medcine 10(1), 69-77.
- Izawa S, Inoue Y and Kimura A (1995). Oxidative stress response in yeast: effect of glutathione on adaptation to hydrogen peroxide stress in *Saccharomyces cerevisiae*. Federation of European Biochemical Societies (FEBS) Letters 368(1), 73-76.

- Izawa S, Inoue Y and Kimura A (1996). Importance of catalase in the adaptive response to hydrogen peroxide: analysis of acatalasaemic *Saccharomyces cerevisiae*. Biochemical Journal 320(1), 61-67.
- Izawa S, Maeda K, Miki T, Mano J, Inoue Y and Kimura A (1998). Importance of glucose-6-phosphate dehydrogenase in the adaptive response to hydrogen peroxide in *Saccharomyces cerevisiae*. Biochemical Journal 330(2), 811-817.
- Jennings DB, Ehrenshaft M, Pharr DM and Williamson JD (1998). Roles for mannitol and mannitol dehydrogenase in active oxygen-mediated plant defense. Proceedings of the National Academy of Science USA 95(25), 15129-15133.
- Jennings DH (1985). Polyol metabolism in fungi. Advances in Microbial Physiology 25, 149-193.
- Jensen LT, Posewitz MC, Srinivasan C and Winge DR (1998). Mapping of the DNA binding domain of the copper-responsive transcription factor Mac1 from *Saccharomyces cerevisiae*. Journal of Biological Chemistry 273(37), 23805-23811.
- Jiang L, Maret W and Vallee BL (1998). The glutathione redox couple modulates zinc transfer from metallothionein to zinc-depleted sorbitol dehydrogenase. Proceedings of the National Academy of Science USA 95, 3483-3488.
- Jiang M and Zhang J (2001). Effect of abscisic acid on active oxygen species, antioxidative defence system and oxidative damage in leaves of maize seedlings. Plant and Cell Physiology 42(11), 1265-1273.
- Johansson MW, Holmblad T, Thornqvist PO, Cammarata M, Parrinello N and Soderhall K (1999) A cell-surface superoxide dismutase is a binding protein for peroxinectin, a cell-adhesive peroxidase in crayfish. Journal of Cell Science 112, 917-925.
- Johnson CH, Klotz MG, York JL, Kruft V and McEwen JE (2002). Redundancy, phylogeny and differential expression of *Histoplasma capsulatum* catalases. Microbiology 148(4), 1129-1142.
- Johnston RB Jr. (2001). Clinical aspects of chronic granulomatous disease. Current Opionions on Hematology 8(1), 17-22.
- Jornvall H, Persson B and Jeffery J (1987). Characteristics of alcohol/polyol dehydrogenases. The zinc-containing long-chain alcohol dehydrogenases. European Journal of Biochemistry 167(2), 195-201.
- Joseph-Horne T, Hollomon DW and Wood PM (2001). Fungal respiration: a fusion of standard and alternative components. Biochimica et Biophysica Acta 1504, 179-195.
- Joshi S, Moore S and Tudzynski P (2002a). Simultaneous targeted deletion of genes coding for the two major secreted AOS-scavenging enzymes, catalase C/D and superoxide dismutase A, has no major effect on pathogenicity. (submitted).
- Joshi S, Oeser B and Tudzynski P (2002b). CPTF1, a bZIP transcription factor of the phytopathogenic fungus Claviceps purpurea, is involved in the oxidative stress response and has an impact on host-pathogen interaction (in preparation).
- Joshi S, Oeser B and Tudzynski P. CPTF1, a bZIP transcription factor of the phytopathogenic fungus *Claviceps purpurea*, is involved in the oxidative stress response and has an impact on host-pathogen interaction (in preparation).
- Kagawa M, Murakoshi N, Nishikawa Y, Matsumoto G, Kurata Y, Mizobata T, Kawata Y and Nagai J (1999). Purification and cloning of a thermostable manganese catalase from a thermophilic bacterium. Archives of Biochemistry and Biophysics 362(2), 346-355.
- Kagi JH, Vasak M, Lerch K, Gilg DE, Hunziker P, Bernhard WR and Good M (1984). Structure of mammalian metallothionein. Environmental Health Perspectives 54, 93-103.
- Karpinska B, Karlsson M, Schinkel H, Streller S, Suss KH, Melzer M and Wingsle G (2001). A novel superoxide dismutase with a high isoelectric point in higher plants. expression, regulation, and protein localization. Plant Physiology 126(4), 1668-1677.
- Kauss H and Jeblick W (1995). Pretreatment of parsley suspension-cultures with salicylic-acid enhances spontaneous and elicited production of hydrogen peroxide. Plant Physiology 108, 1171-1178.
- Kawasaki L and Aguirre J (2001). Multiple catalase genes are differentially regulated in *Aspergillus nidulans*. Journal of Bacteriology 183(4),1434-1440.

- Kawasaki L, Wysong D, Diamond R and Aguirre J (1997). Two divergent catalase genes are differentially regulated during *Aspergillus nidulans* development and oxidative stress. Journal of Bacteriology 179(10), 3284-3292.
- Kehrer JP (2000). The Haber-Weiss reaction and mechanisms of toxicity. Toxicology 149, 43-50.
- Keller NP and Hohn TM (1997). Metabolic pathway gene clusters in filamentous fungi. Fungal Genetics and Biology 21, 17-29.
- Keller U (1983). Highly efficient mutagenesis of *Claviceps purpurea* by using protoplasts. Applied and Environmental Microbiology 46, 580-584.
- Keller U (1999). Biosynthesis of ergot alkaloids. In: Ergot, the Genus *Claviceps*. In: Medicinal and Aromatic Plants - Industrial Profiles (Křen V and Cvak L, Eds.). Harwood Academic Publishers, New York, NY. p. 95-163.
- Keller U and Tudzynski P (2002). Ergot Alkaloids. In: The Mycota X. Industrial Applications (Osiewacz HD, Ed.). Springer-Verlag, Berlin, Heidelberg. p.157-181.
- Keppler LD and Baker CJ (1989). $O_2^{\cdot-}$-initiated lipid peroxidation in a bacteria-induced hypersensitive reaction in tobacco cell suspensions. Phytopathology 79, 555-562.
- Kern M, Haltrich D, Nidetzky B and Kulbe KD (1997). Induction of aldose reductase and xylitol dehydrogenase activities in *Candida tenuis* CBS 4435. Federation of European Microbiological Societies (FEMS) Microbiology Letters 149(1), 31-37.
- Kieffer F, Lherminier J, Simon-Plas F, Nicole M, Paynot M, Elmayan T and Blein JP (2000). The fungal elicitor cryptogein induces cell wall modifications on tobacco cell suspension. Journal of Experimental Botany 51(352), 1799-1811.
- Kim KA, Lee JY, Park KS, Kim MJ and Chung JH (1996). Mechanism of menadione-induced cytotoxicity in rat platelets. Toxicology and Applied Pharmacology 138(1), 12-19.
- Kim YC, Miller CD and Anderson AJ (1999). Transcriptional regulation by iron and role during plant pathogenesis of genes encoding iron- and manganese-superoxide dismutases of *Pseudomonas syringae* pv. *syringae* B728a. Physiological and Molecular Plant Pathology 55, 327-339.
- Kirchhoff H (1929). Beiträge zur Biologie und Physiologie des Mutterkornpilzes. Centralblatt für Bakteriologie Parasitenkunde und Infektionskrankheiten, Zweite Abteilung 71, 310-369.
- Kirkman HN and Gaetani GF (1984). Catalase: a tetrameric enzyme with four tightly bound molecules of NADPH. Proceedings of the National Academy of Science USA 81(14), 4343-4347.
- Klatt P, Molina EP, De Lacoba MG, Padilla CA, Martinez-Galesteo E , Barcena JA and Lamas S (1999). Redox regulation of c-Jun DNA binding by reversible S-glutathiolation. Federation of American Societies for Experimental Biology (FASEB) Journal 13(12), 1481-1490.
- Klotz MG, Klassen GR and Loewen PC (1997). Phylogenetic relationships among prokaryotic and eukaryotic catalases. Molecular Biology and Evolution 14(9), 951-958.
- Kobayashi C, Suga Y, Yamamoto K, Yomo T, Ogasahara K, Yutani K and Urabe I (1997). Thermal conversion from low- to high-activity forms of catalase I from *Bacillus stearothermophilus*. Journal of Biological Chemistry 272(37), 23011-23016.
- Kono Y and Fridovich I (1983). Isolation and characterization of the pseudocatalase of *Lactobacillus plantarum.* Journal of Biological Chemistry 258(10), 6015-6019.
- Kontush A (2001). Amyloid-beta: an antioxidant that becomes a pro-oxidant and critically contributes to Alzheimer's disease. Free Radical Biology and Medicine 31(9), 1120-1131
- Koppenal WH, Butler J and van Leeuwen JW (1978). The Haber-Weiss cycle. Photochemistry and Photobiology 28, 655-660.
- Kragler F, Langeder A, Raupachova J, Binder M and Hartig A (1993). Two independent peroxisomal targeting signals in catalase A of *Saccharomyces cerevisiae*. Journal of Cellular Biology 120(3), 665-673.
- Kuchler K and Thorner J (1992). Secretion of peptides and proteins lacking hydrophobic signal sequences: the role of adenosine triphosphate-driven membrane translocators. Endocrine Reviews 13(3), 499-514.
- Kuchler K and Thorner J(1990). Membrane translocation of proteins without hydrophobic signal peptides. Current Opinion in Cell Biology 2(4), 617-624.

- Kuge S, Jones N and Nomoto A (1997). Regulation of yAP-1 nuclear localization in response to oxidative stress. European Molecular Biology Organisation (EMBO) Journal 16(7), 1710-1720.
- Kwast KE, Burke PV and Poyton RO (1998). Oxygen sensing and the transcriptional regulation of oxygen-responsive genes in yeast. Journal of Experimental Biology 201(8), 1177-1195.
- Labbe S, Peña MM, Fernandes AR, Thiele DJ (1999). A copper-sensing transcription factor regulates iron uptake genes in *Schizosaccharomyces pombe*. Journal of Biological Chemistry 274(51), 36252-36260.
- Labbe S, Zhu Z and Thiele DJ (1997). Copper-specific transcriptional repression of yeast genes encoding critical components in the copper transport pathway. Journal of Biological Chemistry 272(25), 15951-15958.
- Lamb C and Dixon RA (1997). The oxidative burst in plant disease resistance. Annual Review of Plant Physiology and Plant Molecular Biology 48, 251-275.
- Lämmli UK (1970). Cleavage of structural proteins during the assembly of the head of bacteriophage T4. Nature 277, 680-685.
- Lapinskas P, Ruis H and Culotta V (1993). Regulation of *Saccharomyces cerevisiae* catalase gene expresssion by copper. Current Genetics 24, 388-393.
- Lapinskas PJ, Cunningham KW, Liu XF, Fink GR and Culotta VC (1995). Mutations in PMR1 suppress oxidative damage in yeast cells lacking superoxide dismutase. Molecular and Cellular Biology 15(3), 1382-1388.
- Laugé R and De Wit PJGM (1998). Fungal avirulence genes: structure and possible functions. Fungal Genetics and Biology 24, 285-297.
- Leon J, Lawton MA and Raskin I (1995). Hydrogen peroxide stimulates salicylic acid biosyntheseis in tobacco. Plant Physiology 108, 1673-1678.
- Lerch K and Schenk E (1985). Primary structure of copper-zinc superoxide dismutase from *Neurospora crassa*. Journal of Biological Chemistry 260(17), 9559-9566.
- Levine A, Tenhaken R, Dixon R and Lamb C (1994). H_2O_2 from the oxidative burst orchestrates the plant hypersensitive disease resistance response. Cell 79, 583-593.
- Levy E, Eyal Z and Hochman A (1992). Purification and characterization of a catalase-peroxidase from the fungus *Septoria tritici*. Archives of Biochemistry and Biophysics 296(1), 321-327.
- Li W and Brandriss MC (1992). Proline biosynthesis in *Saccharomyces cerevisiae*: molecular analysis of the PRO1 gene, which encodes gamma-glutamyl kinase. Journal of Bacteriology 174 (12), 4148-4156.
- Liddell S and Knox DP (1998). Extracellular and cytoplasmic Cu/Zn superoxide dismutases from *Haemonchus contortus*. Parasitology 116, 383-394.
- Linder MC, Hazegh-Azam M (1996). Copper biochemistry and molecular biology. American Journal of Clinical Nutrition 63(5), 797-811.
- Liochev SI and Fridovich I (1999). Iron and superoxide: partners in crime. International Union of Biochemistry and Molecular Biology (IUBML) Life 48(2), 157-161.
- Litzka O, Then Bergh K, Van den Brulle J, Steidl S and Brakhage AA (1999). Transcriptional control of expression of fungal beta-lactam biosynthesis genes. Antonie Van Leeuwenhoek 75(1-2), 95-105.
- Lledías F, Rangel P and Hansberg W (1999). Singlet oxygen is part of a hyperoxidant state generated during spore germination. Free Radicals in Biology and Medicine 26(11-12), 1396-1404.
- Lodi T and Guiard B (1991). Complex transcriptional regulation of the *Saccharomyces cerevisiae* CYB2 gene encoding cytochrome b2: CYP1(HAP1) activator binds to the CYB2 upstream activation site UAS1-B2. Molecular and Cellular Biology 11(7), 3762-3772.
- Löhr GW and Waller HD (1965). Glucose-6-phosphate dehydrogenase. In: Methods of Enzymatic Analysis (Bergmeyer HU, Ed.). Academic Press, New York and London. p.744-751.
- Lora JM, de la Cruz J, Benitez T, Llobell A and Pintor-Toro JA (1993). .A putative catabolite-repressed cell wall protein from the mycoparasitic fungus *Trichoderma harzianum*. Molecular and General Genetics 242, 461-466.
- Lowry OH, Rosebrough NJ, Farr AL and Randall R (1951). Protein measurement with the Folin phenol reagent. Journal of Biological Chemistry 193, 265-275.

- Lu H and Higgins VJ (1999). The effect of hydrogen peroxide on the viability of tomato cells and on the fungal pathogen *Cladosporium fulvum*. Physiological and Molecular Plant Pathology 54 (5/6), 131-143.
- Lübbe Y (2001). Molekulare Charakterisierung von Genen des Alkaloidbiosynthesewegs bei *Claviceps purpurea*. Diplomarbeit, Westfälische Wilhelms Universität, Münster.
- Luche RM, Sumrada R and Cooper TG (1990). A cis-acting element present in multiple genes serves as a repressor protein binding site for the yeast CAR1 gene. Molecular and Cellular Biology 10(8), 3884-3895.
- Lugones LG, Wösten HAB, Birkenkamp KU, Sjollema KA, Zagers J and Wessels JGH (1999). Hydrophobins line air channels in fruting boidies of *Schizophyllum commune* and *Agaricus bisporus*. Mycological Research 103, 635-640.
- Luttrell ES (1979). Host-parasite relationships and development of the ergot sclerotium in *Claviceps purpurea*. Canadian Jounal of Botany 58, 942-958.
- Mantle PG and Tonolo A (1968). Relationship between the morphology of Claviceps purpurea and the production of alkaloids. Transactions of the British Mycological Society 51, 499-505.
- Mantle PG and Nisbet LJ (1976). Differentiation of *Claviceps purpurea* in axenic culture. Journal of General Microbiology 93, 321-334.
- Marchler G, Schuller C, Adam G and Ruis H (1993). A *Saccharomyces cerevisiae* UAS element controlled by protein kinase A activates transcription in response to a variety of stress conditions. European molecular biology organisation (EMBO) Journal 12(5), 1997-2003.
- Marklund SL (1982). Human copper-containing superoxide dismutase of high molecular weight. Proceedings of the National Academy of Science USA 79(24), 7634-7638.
- Martins LJ, Jensen LT, Simon JR, Keller GL, Winge DR, Simons JR (1998). Metalloregulation of FRE1 and FRE2 homologs in *Saccharomyces cerevisiae*. Journal of Biological Chemistry 273(37), 23716-23721.
- May MJ, Hammond-Kosack KE and Jones JDG (1996). Involvement of reactive oxygen species, glutathione metabolism, and lipid peroixdation in the Cf-gene-dependent defense response of tomato cotyledons induced by race-specific elicitors of *Cladosporium fulvum*. Plant Physiology 110, 1367-1379.
- Mayfield JE and Duvall MR (1996). Anomalous phylogenies based on bacterial catalase gene sequences. Journal of Molecular Evolution 42(4), 469-471.
- McCarty DR (1995). Genetic control and integration of maturation and germination pathways in seed development. Annual Review of Plant Physiology and Plant Molecular Biology 46, 71-93.
- McClung CR (1997). Regulation of catalases in Arabidopsis. Free Radicals in Biology and Medicine 23(3), 489-496
- McCord JM and Fridovich I (1969). Superoxide dismutase- an enzymic function for erythrocuprein (hemocuprein). Journal of Biological Chemistry 244, 6049-6055.
- Mehdy MC (1994). Active oxygen species in plant defense against pathogens. Plant Physiology 105, 467-472.
- Melik-Adamyan WR, Barynin VV, Vagin AA, Borisov VV, Vainshtein BK, Fita I, Murthy MR and Rossmann MG (1986). Comparison of beef liver and Penicillium vitale catalases. Journal of Molecular Biology 188, 63-72.
- Menge M, Mukherjee J and Scheper T (2001). Application of oxygen vectors to *Claviceps purpurea* cultivation. Applied Microbiology and Biotechnology 55(4), 411-416.
- Mey G and Tudzynski P (2002b). CPMK2, an *Slt2*-homologous MAP-kinase is essential for pathogenesis of *Claviceps purpurea* on rye: evidence for a second conserved pathogenesis-related MAP-kinase cascade in phytopathogenic fungi. (submittedb).
- Mey G, Oeser B, Lebrun MH and Tudzynski P (2002a). The biotrophic, non-appressorium-forming grass pathogen *Claviceps purpurea* needs a *Fus3*/*Pmk1* homologous mitogen-activated protein kinase for colonization of rye ovarian tissue. Molecular-Plant Microbe Interactions 15(4), 303-312.
- Miller JH (1972). Experiments in molecular genetics. Cold Spring Harbor Laboratory, Cold Spring Harbor, NY.
- Miller RA and Britigan BE (1997). Role of oxidants in microbial pathophysiology. Clinical Microbiology Reviews 10(1), 1-18.

- Moore S (1997). Biochemische und molekulargenetische Untersuchungen an hydrophobin-ähnlichen Proteinen bei *Claviceps*. Diplomarbeit, Westfälische Wilhelms Universität, Münster.
- Moore S, De Vries OMH and Tudzynski P (2002). The major Cu,Zn SOD of the phytopathogen *Claviceps purpurea* is not essential for pathogenicity. Molecular Plant Pathology 3(1), 9-22.
- Morel F, Doussiere J and Vignais PV (1991). The superoxide-generating oxidase of phagocytic cells: physiological, molecular and pathological aspects. European Journal of Biochemistry 201, 523-546.
- Moskvina E, Schuller C, Maurer CT, Mager WH and Ruis H (1998). A search in the genome of *Saccharomyces cerevisiae* for genes regulated via stress response elements. Yeast 14(11), 1041-1050.
- Mower RL and Hancock JG (1975a). Sugar composition of ergot honeydew. Canadian Journal of Botany 53, 2813-2825.
- Mower RL and Hancock JG (1975b). Mechanism of honeydew formation by *Claviceps* species. Canadian Journal of Botany 53, 2826-2834.
- Müller U (1997). Struktur, Expression und gezielte Inaktivierung von *cel 1*, einem vermutlich Cellobiohydrolase-codierenden Gen von *Claviceps purpurea*. Bibliotheca Mycologia 166, 1-100.
- Munkres KD (1985). The role of genes, antioxidants and antioxygenic enzymes in aging in *Neurospora*: a review. In: Superoxide Dismutases, Vol.3 (Oberly LW, Ed.). CRC Press, Boca Raton, FL. p.237-248.
- Munkres KD (1990). Purification of exocellular superoxide dismutases. In: Methods in Enzymology, Vol. 186 (Packer L and Glazer AN, Eds.). Academic Press, San Diego, CA. p.249-260.
- Mutoh N, Nakagawa CW and Yamada K (1999). The role of catalase in hydrogen peroxide resistance in fission yeast *Schizosaccharomyces pombe*. Canadian Journal of Microbiology 45(2), 125-129.
- Nakagawa CW, Yamada K and Mutoh N (2000). Role of Atf1 and Pap1 in the induction of the catalase gene of fission yeast *Schizosaccharomyces pombe*. Journal of Biochemistry 127(2), 233-238.
- Nakai K and Kanehisa M. (1992), A knowledge base for predicting protein localization sites in eukaryotic cells. Genomics 14, 897-911.
- Narendja FM, Davis MA and Hynes MJ (1999). AnCF, the CCAAT binding complex of *Aspergillus nidulans*, is essential for the formation of a DNase I-hypersensitive site in the 5' region of the amdS gene. Molecular and Cellular Biology 19(10), 6523-6531.
- Navarro RE, Stringer MA, Hansberg W, Timberlake WE and Aguirre J (1996). catA, a new *Aspergillus nidulans* gene encoding a developmentally regulated catalase. Current Genetics 29(4), 352-359.
- Nisbet LJ, Dickerson AG and Mantle PG (1977). Changes in respiration patterns of *Claviceps purpurea* during parasitic development. Transactions of the British Mycological Society 69(1), 11-14.
- Noctor G and Foyer CH (1998). Ascorbate and glutathione: keeping active oxygen under control. Annual Review of Plant Physiology and Plant Molecular Biology 49, 249-279.
- Noventa-Jordão MA, Couto RM, Goldman MHS, Aguirre J, Iyer S, Caplan A, Terenzi HF and Goldman GH (1999). Catalase activity is necessary for heat-shock recovery in *Aspergillus nidulans* germlings. Microbiology 145(11), 3229-3234.
- Nürnberger T, Nennstiel D, Jabs T, Sacks WR, Halbrock K and Scheel D (1994). High affinity binding of a fungal oligopeptide elicitor to parsley plasma membrane triggers multiple defense responses. Cell 78, 449-460.
- Obinger C, Regelsberger G, Strasser G, Burner U and Peschek GA (1997). Purification and characterization of a homodimeric catalase-peroxidase from the cyanobacterium *Anacystis nidulans*. Biochemical and Biophysical Research Communications 235(3), 545-552.
- Oeser B, Heidrich PM, Müller U, Tudzynski P and Tenberge KB (2002). Polygalacturonase is a pathogenicity factor in the *Claviceps purpurea*/rye interaction. Fungal Genetics and Biology (in press).
- Oeser B, Tenberge KB, Moore S, Mihlan M, Heidrich PM and Tudzynski P (2001). Pathogenic development of *Claviceps purpurea*. In: Molecular Biology of Fungal Development (Osiewacz H, Ed.). Marcel Dekker, New York, NY (in press).
- O'Halloran TV and Culotta VC (2000). Metallochaperones, an intracellular shuttle service for metal ions. Journal of Biological Chemistry 275(33), 25057-25060.

- Osiewacz HD and Nuber UN (1996). GRISEA, a putative copper-activated transcription factor from *Podospora anserina* involved in differentiation and senescence. Molecular and General Genetics 252(1-2),115-124.
- Otte O and Barz W (1996). The elicitor-induced oxidative burst in cultured chickpea cells drives the rapid insolublilization of two cell wall structural proteins. Planta 200, 238-246.
- Otte O and Barz W (2000). Characterization and oxidative in vitro crosslinking of an extensin-like protein and a proline-rich protein purified from chickpea cell walls. Phytochemistry 53, 1-5.
- Otte O, Pachten A, Hein F and Barz W (2001). Early elicitor-induced events in chickpea cells: functional links between oxidative burst, sequential occurrence of extracellular alklinisation and acidification, K^+/H^+ exchange and defence-related gene activation. Zeitschrift der Naturforschung 56(1), 65-76.
- Ouf MF, Gazar AA, Shehata ZE, Abdou E and Kiraly Z (1993). The effect of superoxide anion on germination and infectivity of wheat stem rust (*Puccinia graminis pers.* F. Sp. *tritici* Eriks and Henn.) uredospores. Cereal Research Communications 21, 31-37.
- Palmiter RD (1994). Regulation of metallothionein genes by heavy metals appears to be mediated by a zinc-sensitive inhibitor that interacts with a constitutively active transcription factor, MTF-1. Proceedings of the National Academy of Science USA 91(4), 1219-1223.
- Parbery DG (1996). Trophism and the ecology of fungi associated with plants. Biological Reviews 71, 473-527.
- Parmer RJ, Xi XP, Wu HJ, Helman LJ and Petz LN. Secretory protein traffic. Chromogranin A contains a dominant targeting signal for the regulated pathway. Journal of Clinical Investigations 92(2), 1042-1054.
- Pažoutová S and Tudzynski P (1999). *Claviceps* sp. PRL 1980 (ATCC 26245), 59 and Pepty 695/ch-I: their true story. Mycological Research 103(8), 1044-1048.
- Peleg Y and Metzenberg RL (1994). Analysis of the DNA-binding and dimerization activities of *Neurospora crassa* transcription factor NUC-1. Molecular and Cellular Biology 14(12), 7816-7826.
- Pena MM, Lee J and Thiele DJ (1999). A delicate balance: homeostatic control of copper uptake and distribution. Journal of Nutrition 129(7), 1251-1260.
- Peng M and Kuc J (1992). Peroxidase-generated hydrogen peroxide as a source of antifungal activity in vitro and on tobacco leaf disks. Phytopathology 82, 696–699.
- Percy ME (1984). Catalase: an old enzyme with a new role? Canadian Journal of Biochemistry and Cell Biology 62(10), 1006-1014.
- Persson B, Hallborn J, Waldfridsson M, Hahn-Hagerdal B, Keranen S, Penttila M and Jornvall H (1993). Dual relationships of xylitol and alcohol dehydrogenases in families of two protein types. Federation of European Biochemical Societies (FEBS) Letters 324(1), 9-14.
- Pinkham JL and Guarente L (1985). Cloning and molecular analysis of the HAP2 locus: a global regulator of respiratory genes in *Saccharomyces cerevisiae*. Molecular and Cellular Biology 5(12), 3410-3416
- Pirkkala L, Nykanen P and Sistonen L (2001). Roles of the heat shock transcription factors in regulation of the heat shock response and beyond. FASEB Journal 15(7), 1118-1131.
- Platford RG and Bernier CC (1975). Reaction of cultivated cereals to *Claviceps purpurea*. Canadian Journal of Plant Science 56, 51-58.
- Punt PJ, Mattern IE and van den Hondel CA (1988). A vector for *Aspergillus* transformation conferring phleomycin resistance. Fungal Genetics Newsletter 35, 25-30.
- Punt PJ, Oliver RP, Dingemanse MA., Pouwels PH and van den Hondel CA (1987). Transformation of *Aspergillus* based on the hygromycin B resistance marker from *Escherichia coli*. Gene 56(1), 117-124.
- Quandt K, Frech K, Karas H, Wingender E and Werner T (1995). MatInd and MatInspector - New fast and versatile tools for detection of consensus matches in nucleotide sequence data. Nucleic Acids Research 23, 4878-4884.
- Rae TD, Schmidt PJ, Pufahl RA, Culotta VC and O'Halloran TV (1999). Undetectable intracellular free copper: the requirement of a copper chaperone for superoxide dismutase. Science 284(5415), 805-808.
- Raha S and Robinson BH (2000). Mitochondria, oxygen free radicals, disease and ageing. Trends in Biochemical Sciences 25(10), 502-518.

- Ramil E, Agrimonti C, Shechter E, Gervais M and Guiard B (2000). Regulation of the CYB2 gene expression: transcriptional co-ordination by the Hap1p, Hap2/3/4/5p and Adr1p transcription factors. Molecular Microbiology 37(5), 1116-1132.
- Ramstad E and Gjerstad G (1955). The parasitic growth of *Claviceps purpurea* (Fries) Tulasne on rye and its relation to alkaloid formation. The Journal of the American Pharmaceutical Association 44, 741-743.
- Raskin I (1992). Role of salicylic acid in plants. Annual Review of Plant Physiology and Plant Molecular Biology 43, 439-463.
- Raynaud C, Etienne G, Peyron P, Laneelle MA and Daffe M (1998). Extracellular enzyme activities potentially involved in the pathogenicity of *Mycobacterium tuberculosis*. Microbiology 144(2), 577-587.
- Reddy CA and D'Souza TM (1994). Physiology and molecular biology of the lignin peroxidases of *Phanerochaete chrysosporium*. Federation of European Microbiological Societies (FEMS) Microbiology Reviews 13(2-3), 137-152.
- Řeháček Z (1984). Biotechnology of ergot alkaloids. Trends in Biotechnology 2(6), 166-171.
- Reymond P and Farmer EE (1998). Jasmonate and salicylate as global signals for defense gene expression. Current Opinion in Plant Biology 1(5), 404-411.
- Rhie GE, Hwang CS, Brady MJ, Kim ST, Kim YR, Huh WK, Baek YU, Lee BH, Lee JS and Kang SO (1999). Manganese-containing superoxide dismutase and its gene from *Candida albicans*. Biochimica et Biophysica Acta 1426(3), 409-419.
- Rose TM, Schultz ER, Henikoff JG, Pietrokovski S, McCallum CM and Henikoff S (1998). Consensus-degenerate hybrid oligonucleotide primers for amplification of distantly related sequences. Nucleic Acids Research 26(7), 1628-1635.
- Sambrook J, Fritsch EF and Maniatis T (1989). Molecular Cloning: A Laboratory Manual, 2nd Edition. Cold Spring Harbor Laboratory Press, Cold Spring Harbor, NY.
- Sandstrom J, Nilsson P, Karlsson K and Marklund SL (1994). 10-fold increase in human plasma extracellular superoxide dismutase content caused by a mutation in heparin-binding domain. Journal of Biological Chemistry 269(29), 19163-19166.
- Santos R, Franza T, Laporte ML, Sauvage C, Touati D and Expert D (2001). Essential role of superoxide dismutase on the pathogenicity of *Erwinia chrysanthemi* strain 3937. Molecular Plant Microbe Interactions 14(6), 758-767.
- Sarthy AV, Schopp C and Idler KB (1994). Cloning and sequence determination of the gene encoding sorbitol dehydrogenase from *Saccharomyces cerevisiae*. Gene 140(1), 121-126.
- Sasabe M, Takeuchi K, Kamoun S, Ichinose Y, Govers F, Toyoda K, Shiraishi T and Yamada T (2000). Independent pathways leading to apoptotic cell death, oxidative burst and defense gene expression in response to elicitin in tobacco cell suspension culture. European Journal of Biochemistry 267(16), 5005-5013.
- Scandalios JG (1993). Oxygen stress and superoxide dismutases. Plant Physiology 101, 7-12.
- Schmidt DE, Kempken R and Kuek U (2001). Functional analysis of promotor sequences of cephalosporin C biosynthesis genes from *Acremonium chrysogenum*: specific DNA-protein interactions and characterizationof the transcription factor PACC. Molecular Genetics and Genomics 265(3), 508-518.
- Schmidt PJ, Rae TD, Pufahl RA, Hamma T, Strain J, O'Halloran TV and Culotta VC (1999). Multiple protein domains contribute to the action of the copper chaperone for superoxide dismutase. Journal of Biological Chemistry 274(34), 23719-23725.
- Schnell N, Krems B and Entian KD (1992). The PAR1 (YAP1/SNQ3) gene of *Saccharomyces cerevisiae*, a c-jun homologue, is involved in oxygen metabolism. Current Genetics 21(4-5), 269-273
- Schouten A, Tenberge KB, Vermeer J, Stewart J, Wagemakers L, Williamson B and Van Kan JAL (2002). Functional analysis of an extracellular catalase of *Botrytis cinerea* (submitted).
- Segal AW and Abo A (1993) The biochemical basis of the NADPH-oxidase in phagocytes. Trends in Biochemical Sciences 18(2), 43-47.
- Sewell AK, Yokoya F, Yu W, Miyagawa T, Murayama T and Winge DR (1995). Mutated yeast heat shock transcription factor exhibits elevated basal transcriptional activation and confers metal resistance. Journal of Biological Chemistry 270(42), 25079-25086.

- Shardl CL, Jih-Shiou L, White JF Jr., Finkel RA and Siegel MR (1991). Molecular phylogenetic relationships of nonpathogenic grass mycosymbionts and clavicipitaceous plant pathogens. Plant Systematics and Evolution 178, 27-41.
- Shaw B and Mantle PG (1980). Parasitic differentiation of *Claviceps purpurea*. Transactions of the British Mycological Society 75(1), 117-121.
- Shen Q and Ho TH (1995). Functional dissection of an abscisic acid (ABA)-inducible gene reveals two independent ABA-responsive complexes each containing a G-box and a novel cis-acting element. Plant Cell 7(3), 295-307.
- Shima S, Netrusov A, Sordel M, Wicke M, Hartmann GC and Thauer RK (1999). Purification, characterization, and primary structure of a monofunctional catalase from *Methanosarcina barkeri*. Archives of Microbiology 171(5), 317-323
- Shima S, Sordel-Klippert M, Brioukhanov A, Netrusov A, Linder D and Thauer RK (2001). Characterization of a heme-dependent catalase from *Methanobrevibacter arboriphilus*. Applied and Environmental Microbiology 67(7), 3041-3045.
- Shirasu K, Nakajima H, Rasjasekhar VK, Dixon RA and Lamb C (1997) Salicylic acid potentiates an agonist-dependent gain control that amplifies pathogen signals in the activation of defense mechanisms. Plant Cell 9, 1-10.
- Short JM, Fernandez JM, Sorge JA and Huse WD (1988). Lambda ZAP: a bacteriophage lambda expression vector with *in vivo* excision properties. Nucleic Acids Research 16(15), 7583-7600.
- Shull S, Heintz NH, Periasamy M, Manohar M, Janssen YMW, Marsh JP and Mossman BT (1991). Differential regulation of antioxidant enzymes in response to oxidants. Journal of Biological Chemistry 266(36), 24398-24403.
- Sichel G, Corsaro C, Scalia M, Di Biolio AJ and Bomono RP (1991). In vitro scavenger activity of some flavonoids and melanins against O_2^-. Free Radical Biology and Medicine 11, 1-8.
- Simon H-U, Haj-Yehia A and Levi-Schaffer F (2000). Role of reactive oxygen species (ROS) in apoptosis induction. Apoptosis 5, 415-418.
- Singh A and Schugerl K (1992). Induction and regulation of D-xylose catabolizing enzymes in *Fusarium oxysporum*. Biochemistry International 28(3), 481-488.
- Slekar KH, Kosman DJ and Culotta VC (1996). The yeast copper/zinc superoxide dismutase and the pentose phosphate pathway play overlapping roles in oxidative stress protection. Journal of Biological Chemistry 271(46), 28831-28836.
- Smirnoff N and Cumbes Q (1989). Hydroxyl radical scavenging activity of compatible solutes. Phytochemistry 28, 1057-1060.
- Smit R and Tudzynski P (1992). Efficient transformation of *Claviceps purpurea* using pyrimidine auxotrophic mutants: cloning of the OMP decarboxylase gene. Molecular and General Genetics 234, 297-305.
- Soĉiĉ H and Gaberc-Porekar V (1992). Biosynthesis and physiology of ergot alkaloids. In: Handbook of Applied Mycology, Vol. 4, Fungal Biotechnology (Arora DK, Elander RP, Mukerji KG, Eds.). Marcel Dekker, New York, NY. p.475-515.
- Spevak W, Hartig A, Meindl P and Ruis H (1986). Heme control region of the catalase T gene of the yeast *Saccharomyces cerevisiae*. Molecular and General Genetics 203(1), 73-78.
- Srinivasan C, Liba A, Imlay JA, Valentine JS and Gralla EB (2000). Yeast lacking superoxide dismutase(s) show elevated levels of "free iron" as measured by whole cell electron paramagnetic resonance. Journal of Biological Chemistry 275(38), 29187-29192.
- Steidl S, Papagiannopoulos P, Litzka O, Andrianopoulos A, Davis MA, Brakhage AA and Hynes MJ (1999). AnCF, the CCAAT binding complex of *Aspergillus nidulans*, contains products of the hapB, hapC, and hapE genes and is required for activation by the pathway-specific regulatory gene amdR. Molecular and Cellular Biology 19(1), 99-106.
- Steinman HM (1982). Superoxide dismutases: Protein chemistry and structure-function relationships. In: Superoxide dismutases (Oberley LW, Ed.), Vol. I. CRC Press, Boca Raton, FL. p.11-68.
- Stohs SJ and Bagchi D (1995). Oxidative mechanisms in the toxicity of metal ions. Free Radical Biology and Medicine 18(2), 321-336.

- Strålin P and Marklund SL (1994). Effects of oxidative stress on expression of extracellular superoxide dismutase, CuZn-superoxide dismutase and Mn-superoxide dismutase in human dermal fibroblasts. Biochemistry 298, 347-352.
- Strohmeier-Gort A, Ferber DM and Imlay JA (1999). The regulation and role of the periplasmic copper, zinc superoxide dismutase of *Escherichia coli*. Molecular Microbiology 32(1), 179-191.
- Subramani S (1998). Components involved in peroxisome import, biogenesis, proliferation, turnover, and movement. Physiological Reviews 78(1), 171-188
- Sun HW and Plapp BV (1992) Progressive sequence alignment and molecular evolution of the Zn-containing alcohol dehydrogenase family. Journal of Molecular Evolution 34, 522-535.
- Swan DJ and Mantle PG (1991). Parasitic interactions between *Claviceps purpurea* strains in wheat and an acute necrotic host response. Mycology 95, 807–810.
- Taber WA (1985). Biology of *Claviceps*. In: Biotechnology Series, Vol. 6, Biology of Industrial Microorganisms (Demain AL and Nadine AS, Eds.). The Benjamin/Cummings Publishing Company Inc., New York, p.449-486.
- Taglialatela M, Castaldo P, Iossa S, Pannaccione A, Fresi A, Ficker E and Annunziato L (1997). Regulation of the human ether-a-gogo related gene (HERG) K+ channels by reactive oxygen species. Proceedings of the National Academy of Science USA 94(21), 11698-11703.
- Taiz L and Zeiger E (1998). Abscisic Acid. In: Plant Physiology, 2nd Edition. Sinauer Associates, Sunderland, MA. p.671-690.
- Talbot NJ, Ebbole DJ and Hamer JE (1993). Identification and characterization of MPG1, a gene involved in pathogenicity from the rice blast fungus *Magnaporthe grisea*. Plant Cell 5(11), 1575-1590.
- Talbot NJ, Kershaw MJ, Wakley GE, de Vries OMH, Wessels JGH and Hamer JE (1996). MPG1 encodes a fungal hydrophobin involved in surface interactions during infection-related development by the rice blast fungus *Magnaporthe grisea.* Plant Cell 8, 985-999.
- Tamai KT, Gralla EB, Ellerby LM, Valentine JS and Thiele DJ (1993). Yeast and mammalian metallothioneins functionally substitute for yeast copper-zinc superoxide dismutase. Proceedings of the National Academy of Science USA 90(17), 8013-8017.
- ten Have A, Tenberge KB, Benen JAE, Tudzynski P, Visser J and van Kan JAL (2002). The contribution of cell wall degrading enzymes to pathogenesis of fungal plant pathogens. (submitted).
- Tenberge KB (1999). Ergot: the genus *Claviceps*. In: Medicinal and Aromatic Plants - Industrial Profiles. (Křen V, Cvak L, eds.). Harwood Academic Press, London. p.25-56.
- Tenberge KB and Tudzynski P (1994). Early infection of rye ovaries by *Claviceps purpurea* is inter- and intracellular. Bio Engineering Supplement 10(3), 22.
- Then Bergh K and Brakhage A (1998). Regulation of the *Aspergillus nidulans* penicillin biosynthesis gene *acvA* (*pcbAB*) by amino acids: implication for involvement of transcription factor PACC. Applied and Environmental Microbiology 64, 843-849.
- Thiele DJ (1988). ACE1 regulates expression of the *Saccharomyces cerevisiae* metallothionein gene. Molecular and Cellular Biology 8(7), 2745-2752.
- Thompson JE, Legge RL, Barber RF (1987). The role of free radicals in senescence and wounding. New Phytology 105, 317-344.
- Thomson AM, Rogers JT and Leedman PJ (1999). Iron-regulatory proteins, iron-responsive elements and ferritin mRNA translation. International Journal of Biochemistry and Cell Biology 31(10), 1139-1152.
- Thordal-Christensen H, Zhang Z, Wei Y and Collinge DB (1997). Subcellular localization of H_2O_2 in plants. H_2O_2 accumulation in papillae and hypersensitive response during the barley-powdery mildew interaction. Plant Jounal 11(6), 1187-1194.
- Tiburzy R, Rogner UC, Fischer R, Beissmann B, Kreuzaler FM and Reisener HJ (1991). Detection of an elicitor on infection structures of *Puccinia graminis* using momoclonal antibodies. European Journal of Cell Biology 55(1), 174-178.
- Tiedemann AV (1997). Evidence for a primary role of active oxygen species in induction of host cell death during infection of bean leaves with *Botrytis cinerea*. Physiological and Molecular Plant Pathology 50(3), 151-66.

- Toledo I, Aguirre J and Hansberg W (1994). Enzyme inactivation related to a hyperoxidant state during conidiation of *Neurospora crassa*. Microbiology 140(9), 2391-2397.
- Toledo I, Noronha-Dutra AA and Hansberg W (1991). Loss of NAD(P)-reducing power and glutathione disulfide excretion at the start of induction of aerial growth in *Neurospora crassa*. Journal of Bacteriology 173(10), 3243-3249.
- Toledo I, Rangel P and Hansberg W (1995). Redox imbalance at the start of each morphogenetic step of *Neurospora crassa* conidiation. Archives of Biochemistry and Biophysics 319(2), 519-524.
- Toone WM and Jones N (1999). AP-1 transcription factors in yeast. Current Opinion on Genetics and Development 9 (1), 55-61.
- Toone WM, Morgan BA and Jones N (2001). Redox control of AP-1-like factors in yeast and beyond. Oncogene 20(19), 2336-2346.
- Tudzynski B and Hölter K (1998). Gibberellin biosynthetic pathway in *Gibberella fujikuroi*: evidence for a gene cluster. Fungal Genetics and Biology 25(3), 157-170.
- Tudzynski B and Sharon A (2002). Biosynthesis, biological role and application of fungal phytohormones. In: The Mycota X. Industrial Applications (Osiewacz HD, Ed.). Springer-Verlag, Berlin, Heidelberg. p.183-211.
- Tudzynski P, Correia T and Keller U (2001). Biotechnology and genetics of ergot alkaloids. Applied Microbology and Biotechnology 57, 593-605.
- Tudzynski P, Holter K, Correia T, Arntz C, Grammel N and Keller U (1999). Evidence for an ergot alkaloid gene cluster in *Claviceps purpurea*. Molecular and General Genetics 261(1), 133-141.
- Tudzynski P, Tenberge KB and Oeser B (1995). *Claviceps purpurea*. In: Diseases: Histopathological, Biochemical, Genetic and Molecular bases, Vol. II, Eukaryotes (Kohmoto D, Ed.). Pergamon, Elsevier Science Ltd, Oxford, UK. p.161-187.
- Tulasne LR (1853). Mémoire sur l'ergot des glumacées. Annales de Sciences Naturelles (Partie Botanique) 20(5), 5-56
- van de Kamp M, Driessen AJ and Konings WN (1999). Compartmentalization and transport in beta-lactam antibiotic biosynthesis by filamentous fungi. Antonie Van Leeuwenhoek 75(1-2), 41-78.
- van Engelenburg F, Smit R, Goosen T, van den Broek HWJ and Tudzynski P (1989). Transformation of *Claviceps purpurea* using a bleomycin resistance gene. Applied Microbiology and Biotechnology 30, 364-370.
- Vanacker H, Carver TLW and Foyer C (2000). Early H_2O_2 accumulation in mesophyll cells leads to induction of glutathione during the hyper-sensitive response in the barley-powdery mildew interaction. Plant Physiology 123, 1289-1300.
- Vasil V, Marcotte WR Jr, Rosenkrans L, Cocciolone SM, Vasil IK, Quatrano RS and McCarty DR (1995).Overlap of Viviparous1 (VP1) and abscisic acid response elements in the Em promoter: G-box elements are sufficient but not necessary for VP1 transactivation. Plant Cell 7(9), 1511-1518.
- Vianello A, Zancani M and Macri F (1990). Hydrogen peroxide formation and iron ion oxidoreduction linked to NADH oxidation in radish plasmalemma vesicles. Biochimie et Biophysica Acta 1023(1), 19-24.
- Vining LC (1973). Physiological aspects of alkaloid production by *Claviceps* species. In: Genetics of Industrial Microorganisms, Vol II, Actinomycetes and Fungi (Vanék Z, Hostalek S and Cudlin J, Eds.). Elsvier, New York, NY. p.405-419.
- von Heijne G (1986). A new method for predicting signal sequence cleavage sites. Nucleic Acids Research 14(11), 4683-4690.
- von Ossowski I, Hausner G and Loewen PC (1993). Molecular evolutionary analysis based on the amino acid sequence of catalase. Journal of Molecular Evolution 37(1), 71-76.
- Voß T (1996). Untersuchungen zur Gewinnung von Pathogenitätsmutanten bei *Claviceps purpurea* Diplomarbeit, Westfälische Wilhelms Universität Münster.
- Wang W and Ballatori N (1998). Endogenous glutathione conjugates: occurance and biological functions. Pharmacological Reviews 50(3), 335-355.
- Wessels JGH (1997). Hydrophobins: proteins that change the nature of the fungal surface. Advances in Microbial Physiology 38, 1-45.

- White AR, Multhaup G, Maher F, Bellingham S, Camakaris J, Zheng H, Bush AI, Beyreuther K, Masters CL and Cappai R (1999). The Alzheimers disease amyloid precursor protein modulates copper-induced toxicity and oxidative stess in primary neuronal cultures. The Journal of Neuroscience 19(21), 9170-9179.
- Wilson TM, de Lisle GW and Collins DM (1995). Effect of inhA and katG on isoniazid resistance and virulence of *Mycobacterium bovis*. Molecular Microbiology 15(6), 1009-1015.
- Winge DR, Graden JA, Posewitz MC, Martins LJ, Jensen LT and Simon JR (1997). Sensors that mediate copper-specific activation and repression of gene expression. Journal of Biological and Inorganic Chemistry 2, 2-10.
- Winkler H, Adam G, Mattes E, Schanz M, Hartig A and Ruis H (1988). Co-ordinate control of synthesis of mitochondrial and non-mitochondrial hemoproteins: a binding site for the HAP1 (CYP1) protein in the UAS region of the yeast catalase T gene (CTT1). EMBO Journal 7(6), 1799-1804.
- Winterbourn CC, Vile GF, Monteiro HP (1991). Ferritin, lipid peroxidation and redox-cycling xenobiotics. Free Radical Research Communication 12-13(1), 107-114.
- Wiser MF, Grab DJ and Lanners HN (1999). An alternate secretory pathway in *Plasmodium*: more questions than answers. In: Transport and Trafficking in the Malaria-Infected Erythrocyte, Novartis Foundation Symposium 226. John Wiley & Sons, Lt., Chichester, UK. p.199-214.
- Wojtaszek P (1997). Oxidative burst: an early plant response to pathogen infection. Biochemical Journal 322, 681-692.
- Wojtaszek P, Trethowan J, Bolwell GP (1995). Specificity in the immobilisation of cell wall proteins in response to different elicitor molecules in suspension-cultured cells of French bean (*Phaseolus vulgaris* L.). Plant Molecular Biology (6), 1075-1087.
- Worley KC, Culpepper P, Wiese BA and Smith RF (1998). BEAUTY-X: enhanced BLAST searches for DNA queries. Bioinformatics 14(10), 890-891.
- Wösten HA, Schuren FH and Wessels JG (1994b). Interfacial self-assembly of a hydrophobin into an amphipathic protein membrane mediates fungal attachment to hydrophobic surfaces. European molecular biology organisation (EMBO) Journal 13(24), 5848-5854.
- Wösten HAB (2001). Hydrophobins: multipurpose proteins. Annual Review of Microbiology 55, 625-646.
- Wösten HAB, Asgeirsdottir SA, Krook JH, Drenth JH and Wessels JG (1994a). The fungal hydrophobin Sc3p self-assembles at the surface of aerial hyphae as a protein membrane constituting the hydrophobic rodlet layer. European Journal of Cell Biology 63(1), 122-129.
- Wösten HAB, van Wetter MA, Lugones LG, van der Mei HC, Busscher HJ and Wessels JG (1999). How a fungus escapes the water to grow into the air. Current Biology 9(2), 85-88.
- Wu GS, Short BJ, Lawrence EB, Levine EB, Fitzsimmons KC and Shah DM (1995). Disease resistance conferred by expression of a gene encoding H2O2-generating glucose oxidase in transgenic potato plants. Plant Cell 7, 1357-1368.
- Wysong DR, Christin L, Sugar AM, Robbins PW and Diamond RD (1998). Cloning and sequencing of a *Candida albicans* catalase gene and effects of disruption of this gene. Infection and Immunity 66(5),1953-1961.
- Xu JR and Hamer JE (1996). MAP Kinase and cAMP signaling regulate infection structure formation and pathogenic growth in the rice blast fungus *Magnaporthe grisea*. Genes and Development 10, 2696-2706.
- Xu JR, Staiger CJ and Hamer JE (1998). Inactivation of the mitogen-activation protein kinase MPS1 in the rice blast fungus prevents penetration of host cells but allows activation of plant defense responses. Proceedings of the National Academy of Science USA 95, 12713-12718.
- Xu XQ and Pan SQ (2000). An *Agrobacterium* catalase is a virulence factor involved in tumorigenesis. Molecular Microbiology 35(2), 407-414.
- Yamaguchi-Iwai Y, Dancis A and Klausner RD (1995). AFT1: a mediator of iron regulated transcriptional control in *Saccharomyces cerevisiae*. EMBO Journal 14(6), 1231-1239.
- Yoo HY, Chang MS and Rho HM (1999). Heavy metal-mediated activation of the rat Cu/Zn superoxide dismutase gene via a metal-responsive element. Molecular and General Genetics 262, 310-313.

- Young JC and Chen ZJ (1982). Variablility in the content and composition of alkaloid found in Canadian ergot. III. Triticale and barley. Journal of Environmental Sciences and Health - Part B: Pesticides, Food contaminants and Agricultural Wastes 17(2), 93-107.
- Zámocký M and Koller F (1999). Understanding the structure and function of catalases: clues from molecular evolution and in vitro muagenesis. Progress in Biophysics and Molecular Biology 72, 19-66.
- Zhang Z, Collinge DB, and Thordal-Christensen H (1995). Germin-like oxalate oxidase, a H_2O_2-producing enzyme, accumulates in barley attacked by the powdery mildew fungus. Plant Journal 8, 139-145.
- Zhu Z, Labbe S, Pena MM and Thiele DJ (1998). Copper differentially regulates the activity and degradation of yeast Mac1 transcription factor. Journal of Biological Chemistry 273(3), 1277-1280.
- Zitomer RS and Lowry CV (1992). Regulation of gene expression by oxygen in *Saccharomyces cerevisiae*. Microbiological Reviews 56(1), 1-11.

Appendix A: Genomic Sequences

A.1 *cpsod1*

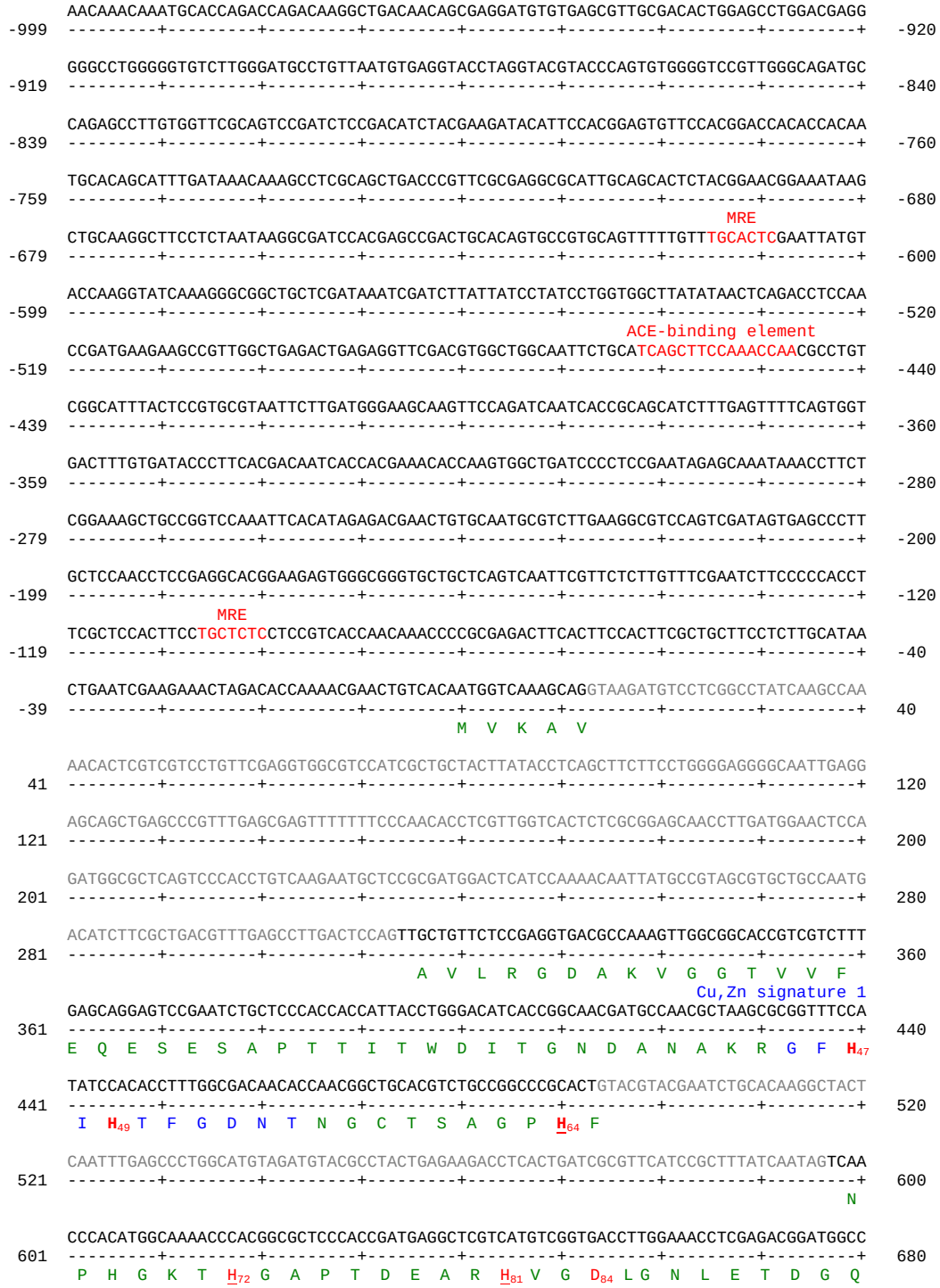

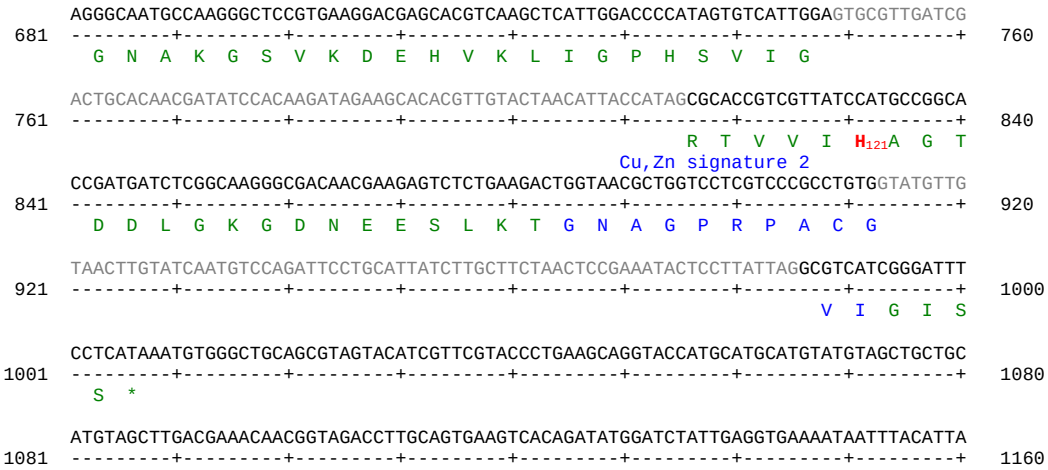

Fig. A.1: Sequences of the *cpsod1* genomic region with putative protein. Putative promotor elements are in red and labelled within the figure. The introns are shown in grey. The derived amino acid sequence is in green; PROSITE signatures for Cu,ZnSOD are in blue. Some of the most important conserved residues are shown in red; those involved in the binding of copper and zinc are in bold or are underlined, respectively (H_{64} is involved in the binding of both metals); numbers indicate sequence position.

A.2 *cpcat2*

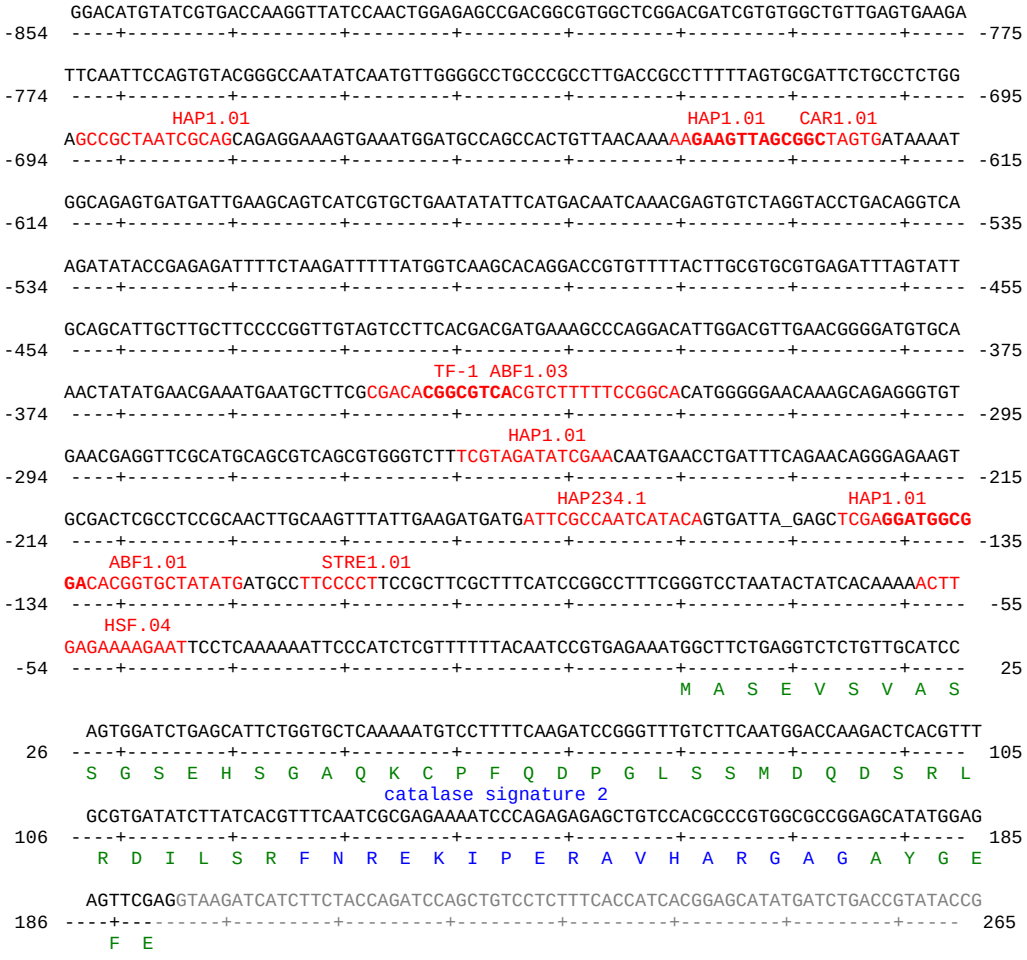

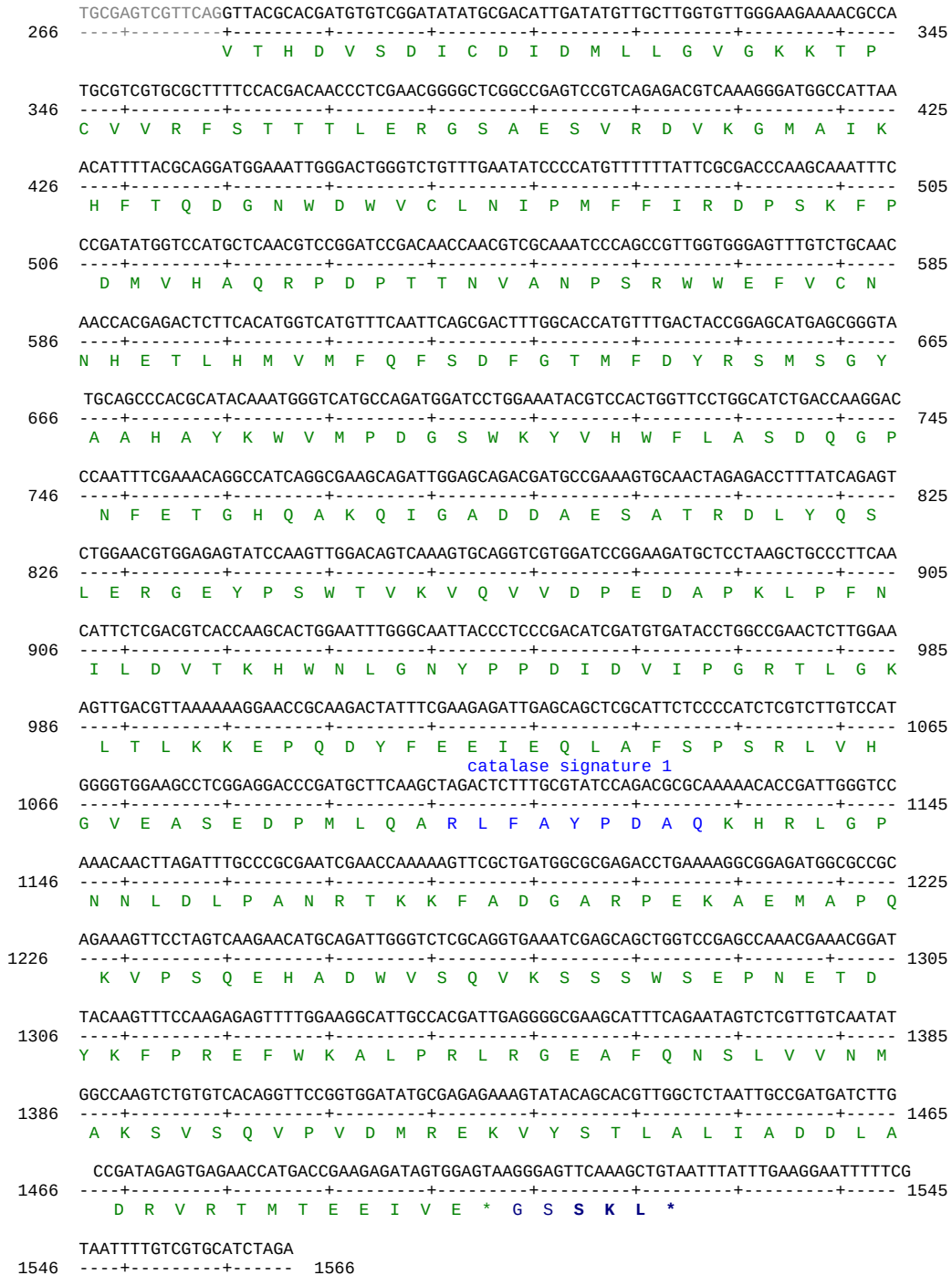

Fig. A.2: Sequences of the *cpcat2* genomic region with putative protein. Putative promotor elements are in red and labelled within the figure. Nucleotides belonging to overlapping elements are depicted in bold type. Conceptual protein sequences are in green type; PROSITE catalase signatures are in blue type (see text). The intron is shown in grey. A protein translation of the six triplets following the stop codon which contain the PTS1 signal are depicted in dark blue type (explanation in text). The adenine of the putative start codon is denominated +1.

A.3 *cph1*

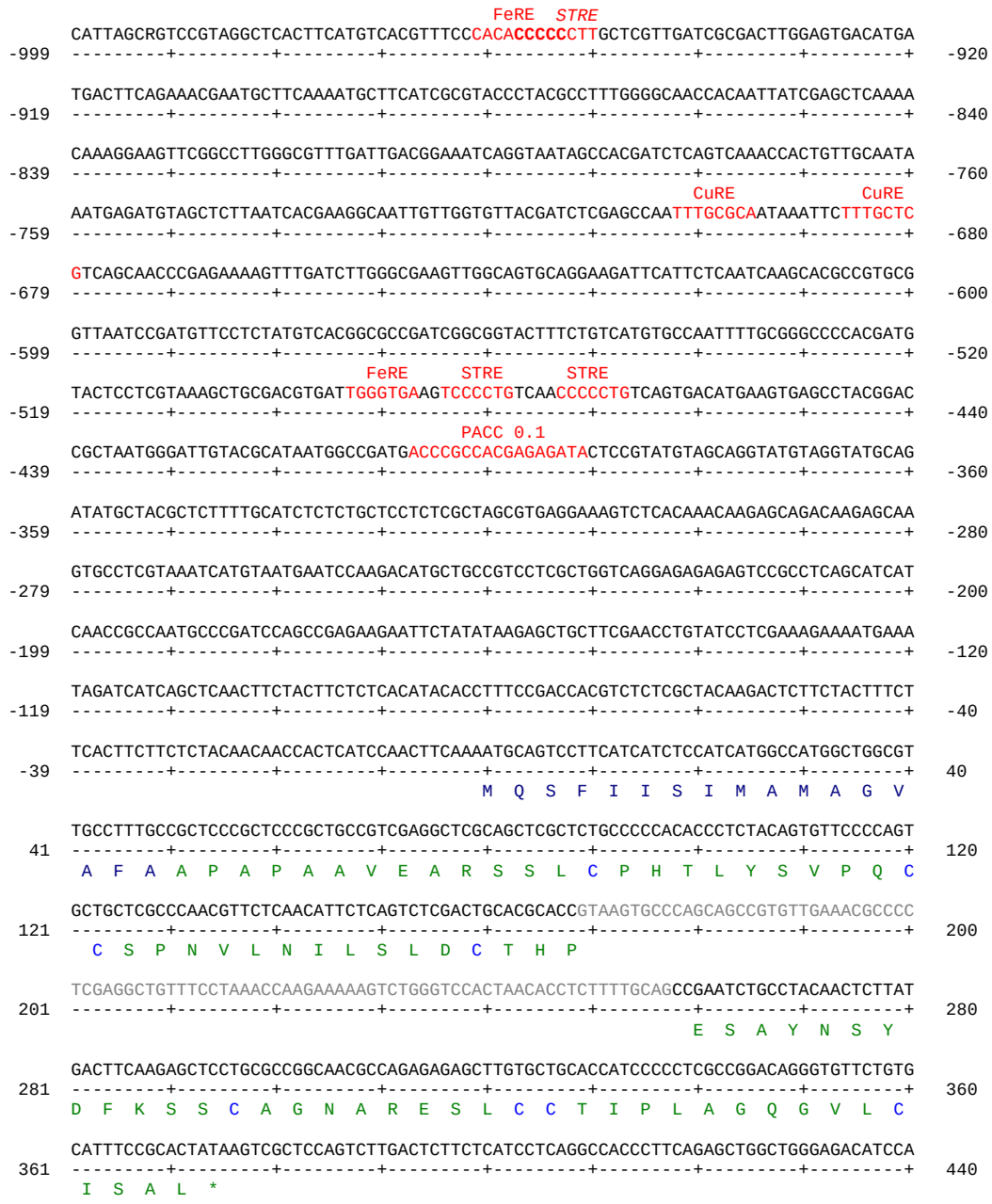

Fig. A.3 Sequence of the *cph1* genomic region with putative protein. Putative promotor elements are in red; nucleotides belonging to overlapping elements are depicted in bold type. Protein sequences are in green type; conserved cysteins are in light blue type, while the putative signal sequence for secretion is in dark blue type. The intron is shown in grey. The adenine of the putative start codon is denominated +1.

A.4 *cpdh1*

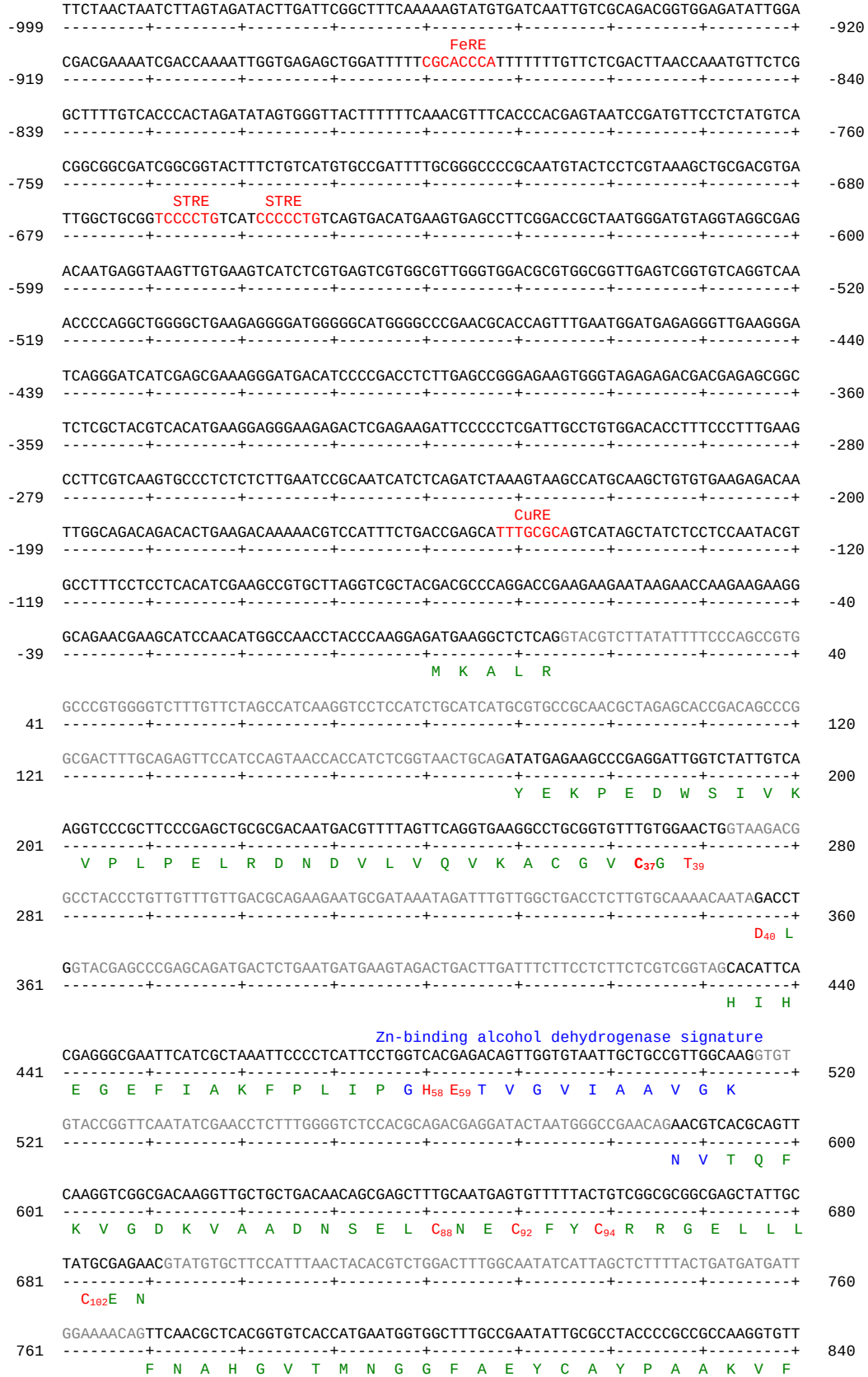
FeRE
STRE
STRE
CuRE
Zn-binding alcohol dehydrogenase signature

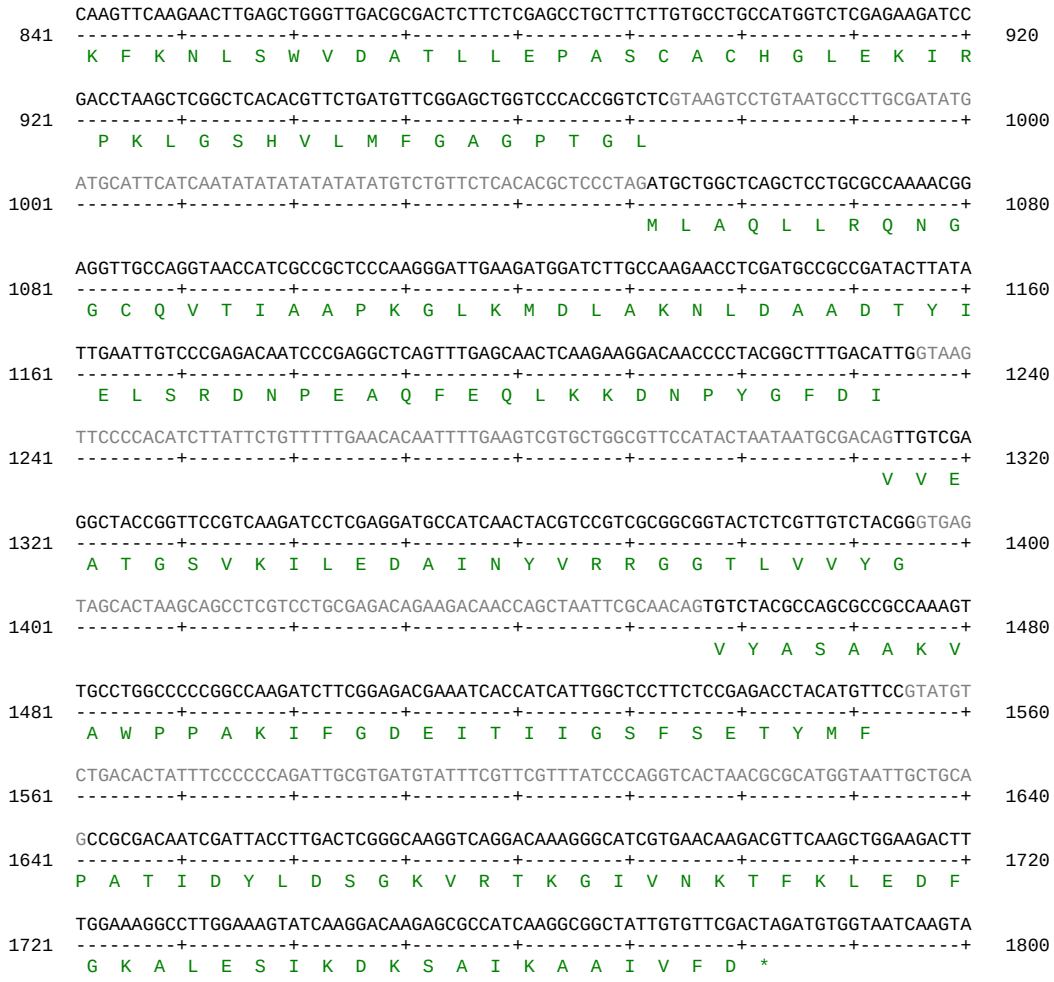

FigA.4: Sequence of the *cpdh1* genomic region with putative protein. The adenine of the putative start codon is denominated +1. Putative promotor elements are shown in red and the introns are in grey. Conceptual protein sequence is in green type while conserved residues, important for enzyme activity, are in red. The PROSITE signature for Zn-binding alcohol dehydrogenases is in blue type.

A.5 *cpsod-ish*

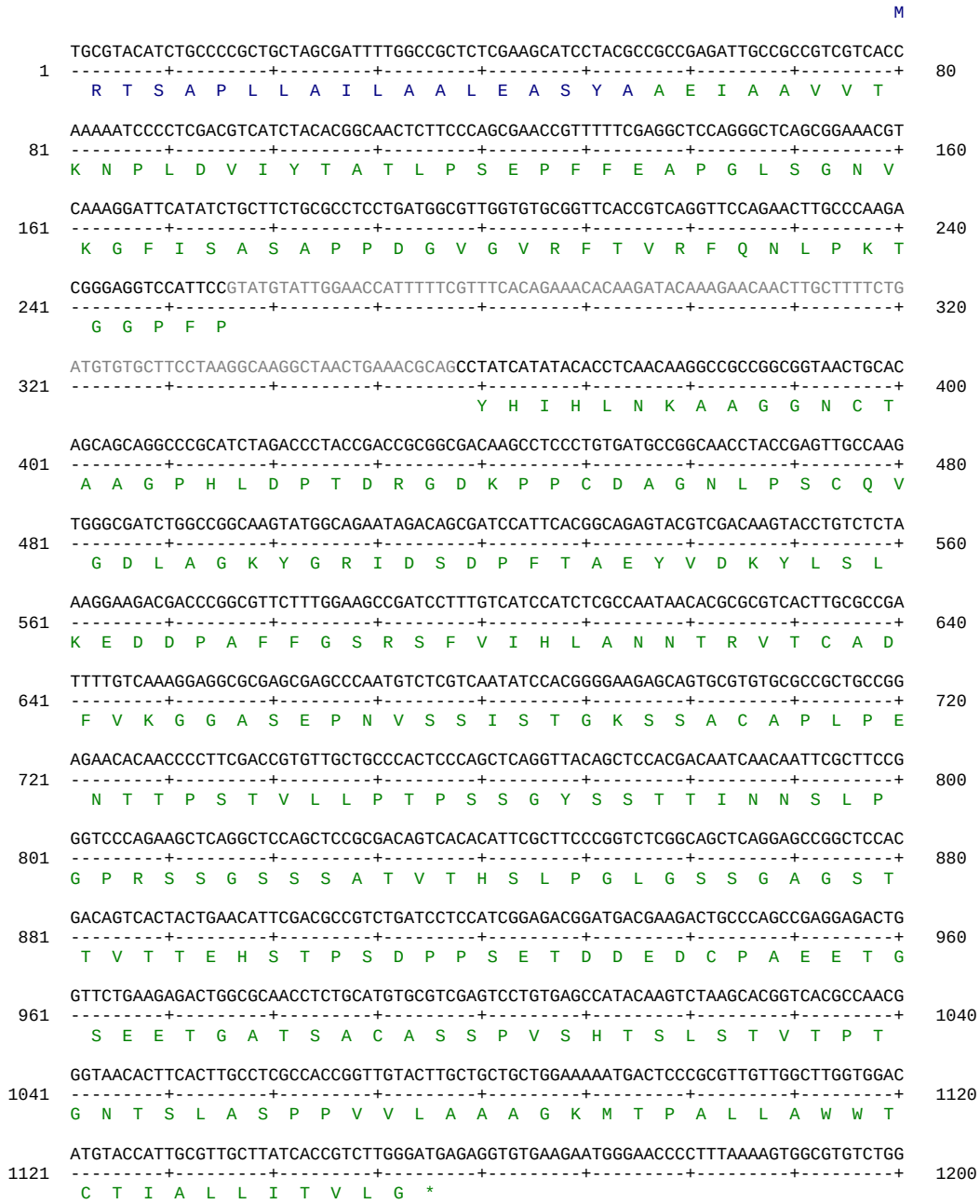

FigA.5: Sequence of the *cpsod-ish* genomic region with putative protein. The adenine of the putative start codon is denominated +1. Conceptual protein sequence is in green type, while the introns are grey. Putative promotor elements are shown in red. The putative signal peptide sequence for secretion is in blue type.

Appendix B: cDNA Sequences

In each case, the entire cDNA sequence is shown with translation of all three open reading frames. Translations which produce homology in BlastX analysis are shaded yellow, conserved residues are highlighted in red.

XA2

red: homology with D-xylose reductase from *Aspergillus niger*.

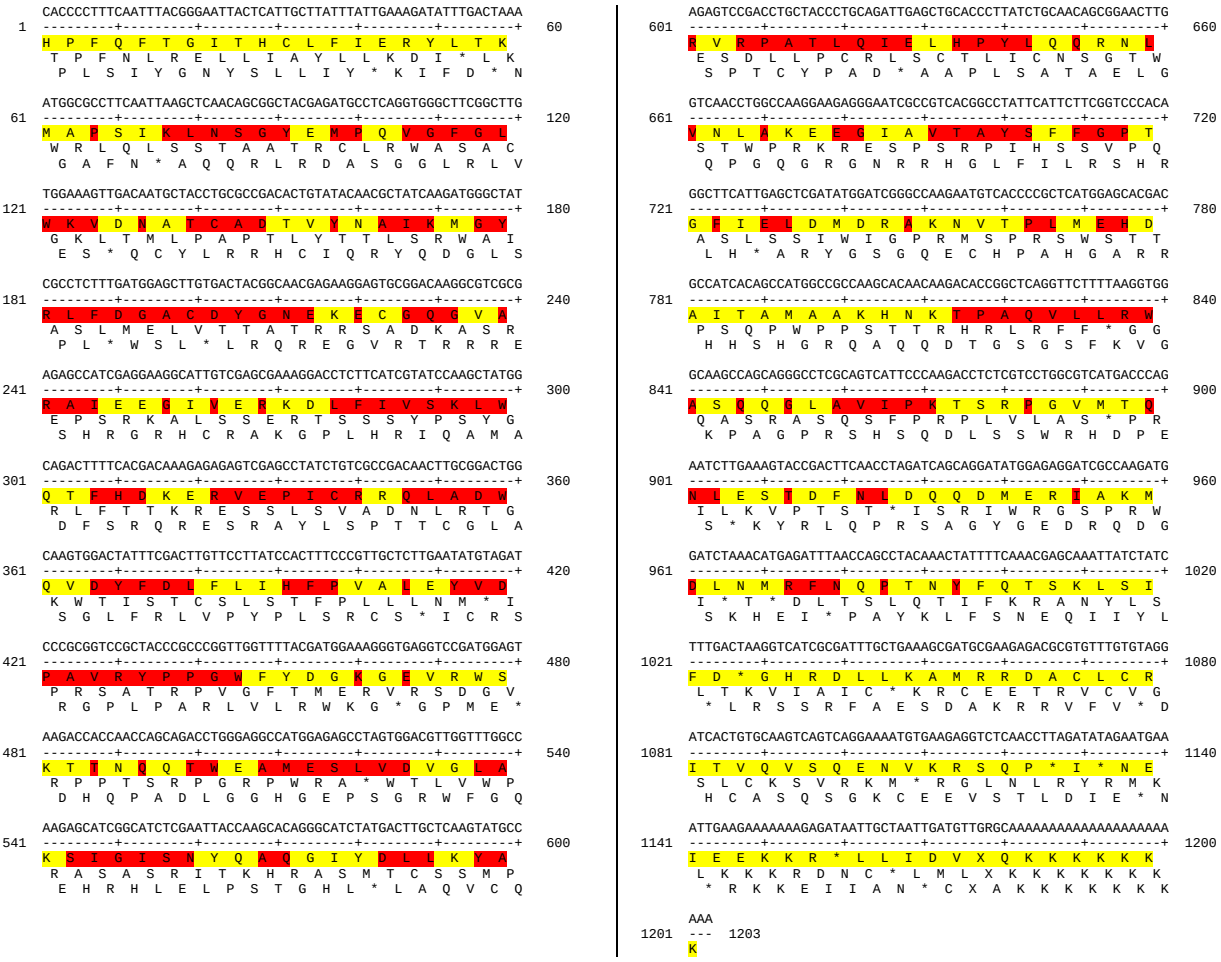

X1

red: homology to hypothetical protein B1D4.110 from *Neurospora crassa*

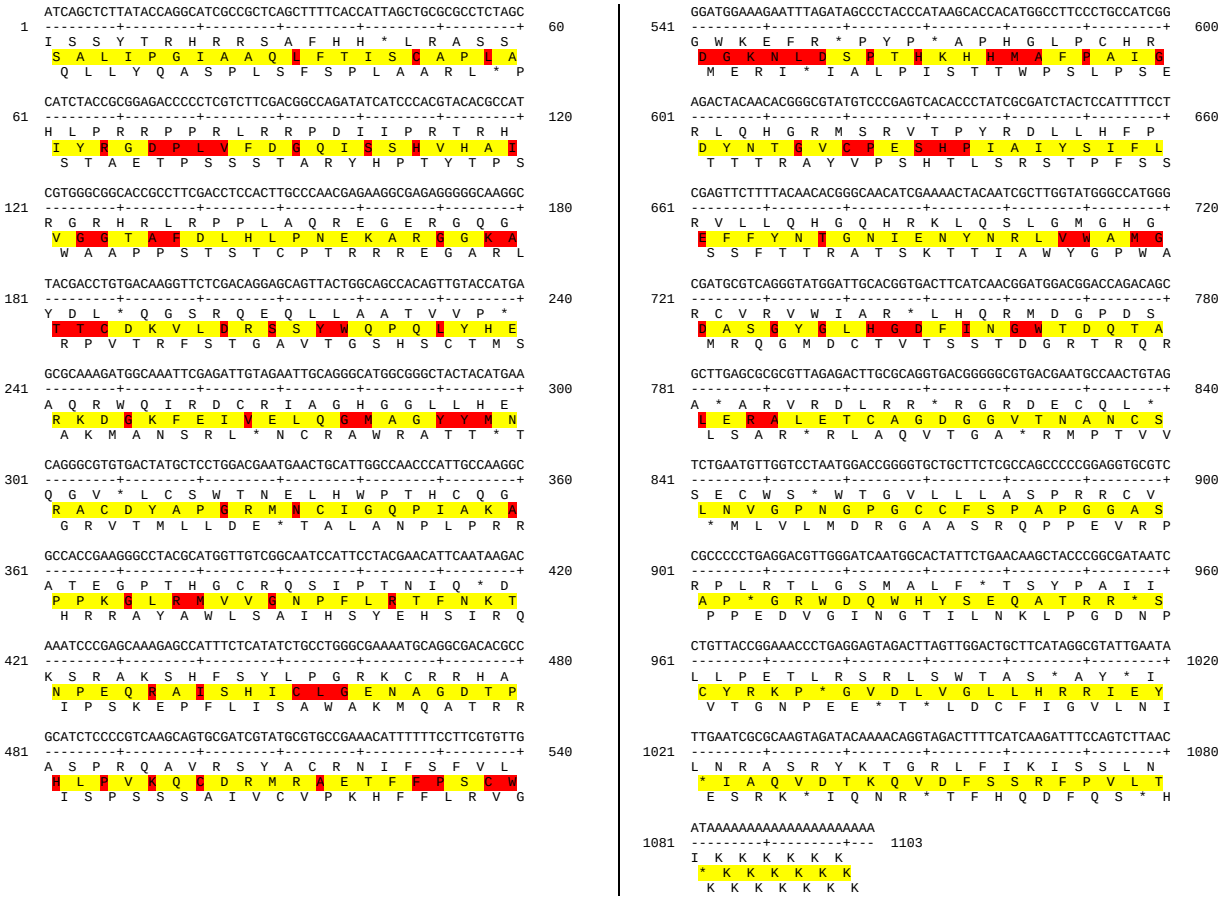

X9

no homologies.

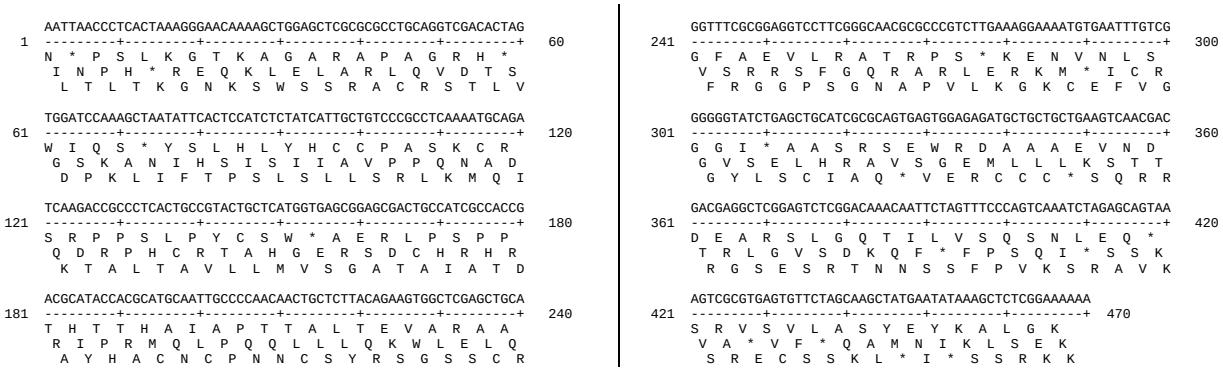

X21

no homologies.

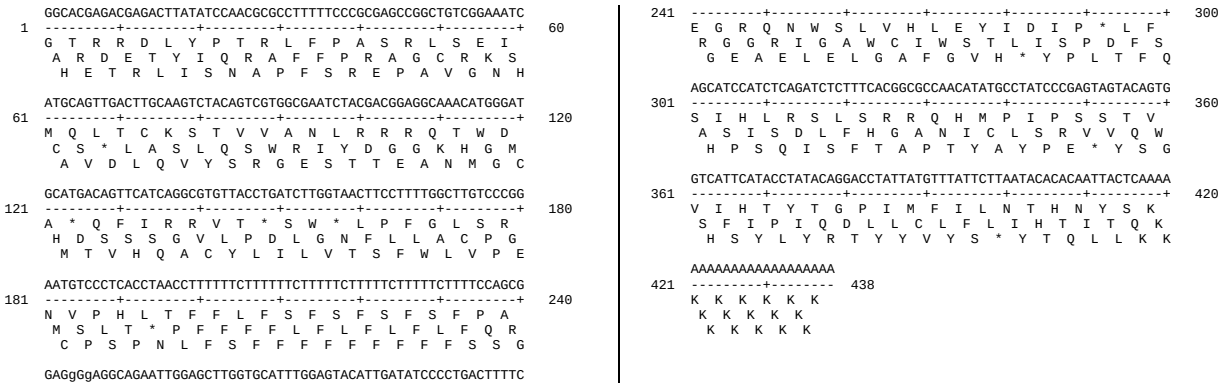

X23

red: homology to $Na^{+}/K^{+}/2C1^{-}$ co-transporter from *Neurospora crassa.*

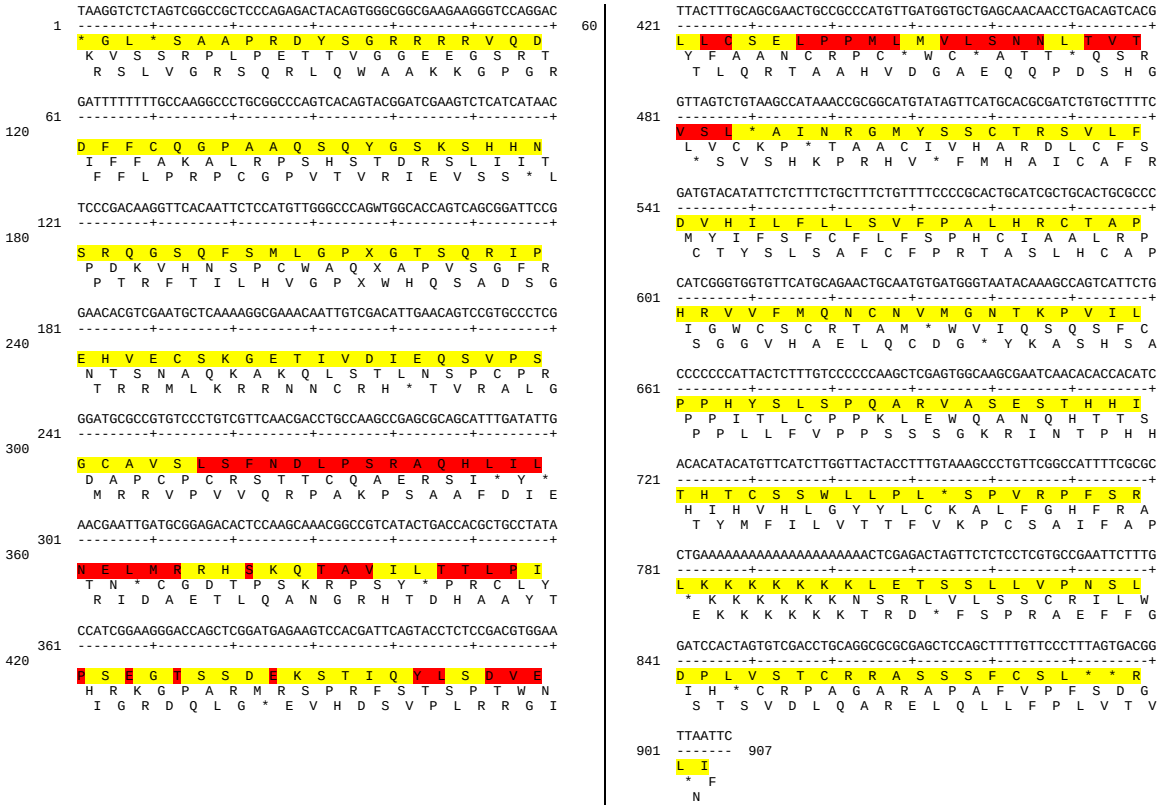

x27a/x68

no homologies..

```
    CCTTTACCAACCTCTTTCAACGGGGCCCTACCACTTGCTCTGGCGGCAGTAACGGGCAGA
1   ---------+---------+---------+---------+---------+---------+   60
    P  L  P  T  S  F  N  G  A  L  P  L  A  L  A  A  V  T  G  R
     L  Y  Q  P  L  S  T  G  P  Y  H  L  L  W  R  Q  *  R  A  D
      F  T  N  L  F  Q  R  G  P  T  T  C  S  G  G  S  N  G  Q  M

    TGAATGGGGGCCCTTTCGATACTCACCGCAGCGCTTGTCTGTCACCACGATGGGCTTGTC
61  ---------+---------+---------+---------+---------+---------+  120
    *  M  G  A  L  S  I  L  T  A  A  L  V  C  H  H  D  G  L  V
     E  W  G  P  F  R  Y  S  P  Q  R  L  S  V  T  T  M  G  L  S
      N  G  G  P  F  D  T  H  R  S  A  C  L  S  P  R  W  A  C  P

    CGGCACCTCGCCTACCTCCCCATCCAGCTTCAATCTTCGCCGTGGTAGCATGTCCACCAA
121 ---------+---------+---------+---------+---------+---------+  180
    R  H  L  A  Y  L  P  I  Q  L  Q  S  S  P  W  *  H  V  H  Q
     G  T  S  P  T  S  P  S  S  F  N  L  R  R  G  S  M  S  T  N
      A  P  R  L  P  P  H  P  A  S  I  F  A  V  V  A  C  P  P  I

    TTCTGACTCTATTGACGAGAGCGTCGTCGAGGATGATGAGGTGCCTGGCACGATGAAGAC
181 ---------+---------+---------+---------+---------+---------+  240
    F  *  L  Y  *  R  E  R  R  R  G  *  *  G  A  W  H  D  E  D
     S  D  S  I  D  E  S  V  V  E  D  D  E  V  P  G  T  M  K  T
      L  T  L  L  T  R  A  S  S  R  M  M  R  C  L  A  R  *  R  L

    TACCCCCACGGCCCCTTTTGGCCGTCGGACGAGCTTTGGTGGCTCTAATTTGAGGACCTA
241 ---------+---------+---------+---------+---------+---------+  300
    Y  P  H  G  P  F  W  P  S  D  E  L  W  W  L  *  F  E  D  L
     T  P  T  A  P  F  G  R  R  T  S  F  G  G  S  N  L  R  T  Y
      P  P  R  P  L  L  A  V  G  R  A  L  V  A  L  I  *  G  P  I

    TCGTCCTAGTGGCAATAGCCCTGGCAATGATCAACCGGGCCTCAACTGGTCGGAGCAACT
301 ---------+---------+---------+---------+---------+---------+  360
    S  S  *  W  Q  *  P  W  Q  *  S  T  G  P  Q  L  V  G  A  T
     R  P  S  G  N  S  P  G  N  D  Q  P  G  L  N  W  S  E  Q  L
      V  L  V  A  I  A  L  A  M  I  N  R  A  S  T  G  R  S  N  S

    CCGCTCTCGCGCCGAGAGCTGCGTCTCCGCCGTTCGTCCTTCATTCTCCCTAGGATCCTC
361 ---------+---------+---------+---------+---------+---------+  420
    P  L  S  R  R  E  L  R  L  R  R  S  S  F  I  L  P  R  I  L
     R  S  R  A  E  S  C  V  S  A  V  R  P  S  F  S  L  G  S  S
      A  L  A  P  R  A  A  S  P  P  F  V  L  H  S  P  *  D  P  H

    ACCTCCACGACCTGCACCACAACACGATCGCACCAAATCCGTCTCCGATATGATGCAGCC
421 ---------+---------+---------+---------+---------+---------+  480
    T  S  T  T  C  T  T  T  R  S  H  Q  I  R  L  R  Y  D  A  A
     P  P  R  P  A  P  Q  H  D  R  T  K  S  V  S  D  M  M  Q  P
      L  H  D  L  H  H  N  T  I  A  P  N  P  S  P  I  *  C  S  R

    GCCTGTTCAGACCCCCAGACCCGCGGCCCAACAACCCAAGCCAGAGCCCCGCAAGCCAGA
481 ---------+---------+---------+---------+---------+---------+  540
    A  C  S  D  P  Q  T  R  G  P  T  T  Q  A  R  A  P  Q  A  R
     P  V  Q  T  P  R  P  A  A  Q  Q  P  K  P  E  P  R  K  P  D
      L  F  R  P  P  D  P  R  P  N  N  P  S  Q  S  P  A  S  Q  M

    TGCGTTCCAGGAGCGGATTCTCAAAGGTGATTTCTACATGGACTGAGCGCATGCTTTTGG
541 ---------+---------+---------+---------+---------+---------+  600
    C  V  P  G  A  D  S  Q  R  *  F  L  H  G  L  S  A  C  F  W
     A  F  Q  E  R  I  L  K  G  D  F  Y  M  D  *  A  H  A  F  G
      R  S  R  S  G  F  S  K  V  I  S  T  W  T  E  R  M  L  L  A
    CAGGTGCCATACACGTCTTCGTATAATCGCCTCTGGTCTCTTCTTTTTTCTCTCACCAGT
601 ---------+---------+---------+---------+---------+---------+  660
    Q  V  P  Y  T  S  S  Y  N  R  L  W  S  L  L  F  S  L  T  S
     R  C  H  T  R  L  R  I  I  A  S  G  L  F  F  F  L  S  P  V
      G  A  I  H  V  F  V  *  S  P  L  V  S  S  F  F  S  H  Q  S

    CCTCTCCACCCGTTGTGCACTCTTTGAGATGCAGGGCCGTGCTGTTGACTGTAAGCTTGT
661 ---------+---------+---------+---------+---------+---------+  720
    P  L  H  P  L  C  T  L  *  D  A  G  P  C  C  *  L  *  A  C
     L  S  T  R  C  A  L  F  E  M  Q  G  R  A  V  D  C  K  L  V
      S  P  P  V  V  H  S  L  R  C  R  A  V  L  L  T  V  S  L  F

    TTGCGGCCCTGATGGATCATTTCCGTGCAGACGCCGCACAGAGAAATGGTCGATCTCTTA
721 ---------+---------+---------+---------+---------+---------+  780
    L  R  P  *  W  I  I  S  V  Q  T  P  H  R  E  M  V  D  L  L
     C  G  P  D  G  S  F  P  C  R  R  R  T  E  K  W  S  I  S  Y
      A  A  L  M  D  H  F  R  A  D  A  A  Q  R  N  G  R  S  L  I

    TATGGTATGGAATATTGCCTCCGTCTTCACCACTGGATTCTCTTGTCTCTTGATGAAGAG
781 ---------+---------+---------+---------+---------+---------+  840
    Y  G  M  E  Y  C  L  R  L  H  H  W  I  L  L  S  L  D  E  E
     M  V  W  N  I  A  S  V  F  T  T  G  F  S  C  L  L  M  K  R
      W  Y  G  I  L  P  P  S  S  P  L  D  S  L  V  S  *  *  R  E

    AATCCAAATCTTTTTTGCCTCTTTCGTGTGTGGAACACATGGAAAGCATCATGTCTAGGA
841 ---------+---------+---------+---------+---------+---------+  900
    N  P  N  L  F  C  L  F  R  V  W  N  T  W  K  A  S  C  L  G
     I  Q  I  F  F  A  S  F  V  C  G  T  H  G  K  H  H  V  *  E
      S  K  S  F  L  P  L  S  C  V  E  H  M  E  S  I  M  S  R  N

    ATGGGTCTGCGTGGCGAATGGCGTAATTTTTATAATTACACTTGCTAGGTCCAATCTGGG
901 ---------+---------+---------+---------+---------+---------+  960
    M  G  L  R  G  E  W  R  N  F  Y  N  Y  T  C  *  V  Q  S  G
     W  V  C  V  A  N  G  V  I  F  I  I  T  L  A  R  S  N  L  G
      G  S  A  W  R  M  A  *  F  L  *  L  H  L  L  G  P  I  W  D

    ACGGGTTACCGTGGTTTACTTGACTTGAGATGCTCAGTGGATATTGAAAGCTTGACACAC
961 ---------+---------+---------+---------+---------+---------+ 1020
    T  G  Y  R  G  L  L  D  L  R  C  S  V  D  I  E  S  L  T  H
     R  V  T  V  V  Y  L  T  *  D  A  Q  W  I  L  K  A  *  H  T
      G  L  P  W  F  T  *  L  E  M  L  S  G  Y  *  K  L  D  T  R

    GGCTGAATTGCCTCGTGACGGATGGCATCATTCATGGTGTACTCTTGTCCCTTCACCGAG
1021--------+---------+---------+---------+---------+---------+ 1080
    G  *  I  A  S  *  R  M  A  S  F  M  V  Y  S  C  P  F  T  E
     A  E  L  P  R  D  G  W  H  H  S  W  C  T  L  V  P  S  P  R
      L  N  C  L  V  T  D  G  I  I  H  G  V  L  L  S  L  H  R  D

    ACACGACATGATGGATGCTTTTCACGAATCGAACAGGTCTAGGTTCGGATGGAATCGGCG
1081--------+---------+---------+---------+---------+---------+ 1140
    T  R  H  D  G  C  F  S  R  I  E  Q  V  *  V  R  M  E  S  A
     H  D  M  M  D  A  F  H  E  S  N  R  S  R  F  G  W  N  R  R
      T  T  *  W  M  L  F  T  N  R  T  G  L  G  S  D  G  I  G  A

    CACAGGGGCGGGACTTGCTTGTAAAATCAGGGTTGTAAGATTCCTGCGCTGGTGAGCAGG
1141--------+---------+---------+---------+---------+---------+ 1200
    H  R  G  G  T  C  L  *  N  Q  G  C  K  I  P  A  L  V  S  R
     T  G  A  G  L  A  C  K  I  R  V  V  R  F  L  R  W  *  A  G
      Q  G  R  D  L  L  V  K  S  G  L  *  D  S  C  A  G  E  Q  A

    CGGAGGGATGTCCCTATAGTTGGCACGCGGGGTCGAGGTTATGAGCATTGAGAAGACGGA
1201--------+---------+---------+---------+---------+---------+ 1260
    R  R  D  V  P  I  V  G  T  R  G  R  G  Y  E  H  *  E  D  G
     G  G  M  S  L  *  L  A  R  G  V  E  V  M  S  I  E  K  T  D
      E  G  C  P  Y  S  W  H  A  G  S  R  L  *  A  L  R  R  R  T

    CTACAAGGGCGAGAGGAATGGATTTCTCTTTTGTTGGTCTTTTAGGAGTTGACGGCGCGG
1261--------+---------+---------+---------+---------+---------+ 1320
    L  Q  G  R  E  E  W  I  S  L  L  L  V  F  *  E  L  T  A  R
     Y  K  G  E  R  N  G  F  L  F  C  W  S  F  R  S  *  R  R  G
      T  R  A  R  G  M  D  F  S  F  V  G  L  L  G  V  D  G  A  V

    TGGCTGGACAAAGGGGCAAGTCCGTGGCGCTGGTCTGAAATTATGGCCACGCCCGGATGA
1321--------+---------+---------+---------+---------+---------+ 1380
    W  L  D  K  G  A  S  P  W  R  W  S  E  I  M  A  T  P  G  *
     G  W  T  K  G  Q  V  R  G  A  G  L  K  L  W  P  R  P  D  E
      A  G  Q  R  G  K  S  V  A  L  V  *  N  Y  G  H  A  R  M  S

    GTATACAGCATCGTGGCTCGATGTCGGGAACGTGGCTCACGCAAAACTTTCGTTTTTCTT
1381--------+---------+---------+---------+---------+---------+ 1440
    V  Y  S  I  V  A  R  C  R  E  R  G  S  R  K  T  F  V  F  L
     Y  T  A  S  W  L  D  V  G  N  V  A  H  A  K  L  S  F  F  L
      I  Q  H  R  G  S  M  S  G  T  W  L  T  Q  N  F  R  F  S  C

    GTGAAACAGATGCTGTAGTTTTGCGCATTTCGGCCATGTGGCCAGCGACTATTGTAGCTG
1441--------+---------+---------+---------+---------+---------+ 1500
    V  K  Q  M  L  *  F  C  A  F  R  P  C  G  Q  R  L  L  *  L
     *  N  R  C  C  S  F  A  H  F  G  H  V  A  S  D  Y  C  S  *
      E  T  D  A  V  V  L  R  I  S  A  M  W  P  A  T  I  V  A  D

    ATTTAAATTGCAAAGCATTCTCTCAAAAA
1501--------+---------+---------  1529
    I  *  I  A  K  H  S  L  K
     F  K  L  Q  S  I  L  S  K
      L  N  C  K  A  F  S  Q  K
```

X34 reverse (rev) and universe (uni) sequences

X34rev

red: homology to ERO1 from *Schizosaccharomyces pombe.*

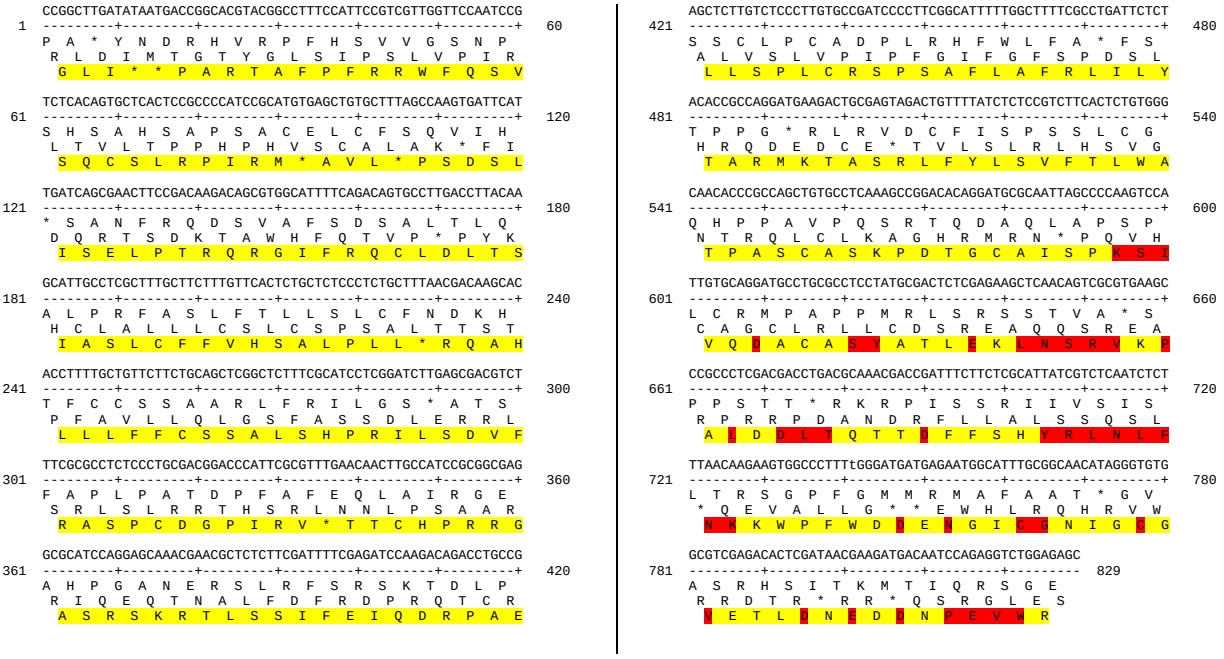

X34uni

red: homology to ERO1 from *Schizosaccaromyces pombe.*

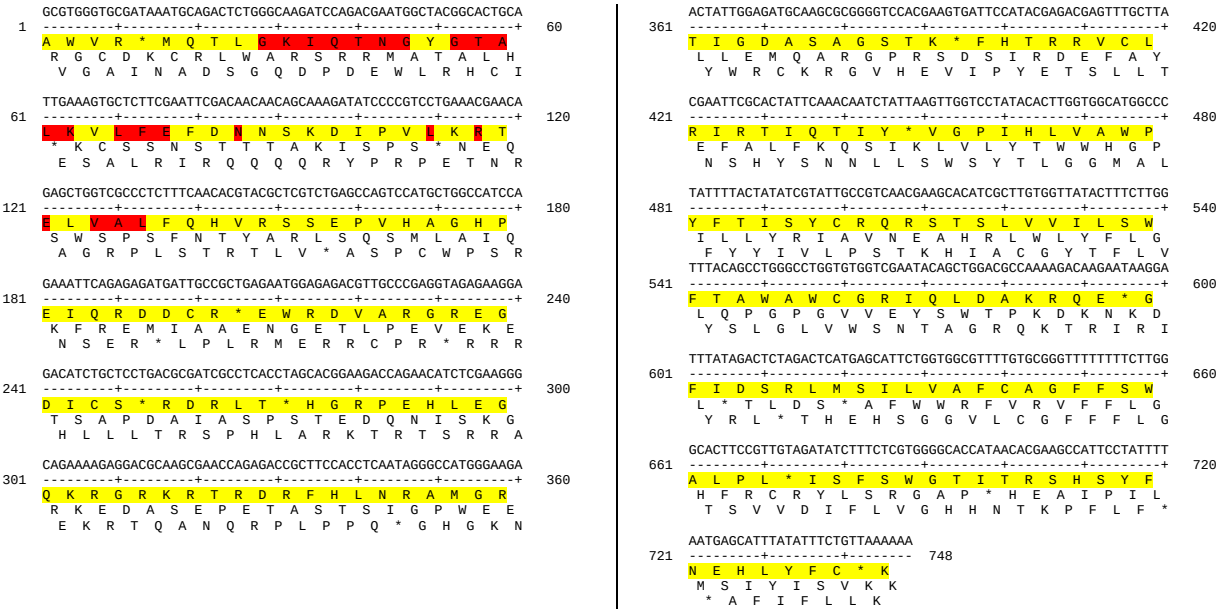

X43

no homologies

```
   CCACCCCTCCTCTCACGCATGCAATGCCCGCATACCCGCCACGACTGCAACGGCCCCTCC
 1 ---------+---------+---------+---------+---------+---------+   60
   P  P  L  L  S  R  M  Q  C  P  H  T  R  H  D  C  N  G  P  S
    H  P  S  S  H  A  C  N  A  R  I  P  A  T  T  A  T  A  P  P
     T  P  P  L  T  H  A  M  P  A  Y  P  P  R  L  Q  R  P  L  L

   TGCGAATAGCGCTGAAGCATCCAGTCGAGGTAGCTCCGTCGGTCCCGAAAAGGGTATTGC
61 ---------+---------+---------+---------+---------+---------+  120
   C  E  *  R  *  S  I  Q  S  R  *  L  R  R  S  R  K  G  Y  C
    A  N  S  A  E  A  S  S  R  G  S  S  V  G  P  E  K  G  I  A
     R  I  A  L  K  H  P  V  E  V  A  P  S  V  P  K  R  V  L  R

   GTTGAGGGGGACAAGGGAAGTGAGGCGGCTGTGATGTGACCATGTGCGAGGACCGCAGAT
121 ---------+---------+---------+---------+---------+---------+  180
   V  E  G  D  K  G  S  E  A  A  V  M  *  P  C  A  R  T  A  D
    L  R  G  T  R  E  V  R  R  L  *  C  D  H  V  R  G  P  Q  I
     *  G  G  Q  G  K  *  G  G  C  D  V  T  M  C  E  D  R  R  S

   CCAGACACTCAGACATGAGTGCCGATGTATTAGACAATGGGAAGGAGGCCCTTGAGAGGC
181 ---------+---------+---------+---------+---------+---------+  240
   P  D  T  Q  T  *  V  P  M  Y  *  T  M  G  R  R  P  L  R  G
    Q  T  L  R  H  E  C  R  C  I  R  Q  W  E  G  G  P  *  E  A
     R  H  S  D  M  S  A  D  V  L  D  N  G  K  E  A  L  E  R  L

   TATATATATAACAAGAGCTGAGAAAGCCGCATTCTGACCTCACCGATCAGTCTGTATGCC
241 ---------+---------+---------+---------+---------+---------+  300
   Y  I  Y  N  K  S  *  E  S  R  I  L  T  S  P  I  S  L  Y  A
    I  Y  I  T  R  A  E  K  A  A  F  *  P  H  R  S  V  C  M  P
     Y  I  *  Q  E  L  R  K  P  H  S  D  L  T  D  Q  S  V  C  P
```

```
   CAGACCAGACATCACGTCACGGCGTCGTGCTTCAGAAGTTCCGCTTCAGCTTCACGTCCC
301 ---------+---------+---------+---------+---------+---------+  360
   Q  T  R  H  H  V  T  A  S  C  F  R  S  S  A  S  A  S  R  P
    R  P  D  I  T  S  R  R  R  A  S  E  V  P  L  Q  L  H  V  P
     D  Q  T  S  R  H  G  V  V  L  Q  K  F  R  F  S  F  T  S  H

   ATGTTCACGTTAATTTTACTCGTTGAATGGTAAAAGTGATGTTGAATGCTCCTCGCTGGC
361 ---------+---------+---------+---------+---------+---------+  420
   M  F  T  L  I  L  L  V  E  W  *  K  *  C  *  M  L  L  A  G
    C  S  R  *  F  Y  S  L  N  G  K  S  D  V  E  C  S  S  L  A
     V  H  V  N  F  T  R  *  M  V  K  V  M  L  N  A  P  R  W  L

   TAAATGCTCTAACGTTACGTTACATGGCTGATGCAGCTAATGTGTCCATGGTGGGTATCA
421 ---------+---------+---------+---------+---------+---------+  480
   *  M  L  *  R  Y  V  T  W  L  M  Q  L  M  C  P  W  W  V  S
    K  C  S  N  V  T  L  H  G  *  C  S  *  C  V  H  G  G  Y  H
     N  A  L  T  L  R  Y  M  A  D  A  A  N  V  S  M  V  G  I  T

   CCGAGGCTTTCCGCTTGGGCTCTTCGTGGTCCTGCTCCTCCCCGCTGTCGCTGGATGACT
481 ---------+---------+---------+---------+---------+---------+  540
   P  R  L  S  A  W  A  L  R  G  P  A  P  P  R  C  R  W  M  T
    R  G  F  P  L  G  L  F  V  V  L  L  L  P  A  V  A  G  *  L
     E  A  F  R  L  G  S  S  W  S  C  S  S  P  L  S  L  D  D  C

   GCTCCATGCCGAGATTGC
541 ---------+-------  558
   A  P  C  R  D  C
    L  H  A  E  I
     S  M  P  R  L
```

X51a

red: homology to cell surface ferroxidase from *Neurospora crassa*.

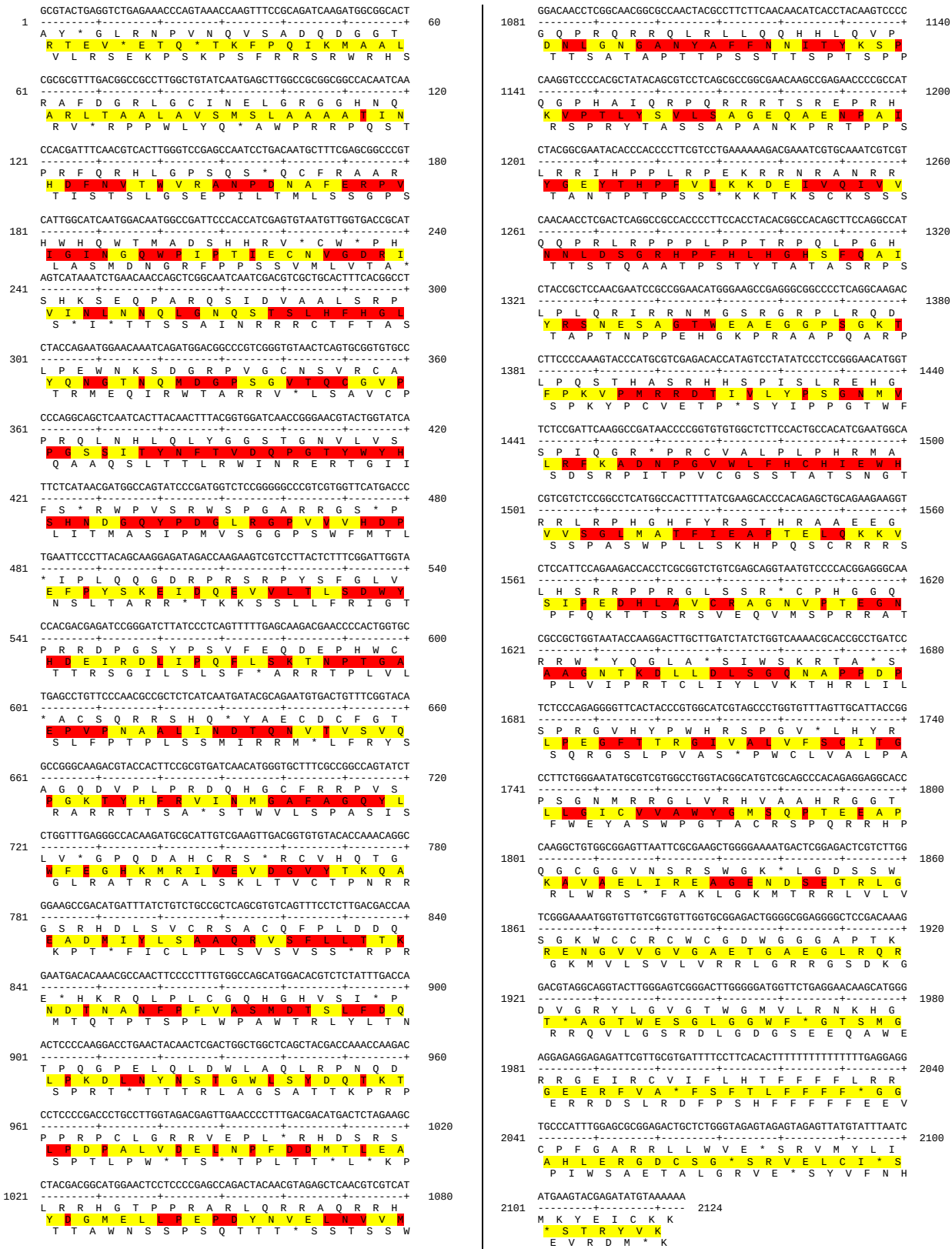

X62

red: homology to putative glutamate 5-kinase from *Schizosaccharomyces pombe.*

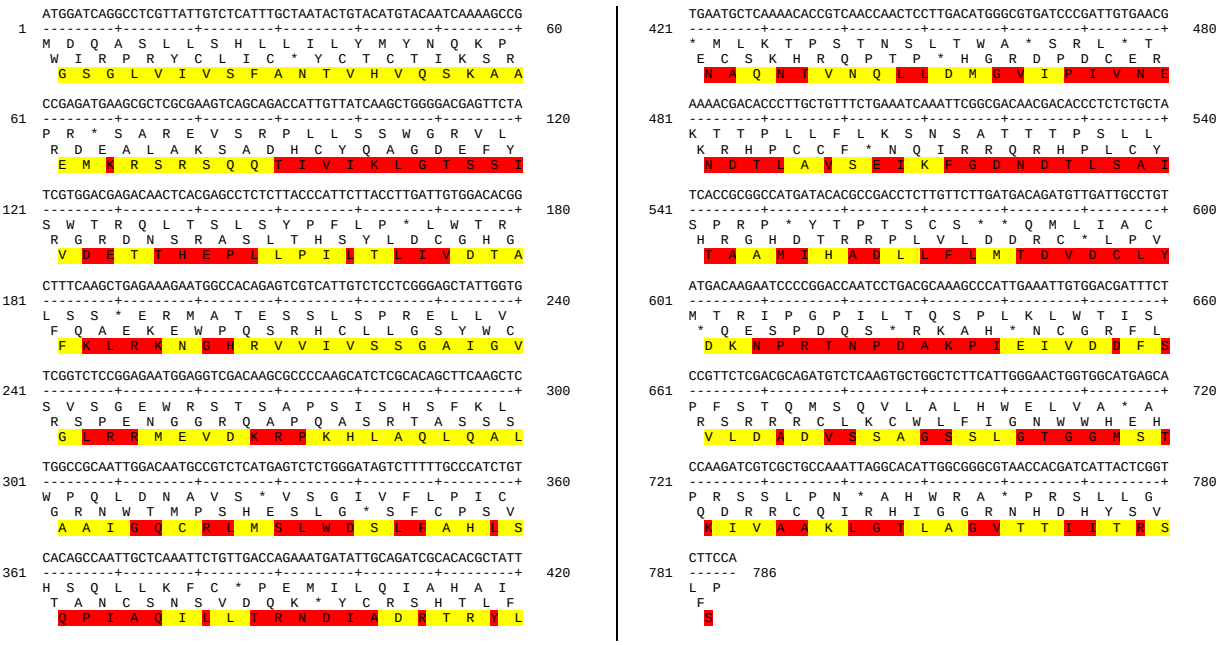

X65

red: homology to probable 20S proteasome subunit Y7 of *Saccharomyces cerevisiae*

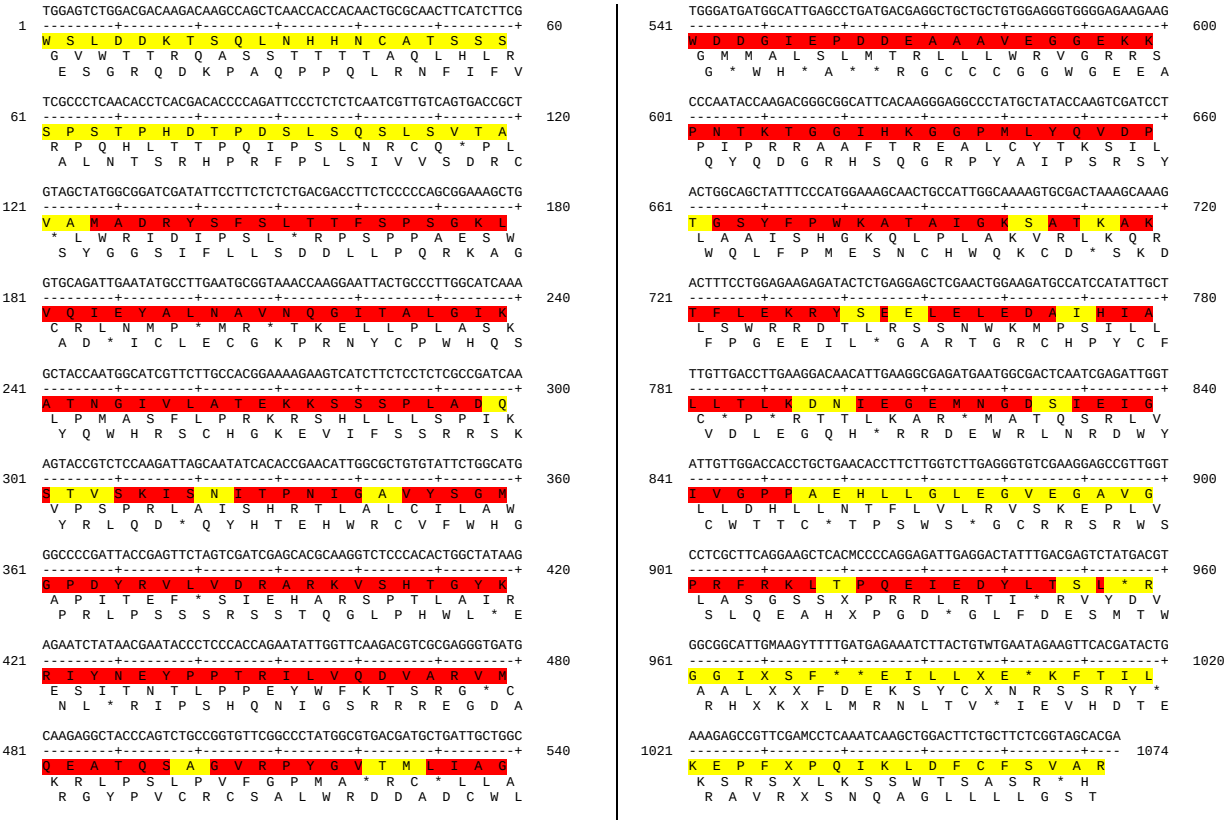

x80c-x98 no homology

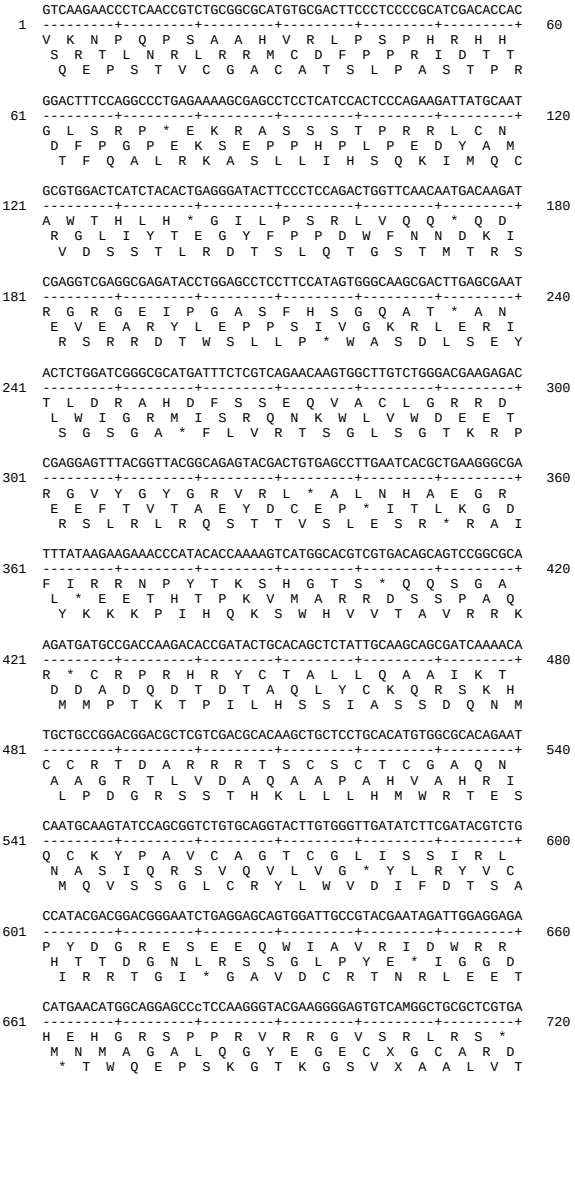

Appendix C: Chemicals

Chemical	*Manufacturer*
λ-ZAP vector	*Stratagene*
1 kb DNA Ladder	*Pharmacia*
Accugel 40% (w/v) 19:1 acrylamide/bisacrylamide	*National Diagnostics*
Acetic acid	*Riedel-de Haën*
Agar (Select)	*Invitrogen*
Agarose ultra pure	*Gibco BRL*
Ammonium acetate	*AppliChem*
Ammonium persulfate	*Serva*
Ampicillin	*Gerbu*
Anti-rabbit IgG, AP conjugate	*Sigma*
Ascorbic acid	*Sigma*
BCA	*Sigma*
BCIP	*Fluka*
Boric acid	*AppliChem*
Bovine liver catalase	*Sigma*
Bromphenol blue	*Serva*
BSA	*Fermentas*
Caesiumchloride	*Gibco BRL*
Calf intestinal alkaline phosphatase	*Pharmacia*
CaN_2O_6 x 4 H_2O	*AppliChem*
Casamino acids	*Difco*
Caseinhydrolysate (peptone #140)	*Gibco BRL*
cDNA library synthesis kit	*Stratagene*
Chloroform	*AppliChem*
Citric acid x 1 H_2O	*AppliChem*
Corresponding buffer	*Sigma*
Cysteine	*Fluka*
DAB	*Fluka*
DDC	*Fluka*
DDT	*Gibco BRL*
DEAE-cellulose NA45 (0,45 µm)	*Schleicher & Schuell*
DEPC	*AppliChem or Serva*
Dextran blue	*Serva*

Chemical	*Manufacturer*
Dextran sulfate	*Eppendorf*
dGTP, dATP and dTTP	*Fermentas*
Dimethylformamide	*Serva*
Dimethylsulphoxide	*Roth*
DNA-Polymerase I (Klenow-Fragment) λ DNA	*MBI Fermentas*
DNaseI	*Boehringer*
Driselase	*Sigma, USA*
DTT (1,4-Dithiothreitol)	*Roth*
DYEnamic Direct Cycle Sequencing Kit with 7d-Z-dGTP	*Amersham*
Dynabeads®	*Dynal*
EDTA	*AppliChem*
Ethanol	*AppliChem*
ExAssist™ helper phages	*Stratagene*
Ficoll® 400	*Pharmacia*
First strand buffer	*Gibco BRL*
GeneQuant II RNA/DNA Calculator	*Pharmacia*
Glucose-6-phosphate	*Calbiochem*
Glycerine	*AppliChem*
Glycine	*AppliChem*
H_2KO_4P	*AppliChem*
Herrings sperm DNA	*Boehringer*
Hygromycin B	*Calbiochem*
IEF protein marker-mix 3.6-9.3	*Sigma*
IPTG	*Biomol*
Isopropanol	*Riedel-de Haën*
Jet Star plasmid isolation and gel extraction kits	*Genomed*
Jet Star Plasmid Miniprep Spin Kit	*Genomed*
KAc	*AppliChem*
Kanamycin-sulfate	*Serva*
KCl	*AppliChem*
KOH	*AppliChem*
L-asparagine	*Biomol*

L-cysteine	*Fluka*
L-glutamine	*Biomol*
LiCl	*AppliChem*
Ligase	*Fermentas or Gibco BRL*
Malt extract	*Oxoid*
Methanol	*Riedel-de Haën*
Methyl viologen	*Sigma*
$MgSO_4$ x 7 H_20	*AppliChem*
Milk powder	*Glücksklee*
Millex GV 0.22 µM filter units	*Millex*
Mineral oil	*Sigma*
Mira-cloth	*Calbiochem*
Molecular weight marker for SDS-PAGE	*Serva*
MOPS (3-(N-Morpholino)propanesulphonic acid)	*USB*
Mutanase	*Interspex Products*
NaCl	*AppliChem*
$NaCO_3$	*AppliChem*
$NADP^+$	*Sigma*
NADPH	*Biomol*
NBT	*Fluka*
Nicotinic acid	*Serva*
Nitrocellulose transfer membrane BA85 (0,45µm) and BA83 (0,2µm)	*Schleicher & Schuell*
N-lauroylsarcosine	*Sigma*
Novozyme 234	*Novo*
Nylonfilter HybondN^+ (0.2 µm und 0,45 µm)	*Amersham*
Oligo dT_{12-18}	*Gibco BRL*
Oligonucleotide N_6 (random hexamers) RNase	*Boehringer*
Oligotex™mRNA Mini Kit	*Quiagen*
Optitran (reinforced) nitrocellulose filters	*Schleicher & Schuell*
PAA	*National Diagnostics*
Paraquat (methyl viologen)	*Sigma*
pCR®2.1-TOPO®	*Invitrogen*
PEG 4000	*Fermentas*
PEG 6000	*Sigma*
Peroxidase (POD) from horse radish, Grade II	*Roche*
Peroxidase (POD) from horse radish, Grade II	*Roche*
Phleomycin	*Cayla*
Polyvinylpolyl-pyrrolidone	*Sigma*
Ponceau S	*Sigma*
Propanol	*AppliChem*
Random hexamers	*Boehringer*
RED-Taq™ DNA polymerase	*Sigma*
Restriction enzymes	*Fermentas*
Riboflavine	*Serva*
RNA Guard RNAse inhibitor	*Pharmacia*
RNAgents® Total RNA Isolation System	*Promega*
RNA-Ladder	*Gibco BRL*
SDS	*Serva or ICN Biomedicals*
Sephadex™ G-50	*Amersham*
Sequagel XR®	*Biozym*
Sequagel® complete buffer reagent	*Biozym*
Servalyt® 3-10 Ampholyte (also pH 5-8, 3-7)	*Serva*
Silver nitrate	*Fluka*
Spermadine	*Sigma*
Spermadine-trihydrochloride	*Fluka*
Sucrose	*Roth*
Superscript™ reverse transcriptase	*Gibco BRL*
T4-Ligase	*Gibco BRL*
TEMED	*Serva*
Thermo-sequencing mix	*Amersham or Biozym*
Thymine	*Serva*
TOPO™ TA Cloning® Kit	*Invitrogen*
Tris	*AppliChem*
Tween® 20	*United States Biochemical*
Uni-ZAP® XR	*Stratagen*
Xanthine	*Sigma*
Xanthine oxidase (XO)	*Sigma*
X-Gal	*Biomol*
Yeast extract	*Gibco BRL*
ZAP Express® cDNA Gigapack III Gold cloning kit	*Stratagene*
ZAP-Express® phagemid vector	*Stratagene*

α-[^{32}P]-dCTP radioactivity *Amersham*

All other chemicals were manufactured by *Merck*

Appendix D: Media

Luria-Bertani Broth (LB)
10 g casamino acids
5 g yeast extract
5 g NaCl
pH 7.2
ad. 1 l with ddH2O

LBM (NZY)
as LB, with:
2 g $MgSO_4$ x 7 H_2O

LBMM
as LB, with:
2 g $MgSO_4$ x 7 H_2O
2 g maltose

Mantle-Medium (MA)
100 g sucrose*
10.0 g L-asparagine
1.0 g $CaNO_3$ x 4 H_2O
0.25 g $MgSO_4$ x 7 H_2O
0.25 g KH_2PO_4
0.125 g KCl
0.10 g yeast extract
0.01 g L-cysteine
0.033 g $FeSO_4$ x 7 H_2O
0.027 g $ZnSO_4$ x 7 H_2O
pH 5.2
ad. 1 l with ddH_2O
*amount of sucrose or other carbon source is specified in experimental procedures, if not 100 g

InocN-Medium
100 g sucrose
0.5 g KH_2PO_4
10.0 g citratex1 H_2O
1.0 g $Ca(NO_3)_2$ x 4 H_2O
0.5 g $MgSO_4$ x 7 H_2O
0.12 g KCl
0.007 g $FeSO_4$ x 7 H_2O
0.006 g $ZnSO_4$ x 7 H_2O
0.75 niacinamide
pH 5.2 with conc. NH_4
ad 1 l with tapwater

Top Agar
0.7 % (w/v) agarose in LBM

T25N-Medium
300 g sucrose
0.5 g KH_2PO_4
15.0 g citratex1 H_2O
1.0 g $Ca(NO_3)_2$ x 4 H_2O
0.5 g $MgSO_4$ x 7 H_2O
0.12 g KCl
0.007 g $FeSO_4$ x 7 H_2O
0.006 g $ZnSO_4$ x 7 H_2O
0.75 niacinamide
pH 5.2 with conc. NH_4
ad 1 l with tapwater

Mimimal Medium (MM)
20 g glucose
1.5 g asparagine
1.0 g K_2HPO_4
0.46 g KH_2PO_4
0.5 g $MgSO_4$ x $7H_2O$
0.005 g $FeCl_3$ x 6 H_2O
0.12 mg thiamine-HCl
1.0 ml trace element stock
ad. 1 l with ddH_2O

Trace element stock
0.06 g HBO_3
0.04 g$(NH_4)_6Mo_7O_{24}$ x 4 H_2O
0.02 g $CuSO_4$ x 5 H_2O
2.0 g $ZnSO_4$ x 7 H_2O
0.1 g $MnSO_4$ x 4 H_2O
0.4 g $CoCl_2$ x 6 H_2O
1.2 g $Ca(NO_3)_2$ x 4 H_2O
ad. 1 l with ddH_2O

BII-Medium
10 g sucrose
5.0 g peptone
5.0 g L-asparagine
1.0 g KH_2PO_4
0.5 g $MgSO_4$,
0.01 g $FeSO_4$x 7 H_2O
pH 5,2
ad. 1 l with ddH_2O

BII/8 (for regeneration of protoplasts)
as BII except: 200 g sucrose

BII/8 Fe-(for selection with phleomycin)
as BII/8 without $FeSO_4$ x $7H_2O$

Media were solidified by the addition of 16 g/l agar, with the exception of media used for the embedding of protoplasts, to which only 12 g/l agar were added.

Acknowledgements:

To Prof. Dr. Paul Tudzynski: for encouragement, discussion, support, time, optimism, clarity and never-ending interest far beyond the call of duty throughout the whole (and the hole) of my time in his lab- (who managed to look both dignified in a too-small sweatshirt of Birgitt's decorated with a smiling teddy-bear, and friendly, even after learning that all his keys were at the bottom of a river)
I could not have wished for a better "Doktorvater"...

To Bettina, who always found time at the drop of a hat (and the paper she was writing) for any problem at hand and whose warmth and enthusiasm never flagged. **To Birgitt,** for always knowing where to look, always being ready to do so and just for being Birgitt and nobody else (which nobody else could be)**To Helga** for the continuous small things-done when no one was looking- which made life hold for two or three days longer (**To both Birgitt and Helga** for their love of EXTREMLEY RIPE bananas), **To Telmo** for some good discussions and all the computer stuff, to **Klaus W**., for always being amused, to **Patrick** for good fellowship in the protein corner and to **Klaus T.** for some fruitful discussions.

TO ANDRE, for always knowing the right thing to say, for the crisis-management, the fast and the slow food and the terrible, terrible movies and most of all, for the **ARGUMENTS** (it was 2.0 ml)

TO MY LONG, LONG (sometimes until after eight o'clock) **SUFFERING S-KURS STUDENTS**: **Christian**, who showed me that life isn't always ampicillin-resistant, **Eva** for the cigarettes, and her tidy ability to mass produce, **Nicole** for coming back (even when she knew what it would be like), **Thomas** (for helping me fit through the door of the isotope lab and those two extra days and those 40 extra filters) and **Jürgen**, **FOR ALL THEIR HELP**.

To MARTINA for her help, her ability to warp time and for her comforting presence behind the teapot, **To GERALDINE** for all that gallic sparkling (and sparkling gall) and all the h's she left in this lab, and to **VERENA** for being such a companionable office-sharer. **TO SABINE GIESBERT** for the first sentence she ever spoke to me (and many after), and for her help and support whenever it was needed, **and to the rest of the lab, past and present,** for making this a nice place to work.

TO DÖRTHE for yet more coffee and all that went into it (!!!!!)

TO MY MOTHER, FATHER, ANDREW AND THE REST OF MY FAMILY, especially to Mom and Elna for spoiling John during the crunch time...

To Prof. Dr. Meinhardt **for his niceness in accepting the role of co-evaluator (and for not asking about the spacing)...**

especially to MARTIN,

whom it would be impossible to thank without offending the censors...

A very grateful thanks-you to my four-headed correction committee MARTIN (chief beast tamer,) BIRGITT (hole-finder), SABINE (for getting up at six!) and ANDRE (for spotting the bugs))and my printing help MARTINAMARTINANDRE (!!!).

Curriculum Vitae

Sabine Ivison, geb. Moore
Weselerstr. 6
48151 Münster

Persönliche Daten

Geburtstag:	19. December, 1969
Geburtsort:	Victoria, B.C., Kanada
Familienstand:	verheiratet
Staatsangehörigkeit:	kanadisch
Eltern:	Robert John Moore und Dorothee Moore, geb. von Scheven

Schulbildung

1975-1979:	Fairlawn Junior School, Thornhill, Ont., Canada
1979-1981:	Wells Street Public School, Aurora, Ont., Canada
1981-1983:	Aurora Senior Public School, Aurora, Ont. Canada
1983-1988:	Dr. G.W. Williams Secondary Secondary, Aurora, Ont., Canada
Abschluss:	Canadian Secondary Honor Graduation

Studium

1989-1990:	Studienkolleg an der Westfälischen Wilhelms-Universität, Münster
1990-1997:	Studium der Biologie an der Westfälischen Wilhelms-Universität, Münster
22. Juli, 1997:	Diplom mit dem Hauptfach Mikrobiologie, Westfälische Wilhelms-Universität, Münster

Promotionsstudiengang

ab Oktober 1997:	Westfälische Wilhelms-Universität Institut für Botanik Lehrstuhl für allgemeine Mikrobiologie und Botanik Bei Prof. Dr. Paul Tudzynski

Berufstätigkeit

ab Oktober 1997:	Wissenschaftliche Mitarbeiterin im Institut für Botanik der Westfälischen Wilhelms-Universität, Münster